U.PORTO

FEUP FACULDADE DE ENGENHARIA
UNIVERSIDADE DO PORTO

Lignin from Pulp Mill Sulfite Liquors: Production of Vanillin and Syringaldehyde by an Integrated Process within the Biorefinery Concept

Dissertation presented to Faculdade de Engenharia da Universidade do Porto for the PhD degree in Chemical and Biological Engineering

by

Filipa Manuela Alves Calvo Casimiro

Supervisor: Prof. Dr. Alírio Egídio Rodrigues
Co-supervisor: Dr. Carina Andreia Esteves da Costa

SRE CM LABORATORY OF SEPARATION AND REACTION ENGINEERING
LABORATORY OF CATALYSIS AND MATERIALS

Laboratory of Separation and Reaction Engineering - Laboratory of Catalysis and Materials
Department of Chemical Engineering, Faculty of Engineering, University of Porto

May, 2023

This thesis was financially supported by LA/P/0045/2020 (Alice), UIDB/50020/2020 and UIDP/50020/2020 (LSRE-LCM), funded by national founds through FCT/MCTES (PIDDAC).

ACKNOWLEDGEMENTS

Começar por agradecer ao meu orientador desta tese, o Professor Alírio Rodrigues, pela oportunidade que me deu não só de integrar na sua equipa como também de poder realizar este grande objectivo, o doutoramento, no seu laboratório. A ele agradeço por todos os conhecimentos e ensinamentos que me transmitiu e que permitiram crescer profissionalmente e aprender.

Um enorme obrigado à minha co-orientadora Dra. Carina Costa pela sua disponibilidade, pelos conhecimentos partilhados e pelo apoio incondicional ao longo deste percurso. Nem sempre o percurso foi fácil, mas além de ser uma excelente orientadora, foi sempre minha amiga e esteve sempre disponível para me apoiar. Os seus conselhos e paciência foram essenciais a este trabalho e deram-me muitas vezes ânimo para continuar em frente e ultrapassar os obstáculos. Obrigado pela ajuda em todos os desafios.

Ao Rui Faria um muito obrigada pela sua disponibilidade e pela sua partilha de conhecimento, foi incansável, a sua ajuda foi muito preciosa na concretização de alguns objectivos do trabalho. Aos meus amigos e colegas de gabinete e de laboratório que me ajudaram de muitas maneiras diferentes e tornam os meus dias mais agradáveis e felizes! Um obrigado especial ao Elson pela sua partilha constante de conhecimento e amizade.

Um agradecimento ao laboratório LSRE-LCM, que foi a minha segunda casa nestes últimos anos, e que contribuiu para a minha evolução profissional e pessoal.

Agradeço de coração às minhas queridas amigas, nomeadamente, Dânia, Vanessa, Raquel, e Mariana pelos convívios na hora de almoço, ultimamente menos frequentes, mas que sem dúvida os momentos passados juntas foram cruciais para enfrentar o dia-a-dia muitas vezes difícil. Obrigado meninas pela alegria contangiante, pelo carinho, pela paciência e apoio.

Os meus últimos agradecimentos, mas não menos importantes, vão para a minha família, para meus pais e irmão, que apesar de estarem um bocadinho longe me apoiam e fazem com que eu acredite que isto seria possível. Ao meu companheiro de vida, Zé, pelo carinho, paciência e por todo o apoio emocional demonstrado, e por fim, ao grande amor da minha vida, ao meu filho, Simão, que me desafia todos os dias a ser uma pessoa melhor e por ser a minha grande motivação no alcance deste grande objectivo.

ABSTRACT

Nowadays, the increasing concern about the decline of fossil fuel reserves and the environmental impact derived from their use has put considerable interest in lignocellulosic biomass exploitation as a renewable source of biofuels and biomaterials. In the biorefinery concept, large quantities of lignin are produced. This biopolymer, the second most abundant on the planet, has long been recognized as a valuable feedstock however, most lignin is burned as a fuel, despite the existence of a great number of potential applications.

The work developed in this thesis intends to validate an integrated process to produce phenolic monomers, namely vanillin and syringaldehyde, from lignin isolated from hardwood and softwood pulp mill sulfite liquors using processes with reduced environmental impact.

The structural characteristics of lignins isolated from hardwood and softwood pulp mill sulfite liquors were evaluated. Lignin was obtained after ultrafiltration and freeze-drying of the sulfite liquors and characterized based on inorganic content, nitrobenzene oxidation, carbon-13 nuclear magnetic resonance, and molecular weight determination. The structural characteristics achieved allow to evaluate the potential of each lignin through oxidative depolymerization to produce added-value phenolic monomers. Hardwood and softwood lignins were submitted to alkaline oxidation with oxygen and the reaction conditions were optimized to obtain a final oxidation mixture with the maximum yield of phenolic monomers. From the results, it is possible to conclude that a phenolic aldehyde-rich oxidation mixture could be obtained, confirming the viability of softwood and hardwood lignins as raw material to produce added-value products such as vanillin and syringaldehyde.

The degradation kinetics of the main phenolic compounds obtained from lignin oxidation in an alkaline medium using oxygen as oxidant, namely vanillin, vanillic acid, acetovanillone, syringaldehyde, syringic acid, and acetosyringone, were studied. The effect of temperature, initial concentration, and oxygen partial pressure was evaluated, and a simple mathematical model was selected to evaluate the degradation of these phenolics during oxidative depolymerization.

In a further stage, the mixture obtained from oxidation of lignin from a pulp mill softwood sulfite liquor, was treated by a two-step filtration using membranes with a

molecular weight cut-off of 2 kDa and 600-800 Da. The membrane filtration was used to concentrate the low molecular phenolic compounds of interest, namely vanillin. The permeate of the nanofiltration membrane (600-800 Da) proceeds to a fixed bed adsorption/desorption process using a non-polar resin (SP700). This chromatographic step allows enriching the final aqueous solution containing vanillin by cyclic mode operation using water and ethanol as eluents to desorb the target phenolic monomer.

The oxidized mixture of lignin isolated from a pulp mill hardwood sulfite liquor was also submitted to a sequential process to obtain the phenolic aldehydes of interest, namely vanillin and syringaldehyde. The main reaction products obtained using this lignin were syringaldehyde, vanillin, vanillic acid, syringic acid, acetosyringone and acetovanillone. The monomers syringaldehyde and vanillin have similar structures and properties, which represents the main challenge in their separation. The first stage of the sequential process was a three-step membrane filtration of the oxidized mixture using ultra and nanofiltration membranes with molecular weight cut-offs of 5 kDa, 2 kDa, and 600-800 Da. After that, the permeate from nanofiltration was treated by a fixed bed adsorption/desorption process using a chromatographic column packed with non-polar resin SP700. To desorb the compounds, two eluents were applied, water and ethanol (99% v/v). In the water desorption phase, an enriched fraction in the target phenolic aldehydes, syringaldehyde and vanillin, was obtained, with minor amounts of phenolic acids (vanillic acid and syringic acid), and phenolic ketones (acetovanillone and acetosyringone).

The last step of the sequential process, contemplate the crystallization of vanillin and syringaldehyde using the aqueous solutions, with low concentrations of these potential food and pharmaceutical phenolic compounds, obtained from the processes of ultra and nanofiltration and preparative chromatography. In the case of V, different approaches of cooling and evaporative crystallization were attempted, and the process yield, purity and thermal stability of crystals were evaluated. For Sy, crystallization was performed based on the solubility of the compounds present in the aqueous solution.

The work developed in this thesis opens good perspectives from the point of view of pulp and paper industry, aiming for diversification of products and side-streams valorization.

RESUMO

Nos últimos anos, a crescente preocupação com a diminuição das reservas de combustíveis fósseis e o consequente impacto ambiental tem gerado um crescente interesse no estudo do potencial da biomassa lenhocelulósica como fonte renovável de biocombustíveis e biomateriais. No contexto das biorrefinarias, são produzidas grandes quantidades de lenhina. Este biopolímero, o segundo mais abundante no planeta, há muito que é reconhecido como uma matéria-prima valiosa, no entanto, a maior parte da lenhina produzida é queimada tornando-se uma fonte de combustível, apesar da existência de uma vasta gama de aplicações.

O trabalho desenvolvido nesta tese pretende validar um processo integrado de produção de monómeros fenólicos, nomeadamente a vanilina e o siringaldeído, a partir de lenhina isolada de licores sulfito, de origem folhosa e de origem resinosa, provenientes da industria da pasta e do papel recorrendo a processos com reduzido impacto ambiental.

As lenhinas isoladas a partir dos licores sulfito de origem folhosa e de origem resinosa, provenientes da industria da pasta e do papel, foram caracterizadas. A lenhina foi obtida após ultrafiltração e liofilização dos licores sulfíto e caracterizada com base no conteúdo inorgânico, oxidação com nitrobenzeno, ressonância magnética nuclear de carbono e determinação do seu peso molecular. As características estruturais permitem avaliar o potencial de cada lenhina face à despolimerização oxidativa para produção de monómeros fenólicos de valor acrescentado, como a vanilina e o siringaldeído. Após a caracterização, as lenhinas, de origem folhosa e de origem resinosa, foram submetidas à oxidação alcalina com oxigénio e as condições de reação foram otimizadas para a obtenção de uma mistura final com o máximo rendimento de produtos fenólicos.

Foi também estudada a cinética de degradação dos principais compostos fenólicos obtidos a partir da oxidação da lenhina em meio alcalino utilizando oxigénio como oxidante, nomeadamente, a vanilina, o ácido vanílico, a acetovanilona, o siringaldeído, o ácido siringico e a acetosiringona. O efeito de parâmetros como a temperatura, a concentração inicial e a pressão parcial de oxigénio foram avaliados. Foi selecionado um modelo matemático simples que permitiu a avaliação da degradação dos produtos fenólicos durante a despolimerização oxidativa.

Numa etapa posterior, a mistura obtida a partir da oxidação da lenhina isolada de de origem resinosa proveniente do licor sulfito foi submetida a um processo de filtração utilizando uma sequência de 2 membranas com um peso molecular de corte de 2 kDa e 600-800 Da. A filtração por membranas foi utilizada para concentrar os compostos fenólicos de interesse , nomeadamente a vanilina. O permeado da membrana de nanofiltração (600-800 Da) segue para um processo de adsorção/dessorção em leito fixo usando uma resina apolar (SP700). Esta etapa de cromatografia permite enriquecer a solução aquosa final que contem vanilina, operando em modo cíclico e utilizando água e etanol como eluentes para dessorção do monómero fenólico de interesse.

Os principais produtos de oxidação obtidos na mistura oxidada da lenhina de origem de madeira folhosa foram o siringaldeído, a vanilina, o ácido vanílico, o ácido siringico, a acetosiringona e a acetovanilona. Os aldeídos, siringaldeído e vanilina, possuem estruturas e propriedades semelhantes, o que representa o principal desafio na sua separação. A primeira etapa do processo sequencial, no caso desta lenhina, foi a filtração da mistura oxidada utilizando uma sequência de 3 membranas de ultra e nanofiltração, com pesos moleculares de corte de 5 kDa, 2 kDa e 600-800 Da. Em seguida, o permeado da nanofiltração foi tratado por um processo de adsorção/dessorção em leito fixo utilizando uma coluna cromatográfica empacotada com resina apolar SP700. Para dessorção dos compostos, dois eluentes foram utilizados, água e etanol. Na fase de dessorção com água, obteve-se uma fração enriquecida nos aldeídos fenólicos, o siringaldeído e a vanilina, com menores quantidades de ácidos fenólicos (ácido vanílico e ácido siringico) e cetonas fenólicas (acetovanilona e acetosiringona).

A última etapa do processo sequencial, contempla a cristalização da vanilina e do siringaldeído utilizando soluções aquosas, com baixas concentrações destes potenciais compostos fenólicos para a indústria alimentar e farmacêutica. No caso da vanilina, diferentes abordagens de cristalização por arrefecimento e por evaporação foram estudadas e no final o rendimento do processo, e a pureza e estabilidade térmica dos cristais formados foram avaliados. No caso do siringaldeído, a cristalização foi realizada com base na solubilidade dos compostos presentes na solução aquosa.

O trabalho desenvolvido nesta tese representa uma importante perspetiva do ponto de vista da indústria da pasta e do papel, visando a diversificação de produtos e valorização das correntes processuais.

ABBREVIATIONS

$A^{\cdot}$ - denomination for phenolic compounds (V, VA, Sy, Hy, SA, VO or SO)

[A] – phenolic concentration in g/L

$[A]_I$ - initial concentration of each phenolic

A_m - membrane surface area

AP1 - aqueous phase from the first liquid-liquid extraction

AP2 - aqueous phase from the first liquid-liquid extraction

C_0 – concentration in the t = 0

C_e - equilibrium concentration of solute in the solution

C_{feed} - initial concentration of solute in the solution

C_i - initial concentration,

$C_{i,feed}$ - initial feed concentration

C_{lignin} – concentration of lignin

C_{NaOH} – sodium hydroxide concentration

DC - degree of condensation

DMF – dimethylformamide

DSC - differential scanning calorimetry

E_a - activation energy

G – guaiacyl units

GPC - gel permeation chromatography

H – *p*-hydroxyphenyl units

$HOO^{\cdot}$ - hydroperoxyl radical

HPLC - high-performance liquid chromatography

HSL – hardwood sulfite liquor

Hy - p-hydroxybenzaldehyde

I – ionic strength

J_p – permeate flux in $m^3.s^{-1}.m^{-2}$

J_w - Water permeate flux

k - reaction rate constant

k_0 - pre-exponential factor

K^+ - potassium

LCM - Laboratory of Catalysis and Materials

LHSL - lignin isolated from hardwood sulfite liquor

LLE – liqui-liquid extraction

LSRE - Laboratory of Separation and Reaction Engineering

LSSL – lignin isolated from softwood sulfite liquor

m - reaction order with respect to oxygen concentration in the liquid phase

MMS – multicomponent model solution

Mn - number-average molecular weight

Mw - weight-average molecular weight

MWCO – molecular weight cut-off

n – reaction order with respect to initial phenolic concentration

NF – nanofiltration

NMR - nuclear magnetic resonance

NO – nitrobenzene oxidation

O_2^{liq}- oxygen in the liquid phase

pKa - acid dissociation constant

pO_2 – oxygen partial pressure

P_{total} – total pressure

q_{ads} - adsorption capacity

q_e - adsorption capacity at equilibrium

Qp - permeate flowrate measured in $m^3.s^{-1}$

R – universal gas constant

r_A - reaction rate

RI - refraction index detector

R_m - membrane hydraulic resistance coefficient

S – syringil units

SA – syringic acid

SO – acetosyringone

SO_3^{2-} - sulfites

SPE - solid phase extraction

SSL – softwood sulfite liquor

Sy – syringaldehyde

t – reaction time

T – temperature

T_i – initial temperature

TDS – total dissolved solids

TMP – transmembrane pressure

TS-1 - titanium silicate-1

UF – ultrafiltration

μ_0 - viscosity of water at 25 ºC

V – vanillin

VA – vanillic acid

VCF – volumetric concentration factor

VO – acetovanillone

VR – volume reduction

W – weight of dry resin

$W_{dry\ resin}$ - weight of the dry SP700 resin,

W_{lignin} – weight of lignin

Table of Contents

List of Figures

List of Tables

1 Introduction

Nowadays, the valorization of side-streams from industrial processes becomes ever more important for the sustainable use of natural resources. Sulfite liquor is a waste stream of the sulfite process used for pulp production, thus, its valorization to produce value-added compounds provides a significant advantage. In this context, an integrated process already developed was improved for the sustainable production of phenolic aldehydes, namely vanillin and syringaldehyde, from lignin from sulfite liquors oxidation.

This chapter described the main objectives of this thesis as well as the main tasks for this work with a brief description of the content of each chapter.

1.1 RELEVANCE AND MOTIVATION

Currently, industries worldwide are developing new strategies concerning environmental and economical sustainable processes to provide efficient biomass conversion into bio-based chemicals, platform chemicals, fuels, and energy. A wide variety of raw materials can be processed in biorefineries, although the selection of the raw material must consider some requirements such as quality, quantity, and associated costs. Biomass represents a valuable feedstock, with a continuous growth in the field of biorefinery, and its use can reduce the existing dependence on fossil feedstocks. The processing of lignocellulosic biomass through the recycling of forest and agricultural waste is one of the main objectives of biorefineries. This type of biomass includes cellulose, hemicellulose, and lignin in its composition (Costa 2017).

With the development of biorefineries aiming the production of fuels, added-value chemicals, and materials the amount of lignin-rich residues has increased, demanding new strategies for lignin valorization (Liu *et al.* 2019). Currently 50 - 70 million tons of lignin are produced annually at pulp and paper facilities worldwide (Sethupathy *et al.* 2022). It is reported that only less than 2% is used for producing value added products and chemicals such as dispersants, adhesives, and surfactants (Strassberger *et al.* 2014, Bajwa *et al.* 2019, Khan *et al.* 2021). Most of the lignin produced from paper industry is burned as low value fuel to generate electricity and heat. Figure 1.1. shows a pyramidal model with the different lignin-derived compounds that it is possible to obtain and their potential market value (Sethupathy *et al.* 2022).

The pulp and paper industry produces pulp and paper from wood or recycled fibers. The process of pulping is classified as chemical, mechanical or semi-chemical. Among chemical process, the kraft and sulfite processes are the most used. However, sulfite process generates large amounts of chemical waste and was being replaced for by kraft process (Dessbesell *et al.* 2020). The global sodium lignosulfonate market size was 673.6 million Euro in 2020, accounting for 69% of the market share, and it is projected to reach 776.1 million Euro in 2027, growing at a compound annual growth rate of 1.6 % during 2021-2027 (Fact.MR 2020). Lignosulphonates are widely used as starting materials in the synthesis of vanillin, a flavoring agent for food, ice cream, and bakery goods. However, the conversion of lignin-rich side streams resulting from processing lignocellulosic biomass to value-added products, such as low-molecular-weight phenolic compounds, is the most straightforward and promising route for lignin valorization (Casimiro *et al.* 2019).

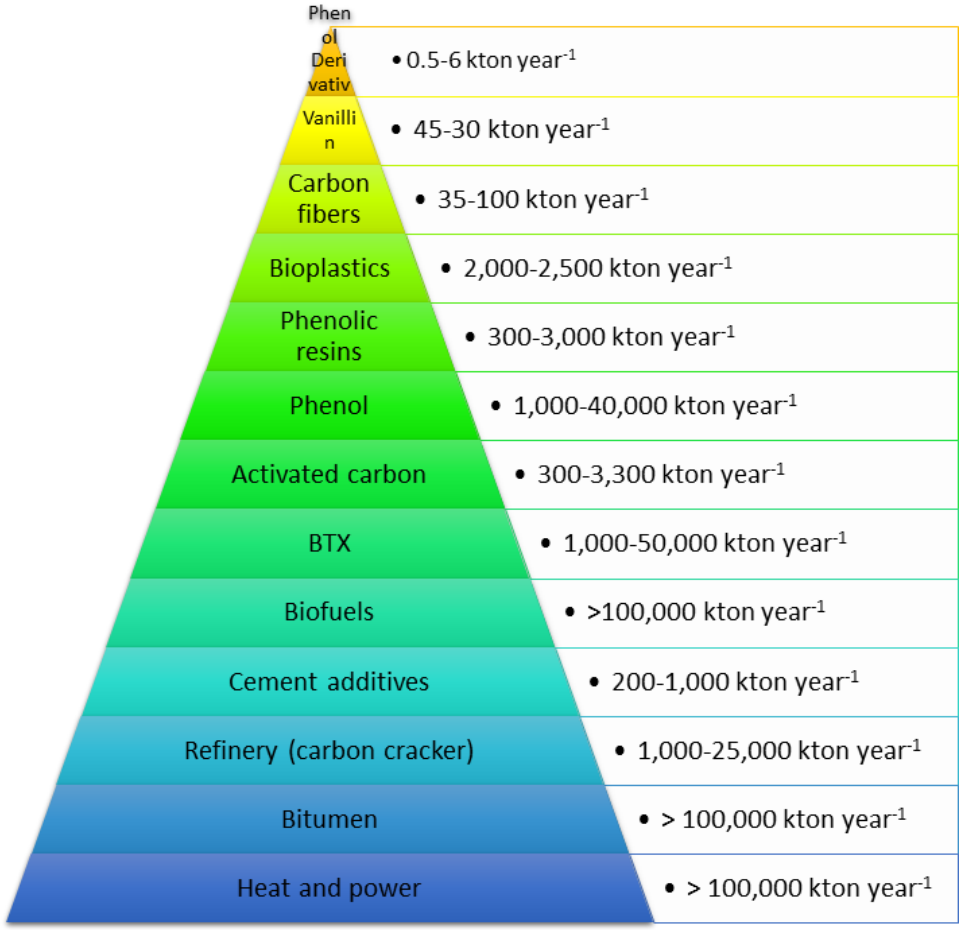

Figure 1.1 – Pyramidal model for lignin valorization (Sethupathy *et al.*, 2022).

Since the 90's that our team in LSRE - LCM (Laboratory of Separation and Reaction Engineering - Laboratory of Catalysis and Materials) develops work on the chemical production of vanillin and syringaldehyde from lignin oxidation (Mathias 1993, Fargues *et al.* 1996 (a), Fargues *et al.* 1996 (b), Zabkova *et al.* 2006, Zabkova *et al.* 2007a, Žabková *et al.* 2007b, Araújo 2008, Araújo *et al.* 2009, Pinto *et al.* 2011, Pinto *et al.* 2012, Pinto *et al.* 2013, Costa *et al.* 2014, Costa 2017, Gomes 2019a). Therefore, an integrated process was developed as the required key piece for the sustainable production of value-added compounds from lignins oxidation, which contributes to decrease the dependence on petroleum derivatives. The present thesis aims to improve the integrated process aiming to produce monomers, namely vanillin and syringaldehyde, from hardwood and softwood lignin from sulfite liquors using processes with reduced environmental impact.

Vanillin global demand is around 20,000 ton per year, mostly supplied by the petrochemical source, with an expected grow by 6.2% from 2017 to 2025. In the same year

(2025), the global vanillin market is expected to reach 724.5 million US dollars (632.9 million Euros) (Oliveira *et al.* 2022). This monomer is widely used as a flavoring and fragrance ingredient in food and cosmetic and a precursor for the synthesis of several second-generation fine chemicals and pharmaceuticals (Munavalli *et al.* 2007, Calvo-Flores and Dobado 2010). Among the major players of vanillin, Solvay SA, Evolva Holding SA, Camlin Fine Sciences, Lesaffre (Ennloys), and Prinova Group LLC, Borregaard is one of the world's leading suppliers of vanillin and the world's only manufacturer of sustainable vanillin from wood. The company has been producing wood-based vanillin in Norway since 1962.

Syringaldehyde is a promising aromatic aldehyde very similar in structure to vanillin with the advantage of already containing two methoxyl groups. This aldehyde is used as flavor and fragrance ingredient in food and cosmetic industries (Rodrigues *et al.* 2018), and has large applicability in the pharmaceutical industry due to its antioxidant, anti-inflammatory, antimicrobial, and antifungal properties (Yancheva *et al.* 2016). Syringaldehyde can be synthesized from gallic acid, pyrogallol, vanillin, or *p*-cresol and its market value is about 22 USD per kilogram (Osorio-González *et al.* 2019). So far, there are few studies in the literature reporting the production of syringaldehyde from hardwood lignin (wood), predominantly this aldehyde is obtained by the synthetic route.

Concerning the valorization of lignin from sulfite liquors, it is necessary to improve a sequence of reaction and separation processes allowing that obtain added-value chemicals, namely vanillin or syringaldehyde. The implementation at an industrial scale depends on the economic sustainability of the process, which, in turn, depends largely on the raw material availability and products yield as well as the separation and purification steps (oxidation reaction, filtration, preparative chromatography, and crystallization processes).

1.2 OBJECTIVES AND OUTLINE

The main objective of this thesis is to assess the potential of hardwood and softwood industrial sulfite liquors to produce vanillin and syringaldehyde. Lignin isolated from sulfite liquors, is submitted to oxidative depolymerization with oxygen in alkaline medium to obtain the maximum yields of the target monomers. Vanillin and syringaldehyde present in the oxidative mixture will be separated and purified through a series of non-toxic physical processes including, ultra and nanofiltration, preparative chromatography, liquid-liquid extraction, and crystallization.

In **Chapter 1**, the main objectives and tasks of this thesis are presented. The relevance and motivation underlying the proposed objectives are briefly exposed.

In **Chapter 2**, the state of the art is presented with a summary of all the themes addressed in this work namely, lignin occurrence and structure, delignification processes, and a brief description of the main stages of the integrated process applied for lignin valorization.

In **Chapter 3**, the structural characterization and oxidative depolymerization of lignins from sulphite liquor (softwood and hardwood lignins) are evaluated. Lignin samples are comprehensively analyzed by selected characterization techniques and methods, evaluating the most important features of their structure. Nitrobenzene oxidation, ^{13}C nuclear magnetic resonance (NMR), gel permeation chromatography (GPC), and inorganics determination allow identifying and quantifying different structural characteristics, functional groups and interunit linkages of lignin structure that would be related with the ability to produce functionalized aldehydes. The lignin depolymerization by oxidation requires alkaline medium and O_2 as oxidant. The oxidation of lignin runs at the optimized conditions to produce an oxidized lignin stream with the highest yield in target phenolic monomers.

Chapter 4 comprises the study of the oxidative degradation kinetics of the main phenolic compounds obtained from lignin oxidation (vanillin, vanillic acid, syringaldehyde, syringic acid, acetovanillone, and acetosyringone). Oxidation reactions are performed in a jacketed reactor, and the effect of temperature, initial concentration of each compound in the model solution, and oxygen partial pressure are evaluated. A simple mathematical model is selected to explain the degradation of these phenolic compounds during oxidation.

Chapter 5 includes the recovery of the phenolic aldehydes from the rich solution obtained by oxidation of lignin from softwood sulfite liquor. Ultra and nanofiltration and adsorption/desorption are the main processes applied to recover our target monomers and described in this chapter. During the filtration process, phenolic compounds are collected in the permeate stream, while compounds with high molecular weight stay in the retentate. The use of different membranes in a sequential mode can significantly reduce the inorganic charge and the lignin content (lignin fractions that were not depolymerized) from the oxidation mixture. Preparative chromatography is used to separate the most representative monomer compounds present in the obtained permeate from nanofiltration of the oxidation mixture. The chromatographic step enriches mixtures containing vanillin by continuous cyclic mode operation using deionized water and ethanol as eluents to desorb the target monomers.

As in the previous chapter, **Chapter 6,** addresses the ultra and nanofiltration processes and the separation of the phenolic monomers of interest by adsorption/desorption but at this time applied to the oxidation mixture of a lignin isolated from a hardwood sulfite liquor. In this chapter, the challenge is the recovery and separation of our target monomers, vanillin and syringaldehyde, from the complex mixture. Due to the similar structure and characteristics, effective and specific separation of these two phenolic compounds is still one of the biggest obstacles to its production from hardwood lignin.

Chapter 7 addresses vanillin and syringaldehyde crystallization using aqueous solutions with low concentrations of these potential phenolic compounds. The crystallization processes are performed using the aqueous solutions enriched with vanillin and syringaldehyde obtained from the steps of filtration and preparative chromatography, described in the previous chapters. In the case of vanillin, different approaches of cooling and evaporative crystallization are attempted using the aqueous solution from lignin isolated from softwood sulfite liquor. For syringaldehyde, the aqueous solution from lignin isolated from hardwood sulfite liquor is used. Crystallization is performed based on the solubility of the compounds present in the solution and taking advantage of the lower solubility of syringaldehyde in water.

The main conclusions and suggestions for future work are presented in **Chapter 8**.

1.3 REFERENCES

Araújo, J. D. P. (2008). Production of vanillin from lignin present in the kraft black liquor of the pulp and paper industry. Ph.D. Dissertation, *Faculty of Engineering University of Porto*.

Araújo, J. D. P., C. A. Grande and A. E. Rodrigues (2009). Structured packed bubble column reactor for continuous production of vanillin from Kraft lignin oxidation. *Catalysis Today* 147: S330-S335.

Bajwa, D. S., G. Pourhashem, A. H. Ullah and S. G. Bajwa (2019). A concise review of current lignin production, applications, products and their environmental impact. *Industrial Crops and Products* 139: 111526.

Calvo-Flores, F. G. and J. A. Dobado (2010). Lignin as renewable raw material. *ChemSusChem* 3(11): 1227-1235.

Casimiro, F. M., C. A. E. Costa, C. M. Botelho, M. F. Barreiro and A. E. Rodrigues (2019). Kinetics of Oxidative Degradation of Lignin-Based Phenolic Compounds in Batch Reactor. *Industrial & Engineering Chemistry Research* 58(36): 16442-16449.

Costa, C. A. E. (2017). Vanillin and syringaldehyde from side streams of pulp and paper industries and biorefineries. PhD, *Faculty of Engineering, University of Porto*.

Costa, C. A. E., P. C. R. Pinto and A. E. Rodrigues (2014). Evaluation of chemical processing impact on E. globulus wood lignin and comparison with bark lignin. *Industrial Crops and Products* 61: 479-491.

Dessbesell, L., M. Paleologou, M. Leitch, R. Pulkki and C. Xu (2020). Global lignin supply overview and kraft lignin potential as an alternative for petroleum-based polymers. *Renewable and Sustainable Energy Reviews* 123: 109768.

Fact.MR. (2020). "Lignin Market." Retrieved November 2021, 2020, from http://www.factmr.com.

Fargues, C., Á. Mathias and A. Rodrigues (1996 (a)). Kinetics of vanillin production from kraft lignin oxidation. *Industrial & Engineering Chemistry Research* 35(1): 28-36.

Fargues, C., A. Mathias, J. Silva and A. Rodrigues (1996 (b)). Kinetics of vanillin oxidation. *Chem. Eng. Technol.* 19: 127- 136.

Gomes, E. D. (2019a). Development of a continuous process for the production of vanillin and syringaldehyde from kraft black liquor. PhD, *Faculty of Engineering, University of Porto*.

Khan, R. J., C. Y. Lau, J. Guan, C. H. Lam, J. Zhao, Y. Ji, H. Wang, J. Xu, D.-J. Lee and S.-Y. Leu (2021). Recent advances of lignin valorization techniques toward sustainable aromatics and potential benchmarks to fossil refinery products. *Bioresource Technology*: 126419.

Liu, Z.-H., R. K. Le, M. Kosa, B. Yang, J. Yuan and A. J. Ragauskas (2019). Identifying and creating pathways to improve biological lignin valorization. *Renewable and Sustainable Energy Reviews* 105: 349-362.

Mathias, A. L. (1993). Produção de Vanilina a partir da Lenhina: Estudo Cinético e do Processo. Ph.D. Thesis, *Faculdade de Engenharia da Universidade do Porto*.

Munavalli, D. S., S. A. Chimatadar and S. T. Nandibewoor (2007). Oxidation of vanillin by a new oxidant diperiodatoargentate(III) in aqueous alkaline medium. *Industrial & Engineering Chemistry Research* 46(5): 1459-1464.

Oliveira, J. P. d. S., R. Garrett, M. G. Bello Koblitz and A. Furtado Macedo (2022). Vanilla flavor: Species from the Atlantic forest as natural alternatives. *Food Chemistry* 375: 131891.

Osorio-González, C. S., K. Hegde, S. K. Brar, A. Kermanshahipour and A. Avalos-Ramírez (2019). Data set of green extraction of valuable chemicals from lignocellulosic biomass using microwave method. *Data in Brief* 26: 104347.

Pinto, P. C. R., C. E. Costa and A. E. Rodrigues (2013). Oxidation of lignin from *eucalyptus globulus* pulping liquors to produce syringaldehyde and vanillin. *Industrial & Engineering Chemistry Research* 52(12): 4421-4428.

Pinto, P. C. R., E. A. B. Silva and A. E. Rodrigues (2012). Lignin as source of fine chemicals: vanillin and syringaldehyde. Biomass Conversion: The Interface of Biotechnology, Chemistry and Materials Science. *C. Baskar, S. Baskar and S. R. Dhillon*. Berlin, Heidelberg, Springer Berlin Heidelberg**:** 381-420.

Pinto, P. C. R., E. A. B. d. Silva and A. E. Rodrigues (2011). Insights into oxidative conversion of lignin to high-added-value phenolic aldehydes. *Industrial & Engineering Chemistry Research* 50(2): 741-748.

Rodrigues, A. E., P. C. d. O. R. Pinto, M. F. Barreiro, C. A. Esteves da Costa, M. I. Ferreira da Mota and I. Fernandes (2018). An integrated approach for added-value products from lignocellulosic biorefineries: Vanillin, syringaldehyde, polyphenols and polyurethane, Springer International Publishing.

Sethupathy, S., G. Murillo Morales, L. Gao, H. Wang, B. Yang, J. Jiang, J. Sun and D. Zhu (2022). Lignin valorization: Status, challenges and opportunities. *Bioresource Technology* 347: 126696.

Strassberger, Z., S. Tanase and G. Rothenberg (2014). The pros and cons of lignin valorisation in an integrated biorefinery. *RSC Advances* 4(48): 25310-25318.

Yancheva, D., E. Velcheva, Z. Glavcheva, B. Stamboliyska and A. Smelcerovic (2016). Insights in the radical scavenging mechanism of syringaldehyde and generation of its anion. *Journal of Molecular Structure* 1108: 552-559.

Zabkova, M., E. A. Borges da Silva and A. E. Rodrigues (2007a). Recovery of vanillin from kraft lignin oxidation by ion-exchange with neutralization. *Separation and Purification Technology* 55(1): 56-68.

Žabková, M., E. A. B. da Silva and A. E. Rodrigues (2007b). Recovery of vanillin from lignin/vanillin mixture by using tubular ceramic ultrafiltration membranes. *Journal of Membrane Science* 301(1): 221-237.

Zabkova, M., M. Otero, M. Minceva, M. Zabka and A. E. Rodrigues (2006). Separation of synthetic vanillin at different pH onto polymeric adsorbent sephabeads SP206. *Chemical Engineering and Processing: Process Intensification* 45(7): 598-607.

2 State of the art

2.1 Lignin: Occurrence and Structure

The production of fuels, added-value chemicals, and materials from lignocellulosic biomass has becoming noticeable in the recent decades, leading to an increase demand on renewable feedstocks instead of fossil resources (Vinoth Kumar *et al.*, 2016). Lignocellulosic biomass is the most promising and abundant renewable resource derived from plants and has a high potential as an alternative to fossil resources. It is used to produce second-generation biofuels, and bio sourced chemicals and materials without compromising global food security (Zoghlami and Paës, 2019). It is mainly composed of cellulose, hemicelluloses, and lignin however, the structure and the quantity of each component on biomass plant cell wall varies according to species, tissues, and maturity (Figure 2.1).

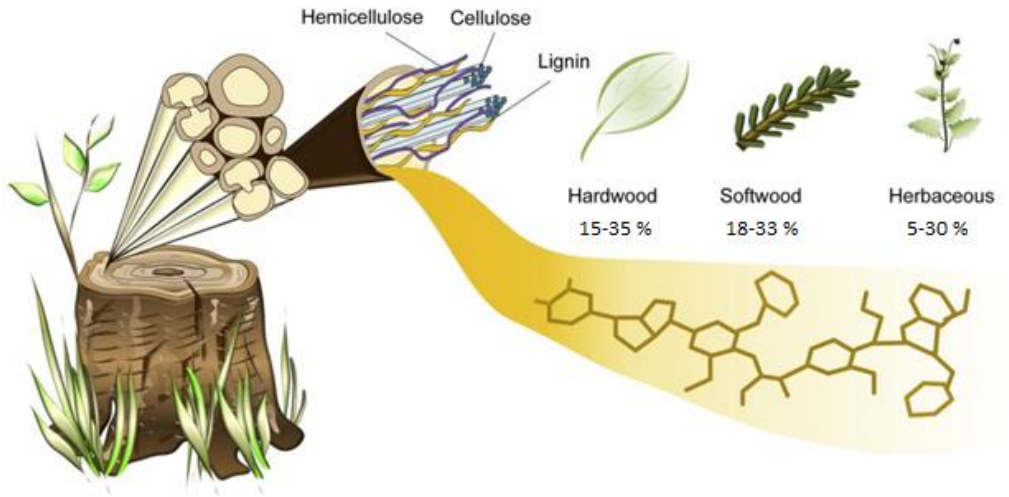

Figure 2.1 - Structure of lignocellulosic biomass in plant cell walls (Becker and Wittmann, 2019).

In general, lignin constitutes about 5–35% of the lignocellulosic materials and is the largest renewable source of aromatics on earth (Rodrigues *et al.*, 2018). The main source groups of lignocellulosic biomass and their chemical composition are shown in Table 2.1.

Table 2.1 - Average organic constituents of some biomass feedstocks (Windeisen and Wegener, 2012, Azadi *et al.*, 2013, Isikgor and Becer, 2015).

Feed	Cellulose (%)	Hemicellulose (%)	Lignin (%)
Softwood	40-50	11-32	18-33
Hardwood	40-55	15-36	15-35
Herbaceous	25-47	12-50	5-30

Current biorefineries are focused mainly on cellulose and hemicellulose valorization, whereas lignin is treated as a waste product. Cellulose and hemicelluloses are polysaccharides, which can be used for many different applications in a variety of areas, such as medicine, energy, chemical industry, in the synthesis of polymeric materials and biosurfactants, as papermaking additives, or in the food industry (Barakat *et al.*, 2013). On the other hand, lignin, which is mostly generated as a side product in the pulp and paper production process, is mainly burned in industrial boilers underestimating its enormous potential (Rinaldi *et al.*, 2016). The limited use of lignin is related to its complexity and structural diversity within the same molecule, which differs from the lignin's origin and the delignification process applied (Fernández-Rodríguez *et al.*, 2019).

Lignin is the second most abundant natural phenolic polymer in the world. It is an amorphous, three-dimensional biopolymer arising from polymerization of three basic units: *p*-hydroxycinnamyl alcohol, coniferyl alcohol, and sinapyl alcohol (Figure 2.2**)**. These monomers differ in the degree of substitution at the phenolic ring and are the precursors of the main moieties present in lignin structure: H (*p*-hydroxyphenyl), G (guaiacyl), and S (syringyl) units. The ratio between G, S and H units in lignin differs among the main groups of plants, namely hardwood, softwood, and annual plants (Casimiro *et al.*, 2019). Softwood lignins are G type, while hardwood and annual plant lignins are S:G:H type. The phenylpropane units of lignin are linked through aryl ether bonds (β-*O*-4, α-*O*-4, 4-*O*-5) and carbon-carbon linkages (5-5', β-5, β-1, β–β), Figure 2.3 (Calvo-Flores and Dobado, 2010, Pinto *et al.*, 2011, Abdelaziz *et al.*, 2022).

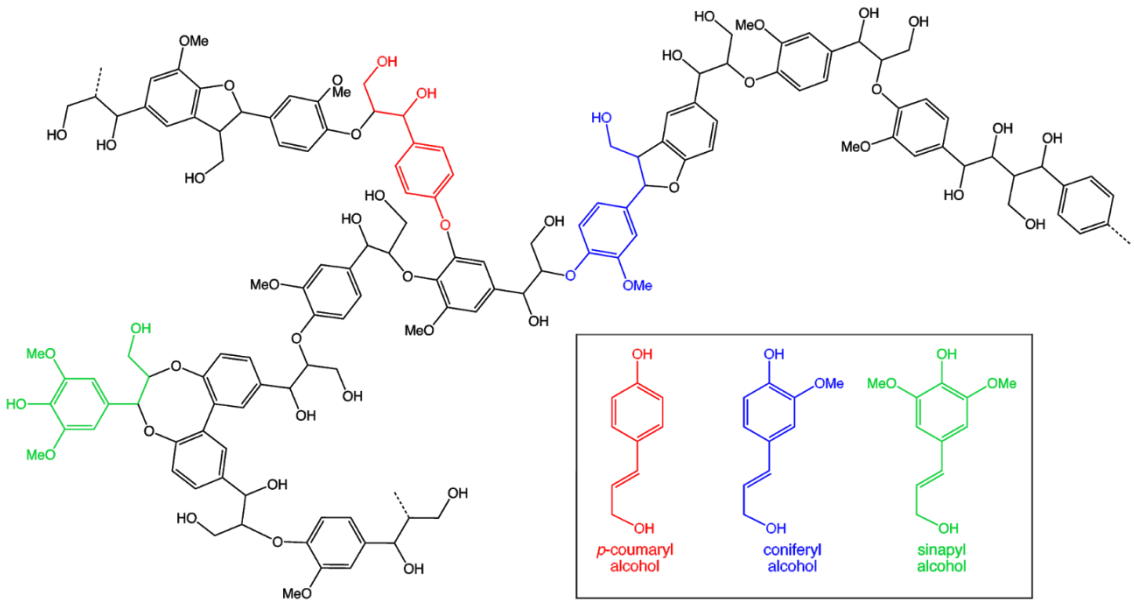

Figure 2.2 – Representative fragment of lignin structure with phenylpropane units highlighted (Serrano *et al.*, 2019).

Ether linkages, particularly β-*O*-4, are, are by far, the most frequent linkages in lignin, followed by carbon-carbon bonds, as 5-5' type (Pinto *et al.*, 2012, Berlin and Balakshin, 2014). Other common lignin interunit linkages include α-*O*-4, phenylcoumaran (β-5), resinol (β–β), 4-*O*-5', and β-1 moieties (Costa, 2017).

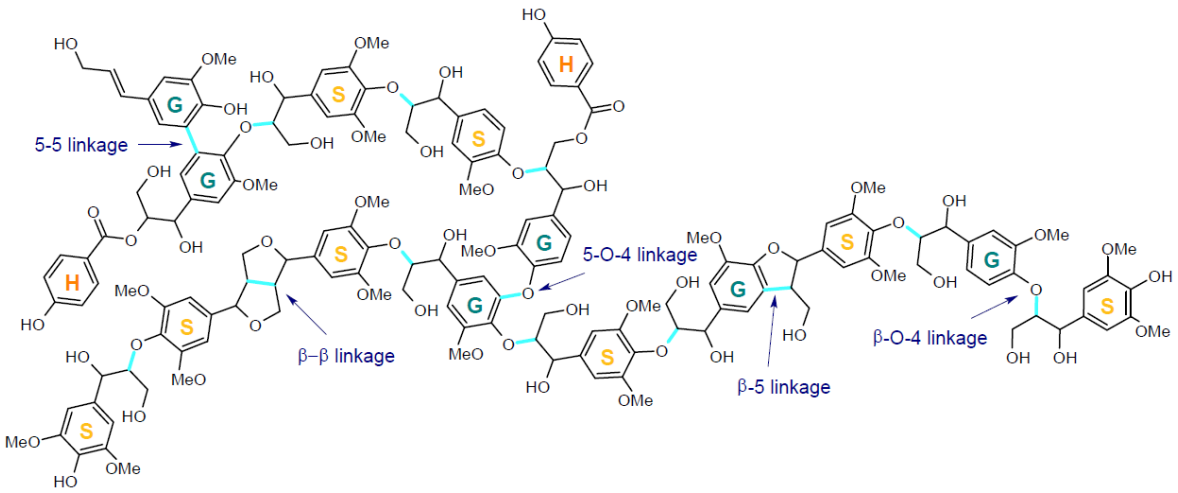

Figure 2.3 - Representative lignin structure (Abdelaziz *et al.*, 2022).

Aryl ether linkages are easier to be cleaved when compared to condensed linkages (C-C, 5-O-4, 5-5') during the lignin depolymerization and conversion, thus the cleavage of the β-*O*-4 is also considered as a critical step of lignin depolymerization for utilizing lignin as

raw materials to produce other chemicals (Chio *et al.*, 2019). The proportion of each type of linkage in lignin structure depends on the relative contribution of a particular monomer to the polymerization process. The frequency of the main linkages in softwood and hardwood lignins are summarized in Table 2.2.

Table 2.2 – Different linkages proportions in lignin molecule (Pinto *et al.*, 2011, Windeisen and Wegener, 2012, Fernández-Rodríguez *et al.*, 2019).

Linkage Type	Softwoods (%)	Hardwoods (%)
Ether Linkage		
β-*O*-4	43-50	50-65
α-*O*-4	6-8	4-8
4-*O*-5	4	6-7
C-C Linkages		
β-5	9-12	4-6
5-5	10-25	4-10
β-1	3-7	5-7
β-β	2-4	3-7
Others	16	7-8

Lignin structure also contains different functional groups, including aliphatic hydroxyl, phenolic hydroxyl, and methoxyl groups. The different functional groups affect the reactivity and chemical properties of lignin, especially the hydroxyl groups. Lignin content, composition, and structure (linkages, and functional groups) depend on the major groups of higher plants, species, morphological parts of the same plant, processing, and isolation conditions, and play an important role in profile and valuable product yields resulting from a conversion route of lignin, aiming its full valorization and conversion (Pu *et al.*, 2008, Costa *et al.*, 2015, Rodrigues *et al.*, 2018).

2.2 PULPING PROCESSES

The pulping process objective is to delignify the wood matrix by chemically degrading and/or sulfonating the lignin into water-soluble fragments (Pinto *et al.*, 2012). The structure of lignin, both in pulp and dissolved lignin, is significantly affected by the origin, the delignification type, and the recovery process from pulping liquors (Rodrigues *et al.*, 2018). Moreover, the isolation of lignin from the lignocellulosic source has a large influence in physical and chemical linkages between lignin and the other components present in plants

(Fernández-Rodríguez *et al.*, 2019). The main industrial processes that are currently used to obtain technical lignins are sulfite, kraft, and organosolv (Figure 2.4).

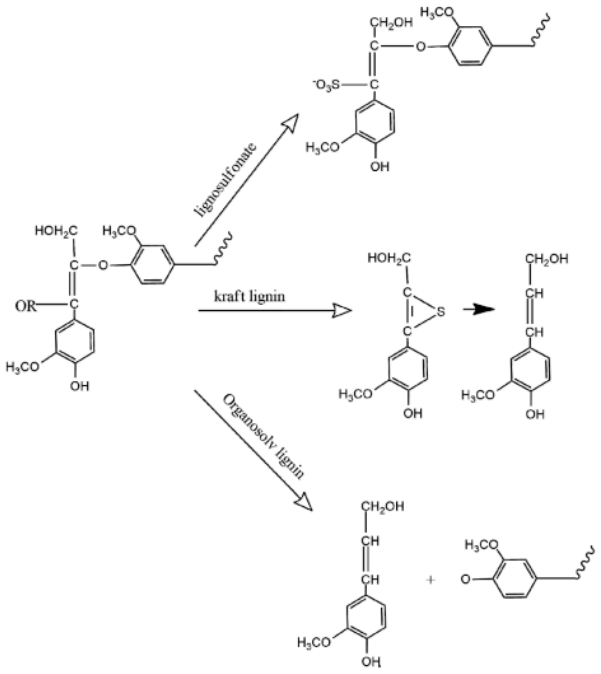

Figure 2.4 – Main lignin extraction processes applied to wood plants (Vásquez-Garay *et al.*, 2021).

The soda process is also used, but it is mainly applied to non-wood plants. Depending on the pulping process, lignins can be chemically modified differently (Windeisen and Wegener, 2012). Several characteristics and properties of different technical lignins are depicted in Table 2.3.

Table 2.3 – Chemical composition of lignin derived from sulfite, kraft, soda and organosolv processes (Vishtal2011,windeisen2012, gosselink2011)(Lebo Jr. *et al.*, 2001, Mansouri and Salvadó, 2006, Gosselink Richard *et al.*, 2010, Windeisen and Wegener, 2012, Tribot *et al.*, 2019).

Parameter	Lignosulfonates	Kraft Lignin	Soda Lignin	Organosolv Lignin
Ash, %	4.0 - 10.0	0.5 - 3.0	0.7 - 2.3	1.7
Nitrogen, %	0.02	0.05	0.2 - 1.0	0 - 0.3
Sulphur, %	3.5 - 8.0	1.0 - 3.0	0	0
Molecular weight (Mw), Da	1k – 5k	1.5k – 5k	1k – 3k	500 – 5k
Polydispersity	4.2 - 7.0	2.5 - 3.5	2.5 - 3.5	1.5
Purity	Low-Medium	High	Medium-High	High

Kraft pulping is the dominant process for production of pulp for paper (Pinto *et al.*, 2012, Rodrigues *et al.*, 2018). Kraft pulping involves the digesting of wood chips at elevated temperature and pressure in ‘‘white liquor’’. During this treatment, the hydroxide and hydrosulfide anions depolymerize the lignin into smaller water/alkali-soluble fragments. One of the major disadvantages of Kraft lignin is a high degree of contaminants, as carbohydrates, present in hemicelluloses as well as in some fatty acids (Cheremisinoff and Rosenfeld, 2010, Alén, 2015, Ahmad and Pant, 2018, Rodrigues *et al.*, 2018). The emission of malodor compounds, and the dark color of pulp are also a negative aspect of kraft lignin.

In the organosolv process low pH, elevated temperature, and a mixture of organic solvents with water are used, obtaining high purity lignin with <1 wt% residual carbohydrate and ash content (Rodrigues *et al.*, 2018). The most used solvents for organosolv delignification include alcohols such as methanol and ethanol, organic acids such as formic and acetic acid, and mixed organic solvent-inorganic alkali chemicals. The higher purity of the isolated lignins is a result of the conditions applied during organosolv process that cause an intensive hydrolysis of lignin-carbohydrate complex (Rodrigues *et al.*, 2018).

Soda pulping process is mainly applied to non-wood plants such as straw, bagasse, kenaf, hemp, and, to some extent, hardwoods (Rodrigues *et al.*, 2018). This process uses sodium hydroxide to dissolve the lignin from lignocellulosic biomass. The resulting lignin from soda process is frequently enriched with carboxylic acids and condensed structures (Lora and Glasser, 2002). Lignin from soda process is free of sulfur, rendering it an attractive raw material for various applications (Abdelaziz *et al.*, 2022). This type of lignin has also low molecular weight and is insoluble in water (Rodrigues *et al.*, 2018).

It is possible to obtain technical lignin via other processes such as hydrolysis or steam explosion of biomass, but these are only at a pilot plant level (Strassberger *et al.*, 2014).

Sulfite pulping was developed and patented by the American chemist Benjamin Chew Tilghman in 1867 (Tilghman, 1867). The first commercial sulfite pulp mill was built in Sewden in 1874. Almost simultaneously with Ekman, A. Mitscherlich in Germany worked on the sulfite cooking process of wood and, in 1880, he started a sulfite pulp mill in Zell, in south Germany. The first sulfite mill in the United States was the Richmond Paper Company in Rumford, Rhode Island in the mid-1880s. Lignosulfonate is the resulting lignin from acid sulfite pulping of wood, which was the dominant process for cellulose production until it was exceeded by the kraft process in the 1940s. Sulfite pulping has been used for a long time in the industry but, nowadays, it has been replaced by the Kraft process, which is capable of

processing different wood species to produce strong fibers for paper manufacturing (Pinto *et al.*, 2012, Rodrigues *et al.*, 2018).

In the sulfite process, sulfites (SO_3^{2-}), or bisulfites (HSO_3^-) are the pulping agents depending on the pH (Rodrigues *et al.*, 2018), sulfur dioxide or sulfuric acid could be also used. The most common counter ion of the sulfite and bisulfite salts is sodium (Na^+) but calcium (Ca^{2+}), potassium (K^+), magnesium (Mg^{2+}), or ammonium (NH_4^+) have been employed as well (Pinto *et al.*, 2012). Typically, in lignosulfonates a high quantity of impurities (around 30% in weight), like ash or carbohydrates can be found (Fernández-Rodríguez *et al.*, 2019). Lignosulfonates present both hydrophobic and hydrophilic properties, they are water-soluble and chemically modified with sulfonate groups, carbohydrates, and small amounts of wood extracts and inorganic compounds (Calvo-Flores and Dobado, 2010). Carbohydrates cannot be removed selectively, consequently further purified lignosulfonates are obtained by removing these types of impurities by fermentation, chemical removal, ultrafiltration, or selective precipitation (Strassberger *et al.*, 2014). However, precipitation may not be an effective process to obtain lignosulfonates since they are water-soluble products. Membrane filtration has been recognized as a commercial process for recovering lignosulfonates from spent sulfite liquors because lignosulfonates have a higher molecular weight than that of other components in the spent liquors, and the difference in molecular weights allows for effective separation (Aro and Fatehi, 2017). The high average molecular weight is another structural characteristic of lignins from sulfite process, even higher than Kraft lignins (Galkin and Samec, 2016). Furthermore, in the sulfite pulping processes, ether bonds are cleaved, methoxyl groups are destroyed, and new carbon-carbon bonds are formed (Li *et al.*, 2015). The diversity of functional groups (phenolic, carboxylic, and sulfur-containing groups) on lignosulfonate lignins offer some properties, and it can be used in many applications such as dispersants, additives, surfactants, and flocculants (Aro and Fatehi, 2017). Besides that, lignins can be used in the food industry as they are easily depolymerized to produce value-added compounds, as vanillin and syringaldehyde (Fernández-Rodríguez *et al.*, 2019).

2.3 INTEGRATED PROCESS

An integrated process has been developed for the production of high value-added products from lignin by our research group in LSRE - LCM since 90's. The employment of the integrated process is recommended for pulp and paper mills where part of the pulping

liquor stream is deviated to lignin extraction/precipitation and subsequent manufacture of high value-added products and not only burned to generate energy. Over the years, our team has been working in this process, and it has suffered several changes, contributing to its improvement. Borges da Silva reported an integrated process to produce vanillin and lignin-based polyurethanes from kraft lignin oxidation (E. A. Borges da Silva *et al.*, 2009), Figure 2.5.

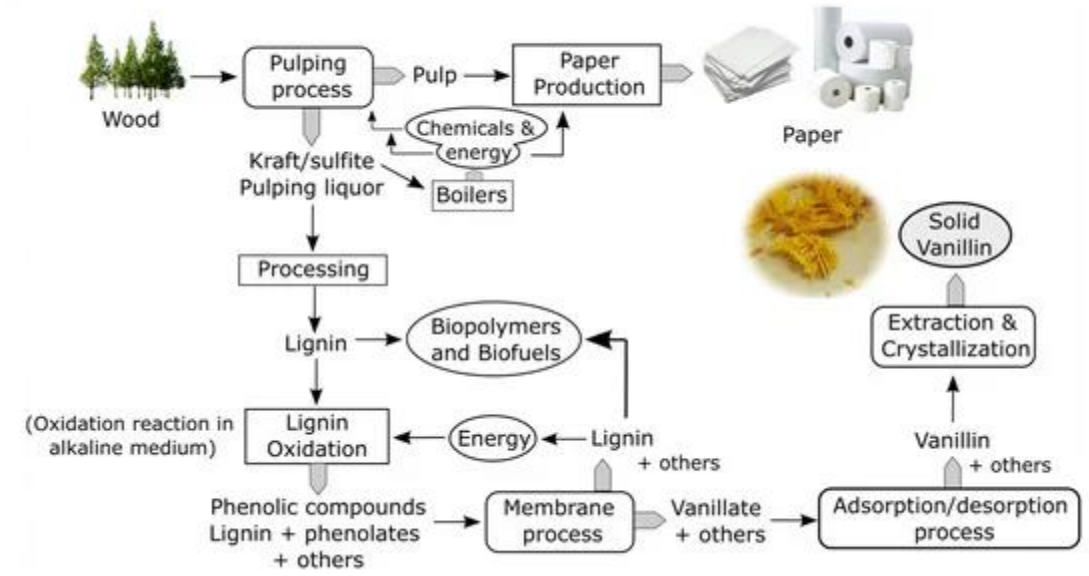

Figure 2.5 – Integrated process for production of value-added products and polymers from kraft lignin in a biorefinery concept (Costa *et al.*, 2021).

The strategy for converting lignin from pulping spent liquors into value-added products combines reaction engineering and efficient separation processes (Zabkova *et al.*, 2007a, Žabková *et al.*, 2007b, Araújo *et al.*, 2009, Gomes *et al.*, 2018, Mota *et al.*, 2018, Gomes and Rodrigues, 2019b, Gomes and Rodrigues, 2020a, Gomes and Rodrigues, 2020b). The whole process involves three main levels. The first level is the alkaline oxidation with O_2. Then, the reactor stream follows to a filtration process where the lignin higher molecular residues are retained, while low molecular weight species go to the permeate stream. Finally, the permeate containing smaller molecules and excess of NaOH flows through a packed bed, in order to convert the phenolates into phenolic compounds. Recent works developed in our team updated the integrated process improving the unit operations, namely oxidation, separation, adsorption, and crystallization, as described in the next sections.

2.3.1 Lignin Depolymerization

Within lignocellulosic biorefineries, lignin conversion to value-added products, such as low molecular weight phenolic compounds, is one of the most straightforward and promising routes to expand lignin applications (Figure 2.6). In literature it is possible to find different methods for lignin depolymerization, including pyrolysis (thermolysis), hydrogenolysis, reductive and biological depolymerization, gasification, hydrolysis, ionic liquid-assisted, supercritical fluids assisted and oxidative depolymerization (Pandey and Kim, 2011, Wang *et al.*, 2013, Sun *et al.*, 2018, Chio *et al.*, 2019, Wong *et al.*, 2020).

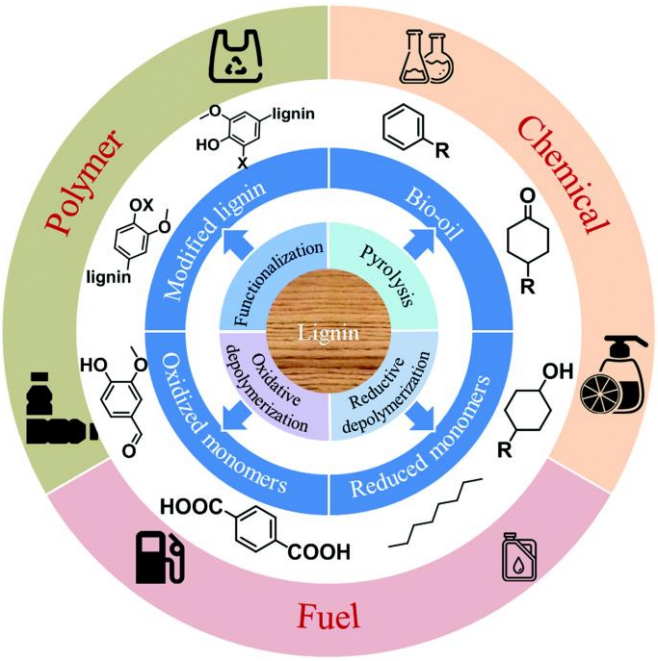

Figure 2.6 - Lignin upstream (inner cycle) and downstream (outer cycle) processes for the production of valuable products (Wong *et al.*, 2020).

Despite all the existing methods, some of them with higher yields of products, the advantage of oxidation is related to the existent market for specific fine chemicals obtained from this process, such as vanillin and syringaldehyde, which is well established, while the market for produced monomers from other depolymerization methods is smaller and/or less defined.

2.3.1.1 Oxidative depolymerization of lignin

Oxidation has been the most studied method for lignin depolymerization (Mathias and Rodrigues, 1995, Araújo, 2008, Pinto *et al.*, 2011, Pinto *et al.*, 2012, Pinto *et al.*, 2013, Ma *et al.*, 2018). The oxidative depolymerization of lignin involves the cleavage of aromatic rings, aryl ether linkages and/or other linkages in the lignin structure. Moreover, this method represents an energy-efficient means of lignin decomposition while generating targeted products in a selective way, including valuable chemicals such as phenolic aldehydes, phenolic acids, and carboxylic acids, depending on the lignin source and the applied reaction conditions (Pandey and Kim, 2011, Pinto *et al.*, 2011, Pinto *et al.*, 2013, Abdelaziz *et al.*, 2019, Rawat *et al.*, 2020).

The production of dicarboxylic acids from lignin oxidation was studied by Vega-Aguilar and co-workers using H_2O_2 as the oxidizer and TS-1 (titanium silicate-1) as the heterogeneous catalyst. The authors achieved yields of up to 11.3 wt % for succinic acid when Indulin AT lignin (Vega-Aguilar *et al.*, 2021) was used, and up to 34 wt% for malic acid when the microwave-assisted reaction was applied, without using a catalyst (Vega-Aguilar *et al.*, 2022). Many oxidizing agents, such as oxygen, ozone, hydrogen peroxide, chlorine dioxide, and peroxy acids, have been used for oxidative depolymerization of lignin (Lyu *et al.*, 2018). However, molecular oxygen is the most attractive oxidant because it is inexpensive, abundant, nontoxic, and environmentally friendly (Azarpira *et al.*, 2014). Catalysts have also been used to increase the yield of phenolic products obtained from lignin oxidation. The most frequent catalysts used in lignin oxidation with O_2 in alkaline medium are transition metal salts such as CuO, $CuSO_4$, $FeCl_3$, and Fe_2O_3. These catalysts have high oxidation potential and allow electron transference from the aromatic rings of lignin; at the same time, this high oxidation potential turns the regeneration of the metal salt in the catalytic cycle more difficult (Pinto *et al.*, 2012). The desired products are low molecular weight compounds such as phenolic aldehydes including vanillin and syringaldehyde, ketones, and acids (Paananen *et al.*, 2020).

Vanillin is a high-value market compound that is widely used as flavoring and fragrance ingredient in food, cosmetic and as a precursor for the synthesis of several second-generation fine chemicals and pharmaceuticals (Munavalli *et al.*, 2007, Calvo-Flores and Dobado, 2010). The world demand of vanillin is approximately over 20 000 t/y, most of which is supplied by the petrochemical source via the catechol synthesis route, and only 15 % comes from lignin (E. A. Borges da Silva *et al.*, 2009, Ponnusamy *et al.*, 2019). It is

expected that vanillin demand grows by 6.2% from 2016 to 2025, and the global vanillin market is expected to reach 724.5 million US dollars (Oliveira *et al.*, 2022). The majority of vanillin sold in the market is chemically synthesized rather than naturally extracted from vanilla beans. This is because natural vanillin is relatively expensive when compared to synthetic vanillin, about 2000-4000 euros/kg for the naturally extracted vanillin and about 15-100 euros/kg for the synthetic one (Khwanjaisakun *et al.*, 2020). Vanillin has the potential to be a key renewable aromatic building-block and can be produced from lignin which has been known as the lignin-based process. For the last 20 years, the Norwegian company Borregaard have been the only one that produce vanillin from lignin, more precisely from lignosulfonates (Fache *et al.*, 2015). The process starts with sulfite pulping of wood, which gives the lignosulfonate-rich sulfite liquor as a by-product. This liquor is further processed as shown in Figure 2.7 (Lora, 2008).

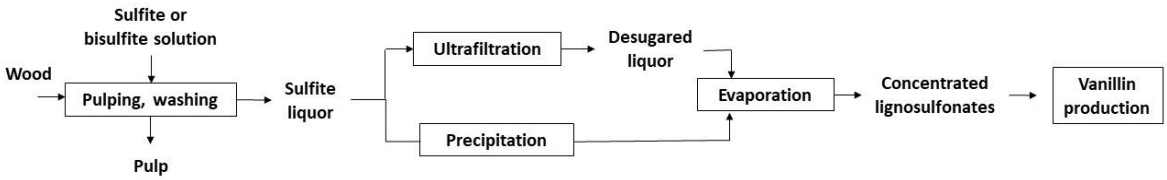

Figure 2.7 – Schematic process to produce vanillin from wood.

This process to produce vanillin comprises ultrafiltration of sulfite liquor to obtain a concentrated fraction rich in lignin and oxidation of this fraction by conventional processes (Evju, 1979). The oxidation of the waste liquor is performed with strongly alkaline conditions and molecular oxygen, and the reaction mixture is kept during the reaction period at a temperature of around 170° C (Gomes, 2019a).

Syringaldehyde is very similar in structure to vanillin, and it has similar applications. Although it is not as well-commercialized as vanillin, syringaldehyde has been gaining prominence, especially after the discovery of its role as an essential intermediate of the antibacterial drugs Trimethoprim, Bactrim, and Biseptol (Manchand, 1978). Syringaldehyde is a naturally occurring unique compound with assorted bioactive characteristics that belongs to the phenolic aldehyde family. This phenolic is important in pharmaceutical applications due to their antioxidant, anti-inflammatory, antimicrobial and antifungal properties (Yancheva *et al.*, 2016). Syringaldehyde has been synthesized from gallic acid, pyrogallol, and V itself (Ibrahim *et al.*, 2012). An excellent natural source of syringaldehyde lies within the cell walls of plants. Recently, the demand for chemicals from renewable sources has

brought new life on the lignin route to produce vanillin (V). Furthermore, there is an increasing interest also for homologous compounds such as syringaldehyde (Sy), for direct applications, or as precursors of fine chemicals and drugs (Erofeev *et al.*, 1990, Lee *et al.*, 2009, Ibrahim *et al.*, 2012).

Products from alkaline lignin oxidation are predominantly aromatic aldehydes, acids and ketones depending on the reaction conditions. In addition to V and Sy and other phenolics like p-hydroxybenzaldehyde (Hy), vanillic acid (VA), syringic acid (SA), acetovanillone (VO) and acetosyringone (SO) are the most important and their occurrence plays a decisive role to determine the reaction efficiency (Wu *et al.*, 1994, Pinto *et al.*, 2012). The phenolic acid VA, an oxidized form of V, is most often used as preservative in argan oil and as acidity regulator in wine and vinegar. VO, also known as apocynin, is structurally related to vanillin, and has been studied due to their important pharmacological properties (T Hart *et al.*, 1990, Stefanska *et al.*, 2012, Stefanska *et al.*, 2012). SA is extensively used as therapeutic agent, antioxidant, antimicrobial, anti-inflammatory and anticancer (Karthik *et al.*, 2014, Srinivasulu *et al.*, 2018), while SO is a chemical compound related to acetophenone and is used as a plant hormone and insect attractor (Baker *et al.*, 2005). A summary of some of the representative studies, for non-catalytic and catalytic oxidation in alkaline medium with O_2, concerning raw material, reaction conditions, and the yields of V and Sy are presented in Figure 2.8**.** The reported yields ranged from 1.2 to 12.5 % w/w_{lignin} in the case of V and 2.5 to 20.0 % w/w_{lignin} for Sy.

Valorization of lignin by oxidative depolymerization in an alkaline medium with oxygen was the main method studied in literature and by our research group, LSRE-LCM (Mathias, 1993, Fargues *et al.*, 1996 (a), Araújo, 2008, Pinto *et al.*, 2013). Vanillin production from the oxidation of lignin obtained from side streams of pulp and paper industries and biorefineries is widely studied and reported in literature (Sandborn *et al.*, 1936, Tomlinson and Hibbert, 1936, Mathias, 1993, Hocking, 1997, Araújo, 2008, E. A. Borges da Silva *et al.*, 2009, Pinto *et al.*, 2013, Aarabi *et al.*, 2017, Gomes, 2019a). Sandborn and co-workers patented a process to produce V by a hydrolysis process but pointed out the need to use oxidation in order to achieve higher production yields (Sandborn *et al.*, 1936).

Mathias and Rodrigues reported the production of V by oxidation of kraft lignin with oxygen, as well as the effect of the operating process parameters (total pressure, temperature, oxygen partial pressure, lignin concentration and sodium hydroxide concentration) on the kinetics of lignin oxidation reaction (Mathias *et al.*, 1995). Since then, the conditions of the lignin in the oxidation stage were improved to increase phenolic monomers yields. Araujo

(Araújo, 2008), reported that oxygen mass transfer was the limiting step to vanillin formation, using the structured packed bubble column reactor. Therefore, Gomes (Gomes, 2019a) made some improvements at this point and made some modifications in the reaction conditions. And concluded that, increasing the gas volumetric flow rate (which increased the turbulence inside the reactor) and utilization of a pure feed of oxygen (increasing the driving force for the dissolution of oxygen) the concentration of vanillin increases (Gomes, 2019a).

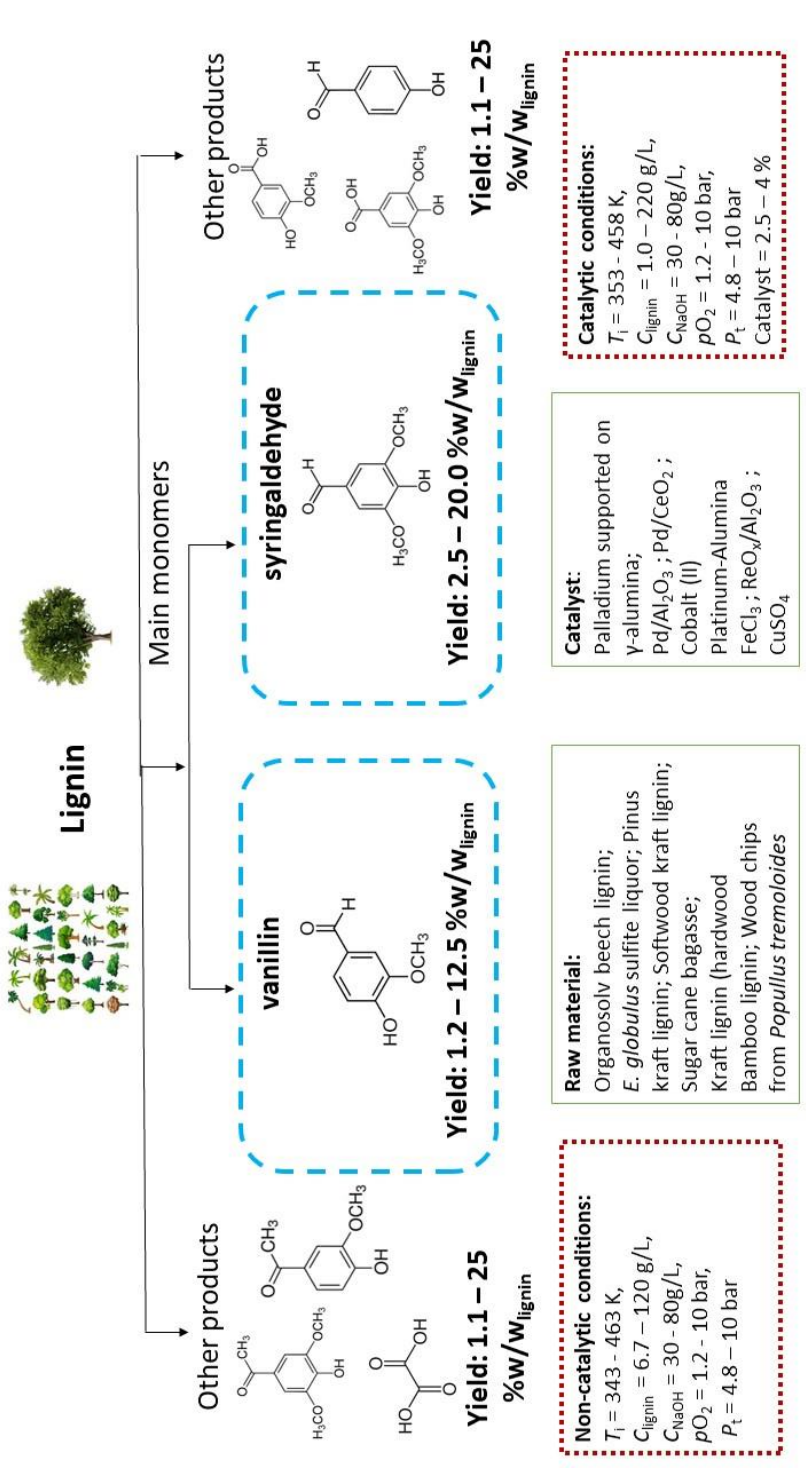

Figure 2.8 – Summary of some of the representative studies, for non-catalytic and catalytic oxidation in alkaline medium with O_2, concerning raw material, reaction conditions, and the yields of V and Sy (Mathias, 1993, Mathias and Rodrigues, 1995, Tarabanko *et al.*, 1995, Wu and Heitz, 1995, Fargues *et al.*, 1996 (a), Villar *et al.*, 2001, Sales *et al.*, 2004, Sales *et al.*, 2007, Araújo *et al.*, 2010, Deng *et al.*, 2010, Voitl and Rohr, 2010, Pinto *et al.*, 2011, Santos *et al.*, 2011, Pacek *et al.*, 2013, Alunga *et al.*, 2015, Deng *et al.*, 2015, Luo *et al.*, 2016, Aarabi *et al.*, 2017, Lyu *et al.*, 2018, Abdelaziz *et al.*, 2019, Gomes, 2019a, Rawat *et al.*, 2020, Kumar *et al.*, 2022).

2.3.2 Membrane Separation Process

The membrane separation process is the first step of the separation and purification process of high added value phenolic compounds present in oxidized solution resulting from the oxidative depolymerization of lignin in alkaline medium with O_2. Depending on the lignin-based raw materials, it is expected that oxidized lignin solutions contain lignin oligomers, dimers, simple phenolic compounds (e.g., aldehydes, ketones, and acids), and other secondary products such as lactones, guaiacol, and syringol (Rodrigues *et al.*, 2018). The main processes studied to separate and purify oxidized lignin streams are related with pressure driven processes encompassing ultrafiltration (UF) (Žabková *et al.*, 2007b) and nanofiltration (NF) (Werhan *et al.*, 2012). Pervaporation and membrane contactors have been suggested as well (Mota *et al.*, 2016) for vanillin recovery from fermented broths.

The use of membrane filtration system to separate low molecular weight phenolic compounds, promotes the reduction of the organic load of the mixture coming from the lignin oxidation (Werhan *et al.*, 2012). The oligomers and other higher molecular weight fractions will be retained by the membrane, while the low molecular weight compounds will cross the membrane pores into the permeate stream.

Mota and co-workers (Mota *et al.*, 2018) reported a membrane fractionation study of an oxidized industrial kraft liquor to improve the effectiveness of the purification step, and Žabková *et al.* (2007b) use an UF process as an efficient way for the recovery of vanillin from Kraft lignin oxidation product. The complexity of the oxidized lignin mixture can be reduced using the membrane separation process, where the high-molecular-weight fractions of degraded lignin are separated from the lower molecular-weight species. The membrane selection depends on its characteristics, with the commitment to have a balance between a high selectivity and a high recovery (Caus *et al.*, 2009). UF and NF sequence (Gomes and Rodrigues, 2020a) and NF cascades (Caus *et al.*, 2009) have already been studied and demonstrated to be successful in the separation of fractions with different molecular weights, overcoming some existing limitations, such as low fluxes, fouling, and rejections. However, membrane separation by itself is not enough for effective separation of fractions rich in the desired aromatic compounds, and it needs to be combined with other techniques (Abdelaziz *et al.*, 2022).

2.3.3 Preparative Chromatography

The second step for the separation and purification sequence is the use of preparative chromatography process. In several studies reported in the literature, adsorbents as Sephabeads SP206, macroporous adsorption resins with crosslinked-polystyrene framework, and Sepabeads SP700 resin were used to recover V and Sy from synthetic solutions (Zabkova *et al.*, 2006, Zhang *et al.*, 2008, Samah *et al.*, 2013, Mota *et al.*, 2016). These studies lack explaining the competitiveness among V or Sy and the other compounds present in the permeate resulting from the filtration, many of which have very similar physical and chemical properties. However, the number of studies with real oxidized lignin mixtures has been increasing (Wang *et al.*, 2010, Mota, 2017, Gomes *et al.*, 2018). Wang and co-workers reported an approach for separating V and Sy from oxygen delignification spent liquor using non-polar macroporous resin D101. The separated mixture contained 37.5% of vanillin and 31.9 % of syringaldehyde with recoveries of 96.2 and 94.7%, respectively (Wang *et al.*, 2010). Hence, several works have been developed by our group in LSRE-LCM in this field, with the main focus in high added value phenolic monomers recovery, namely vanillin and syringaldehyde from real oxidized mixtures. The separation of the different species by adsorption, where the permeate resulting from the filtration (butanol organosolv lignin, tobacco stalks) is fractionated in families of chemicals namely phenolic acids, aldehydes, and ketones, is successfully achieved. However, this mixture is purified by the membrane process before the adsorption stage (Gomes *et al.*, 2018). A similar study was reported by Mota *et al.* (2020), where the permeate resulting from the filtration was fractionated by a chromatographic process using a polymeric resin SP700 prior to a pH value correction to 7.5-8, and concentrations of 1.98 and 1.92 g/L of V and Sy were found in the eluates. High recoveries of the monomers were achieved by Gomes and Rodrigues with Indulin AT (MeadWestvaco Co.), with values of 94.1%, 96.2%, and 52.7% were found for VA, V, and VO, respectively (Gomes and Rodrigues, 2019b). In that work it was applied a non-polar resin SP700 as adsorbent, and it was implemented a cyclic mode operation without regeneration of the resin, the eluents used in desorption phase were water deionized and ethanol (feed pH of 13.7). A similar work was reported by the same author, by using only water deionized as an eluent in desorption phase. The chromatographic step enriches solutions containing V by alternating the feed phase with desorption with deionized water only. In 22 cycles, 71% of the V fed is recovered with at an average 1.5 g/cycle (Gomes and Rodrigues, 2020a).

Methods to the separation of the monomers obtained after depolymerization as non-polar resins (Gomes *et al.*, 2018), ion exchange resins (Schmitt *et al.*, 2017), chemical derivatizations with ammonia (Tarabanko *et al.*, 2013), and sulfur dioxide (carbonyl-bisulfite adduct formation) (Sandborn *et al.*, 1936) were successfully applied in different works. However, the use of ion exchange resins to separate phenolic acids, ketones and aldehydes, proved to be inefficient (Forss *et al.*, 1986, Zabkova *et al.*, 2007a). Recently, a promising process to separate V and Sy from standard solutions was proposed in literature: the simulated moving-bed chromatography (Yao *et al.*, 2018).

2.3.4 Crystallization

The purification step represents a significant challenge due to the presence, in the lignin oxidized mixture, of phenolic side-products with similar chemical and physical properties, as V and Sy. Crystallization is a significant process in chemical engineering industries, especially in pharmaceutical ones, where purity is extremely important. Through this process some properties of the crystallized product could be controlled (Wang *et al.*, 2017).

Crystallization usually requires several steps in order to achieve a high-purity final product. In the integrated process, it should be applied after the step of separation and purification, when the compounds of interest, V and/or Sy, are present at low volumes and low concentrations (Abdelaziz *et al.*, 2022).

So far, the integrated process developed in our group has been applied only to a highly purified, unsulfonated raw softwood kraft lignin, so it would be an advantage to extend this study to other types of lignins, as softwood and hardwood lignins isolated from sulfite liquors.

2.4 REFERENCES

Aarabi, A., M. Mizani and M. Honarvar (2017). The use of sugar beet pulp lignin for the production of vanillin. *International Journal of Biological Macromolecules* 94: 345-354.

Abdelaziz, O. Y., I. Clemmensen, S. Meier, C. A. E. Costa, A. E. Rodrigues, C. P. Hulteberg and A. Riisager (2022). On the oxidative valorization of lignin to high-value chemicals: A critical review of opportunities and challenges. *ChemSusChem* e202201232.

Abdelaziz, O. Y., K. Ravi, F. Mittermeier, S. Meier, A. Riisager, G. Lidén and C. P. Hulteberg (2019). Oxidative Depolymerization of Kraft Lignin for Microbial Conversion. *ACS Sustainable Chemistry & Engineering* 7(13): 11640-11652.

Ahmad, E. and K. K. Pant (2018). Chapter 14 - Lignin Conversion: A Key to the Concept of Lignocellulosic Biomass-Based Integrated Biorefinery. Waste Biorefinery. *T. Bhaskar, A. Pandey, S. V. Mohan, D.-J. Lee and S. K. Khanal*, Elsevier**:** 409-444.

Alén, R. (2015). Chapter 3A - Pulp Mills and Wood-Based Biorefineries. Industrial Biorefineries & White Biotechnology. *A. Pandey, R. Höfer, M. Taherzadeh, K. M. Nampoothiri and C. Larroche*. Amsterdam, Elsevier**:** 91-126.

Alunga, K. R., Y.-Y. Ye, S.-R. Li, D. Wang and Y.-Q. Liu (2015). Catalytic oxidation of lignin-acetoderivatives: a potential new recovery route for value-added aromatic aldehydes from acetoderivatives. *Catalysis Science & Technology* 5(7): 3746-3753.

Araújo, J. D. P. (2008). Production of vanillin from lignin present in the kraft black liquor of the pulp and paper industry. Ph.D. Dissertation, *Faculty of Engineering University of Porto*.

Araújo, J. D. P., C. A. Grande and A. E. Rodrigues (2009). Structured packed bubble column reactor for continuous production of vanillin from Kraft lignin oxidation. *Catalysis Today* 147: S330-S335.

Araújo, J. D. P., C. A. Grande and A. E. Rodrigues (2010). Vanillin production from lignin oxidation in a batch reactor. *Chemical Engineering Research and Design* 88(8): 1024-1032.

Aro, T. and P. Fatehi (2017). Production and Application of Lignosulfonates and Sulfonated Lignin. *ChemSusChem* 10(9): 1861-1877.

Azadi, P., O. R. Inderwildi, R. Farnood and D. A. King (2013). Liquid fuels, hydrogen and chemicals from lignin: A critical review. *Renewable and Sustainable Energy Reviews* 21: 506-523.

Azarpira, A., J. Ralph and F. Lu (2014). Catalytic Alkaline Oxidation of Lignin and its Model Compounds: a Pathway to Aromatic Biochemicals. *BioEnergy Research* 7(1): 78-86.

Baker, C. J., N. M. Mock, B. D. Whitaker, D. P. Roberts, C. P. Rice, K. L. Deahl and A. A. Aver'yanov (2005). Involvement of acetosyringone in plant–pathogen recognition. *Biochemical and Biophysical Research Communications* 328(1): 130-136.

Barakat, A., H. de Vries and X. Rouau (2013). Dry fractionation process as an important step in current and future lignocellulose biorefineries: A review. *Bioresource Technology* 134: 362-373.

Becker, J. and C. Wittmann (2019). A field of dreams: Lignin valorization into chemicals, materials, fuels, and health-care products. *Biotechnology Advances* 37(6): 107360.

Berlin, A. and M. Balakshin (2014). Chapter 18 - Industrial Lignins: Analysis, Properties, and Applications. Bioenergy Research: Advances and Applications. *V. K. Gupta, M. G. Tuohy, C. P. Kubicek, J. Saddler and F. Xu*. Amsterdam, Elsevier**:** 315-336.

Calvo-Flores, F. G. and J. A. Dobado (2010). Lignin as renewable raw material. *ChemSusChem* 3(11): 1227-1235.

Casimiro, F. M., C. A. E. Costa, C. M. Botelho, M. F. Barreiro and A. E. Rodrigues (2019). Kinetics of Oxidative Degradation of Lignin-Based Phenolic Compounds in Batch Reactor. *Industrial & Engineering Chemistry Research* 58(36): 16442-16449.

Caus, A., L. Braeken, K. Boussu and B. Van der Bruggen (2009). The use of integrated countercurrent nanofiltration cascades for advanced separations. *Journal of Chemical Technology & Biotechnology* 84(3): 391-398.

Cheremisinoff, N. P. and P. E. Rosenfeld (2010). Chapter 6 - Sources of air emissions from pulp and paper mills. Handbook of Pollution Prevention and Cleaner Production. *N. P. Cheremisinoff and P. E. Rosenfeld*. Oxford, William Andrew Publishing**:** 179-259.

Chio, C., M. Sain and W. Qin (2019). Lignin utilization: A review of lignin depolymerization from various aspects. *Renewable and Sustainable Energy Reviews* 107: 232-249.

Costa, C. A. E. (2017). Vanillin and syringaldehyde from side streams of pulp and paper industries and biorefineries. PhD, *Faculty of Engineering, University of Porto*.

Costa, C. A. E., P. C. R. Pinto and A. E. Rodrigues (2015). Radar Tool for Lignin Classification on the Perspective of Its Valorization. *Industrial & Engineering Chemistry Research* 54(31): 7580-7590.

Costa, C. A. E., C. A. Vega-Aguilar and A. E. Rodrigues (2021). Added-Value Chemicals from Lignin Oxidation. *Molecules* 26(15): 4602.

Deng, H., L. Lin and S. Liu (2010). Catalysis of Cu-Doped Co-Based Perovskite-Type Oxide in Wet Oxidation of Lignin To Produce Aromatic Aldehydes. *Energy & Fuels* 24(9): 4797-4802.

Deng, W., H. Zhang, X. Wu, R. Li, Q. Zhang and Y. Wang (2015). Oxidative conversion of lignin and lignin model compounds catalyzed by CeO2-supported Pd nanoparticles. *Green Chemistry* 17(11): 5009-5018.

E. A. Borges da Silva, M. Zabkova, J. D. Araújo, C. A. Cateto, F. Barreiro, M. N. Belgacem and A. E. Rodrigues (2009). Valorisation of Kraft Lignin by producing vanillin and ligninbased

polyurethanes: Use of the biorefinery concept. Nordic Wood Biorefinery Conference. Helsinki, Finland: 8.

Erofeev, Y. V., V. L. Afanas'eva and R. G. Glushkov (1990). Synthetic routes to 3,4,5-trimethoxybenzaldehyde (review). *Pharmaceutical Chemistry Journal* 24(7): 501-510.

Evju, H., (1979), Process for preparation of 3-methoxy-4-hydroxybenzaldehyde. US4151207A, Borregaard Industries Ltd, 1979-04-24

Fache, M., B. Boutevin and S. Caillol (2015). Vanillin, a key-intermediate of biobased polymers. *European Polymer Journal* 68: 488-502.

Fargues, C., Á. Mathias and A. Rodrigues (1996 (a)). Kinetics of vanillin production from kraft lignin oxidation. *Industrial & Engineering Chemistry Research* 35(1): 28-36.

Fernández-Rodríguez, J., X. Erdocia, F. Hernández-Ramos, M. G. Alriols and J. Labidi (2019). Chapter 7 - Lignin Separation and Fractionation by Ultrafiltration. Separation of Functional Molecules in Food by Membrane Technology. *C. M. Galanakis*, Academic Press**:** 229-265.

Forss, K. G., E. T. Talka and K. E. Fremer (1986). Isolation of vanillin from alkaline oxidized spent sulfite liquor. *Industrial & Engineering Chemistry Product Research and Development* 25(1): 103-108.

Galkin, M. V. and J. S. M. Samec (2016). Lignin Valorization through Catalytic Lignocellulose Fractionation: A Fundamental Platform for the Future Biorefinery. *ChemSusChem* 9(13): 1544-1558.

Gomes, E. D. (2019a). Development of a continuous process for the production of vanillin and syringaldehyde from kraft black liquor. PhD, *Faculty of Engineering, University of Porto*.

Gomes, E. D., M. I. Mota and A. E. Rodrigues (2018). Fractionation of acids, ketones and aldehydes from alkaline lignin oxidation solution with SP700 resin. *Separation and Purification Technology* 194: 256-264.

Gomes, E. D. and A. E. Rodrigues (2019b). Lignin biorefinery: Separation of vanillin, vanillic acid and acetovanillone by adsorption. *Separation and Purification Technology* 216: 92-101.

Gomes, E. D. and A. E. Rodrigues (2020a). Recovery of vanillin from kraft lignin depolymerization with water as desorption eluent. *Separation and Purification Technology* 239: 116551.

Gomes, E. D. and A. E. Rodrigues (2020b). Crystallization of vanillin from kraft lignin oxidation. *Separation and Purification Technology* 247: 116977.

Gosselink Richard, J. A., E. G. van Dam Jan, E. de Jong, L. Scott Elinor, P. M. Sanders Johan, J. Li and G. Gellerstedt (2010). Fractionation, analysis, and PCA modeling of properties of four technical lignins for prediction of their application potential in binders. Holzforschung. 64: 193.

Hocking, M. B. (1997). Vanillin: Synthetic Flavoring from Spent Sulfite Liquor. *Journal of Chemical Education* 74(9): 1055.

Ibrahim, M., R. B. Sriprasanthi, S. Shamsudeen, F. Adam and S. Bhawani (2012). A concise review of the natural existence, synthesis, properties, and applications of syringaldehyde.

Isikgor, F. H. and C. R. Becer (2015). Lignocellulosic biomass: a sustainable platform for the production of bio-based chemicals and polymers. *Polymer Chemistry* 6(25): 4497-4559.

Karthik, G., M. Angappan, A. VijayaKumar and S. Natarajapillai (2014). Syringic acid exerts antiangiogenic activity by downregulation of VEGF in zebrafish embryos. *Biomedicine & Preventive Nutrition* 4(2): 203-208.

Khwanjaisakun, N., S. Amornraksa, L. Simasatitkul, P. Charoensuppanimit and S. Assabumrungrat (2020). Techno-economic analysis of vanillin production from Kraft lignin: Feasibility study of lignin valorization. *Bioresource Technology* 299: 122559.

Kumar, A., B. Biswas, R. Kaur, S. Rawat, B. B. Krishna, P. Kumbhar, S. Pal, S. Padmanabhan and T. Bhaskar (2022). Oxidative catalytic valorization of industrial lignin into phenolics: Effect of reaction parameters and metal oxides. *Bioresource Technology* 352: 127032.

Lebo Jr., S. E., J. D. Gargulak and T. J. McNally (2001). Lignin. Kirk-Othmer Encyclopedia of Chemical Technology.

Lee, C. Y., A. Sharma, J. E. Cheong and J. L. Nelson (2009). Synthesis and antioxidant properties of dendritic polyphenols. *Bioorganic & Medicinal Chemistry Letters* 19(22): 6326-6330.

Li, C., X. Zhao, A. Wang, G. W. Huber and T. Zhang (2015). Catalytic Transformation of Lignin for the Production of Chemicals and Fuels. *Chemical Reviews* 115(21): 11559-11624.

Lora, J. (2008). Chapter 10 - Industrial Commercial Lignins: Sources, Properties and Applications. Monomers, Polymers and Composites from Renewable Resources. *M. N. Belgacem and A. Gandini*. Amsterdam, Elsevier**:** 225-241.

Lora, J. H. and W. G. Glasser (2002). Recent Industrial Applications of Lignin: A Sustainable Alternative to Nonrenewable Materials. *Journal of Polymers and the Environment* 10(1): 39-48.

Luo, J., P. Melissa, W. Zhao, Z. Wang and Y. Zhu (2016). Selective Lignin Oxidation towards Vanillin in Phenol Media. *ChemistrySelect* 1(15): 4596-4601.

Lyu, G., C. G. Yoo and X. Pan (2018). Alkaline oxidative cracking for effective depolymerization of biorefining lignin to mono-aromatic compounds and organic acids with molecular oxygen. *Biomass and Bioenergy* 108: 7-14.

Ma, R., M. Guo and X. Zhang (2018). Recent advances in oxidative valorization of lignin. *Catalysis Today* 302: 50-60.

Manchand, P., (1978), Process for preparing 2,4-diamino-5-(substituted benzyl)-pyrimidines. US 4115650A,

Mansouri, N.-E. E. and J. Salvadó (2006). Structural characterization of technical lignins for the production of adhesives: Application to lignosulfonate, kraft, soda-anthraquinone, organosolv and ethanol process lignins. *Industrial Crops and Products* 24(1): 8-16.

Mathias, A. L. (1993). Produção de Vanilina a partir da Lenhina: Estudo Cinético e do Processo. Ph.D. Thesis, *Faculdade de Engenharia da Universidade do Porto*.

Mathias, A. L., M. I. Lopretti and A. E. Rodrigues (1995). Chemical and biological oxidation of Pinus pinaster lignin of the production of vanillin. *Journal of Chemical Technology & Biotechnology* 64(3): 225-234.

Mathias, A. L. and A. E. Rodrigues (1995). Production of Vanillin by Oxidation of Pine Kraft Lignins with Oxygen. Holzforschung - International Journal of the Biology, Chemistry, Physics and Technology of Wood. 49: 273.

Mota, I. F., P. R. Pinto, J. M. Loureiro and A. E. Rodrigues (2020). Purification of syringaldehyde and vanillin from an oxidized industrial kraft liquor by chromatographic processes. *Separation and Purification Technology* 234: 116083.

Mota, I. F., P. R. Pinto, A. M. Ribeiro, J. M. Loureiro and A. E. Rodrigues (2018). Downstream processing of an oxidized industrial kraft liquor by membrane fractionation for vanillin and syringaldehyde recovery. *Separation and Purification Technology* 197: 360-371.

Mota, M. I. F., P. C. R. Pinto, J. M. Loureiro and A. E. Rodrigues (2016). Adsorption of vanillin and syringaldehyde onto a macroporous polymeric resin. *Chemical Engineering Journal* 288: 869-879.

Mota, M. I. F., P. C. Rodrigues Pinto, J. M. Loureiro and A. E. Rodrigues (2016). Recovery of Vanillin and Syringaldehyde from Lignin Oxidation: A Review of Separation and Purification Processes. *Separation & Purification Reviews* 45(3): 227-259.

Mota, M. I. F. d. (2017). Fractionation and purification of syringaldehyde and vanillin from oxidation of lignin. PhD *Faculty of Engineering, University of Porto*.

Munavalli, D. S., S. A. Chimatadar and S. T. Nandibewoor (2007). Oxidation of vanillin by a new oxidant diperiodatoargentate(III) in aqueous alkaline medium. *Industrial & Engineering Chemistry Research* 46(5): 1459-1464.

Oliveira, J. P. d. S., R. Garrett, M. G. Bello Koblitz and A. Furtado Macedo (2022). Vanilla flavor: Species from the Atlantic forest as natural alternatives. *Food Chemistry* 375: 131891.

Paananen, H., E. Eronen, M. Mäkinen, J. Jänis, M. Suvanto and T. T. Pakkanen (2020). Base-catalyzed oxidative depolymerization of softwood kraft lignin. *Industrial Crops and Products* 152: 112473.

Pacek, A. W., P. Ding, M. Garrett, G. Sheldrake and A. W. Nienow (2013). Catalytic Conversion of Sodium Lignosulfonate to Vanillin: Engineering Aspects. Part 1. Effects of Processing Conditions on Vanillin Yield and Selectivity. *Industrial & Engineering Chemistry Research* 52(25): 8361-8372.

Pandey, M. P. and C. S. Kim (2011). Lignin Depolymerization and Conversion: A Review of Thermochemical Methods. *Chemical Engineering & Technology* 34(1): 29-41.

Pinto, P. C. R., C. E. Costa and A. E. Rodrigues (2013). Oxidation of lignin from *eucalyptus globulus* pulping liquors to produce syringaldehyde and vanillin. *Industrial & Engineering Chemistry Research* 52(12): 4421-4428.

Pinto, P. C. R., E. A. B. Silva and A. E. Rodrigues (2012). Lignin as source of fine chemicals: vanillin and syringaldehyde. Biomass Conversion: The Interface of Biotechnology, Chemistry and Materials Science. *C. Baskar, S. Baskar and S. R. Dhillon*. Berlin, Heidelberg, Springer Berlin Heidelberg**:** 381-420.

Pinto, P. C. R., E. A. B. d. Silva and A. E. Rodrigues (2011). Insights into oxidative conversion of lignin to high-added-value phenolic aldehydes. *Industrial & Engineering Chemistry Research* 50(2): 741-748.

Ponnusamy, V. K., D. D. Nguyen, J. Dharmaraja, S. Shobana, J. R. Banu, R. G. Saratale, S. W. Chang and G. Kumar (2019). A review on lignin structure, pretreatments, fermentation reactions and biorefinery potential. *Bioresource Technology* 271: 462-472.

Pu, Y., D. Zhang, P. M. Singh and A. J. Ragauskas (2008). The new forestry biofuels sector. *Biofuels, Bioproducts and Biorefining* 2(1): 58-73.

Rawat, S., P. Gupta, B. Singh, T. Bhaskar, K. Natte and A. Narani (2020). Molybdenum-catalyzed oxidative depolymerization of alkali lignin: Selective production of Vanillin. *Applied Catalysis A: General* 598: 117567.

Rinaldi, R., R. Jastrzebski, M. T. Clough, J. Ralph, M. Kennema, P. C. A. Bruijnincx and B. M. Weckhuysen (2016). Paving the Way for Lignin Valorisation: Recent Advances in Bioengineering, Biorefining and Catalysis. *Angewandte Chemie International Edition* 55(29): 8164-8215.

Rodrigues, A., P. Pinto, F. Barreiro;, C. A. E. Costa, M. I. F. Mota and I. Fernandes (2018). An Integrated Approach for Added-Value Products from Lignocellulosic Biorefineries. *Springer Nature Switzerland AG*, Springer International Publishing.

Sales, F. G., C. A. M. Abreu and J. A. F. R. Pereira (2004). Catalytic wet-air oxidation of lignin in a three-phase reactor with aromatic aldehyde production. *Brazilian Journal of Chemical Engineering* 21: 211-218.

Sales, F. G., L. C. A. Maranhão, N. M. L. Filho and C. A. M. Abreu (2007). Experimental evaluation and continuous catalytic process for fine aldehyde production from lignin. *Chemical Engineering Science* 62(18–20): 5386-5391.

Samah, R. A., N. Zainol, P. L. Yee, C. M. Pawing and S. Abd-Aziz (2013). Adsorption of Vanillin Using Macroporous Resin H103. *Adsorption Science & Technology* 31(7): 599-610.

Sandborn, L. T., J. R. Salvesen and G. C. Howard, (1936), Process of making vanillin.

Santos, S. G., A. P. Marques, D. L. D. Lima, D. V. Evtuguin and V. I. Esteves (2011). Kinetics of Eucalypt Lignosulfonate Oxidation to Aromatic Aldehydes by Oxygen in Alkaline Medium. *Industrial & Engineering Chemistry Research* 50(1): 291-298.

Schmitt, D., N. Beiser, C. Regenbrecht, M. Zirbes and S. R. Waldvogel (2017). Adsorption and separation of black liquor-derived phenol derivatives using anion exchange resins. *Separation and Purification Technology* 181: 8-17.

Serrano, L., J. A. Cecilia, C. García-Sancho and A. García (2019). Lignin Depolymerization to BTXs. *Topics in Current Chemistry* 377(5): 26.

Srinivasulu, C., M. Ramgopal, G. Ramanjaneyulu, C. M. Anuradha and C. Suresh Kumar (2018). Syringic acid (SA) – A Review of Its Occurrence, Biosynthesis, Pharmacological and Industrial Importance. *Biomedicine & Pharmacotherapy* 108: 547-557.

Stefanska, J., A. Sarniak, A. Wlodarczyk, M. Sokolowska, Z. Doniec, P. Bialasiewicz, D. Nowak and R. Pawliczak (2012). Hydrogen peroxide and nitrite reduction in exhaled breath condensate of COPD patients. *Pulmonary Pharmacology & Therapeutics* 25(5): 343-348.

Stefanska, J., A. Sarniak, A. Wlodarczyk, M. Sokolowska, E. Pniewska, Z. Doniec, D. Nowak and R. Pawliczak (2012). Apocynin reduces reactive oxygen species concentrations in exhaled breath condensate in asthmatics. *Experimental Lung Research* 38(2): 90-99.

Strassberger, Z., S. Tanase and G. Rothenberg (2014). The pros and cons of lignin valorisation in an integrated biorefinery. *RSC Advances* 4(48): 25310-25318.

Sun, Z., B. Fridrich, A. de Santi, S. Elangovan and K. Barta (2018). Bright Side of Lignin Depolymerization: Toward New Platform Chemicals. *Chemical Reviews* 118(2): 614-678.

T Hart, B. A., J. M. Simons, K.-S. Shoshan, N. P. M. Bakker and R. P. Labadie (1990). Antiarthritic activity of the newly developed neutrophil oxidative burst antagonist apocynin. *Free Radical Biology and Medicine* 9(2): 127-131.

Tarabanko, V. E., Y. V. Chelbina, A. V. Kudryashev and N. V. Tarabanko (2013). Separation of Vanillin and Syringaldehyde Produced from Lignins. *Separation Science and Technology* 48(1): 127-132.

Tarabanko, V. E., N. A. Fomova, B. N. Kuznetsov, N. M. Ivanchenko and A. V. Kudryashev (1995). On the mechanism of vanillin formation in the catalytic oxidation of lignin with oxygen. *Reaction Kinetics and Catalysis Letters* 55(1): 161-170.

Tilghman, B. C., (1867), Improved mode of treating vegetable substances for making paper-pulp. Letter Patent No. 70,485,

Tomlinson, G. H. and H. Hibbert (1936). Studies on Lignin and Related Compounds. XXV. Mechanism of Vanillin Formation from Spruce Lignin Sulfonic Acids in Relation to Lignin Structure1. *Journal of the American Chemical Society* 58(2): 348-353.

Tribot, A., G. Amer, M. Abdou Alio, H. de Baynast, C. Delattre, A. Pons, J.-D. Mathias, J.-M. Callois, C. Vial, P. Michaud and C.-G. Dussap (2019). Wood-lignin: Supply, extraction processes and use as bio-based material. *European Polymer Journal* 112: 228-240.

Vásquez-Garay, F., I. Carrillo-Varela, C. Vidal, P. Reyes-Contreras, M. Faccini and R. Teixeira Mendonça (2021). A Review on the Lignin Biopolymer and Its Integration in the Elaboration of Sustainable Materials. *Sustainability* 13(5): 2697.

Vega-Aguilar, C. A., M. F. Barreiro and A. E. Rodrigues (2021). Lignin conversion into C4 dicarboxylic acids by catalytic wet peroxide oxidation using titanium silicalite-1. *Industrial Crops and Products* 173: 114155.

Vega-Aguilar, C. A., C. Costa, M. F. Barreiro and A. E. Rodrigues (2022). Microwave-Assisted Lignin Wet Peroxide Oxidation to C4 Dicarboxylic Acids. *Industrial & Engineering Chemistry Research* 61(10): 3570-3581.

Villar, J. C., A. Caperos and F. García-Ochoa (2001). Oxidation of hardwood kraft-lignin to phenolic derivatives with oxygen as oxidant. *Wood Science and Technology* 35(3): 245-255.

Vinoth Kumar, R., K. Pakshirajan and G. Pugazhenthi (2016). Chapter 3 - Petroleum Versus Biorefinery-Based Platform Chemicals. Platform Chemical Biorefinery. *S. Kaur Brar, S. Jyoti Sarma and K. Pakshirajan*. Amsterdam, Elsevier**:** 33-53.

Voitl, T. and P. R. v. Rohr (2010). Demonstration of a Process for the Conversion of Kraft Lignin into Vanillin and Methyl Vanillate by Acidic Oxidation in Aqueous Methanol. *Industrial & Engineering Chemistry Research* 49(2): 520-525.

Wang, H., M. Tucker and Y. Ji (2013). Recent Development in Chemical Depolymerization of Lignin: A Review. *Journal of Applied Chemistry* 2013: 9.

Wang, T., H. Lu, J. Wang, Y. Xiao, Y. Zhou, Y. Bao and H. Hao (2017). Recent progress of continuous crystallization. *Journal of Industrial and Engineering Chemistry* 54: 14-29.

Wang, Z., K. Chen, J. Li, Q. Wang and J. Guo (2010). Separation of Vanillin and Syringaldehyde from Oxygen Delignification Spent Liquor by Macroporous Resin Adsorption. *CLEAN – Soil, Air, Water* 38(11): 1074-1079.

Werhan, H., A. Farshori and P. Rudolf von Rohr (2012). Separation of lignin oxidation products by organic solvent nanofiltration. *Journal of Membrane Science* 423–424: 404-412.

Windeisen, E. and G. Wegener (2012). Lignin as Building Unit for Polymers. *Polymer Science: A Comprehensive Reference, 10 Volume Set* 10: 255-265.

Wong, S. S., R. Shu, J. Zhang, H. Liu and N. Yan (2020). Downstream processing of lignin derived feedstock into end products. *Chemical Society Reviews* 49(15): 5510-5560.

Wu, G. and M. Heitz (1995). Catalytic Mechanism of Cu2+ and Fe3+ in Alkaline O2 Oxidation of Lignin. *Journal of Wood Chemistry and Technology* 15(2): 189-202.

Wu, G., M. Heitz and E. Chornet (1994). Improved Alkaline Oxidation Process for the Production of Aldehydes (Vanillin and Syringaldehyde) from Steam-Explosion Hardwood Lignin. *Industrial & Engineering Chemistry Research* 33(3): 718-723.

Yancheva, D., E. Velcheva, Z. Glavcheva, B. Stamboliyska and A. Smelcerovic (2016). Insights in the radical scavenging mechanism of syringaldehyde and generation of its anion. *Journal of Molecular Structure* 1108: 552-559.

Yao, C., J. Chen, Y. Lu, S. Tang and E. Fan (2018). Construction of an asynchronous three-zone simulated-moving-bed chromatography and its application for the separation of vanillin and syringaldehyde. *Chemical Engineering Journal* 331: 644-651.

Zabkova, M., E. A. Borges da Silva and A. E. Rodrigues (2007a). Recovery of vanillin from kraft lignin oxidation by ion-exchange with neutralization. *Separation and Purification Technology* 55(1): 56-68.

Žabková, M., E. A. B. da Silva and A. E. Rodrigues (2007b). Recovery of vanillin from lignin/vanillin mixture by using tubular ceramic ultrafiltration membranes. *Journal of Membrane Science* 301(1): 221-237.

Zabkova, M., M. Otero, M. Minceva, M. Zabka and A. E. Rodrigues (2006). Separation of synthetic vanillin at different pH onto polymeric adsorbent sephabeads SP206. *Chemical Engineering and Processing: Process Intensification* 45(7): 598-607.

Zhang, Q.-F., Z.-T. Jiang, H.-J. Gao and R. Li (2008). Recovery of vanillin from aqueous solutions using macroporous adsorption resins. *European Food Research and Technology* 226(3): 377-383.

Zoghlami, A. and G. Paës (2019). Lignocellulosic Biomass: Understanding Recalcitrance and Predicting Hydrolysis. *Frontiers in chemistry* 7: 874-874.

3 Hardwood and Softwood Lignins from Sulfite liquors: Structural Characterization and Valorization through Depolymerization

Researchers worldwide confirms the importance of lignin in the scenario of the integration of biorefinery concept and the efforts are focused on the study of alternatives as sources of chemicals. Lignin is an aromatic biopolymer naturally abundant (about 25% of wood) with high potential for the conversion into value-added phenolic monomers.

In this chapter, structural characteristics of lignins obtained from hardwood and softwood sulfite liquors were evaluated. The structural characteristics achieved allow evaluating the potential of each lignin through depolymerization to produce added-value phenolic monomers. Hardwood and softwood lignins were submitted to alkaline oxidation with oxygen and the reaction conditions optimized to obtain a final oxidation mixture with the maximum yield of phenolic monomers of interest namely vanillin and syringaldehyde.

This chapter is based on the following publication:

- Casimiro, F. M., C. A. E. Costa, C. Vega-Aguilar and A. E. Rodrigues (2022). "Hardwood and softwood lignins from sulfite liquors: Structural characterization and valorization through depolymerization." International Journal of Biological Macromolecules **215**: 272-279.

3.1 INTRODUCTION

Lignin is the most abundant natural phenolic polymer in the world. It is an amorphous, three-dimensional biopolymer arising from polymerization of three basic units: *p*-hydroxycinnamyl, coniferyl, and sinapyl alcohol. These monomers differ in the degree of substitution at the phenolic ring and are the precursors of the main moieties present in lignin structure: H (*p*-hydroxyphenyl), G (guaiacyl), and S (syringyl) units. The ratio between G, S and H units, type of structures, linkages, and functional groups in lignin differ with the biomass species, processing, and isolation conditions (Pu *et al.*, 2008, Costa *et al.*, 2015, Rodrigues *et al.*, 2018).

Nowadays, technical lignins can be generated as a byproduct of the pulping process. The major commercial lignins are obtained from kraft and sulfite processes however, other lignins such as organosolv are obtained from pulping processes using organic solvents. Kraft pulping is the main process for production of pulp and paper and originates kraft lignin while sulfite pulping is the predominant lignin-producing process (Strassberger *et al.*, 2014). Lignins from sulfite pulping process are denoted as lignosulfonates and are produced using sulfites (SO_3^{2-}), or bisulfites (HSO_3^-) as the pulping agents, at different pH levels (Rodrigues *et al.*, 2018). The most common counter ion of sulfite and bisulfite salts is magnesium (Mg^{2+}), but calcium (Ca^{2+}), sodium (Na^+) or ammonium (NH_4^+) have been employed as well in sulfite process (Pinto *et al.*, 2012).

Currently, lignosulfonates account for 90 % of the total market of commercial lignin, and its total annual worldwide production is approximately 1.8 million tons (Aro and Fatehi, 2017). Lignosulfonates are water-soluble and have quite high inorganic content (Calvo-Flores and Dobado, 2010, Fernández-Rodríguez *et al.*, 2019). Moreover, these types of lignins are typically highly cross-linked lignins and its weight-average molecular weight is higher than kraft lignins, values in the range 10-60 kDa have been reported in literature, with a corresponding broad polydispersity (Berlin and Balakshin, 2014, Galkin and Samec, 2016). Lignins from sulfite process have an established market being used mainly as dispersants in cement admixtures, additives, surfactants, pesticides, stabilizers, flocculants, and binder for pelleting animal feed (Aro and Fatehi, 2017, Rodrigues *et al.*, 2018, Fernández-Rodríguez *et al.*, 2019).

The variability of lignin structure and composition is one of the main challenges considering lignin valorization through the production of value-added products. Vanillin (V), syringaldehyde (Sy), vanillic acid (VA), syringic acid (SA), acetovanillone (VO), and

acetosyringone (SO) are main reaction products derived from lignin depolymerization through alkaline oxidation using oxygen as oxidant. V is one of the most widely used flavoring agents, it is known for its vanilla scent and flavor, and it is used as a precursor for the synthesis of several second-generation fine chemicals and pharmaceuticals, and in the food and fragrances industries as well (Munavalli *et al.*, 2007, Calvo-Flores and Dobado, 2010). Nowadays, 85% of vanillin supply is synthesized from oil derived guaiacol and glyoxylic acid, attaining around 15,000 tons per year at the price 6 - 15 USD/kg, the remaining 15% come from softwood lignin (Tarabanko and Tarabanko, 2017). Only, about 1% of the global demand for vanillin is assured by natural origin (vanilla beans) (Pinto *et al.*, 2012). VA, an oxidized form of V, is used as a flavoring agent and is often applied as preservative in argan oil. VO, also known as apocynin, is structurally related to V, and has been studied due to their important pharmacological properties (T Hart *et al.*, 1990, Stefanska *et al.*, 2012). Sy is an organic compound occurring, in small quantities, in nature. This phenolic is important in pharmaceutical applications due to their antioxidant, anti-inflammatory, antimicrobial and antifungal properties (Yancheva *et al.*, 2016). SA is extensively used as therapeutic agent, antioxidant, antimicrobial, anti-inflammatory and anticancer (Karthik *et al.*, 2014, Srinivasulu *et al.*, 2018), while SO is a chemical compound related to acetophenone and is used as a plant hormone and insect attractor (Baker *et al.*, 2005).

The depolymerization of lignosulfonates by alkaline oxidation has been a commercial process since at least 1945 (Salvesen *et al.*, 1945, Schoeffel, 1950, David and Logan, 1958). Moreover, oxidation in alkaline medium with oxygen was the main method studied in literature and by our research group, in associate laboratory LSRE-LCM, for lignin valorization through depolymerization to produce high-added-value chemicals (Mathias, 1993, Mathias and Rodrigues, 1995, Fargues *et al.*, 1996 (a), Araújo, 2008, Pinto *et al.*, 2011, Pinto *et al.*, 2013, Costa *et al.*, 2014, Costa, 2017, Gomes, 2019a). In this work, lignins from hardwood and softwood sulfite liquors, LHSL and LSSL, were evaluated as potential sources of phenolic monomers, mainly Sy and V, through oxidation with O_2 in alkaline medium. The profiles of Sy, V, and other minor products were established, and some reaction conditions optimized. Characterization of both lignins was also achieved.

3.2 EXPERIMENTAL SECTION: MATERIALS AND METHODS

3.2.1 Sulfite Liquors and Lignins

Two spent sulfite liquors from different origins were studied. A hardwood sulfite liquor (HSL, total solids, 15.0 % w/w_{liquor}) from *Eucalyptus globulus*, gently provided by Caima (Constância, Portugal), and a softwood sulfite liquor (SSL, total solids, 11.3 % w/w_{liquor}), supplied by a pulp mill of Company A, from a mixture of 90 % of spruce (softwood material) and 10 % of beech (hardwood biomass).

HSL and SSL were submitted to ultrafiltration performed in a G.E. Osmonics SEPA CF II crossflow filtration system using a Synder MT membrane with a molecular weight cutoff (MWCO) of 5 kDa. The experiment was carried out with a total recirculation of the feed solution. The operating conditions of the ultrafiltration of each liquor are presented in Table 3.1.

The resulting retentates were freeze-dried (-80 ºC and 0.05 bar) and the yields on lignin recovered from this isolation procedure were 39% for LHSL and 53% for LSSL, calculated with reference to the total nonvolatile solids on the respective liquors. The obtained lignins, LHSL and LSSL, were characterized and submitted to oxidation using the methods and techniques described in the following sections.

Table 3.1 - SSL and HSL ultrafiltration operating conditions.

	HSL	**SSL**
Membrane MWCO, Da	5000	
Pressure, bar	9	
Initial volume, mL	4000	
Liquor pH	2.3	3.4
Temperature*, ºC	28	27
Retentate volume, mL	800	900

*average value

3.2.2 Inorganic Content of Lignins

The inorganic content of LSSL and LHSL was determined by gravimetric quantification after incineration of about 100 mg of each lignin in a muffle furnace at 600

ºC during 6 h (Pinto *et al.*, 2011, Costa *et al.*, 2015). Inorganics determination was performed in duplicated. The results, as component weigh per 100 g of lignin, are depicted in Table 3.2.

Table 3.2 - Inorganic content of LHSL and LSSL lignins, presented in $\%w/w_{lignin}$ (dry weight).

	LHSL	**LSSL**
Inorganic content, $\%w/w_{lignin}$	7.2 ± 0.2	10.1 ± 0.3

The inorganic content found for LHSL and LSSL are in accordance with other studies in literature concerning lignosulfonates characterization, where values of inorganics in the range 4 - 10 % w/w_{lignin} were reported (Lebo Jr. *et al.*, 2001, Mansouri and Salvadó, 2006, Vishtal and Kraslawski, 2011, Tribot *et al.*, 2019).

3.2.3 Nitrobenzene Oxidation (NO)

Lignins, LHSL and LSSL, were submitted to alkaline NO as already described in the literature (Pinto *et al.*, 2010, Costa *et al.*, 2015). Briefly, 30 mg of each lignin was dissolved in 7 ml of 2M NaOH aqueous solution in a teflon vessel and, after adding 450 µL of nitrobenzene the vessel was placed into a stainless steel reactor and heated up to 170 ºC for 4 h. The oxidized material was extracted twice with chloroform. The organic phase collected was evaporated under reduce pressure, the dried sample was dissolved in methanol and made up to 10 mL with methanol. Quantification of reaction products was made by high-performance liquid chromatography (HPLC) (Pinto *et al.*, 2010). A Knauer HPLC system equipped with a Smartline 5000 online degasser, a Smartline 1000 quaternary pump, and a Smartline 2600 UV-DAD detector was used. The analytical column was an ACE 5 C18-pentafluorophenyl group (250 x 3.0 mm, 5 µm) with a guard column of the same material. The detection wavelength was set to 280 nm and the injection volume was 20 µL. Chromatograms were acquired at 30 ºC with a flowrate of 0.6 mL min^{-1} using an elution gradient composed by two eluents: A) methanol:water (5:95 % v/v) and B) methanol:water (95:5 % v/v), both acidified with formic acid (0.1 % v/v). The elution gradient was [0-3.30] min 90% A; 6.70 min 80 % A; [6.70-20] min 80 % A; 35 min 50 % A; 38.3 min 0 % A, [38.3-41.7] min 0 % A; 45 min 90 % A; [45-55] min 90 % A. Quantification of all compounds was done based on calibration curves previously prepared from standard solutions in the needed concentration range. NO and HPLC analysis were performed in duplicated.

3.2.4 ^{13}C NMR

Quantitative ^{13}C NMR procedure was reported elsewhere (Costa *et al.*, 2014). ^{13}C NMR spectra were recorded using a Bruker AVANCE III 400 spectrometer operating at 400 MHz, with a temperature of 45 ℃, during 72 h. Approximately 160 mg of each lignin was dissolved in 0.5 mL deuterated dimethyl sulfoxide (DMSO-d^6). Conditions for ^{13}C NMR measurements: simple 1D pulse sequence, recycling time of 12 s, 17000 scans, and 1D sequence with power-gated coupling using 90º flip angle.

3.2.5 Gel Permeation Chromatography (GPC)

Molecular weight analyses were performed using a Shimadzu UFLC, equipped with a diode array detector (operating at 268 nm wavelength) and a refraction index detector (RI). Two Agilent gel columns were used: an OligoPore column 300×7.5 mm and a MesoPore column 300 ×7.5 mm. A guard column Oligopore 50×7.5 mm was assembled prior to the columns. GPC analyses were performed according to the procedure used in the literature (Costa *et al.*, 2018). Briefly, GPC analysis were performed at 70 ℃ with a flowrate of 0.8 mL.min^{-1} and using an isocratic mobile phase of dimethylformamide (DMF) with 0.5 %w/v of lithium chloride (LiCl) to avoid lignin agglomeration. The system was calibrated with polystyrene molecular weight standards ranging from 162 to 55000 g/mol, before the analysis. Solutions of about 5 mg/mL of each polystyrene standard and lignin samples were dissolved in the mobile phase solvent. Prior to analysis, lignin samples were stirred and filtered through a 0.2 μm syringe filter.

3.2.6 Alkaline Oxidation with O_2

Oxidation of lignins in alkaline medium using O_2 were performed in a Büchi AG laboratory autoclave with a capacity of 1 L (model BEP280 type II, Switzerland). The heating and temperature control was assured by a Haake thermostatic bath (model N2-B, Karlsruhe, Germany). Temperature and total pressure inside the reactor were measured using a thermocouple type K and a pressure transducer (Kulite model XYME-190 M G, Leonia, USA), respectively. The O_2 flow rate was measured by means a mass flow meter EL FLOW (Bronkhorst High-Tech B.V., model F-201C-FAC-11-V, Ruurlo, Netherlands). The reaction samples were collected at preset time intervals.

For each oxidation reaction, about 30 g of lignin was dissolved in 500 mL of NaOH (80 g/L) solution, introduced into the reactor, heated to 120 ℃, and pressurized. The reaction time started when the initial temperature reached 120 ℃. At this time, O_2 was introduced starting the data acquisition. The total pressure in the reactor was kept at 9.8 bar with a partial pressure of O_2 of 3.0 bar by continuous supply of O_2 along the time.

The low molecular weight phenolic compounds produced during LHSL and LSSL oxidation were extracted by solid phase extraction (SPE) and analyzed by HPLC. For the SPE procedure, LiChrolut EN (40 - 120 μm) 500 mg, 6 mL (Merck) SPE cartridges were used. First, 7 mL of methanol was applied on the column for the sorbent bed solvation. Prior to sample loading, 12 mL of 95:5 (v/v) water:methanol with 0.1% (v/v) formic acid was used for SPE column equilibration. The samples were diluted with distilled water (1:1), acidified to pH 2 with H_2SO_4 solution (6 M), and loaded on the prepared cartridge. The cartridge was then washed with 12 mL of solution 95:5 (v/v) water:methanol with 0.1% (v/v) formic acid for interference elution. Finally, the phenolic compounds were eluted using 7 mL of 5:95 (v/v) water:methanol with 0.1% (v/v) formic acid. The volume was collected to a volumetric flask and brought up to 10 mL in volume with the same solution. The analysis of the extracted products was performed using the equipment and the conditions as previously described in section 3.2.3.

3.3 RESULTS AND DISCUSSION

3.3.1 LSSL and LHSL Characterization by NO

Nitrobenzene oxidation in alkaline medium represents an important method for qualitatively and quantitatively determining lignin composition, providing information about the phenolic monomers in the non-condensed fraction of lignin (Sun *et al.*, 1995). Studies on the nitrobenzene oxidation of lignin model compounds indicated that phenolic monomers are derived from oxidative degradation of the corresponding 4-hydroxyphenylpropane units and their eters, in particular the corresponding 4-*O*-alkylated and α-*O*-4 and β-*O*-4 lignin structures (Lin and Dence, 1992).

The yields and types of phenolic aldehydes, acids, and ketones obtained for LHSL and LSSL by nitrobenzene oxidation are depicted in Table 3.3. The quantification of the maximum individual yield of the referred phenolic monomers represents an important

parameter for the evaluation of lignin potential through lignin oxidative depolymerization (Pinto *et al.*, 2010, Costa *et al.*, 2014).

Table 3.3 – Yields of monomeric phenolic obtained by NO of LHSL and LSSL lignins.

	Products, % w/w$_{lignin}$*					
	Hy	**VA**	**SA**	**V**	**Sy**	**Total yield**
LHSL	0.07	0.52	1.90	6.20	18.7	27.4
LSSL	0.27	1.96	0.19	19.3	1.55	23.3

* reported to nonvolatile solids weight after removing inorganic content.

As shown in Table 3.3, V and Sy are the main products, accounting about 90% of the total phenolic monomers identified in both lignins. Minor contents of their corresponding acids (VA and SA, respectively) and Hy were also obtained. As expected, the softwood lignin (LSSL) has mostly G units, with V and VA accounting 91 % of the total yield, with a lower content of S units. On the other hand, LHSL have a percentage of Sy higher than 18 % w/w$_{lignin}$, accounting about 68% of the total yield of the phenolic monomers identified.

From a perspective of lignins valorization to added-value products, the results from NO allow anticipate the maximum yields that could be achieve through lignin depolymerization however, it is reported that the oxidation of lignin in alkaline medium using O_2 as oxidant only can reach up to 50% of the total yields obtained by NO (Tarabanko *et al.*, 1995, Costa *et al.*, 2015). Moreover, it is well known that high aldehyde/acid ratios are also an advantage in the perspective of lignin valorization. In this study, both lignins, LSSL and LHSL, show a value of Sy/SA and V/VA ratio in the range from 8.0 to12. The obtained values are higher than the ones obtained for hardwood kraft liquors and lignins, that showed ratios between 3 and 4.6 (Pinto *et al.*, 2013), confirming the advantage of lignins from sulfite liquors from the point of view of selectivity for phenolic aldehydes.

3.3.2 Lignins Characterization by ^{13}C NMR

^{13}C NMR provides important information about the carbons in different structural and chemical environments in the condensed and non-condensed fractions of lignin structure. The carbon chemical shifts of each functional group, linkage, or structure present in lignins was made based on reference spectra and data available on literature (Evtuguin *et al.*, 2001,

Capanema *et al.*, 2004, Lin and Dence, 2012, Costa *et al.*, 2014). The ^{13}C NMR spectra of LSSL and LHSL, with the main assignments identified, are shown in Figure 3.1.

The assignments and the corresponding chemical shifts of the main structures, linkages, and functional groups, as well as the resulting content, reported as the ratio of the integral of a given carbon signal to one-sixth of the integral of aromatic carbons (Ar), are presented in Table 3.4. The integral of the δ 103 - 162 ppm region was set as the reference, assuming that it includes six aromatic carbons (Lin and Dence, 1992, Capanema *et al.*, 2004).

From the quantitative data from ^{13}C NMR it is possible to calculate basic parameters that summarizes the main structural characteristics of lignins: the content of β-*O*-4 structures, the degree of condensation (DC), and the S/G ratio. The content of β-*O*-4 and the DC value of each lignin were estimated as described in detail in a previous work (Costa *et al.*, 2014). The referred parameters, calculated for LHSL and LSSL, are depicted in Table 3.5.

The most significant difference in LHSL and LSSL structure, besides the proportion of S:G:H units, is the highest content of condensed structures in LSSL, reflected by the DC value found for this lignin. The higher DC is related with the high proportion of G units in LSSL, also confirmed by S/G ratio. G units have more ability to form C–C linkages, present in the most common condensed moieties in lignin structure such as 5-5', β-5, and 4-O-5', due to the availability of the C_5 position in the aromatic ring (Berlin and Balakshin, 2014, Fernández-Costas *et al.*, 2014). For hardwood lignins, as LHSL, the higher proportion of S units makes it difficult the formation of these type of linkages, since they have both C_3 and C_5 positions substituted by a methoxyl group (Alriols *et al.*, 2010).

Considering the lowest value of DC and the highest number of β-*O*-4 structures obtained for LHSL, it is expected that this lignin give origin to higher yields of phenolic monomers through depolymerization, which are also confirmed by the results obtained by NO (Table 3.3).

Table 3.4 - Assignments and quantification (number per aryl unit) of the structures/linkages and functional groups identified by ^{13}C NMR.

Assignments (spectroscopic range)	**amount (number per Ar)**	
	LHSL	**LSSL**
C_β in β-5 and β-β structures (δ 51.0 - 53.8 ppm)	0.15	0.26
Aromatic OCH_3 (δ 54.3 - 57.3 ppm)	1.35	1.44
Cγ in β-*O*-4 structures without Cα=O (δ 59.3 - 60.8 ppm)	0.26	0.30
Cγ in β-5, β-*O*-4 structures with Cα=O and β-1	0.14	0.24

(δ 62.5 - 63.8 ppm)		
Cα in β-*O*-4 structures; Cγ in pinoresinol/syringaresinol and β-β structures (δ 70.0 - 76.0 ppm)	1.24	1.00
C_β in β-*O*-4 structures; Cα in β-5 and β-β structures (δ 80.0 - 90.0 ppm)	0.57	0.66
Aromatic C_{Ar}-H (δ 103.0 - 123.0 ppm)	2.06	2.37
Aromatic C_{Ar}-C (δ 123.0 - 137.0 ppm)	1.61	1.57
Aromatic C_{Ar}-O (δ 137.0 - 156.0 ppm)	2.28	2.00
C_4 in H units (δ 157.0 - 162.0 ppm)	0.05	0.07
CHO in benzaldehyde structures (δ 191.0-192.0 ppm)	0.00	0.02
CHO in cinnamaldehyde structures (δ 193.5-194.5 ppm)	0.01	0.03
CO in aldehydes and ketones (δ 195.0 - 210.0 ppm)	0.59	0.40

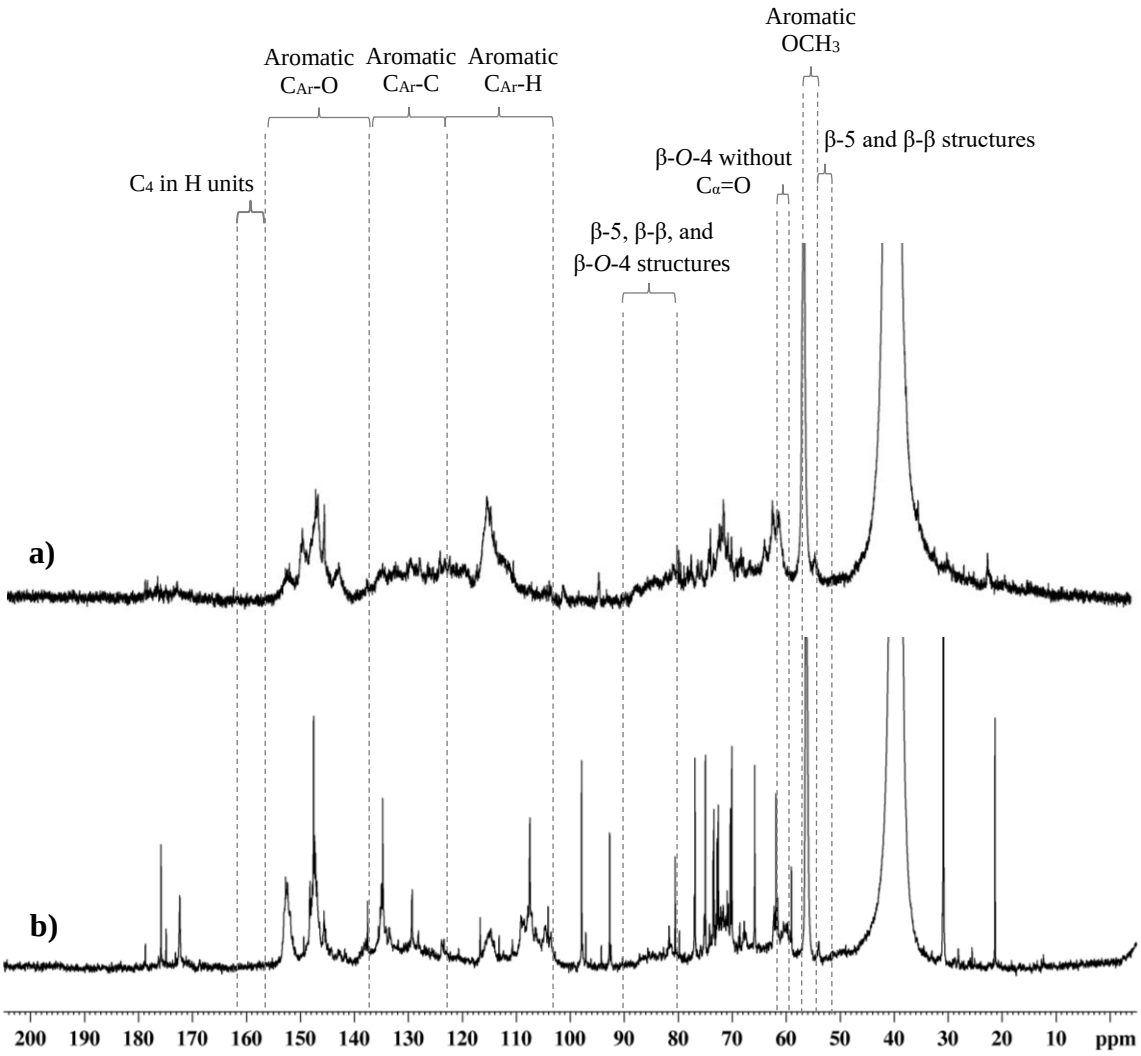

Figure 3.1 - Quantitative ^{13}C NMR spectra of lignins: a) LSSL and b) LHSL, in DMSO-d^6.

Table 3.5 - β-*O*-4 structures content (number per 100 Ar), DC, and S/G ratio calculated for LHSL and LSSL.

	β-*O*-4, n/100 Ar	**DC**, %	**S/G**
LHSL	42	24	2.1
LSSL	40	38	0.24

3.3.3 Molecular Weight Distribution

Gel permeation chromatography (GPC) allow to obtain the molecular weight distribution of the lignins obtained from ultrafiltration of hardwood and softwood sulfite liquors. The chromatograms obtained for LHSL and LSSL were normalized, overlaid, and presented in Figure 3.2 and the weight-average molecular weight (Mw) and polydispersity index (Mw/Mn) found are shown in Table 3.6. As already stated in section 3.2.5, the GPC calibration was performed with polystyrene standards thus, the obtained values of Mw are relative to this polymer and the analysis of lignin only provides relative molecular weight values (Costa *et al.*, 2018).

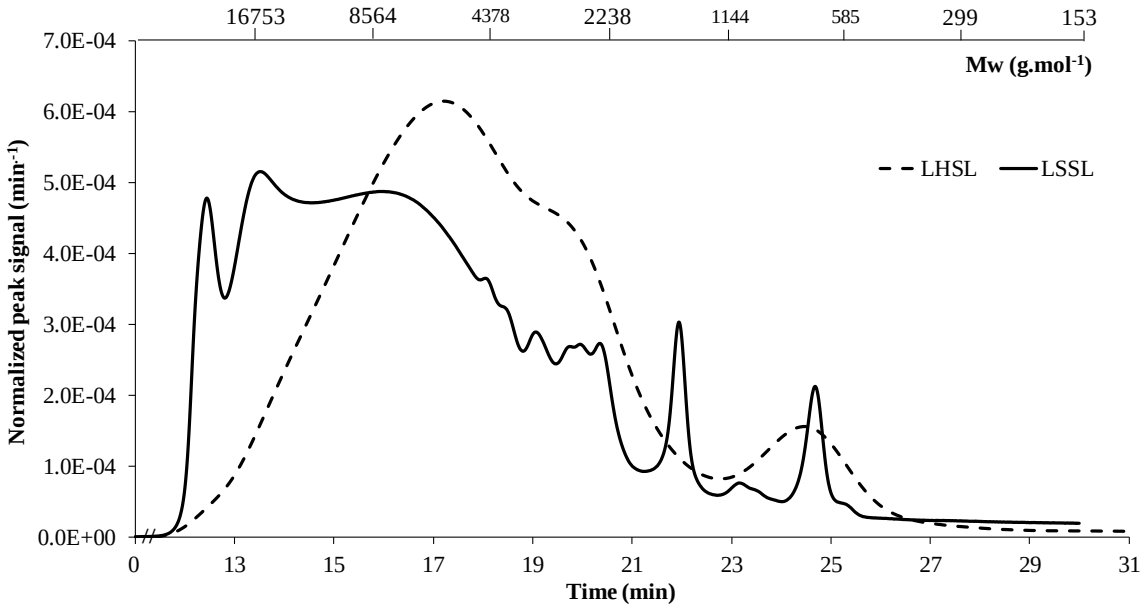

Figure 3.2 - Molecular weight distribution curves obtained from GPC analyses of LHSL and LSSL lignins.

Table 3.6 - Molecular weight (Mw) and polydispersity (Mw/Mn) of LHSL and LSSL lignins analyzed by GPC.

	Mw (g/mol)	**Mw/Mn**
LHSL	31347	1.64
LSSL	48566	1.57

The molecular weight distribution curve obtained for LSSL lignin shows two peaks in the high molecular weight region, not visible for LHSL that corresponds to a low elution time. This lignin has the highest value of molecular weight, which is coherent with the described peaks and the presence of more condensed moieties in its structure (Table 3.5). In literature other authors already stated that lignins mostly composed by G units are expected to show higher Mw than those presenting high contents of S units due to the higher probability to form condensed structures (Toledano *et al.*, 2010). In the low molecular weight region, LSSL and LHSL show the presence of peaks, albeit in different intensities, indicated that low molecular weight fragments are present in both lignins. The lower polydispersity found for LSSL confirms that this lignin has a structure slightly more homogeneous, with narrower molecular weight distribution.

3.3.4 Oxidation of LSSL and LHSL with O_2 in Alkaline Medium

The oxidation experiments of LHSL and LSSL lignins were carried out in 0.5 L of a 2 M NaOH solution (80 g/L) with a lignin initial concentration of 60 g/L, an initial temperature of 120 ºC, and a partial pressure of O_2 of 3 bar (total pressure of 9.8 bar), as already described in section 3.2.6. The first oxidation reaction of both lignins was performed for 120 minutes, to evaluate the complete profile of all the oxidation phenolic products, including their formation and consequent degradation. The second oxidation experiment was interrupted just before the maximum yield of the main phenolics is achieved, the admission of O_2 was stopped and the temperature of the reactor decreased. These oxidation reactions were over after 26 and 8 minutes, for LSSL and LHSL, respectively. The objective is to avoid further degradation of the oxidation products and consequently achieve a final mixture with the maximum yields of the valuable phenolics of interest, namely V and Sy.

The profiles of the phenolic monomers identified in oxidation experiment 1, for 120 minutes, and experiment 2, for 26 and 8 minutes, for LSSL and LHSL, respectively, are presented in Figure 3.3 and Figure 3.4. As expected, V and VA are the main products from

the oxidation of LSSL, with minor yields of Sy and VO (Figure 3.4). In the case of LHSL, the main phenolic products identified in the oxidation mixture were Sy and V; however, the carboxylic acids SA and VA were also identified, as the phenolic ketones VO and SO (Figure 3.3). During the hardwood lignin oxidation Sy reaches to a maximum yield of 2.5 % w/w_{lignin} at a reaction time between 10 and 15 min followed by an accentuated decrease for longer reaction times. For V, the time to maximum is higher, about 20 min, and, after the maximum (1.2 % w/w_{lignin}), a smooth drop occurs when compared with Sy. In the case of LSSL lignin V reaches the maximum yield of 4.7 % w/w_{lignin} after 30 minutes and Sy reaches 0.23 % w/w_{lignin} between 15 and 20 minutes of oxidation reaction. The degradation profile of both phenolic aldehydes in this lignin is similar to the described for LHSL.

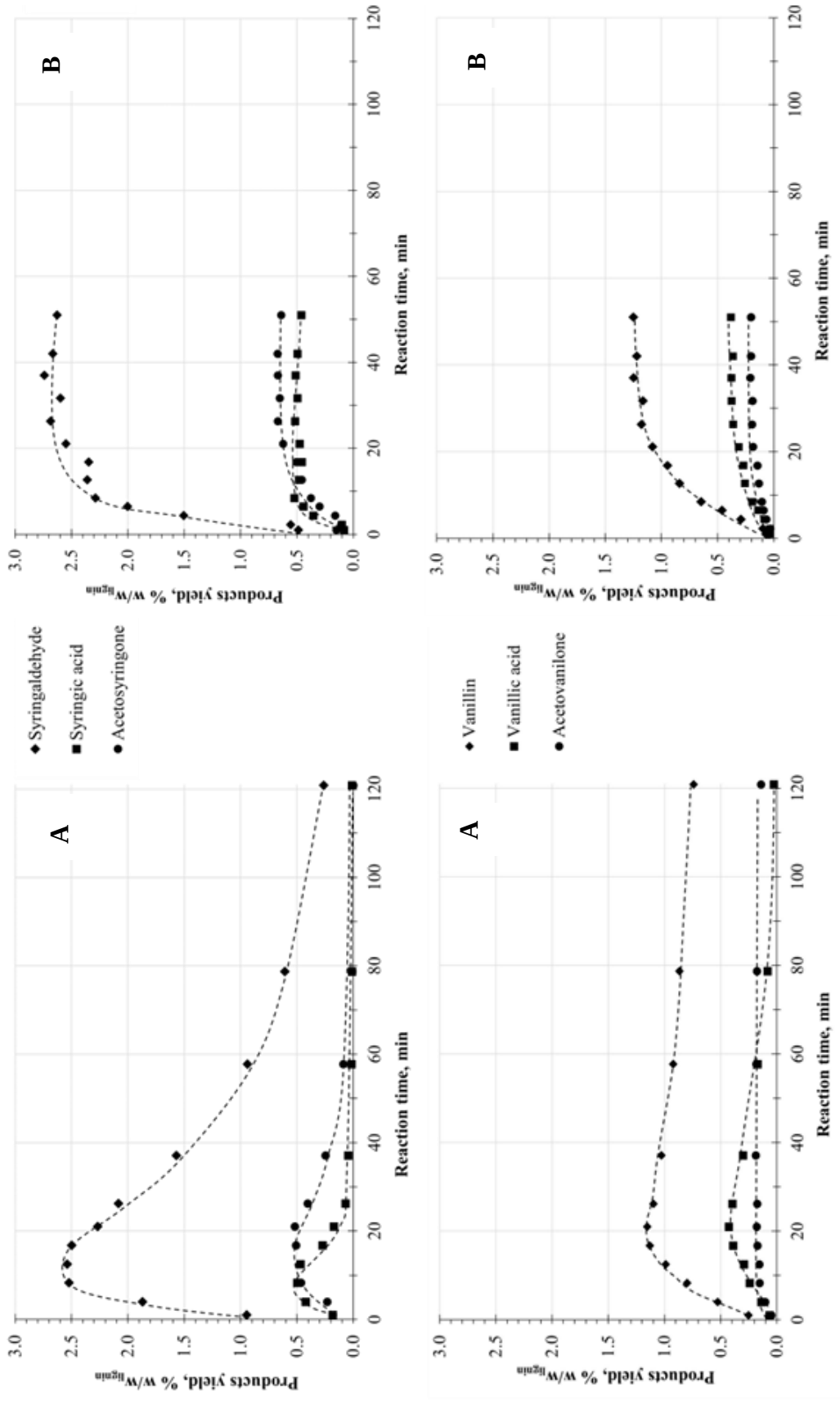

Figure 3.3 – Profiles of monomeric products: Sy, SA, SO, V, VA and VO during oxidation experiment 1 (A) and experiment 2 (B) of LHSL lignin. General conditions: lignin concentration 60 g/L, [NaOH] = 80/g.L, pH $_{initial} \geq 13.8$, pO_2 = 3bar, P_{total} = 9.8 bar, T_i = 393 K.

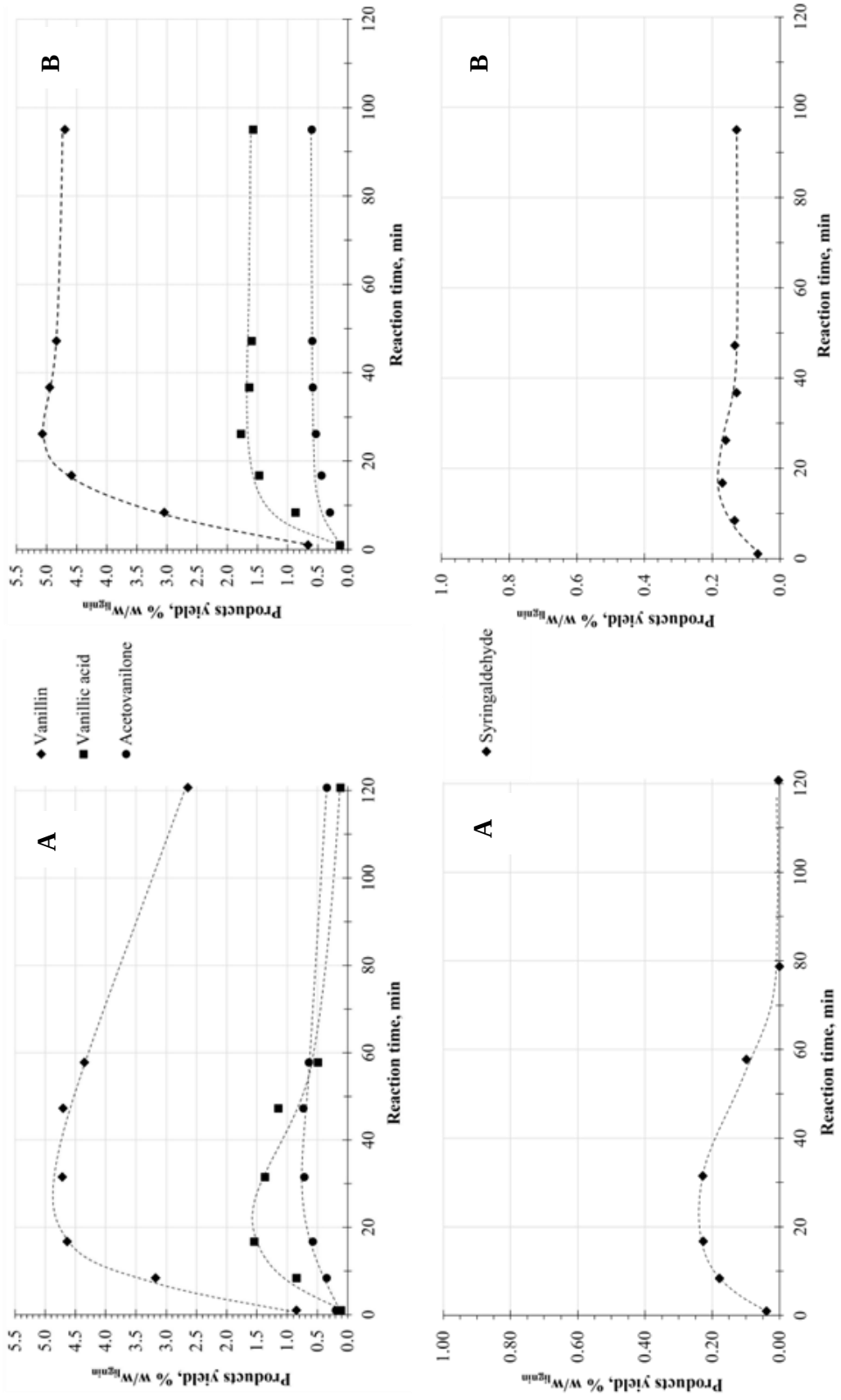

Figure 3.4 - Profiles of monomeric products: V, VA, VO and Sy during oxidation experiment 1 (A) and experiment 2 (B) of LSSL lignin. General conditions: lignin concentration 60 g/L, [NaOH] = 80 g/L, pH $_{initial} \geq 13.8$, pO_2 = 3bar, P_{total} = 9.8 bar, T_i = 393 K.

The lower reaction times to reach the maximum yield of the phenolic aldehydes observed for LHSL confirms the higher reactivity of this lignin comparatively to LSSL, related with the presence of high contents of S units. Sy is more sensitive than V to oxygen pressure; it forms quickly but it readily degrades under a high oxygen pressure. A similar trend in the reactivity of the S nuclei comparatively to the G nuclei was also found by other authors in studies about the effect of O_2 pressure in lignin oxidation (Sultanov and Wallis, 1991, Wu *et al.*, 1994, Pinto *et al.*, 2013).

When the time of the oxidation reaction of LSSL and LHSL is reduced, and the admission of O_2 is interrupted just before the maximum yield of the main products is reached, it is possible to see a decrease in V and Sy degradation, resulting in a final oxidation mixture with higher yield of these phenolics (Figure 3.5). For LHSL, the influence in the degradation of V and Sy is more evidenced since in the case of this lignin, the oxidation reaction is interrupted after 8 minutes, and it is not observed any decrease in the yield of these oxidation products after this time. Considering V, the yield in the final oxidation mixture is about 40 % higher in the reaction stopped at 8 and 26 minutes, for LHSL and LSSL, respectively, comparatively to the content of this phenolic compound in the final mixture obtained after the oxidation reaction for 120 minutes (Figure 3.5). For Sy, due to its higher reactivity, an increase of 95 % in the final yield of this aldehyde was obtained when the oxidation is performed only for 8 minutes. These results indicate that an initial high pressure of oxygen rapidly breaks down the lignin and then a decrease in the oxygen pressure allows proceeding the oxidation of the lignin fragments but prevents the degradation of the phenolic monomers. Since the main objective of lignin depolymerization is to attain an oxidation mixture with the maximum yield of the phenolic compounds of interest, it is essential to select the experimental conditions that allow reaching the best compromise between the formation and the degradation of the oxidation products.

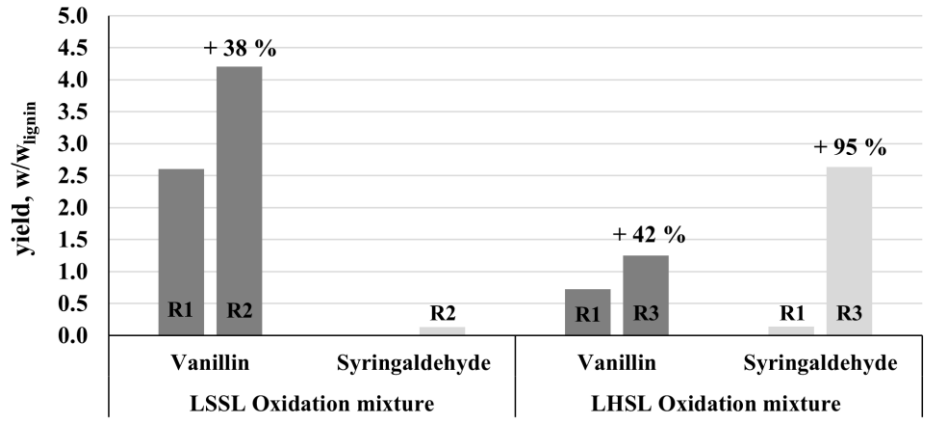

Figure 3.5 – Yield of V and Sy in the final solution obtained from the oxidation for 120 minutes (R1), 26 minutes (R2), and 8 minutes (R3) for LSSL and LHSL lignins. The percentages refer to the increase of yield comparatively to reaction 1 for V and Sy.

3.3.5 Evaluation of the S:G:H Units Proportion

The proportion of S:G:H in LSSL and LHSL was determined from the results of NO, oxidation with O_2, and ^{13}C NMR - Table 3.7. Through NO only uncondensed lignin structural units are accessible, consequently the proportion of G, S, and H in the uncondensed fraction of lignins were calculated using the phenolic monomers yields obtained from this method. G units were determined from the contribution of V and VA, while for S units only Sy and SA were considered. Hy yield allow the calculation of H units. The same procedure was performed to achieve the ratio S:G:H from oxidation with O_2, with the difference that this method is not restrict only to the non-condensed fraction of lignin. ^{13}C NMR results also reflect the structural features of the whole lignin, accessing both condensed and non-condensed moieties, and the proportion of S, G, and H structures obtained from this technique was also achieved.

Table 3.7 – Proportion of S:G:H units obtained from the results of ^{13}C NMR, NO, and alkaline oxidation with O_2.

		^{13}C NMR	**NO**	**Oxid. O_2**
LSSL	**S** units	18	8	7
	G units	75	91	92
	H units	7	1	1
LHSL	**S** units	64	75	65
	G units	30	24	32
	H units	6	1	2

For LSSL lignin it is observed that the proportion of S:G:H units obtained from the results of NO is similar to that obtained from the results from alkaline oxidation with O_2. This behavior suggests that alkaline oxidation with O_2 mainly attacks the non-condensed structures of this lignin. Moreover, the proportion of S:G:H from ^{13}C NMR, that reflects the structural features of the whole lignin, shows a higher content of S units, suggesting that a significant part of these units are involved in condensed structures. Since the main condensed structures present in lignin are 5-5', β-5, and 4-O-5' it could be concluded that in this lignin, obtained from softwood biomass, S units are mainly involved in condensed structures through C_β in β-5 structures (phenylcoumarin structure), since this type of units have the C_5 position already substituted by a methoxyl group. This statement is also evidenced by the data from quantitative ^{13}C NMR, (first row of Table 3.4), that shows higher amounts of C_β in β-5 and β-β structures in LSSL lignin. In literature, other authors also noted the higher content of β-5 linkages in softwood lignins (Constant *et al.,* 2016, Lahive *et al.,* 2018). In opposition, LHSL shows that the proportion of S:G:H units obtained from the results of ^{13}C NMR is similar to that obtained from the results from alkaline oxidation with O_2. This indicate that for this lignin the alkaline oxidation using O_2 as oxidant attacks the whole lignin structure (condensed and uncondensed structures) in the same proportion, instead of showing more propensity to cleave the structures in the non-condensed fraction of lignin, as observed in the case of LSSL. This type of structural information about lignin is essential to evaluate its reactivity and to understand its efficient utilization either through depolymerization reactions or in material applications.

3.4 CONCLUSIONS

The hardwood and softwood lignins obtained from the ultrafiltration of the sulfite liquors were characterized and the results showed that LHSL has the lowest value of DC and the highest number of β-*O*-4 structures, consequently this lignin give origin to higher yields of phenolic monomers through depolymerization by NO. Concerning LSSL, lignin from softwood biomass, the GPC analysis confirmed its highest value of molecular weight, which is coherent with presence of more condensed moieties in its structure related with the higher availability of G units in this lignin. Both lignins were subjected to alkaline oxidation with O_2 and the yield of aromatic monomers and the selectivity of the target products were

evaluated. When the O_2 pressure is maintained constant, a higher rate of oxygen is transferred from the gas phase into the liquid phase, the conversion takes place and the yields of phenolic monomers increase in a very short time, followed by their accentuated degradation. It was found that it is preferable to keep an initial high pressure of oxygen and then decrease it to continue the oxidation of the lignin fragments but prevent the degradation of the phenolic monomers. With the experimental conditions optimized, LSSL showed to be the raw material with better performance toward oxidation, producing a maximum of 2.7 $g.L^{-1}$ of V in the final oxidation mixture. In the end of this work, it is possible to conclude that alkaline oxidation of the studied lignins allow obtaining a final oxidized mixture rich in the produced phenolic monomers what is an extremely important point from a techno-economic approach.

3.5 REFERENCES

Alriols, M. G., A. García, R. Llano-ponte and J. Labidi (2010). Combined organosolv and ultrafiltration lignocellulosic biorefinery process. *Chemical Engineering Journal* 157(1): 113-120.

Araújo, J. D. P. (2008). Production of vanillin from lignin present in the kraft black liquor of the pulp and paper industry. Ph.D. Dissertation, *Faculty of Engineering University of Porto*.

Aro, T. and P. Fatehi (2017). Production and Application of Lignosulfonates and Sulfonated Lignin. *ChemSusChem* 10(9): 1861-1877.

Baker, C. J., N. M. Mock, B. D. Whitaker, D. P. Roberts, C. P. Rice, K. L. Deahl and A. A. Aver'yanov (2005). Involvement of acetosyringone in plant–pathogen recognition. *Biochemical and Biophysical Research Communications* 328(1): 130-136.

Berlin, A. and M. Balakshin (2014). Chapter 18 - Industrial lignins: Analysis, properties, and applications. Bioenergy Research: Advances and Applications. *V. K. Gupta, M. G. Tuohy, C. P. Kubicek, J. Saddler and F. Xu*. Amsterdam, Elsevier**:** 315-336.

Calvo-Flores, F. G. and J. A. Dobado (2010). Lignin as renewable raw material. *ChemSusChem* 3(11): 1227-1235.

Capanema, E. A., M. Y. Balakshin and J. F. Kadla (2004). A Comprehensive Approach for Quantitative Lignin Characterization by NMR Spectroscopy. *Journal of Agricultural and Food Chemistry* 52(7): 1850-1860.

Constant, S., H. L. J. Wienk, A. E. Frissen, P. d. Peinder, R. Boelens, D. S. van Es, R. J. H. Grisel, B. M. Weckhuysen, W. J. J. Huijgen, R. J. A. Gosselink and P. C. A. Bruijnincx (2016). New insights into the structure and composition of technical lignins: A comparative characterisation study. *Green Chemistry* 18(9): 2651-2665.

Costa, C. A. E. (2017). Vanillin and syringaldehyde from side streams of pulp and paper industries and biorefineries. PhD, *Faculty of Engineering, University of Porto*.

Costa, C. A. E., P. C. R. Pinto and A. E. Rodrigues (2014). Evaluation of chemical processing impact on E. globulus wood lignin and comparison with bark lignin. *Industrial Crops and Products* 61: 479-491.

Costa, C. A. E., P. C. R. Pinto and A. E. Rodrigues (2015). Radar Tool for Lignin Classification on the Perspective of Its Valorization. *Industrial & Engineering Chemistry Research* 54(31): 7580-7590.

Costa, C. A. E., P. C. R. Pinto and A. E. Rodrigues (2018). Lignin fractionation from E. Globulus kraft liquor by ultrafiltration in a three stage membrane sequence. *Separation and Purification Technology* 192: 140-151.

David, C. and C. D. Logan, (1958), Method of producing vanillin and other useful products from lignosulfonic acid compounds.

Evtuguin, D. V., C. P. Neto, A. M. S. Silva, P. M. Domingues, F. M. L. Amado, D. Robert and O. Faix (2001). Comprehensive Study on the Chemical Structure of Dioxane Lignin from Plantation Eucalyptus globulus Wood. *Journal of Agricultural and Food Chemistry* 49(9): 4252-4261.

Fargues, C., Á. Mathias and A. Rodrigues (1996 (a)). Kinetics of vanillin production from kraft lignin oxidation. *Industrial & Engineering Chemistry Research* 35(1): 28-36.

Fernández-Costas, C., S. Gouveia, M. A. Sanromán and D. Moldes (2014). Structural characterization of Kraft lignins from different spent cooking liquors by 1D and 2D Nuclear Magnetic Resonance spectroscopy. *Biomass and Bioenergy* 63: 156-166.

Fernández-Rodríguez, J., X. Erdocia, F. Hernández-Ramos, M. G. Alriols and J. Labidi (2019). Chapter 7 - Lignin Separation and Fractionation by Ultrafiltration. Separation of Functional Molecules in Food by Membrane Technology. *C. M. Galanakis*, Academic Press**:** 229-265.

Galkin, M. V. and J. S. M. Samec (2016). Lignin Valorization through Catalytic Lignocellulose Fractionation: A Fundamental Platform for the Future Biorefinery. *ChemSusChem* 9(13): 1544-1558.

Gomes, E. D. (2019a). Development of a continuous process for the production of vanillin and syringaldehyde from kraft black liquor. PhD, *Faculty of Engineering, University of Porto*.

Karthik, G., M. Angappan, A. VijayaKumar and S. Natarajapillai (2014). Syringic acid exerts antiangiogenic activity by downregulation of VEGF in zebrafish embryos. *Biomedicine & Preventive Nutrition* 4(2): 203-208.

Lahive, C. W., C. S. Lancefield, A. Codina, P. C. J. Kamer and N. J. Westwood (2018). Revealing the fate of the phenylcoumaran linkage during lignin oxidation reactions. *Organic & Biomolecular Chemistry* 16(11): 1976-1982.

Lebo Jr., S. E., J. D. Gargulak and T. J. McNally (2001). Lignin. Kirk-Othmer Encyclopedia of Chemical Technology.

Lin, S. Y. and C. W. Dence (1992). Methods in lignin chemistry, Springer-Verlag.

Lin, S. Y. and C. W. Dence (2012). Methods in Lignin Chemistry, Springer Berlin Heidelberg.

Mansouri, N.-E. E. and J. Salvadó (2006). Structural characterization of technical lignins for the production of adhesives: Application to lignosulfonate, kraft, soda-anthraquinone, organosolv and ethanol process lignins. *Industrial Crops and Products* 24(1): 8-16.

Mathias, A. L. (1993). Produção de vanilina a partir da lenhina: estudo cinético e do processo. Ph.D. Thesis, *Faculdade de Engenharia da Universidade do Porto*.

Mathias, A. L. and A. E. Rodrigues (1995). Production of vanillin by oxidation of *Pine* kraft lignins with oxygen. *Holzforschung* 49(3): 273-278.

Munavalli, D. S., S. A. Chimatadar and S. T. Nandibewoor (2007). Oxidation of vanillin by a new oxidant diperiodatoargentate(III) in aqueous alkaline medium. *Industrial & Engineering Chemistry Research* 46(5): 1459-1464.

Pinto, P. C. R., C. E. Costa and A. E. Rodrigues (2013). Oxidation of lignin from *eucalyptus globulus* pulping liquors to produce syringaldehyde and vanillin. *Industrial & Engineering Chemistry Research* 52(12): 4421-4428.

Pinto, P. C. R., E. A. B. Silva and A. E. Rodrigues (2012). Lignin as source of fine chemicals: vanillin and syringaldehyde. Biomass Conversion: The Interface of Biotechnology, Chemistry and Materials Science. *C. Baskar, S. Baskar and S. R. Dhillon*. Berlin, Heidelberg, Springer Berlin Heidelberg**:** 381-420.

Pinto, P. C. R., E. A. B. d. Silva and A. E. Rodrigues (2011). Insights into oxidative conversion of lignin to high-added-value phenolic aldehydes. *Industrial & Engineering Chemistry Research* 50(2): 741-748.

Pinto, P. R., E. B. d. Silva and A. E. Rodrigues (2010). Comparative Study of Solid-Phase Extraction and Liquid−Liquid Extraction for the Reliable Quantification of High Value Added Compounds from Oxidation Processes of Wood-Derived Lignin. *Industrial & Engineering Chemistry Research* 49(23): 12311-12318.

Pu, Y., D. Zhang, P. M. Singh and A. J. Ragauskas (2008). The new forestry biofuels sector. *Biofuels, Bioproducts and Biorefining* 2(1): 58-73.

Rodrigues, A., P. Pinto, F. Barreiro, C. A. E. Costa, M. I. F. Mota and I. Fernandes (2018). An integrated approach for added-value products from lignocellulosic biorefineries. *Springer Nature Switzerland AG*, Springer International Publishing.

Salvesen, J. R., D. L. Brink, D. G. Diddams and O. Peter, (1945), Process for making vanillin.

Schoeffel, E. W., (1950), Manufacture of vanillin.

Srinivasulu, C., M. Ramgopal, G. Ramanjaneyulu, C. M. Anuradha and C. Suresh Kumar (2018). Syringic acid (SA) – A Review of Its Occurrence, Biosynthesis, Pharmacological and Industrial Importance. *Biomedicine & Pharmacotherapy* 108: 547-557.

Stefanska, J., A. Sarniak, A. Wlodarczyk, M. Sokolowska, Z. Doniec, P. Bialasiewicz, D. Nowak and R. Pawliczak (2012). Hydrogen peroxide and nitrite reduction in exhaled breath condensate of COPD patients. *Pulmonary Pharmacology & Therapeutics* 25(5): 343-348.

Strassberger, Z., S. Tanase and G. Rothenberg (2014). The pros and cons of lignin valorisation in an integrated biorefinery. *RSC Advances* 4(48): 25310-25318.

Sultanov, V. S. and A. F. A. Wallis (1991). Reactivities of guaiacyl and syringyl lignin model phenols towards oxidation with oxygen-alkali. *Journal of Wood Chemistry and Technology* 11(3): 291-305.

Sun, R., J. M. Lawther and W. B. Banks (1995). The effect of alkaline nitrobenzene oxidation conditions on the yield and components of phenolic monomers in wheat straw lignin and compared to cupric(II) oxidation. *Industrial Crops and Products* 4(4): 241-254.

T Hart, B. A., J. M. Simons, K.-S. Shoshan, N. P. M. Bakker and R. P. Labadie (1990). Antiarthritic activity of the newly developed neutrophil oxidative burst antagonist apocynin. *Free Radical Biology and Medicine* 9(2): 127-131.

Tarabanko, V. E., N. A. Fomova, B. N. Kuznetsov, N. M. Ivanchenko and A. V. Kudryashev (1995). On the mechanism of vanillin formation in the catalytic oxidation of lignin with oxygen. *Reaction Kinetics and Catalysis Letters* 55(1): 161-170.

Tarabanko, V. E. and N. Tarabanko (2017). Catalytic oxidation of lignins into the aromatic aldehydes: General process trends and development prospects. *International Journal of Molecular Sciences* 18(11).

Toledano, A., L. Serrano, A. Garcia, I. Mondragon and J. Labidi (2010). Comparative study of lignin fractionation by ultrafiltration and selective precipitation. *Chemical Engineering Journal* 157(1): 93-99.

Tribot, A., G. Amer, M. Abdou Alio, H. de Baynast, C. Delattre, A. Pons, J.-D. Mathias, J.-M. Callois, C. Vial, P. Michaud and C.-G. Dussap (2019). Wood-lignin: Supply, extraction processes and use as bio-based material. *European Polymer Journal* 112: 228-240.

Vishtal, A. and A. Kraslawski (2011). Challenges in industrial applications of technical lignins. *Bioresources* 6: 3547-3568.

Wu, G., M. Heitz and E. Chornet (1994). Improved alkaline oxidation process for the production of aldehydes (vanillin and syringaldehyde) from steam-explosion hardwood lignin. *Industrial and Engineering Chemistry Research* 33(3): 718-723.

Yancheva, D., E. Velcheva, Z. Glavcheva, B. Stamboliyska and A. Smelcerovic (2016). Insights in the radical scavenging mechanism of syringaldehyde and generation of its anion. *Journal of Molecular Structure* 1108: 552-559.

4 Kinetics of oxidative degradation of lignin-based phenolic compounds in batch reactor

The increase of the reaction yields of phenolic monomers from lignin oxidation in alkaline medium still needs deeper knowledge about the behavior of each individual compound since it can be easily degraded. The evaluation of reaction products degradation under oxidation conditions simulating lignin oxidation is an important tool to better understand this reaction and maximize the yield of target value-added products like vanillin and syringaldehyde as the major phenolic aldehydes.

In this chapter, the main objective was to study the degradation kinetics of the main phenolic compounds obtained from lignin oxidation namely vanillin, vanillic acid acetovanillone, syringaldehyde, syringic acid and acetosyringone. The effect of temperature, initial concentration and oxygen partial pressure was also evaluated, and a simple mathematical model was selected to explain the degradation of these phenolics during lignin oxidative depolymerization.

This chapter is based on the following publication:

- Casimiro, F. M.; Costa, C. A. E.; Botelho, C. M.; Barreiro, M. F.; Rodrigues, A. E., Kinetics of Oxidative Degradation of Lignin-Based Phenolic Compounds in Batch Reactor. *Ind. Eng. Chem. Res.* **2019,** 58, 16442-16449.

4.1 INTRODUCTION

Within lignocellulosic biorefineries, lignin conversion to value-added products, such as low molecular weight phenolic compounds, is one of the most straightforward and promising routes to expand lignin applications. In this context, oxidation has been the most studied method for lignin depolymerization (Mathias *et al.*, 1995, Araújo, 2008, Pinto *et al.*, 2011, Pinto *et al.*, 2012, Pinto *et al.*, 2013, Ma *et al.*, 2018). The oxidative depolymerization of lignin involves the cleavage of aromatic rings, aryl ether linkages and/or other linkages in the lignin structure. Lignin oxidation products range from aromatic aldehydes to carboxylic acids, depending on the lignin source and the harshness of the applied reaction conditions (Pandey and Kim, 2011, Pinto *et al.*, 2011, Pinto *et al.*, 2013). Among the possible routes, oxidation in alkaline medium with oxygen was the main method studied by our research group for lignin valorization (Mathias, 1993, Fargues *et al.*, 1996 (a), Araújo, 2008, Pinto *et al.*, 2013).

In general, the improvement of the reaction yields of phenolics from lignin oxidation, still needs deeper knowledge about the behavior of each individual compound. In the literature, there is a lack of studies that report kinetic of oxidation of lignin derived compounds in alkaline medium with oxygen and without heterogeneous catalyst. The main works published use oxidants like H_2O_2 or ozone and heterogeneous catalyst (Benitez *et al.*, 1996, Benitez *et al.*, 2005, Jose *et al.*, 2006, Munavalli *et al.*, 2007, Alunga *et al.*, 2015, Ansaloni *et al.*, 2016, Fawzy *et al.*, 2016, Liu and Zeng, 2018, Singh and Kumar, 2018). Sales and co-workers studied V degradation with similar experimental conditions to those used in this work but with a heterogeneous catalyst (palladium catalyst supported on γ-alumina) (Sales *et al.*, 2006). On the other hand, kinetics of V degradation using oxygen in alkaline medium (NaOH) without heterogeneous catalyst was investigated by Fargues and co-workers who developed a kinetic model to evaluate the degradation of this phenolic compound. This chapter presents an evaluation of the degradation of the main phenolic products derived from lignin oxidation (V, VA, VO, Sy, SA and SO). The kinetic study considering these products individually is of great interest since during oxidation their formation can be simultaneously accompanied by their degradation, process that is dependent on the applied oxidation conditions. Oxidation reactions were made in alkaline medium ([NaOH] = 80 g/L; pH ≈ 14) with molecular oxygen, and the effect of temperature, oxygen partial pressure, and initial concentration of the phenolics was evaluated. A simple mathematical model was developed to describe phenolic compounds degradation using

general PROcess Modelling System software (gPROMS). The study was completed through the determination of activation energy (E_a) and reaction rate constants (k) for all the studied low molecular weight phenolic compounds.

4.2 EXPERIMENTAL SECTION: MATERIALS AND METHODS

4.2.1 Chemicals

Phenolic compounds standards (V, VA, VO, Sy, SA, and SO) were supplied by Sigma – Aldrich (Madrid, Spain), all of them with a purity grade higher than 95 %. Methanol (grade ≥99.8%), formic acid (grade ≥ 99.9%), and sodium hydroxide were provided from Merck (Darmstadt, Germany), oxygen (Alphagaz1 O_2 L50, 10.6 m^3) and nitrogen (Alphagaz1 N_2 L50 9.4 m^3) were supplied from Air Liquid (Maia, Portugal).

4.2.2 Phenolic Compounds Oxidation in Batch Reactor

Oxidation experiments were performed in a Büchi AG laboratory autoclave with a capacity of 1 L (model BEP280 type II, Switzerland). The heating and temperature control was assured by a Haake thermostatic bath (model N2-B, Karlsruhe, Germany). Temperature and total pressure inside the reactor were measured using a thermocouple type K and a pressure transducer (Kulite model XYME-190 M G, Leonia, USA), respectively. The O_2 flow rate was measured by means a mass flow meter EL FLOW (Bronkhorst High-Tech B.V., model F-201C-FAC-11-V, Ruurlo, Netherlands) and expressed as standard cubic centimeters per minute (sccpm). The reaction samples were collected at preset time intervals through an electro valve (Asco Netherlands) assisted by a universal fraction collector Eldex (model 1243, Napa, USA). The signals of the thermocouple, flowmeter, and pressure transducer were recorded using an acquisition board and LabView program. Experimental set-up is presented in Figure 4.1**.** For the oxidation reactions, a selected amount of each phenolic compound (V, VA, VO, Sy, SA or SO) was dissolved in 500 mL of NaOH (80 g/L) solution, introduced into the reactor, heated to the defined temperature, and pressurized. The reaction starts with the admission of O_2. Samples from the reaction mixture were collected at regular time intervals. The analyses of the products were performed by the procedure and equipment/conditions as described in the section 3.2.3.

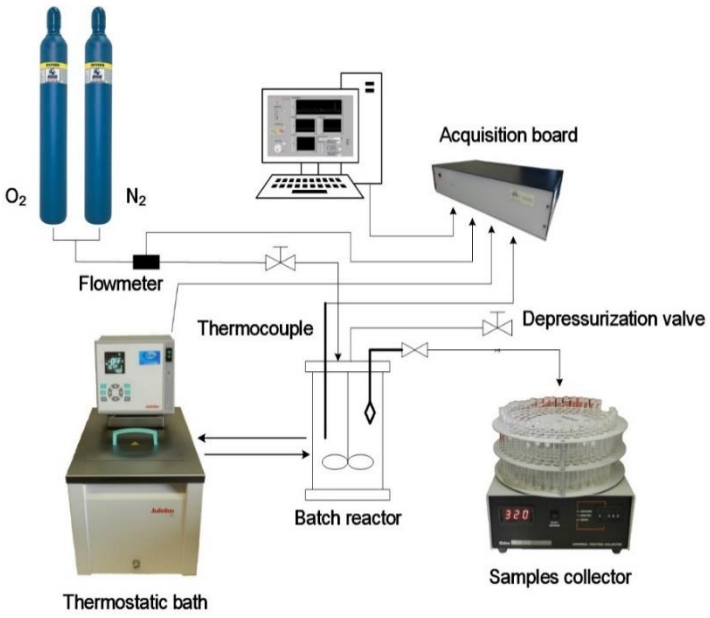

Figure 4.1 - Experimental set-up for kinetic studies of lignin-based phenolic compounds oxidation.

4.3 RESULTS AND DISCUSSION

4.3.1 Kinetic Analysis of V, VA, VO, Sy, SA and SO Degradation

The understanding of the reaction pathways for lignin oxidation can be improved through a preliminary study of the oxidation of model compounds (Alunga *et al.*, 2015). Mathias (Mathias, 1993) developed a simple model for V oxidation in alkaline medium with oxygen, while Fargues, *et al.* (Fargues *et al.*, 1996 (b)) reported a kinetic study of V oxidation using the same conditions.

In this work, the mechanism proposed for V, VA VO, Sy, SA and SO oxidation in alkaline medium with oxygen is based on previously published works (Mathias, 1993, Fargues *et al.*, 1996 (a), Fargues *et al.*, 1996 (b), Alunga *et al.*, 2015). Considering the proposed mechanism, phenolics are dissolved in an alkaline medium to guarantee a high pH (≈14), which implies the dissociation of the phenolics into the ionic forms, and thus react with molecular oxygen. The oxidation of phenolics results from the action of $HOO^{\cdot}$ or $O_2^{\cdot -}$ radicals on the radical $A^{\cdot}$, or from the direct action of molecular oxygen. The degradation mechanism of the phenolic compound *A*, which can be V, VA, VO, Sy, SA or SO, can be represented as:

Initiation	$AH + O_2 \rightarrow A^{\cdot} + HOO^{\cdot}$
Propagation	$A^{\cdot} + O_2 \rightarrow AOO^{\cdot}$
	$AOO^{\cdot} + AH \rightarrow AOOH + A^{\cdot}$
Termination	$AOO^{\cdot} + AOO^{\cdot} \rightarrow$ Products

The equation used to relate the reaction rate with the phenolic compound concentration and oxygen concentration in the liquid phase, $[O_2^{liq}]$, is presented below,

$$r_A = k\,[A]^n \left[O_2^{liq}\right]^m \qquad (4.1)$$

where, r_A is the reaction rate of the phenolic compound in g/(L·min), [A] represent the phenolic concentration in g/L (V, VA, VO, Sy, SA or SO), *k* is the oxidation rate constant in L/(mol·min), and *n* and *m* the reaction orders with respect to initial [A] and $\left[O_2^{liq}\right]$, respectively. The values of pO_2 of the gas phase were converted to concentration of O_2 in the liquid phase using a correlation published by Mathias (Mathias, 1993), equation (2).

$$\left[O_2^{liq}\right] = \left(3.559 - 6.659 * 10^{-3} * T - 5.606 * pO_2 + 1.594 * 10^{-5} * pO_2 * T^2 + 1.498 * 10^3 * \frac{pO_2}{T}\right) * (10^{-0.144*I}) * (10^{-3}) \text{ in mol/L} \qquad (4.2)$$

where I is the ionic strength of the solvent in mol/L. The kinetic model developed was applied to describe the degradation of phenolic compounds in batch reactor during oxidation. The model was solved using general PROcess Modelling System (gPROMS) (PSA Enterprise, United Kingdom) and the Differential-Algebraic equation SOLVer (DASOLV), was used to solve the ordinary differential equation in time. For the model, different assumptions were considered: a) isothermal conditions; b) perfectly mixed reactor; c) constant liquid and gas volumes; d) closed system with respect to the liquid phase; e) constant total pressure; f) mass transfer resistances negligible; g) degradation reactions irreversible. The material balance, described in equation (3), is defined considering the previous assumptions:

$$\frac{d[A]}{dt} = -\ r_A \qquad (4.3)$$

where, *t* is the reaction time. Since the starting liquid mixture consists in an aqueous alkaline solution of the phenolic compound with known concentration, the initial conditions for the material balance are: t = 0 and [A] = [A]i, where [A]i is the initial concentration of each phenolic. The performed oxidation reactions were simulated, fitting the developed kinetic model to the experimental data, and the results are presented in the following sections. Moreover, it can be stated that the developed kinetic model fits all the experimental results concerning the oxidation reactions of the phenolic compounds.

4.3.2 Effect of the Phenolic Initial Concentration

The effect of the initial concentration on the degradation of the selected phenolic compounds (V, VA, VO, Sy, SO, and SA) was evaluated though different oxidation reactions performed at constant temperature, T = 393 K, constant oxygen partial pressure, pO_2 = 3.1 bar, and constant total pressure, P_T = 9.8 bar. The initial concentration of each phenolic compound ranged between 1.3 – 5.0 g/L for V, VA, and VO and 0.75 – 2.5 g/L for Sy, SA and SO. The alkaline medium contained a [NaOH] = 80 g/L. The solubility of each compound influenced the selected concentration range, reason why the derivatives from S units were tested at lower initial concentrations than the G units derivatives.

Figure 4.2 shows the effect of initial concentration on the degradation yield, for each studied phenolic compound. For V, VA, and VO it was verified that initial concentration does not affect degradation yields. After 100 minutes of reaction time, V has a degradation level comprised between 14 and 17 %, independently of the used initial concentration. After the same reaction time, VA shows a complete degradation in all the performed oxidation reactions, being the most reactive compound considering G units derivatives. VO shows a degradation level between 23 and 28 % for the performed oxidation reactions, which means that initial concentration does not significantly affect its degradation. In a previous study addressing the kinetics of V oxidation, Fargues and co-workers also stated that the initial concentration does not affect V degradation yield, i.e. the degradation is almost the same independently of the tested initial concentration (Fargues *et al.*, 1996 (b)).

Concerning Sy, SA and SO, a similar behavior was observed; the initial concentration of these phenolic compounds does not impact their degradation yield. Sy shows a degradation around 84 % after 100 minutes of reaction time independently of the used initial concentration. Considering SA, it appears to be a very reactive compound, with a complete

degradation in less than 15 minutes for all the experimental oxidation conditions. SO also showed a complete degradation, whatever the used initial concentration, but only after surpassing a reaction time of 100 minutes.

4.3.3 Effect of Oxygen Partial Pressure

To evaluate the effect of the oxygen partial pressure, pO_2 on the phenolic compounds (V, VA, VO, Sy, SA, SO) degradation, during oxidation in batch reactor, oxidation reactions were performed in alkaline medium, [NaOH] = 80 g/L, at constant total pressure, P_T = 9.8 bar, constant temperature, T = 413 K, and constant initial concentration of the phenolic compound, 2.5 g/L. The tested pO_2 in the various runs was 2.0, 3.1 and 5.1 bar.

The concentration of V, VA, VO, Sy, SA and SO versus reaction time, for each oxidation performed with different pO_2 is shown in Figure 4.3. The results indicated that VA, Sy, SA and SO have a complete degradation after 80 minutes of reaction, independently of the used pO_2. In the case of V and VO the degradation was not complete even after 140 minutes of reaction, independently of the used pO_2. Moreover, in the reaction conducted under a pO_2 of 5 bar, 44 % of the initially used V was degraded after 80 minutes, while for the reactions using a pO_2 of 3 and 2 bar, for the same reaction time, 32 % and 26 % of degradation was obtained, respectively. Considering VO, it was also observed that the increase in pO_2 enhances the degradation of this phenolic; in the reaction with 2 bar of pO_2, only 42 % of the initial VO was degraded after 80 minutes, comparatively with 55 % and 70 % when 3 and 5 bar of pO_2 was used, respectively. In general, the increase of pO_2 led to an increase in the degradation of the phenolic compound.

4.3.4 Effect of Temperature on the Reaction Rate

In this series of experiments V, VA, VO, Sy, SA and SO oxidation was performed in alkaline medium, [NaOH] = 80 g/L], at constant total pressure, P_T = 9.8 bar, constant oxygen partial pressure, pO_2 = 3.1 bar (except for Sy, SA and SO, pO_2 = 3.0 bar) and an initial concentration of 2.5 g/L. Temperature was 373, 393 and 413 K.

The results showed that the increase of temperature enhanced the degradation of all studied phenolic compounds (Figure 4.4). When an initial T of 413 K was used, a degradation of 24%, 100% and 39% was found for V, VA, and VO, respectively, after 1 hour of reaction. It can also be observed that VA is the compound most susceptible to

degradation, with 41 % of degradation before 60 minutes of reaction when an initial temperature of 373 K was used.

With a temperature of 413 K it was observed a complete degradation for SA and SO at the end of a reaction time of 1 hour, and a degradation of 94 % for Sy. Lower degradations were detected when a temperature of 373 K was used, achieving a degradation of 46 %, 100 % and 57 % for Sy, SA and SO respectively after one hour of reaction time.

In the oxidation of phenolic ketones (VO and SO) a small amount of the corresponding phenolic aldehydes, V and Sy, respectively, were produced. This is most noticeable when the reactions are performed using an initial temperature of 413 K. Fung and Hrutfiord (Fung and Hrutfiord, 1987) published a patent concerning the alkaline oxidation of VO to produce V, where it was stated that the applied reaction conditions affected the conversion yield. Alunga and co-workers have also reported V and Sy formation through VO and SO oxidation, respectively (Alunga *et al.*, 2015). The authors used $CuSO_4$ as the catalyst on the oxidation reactions concluding that the rate of V formation increases with the use of higher temperatures.

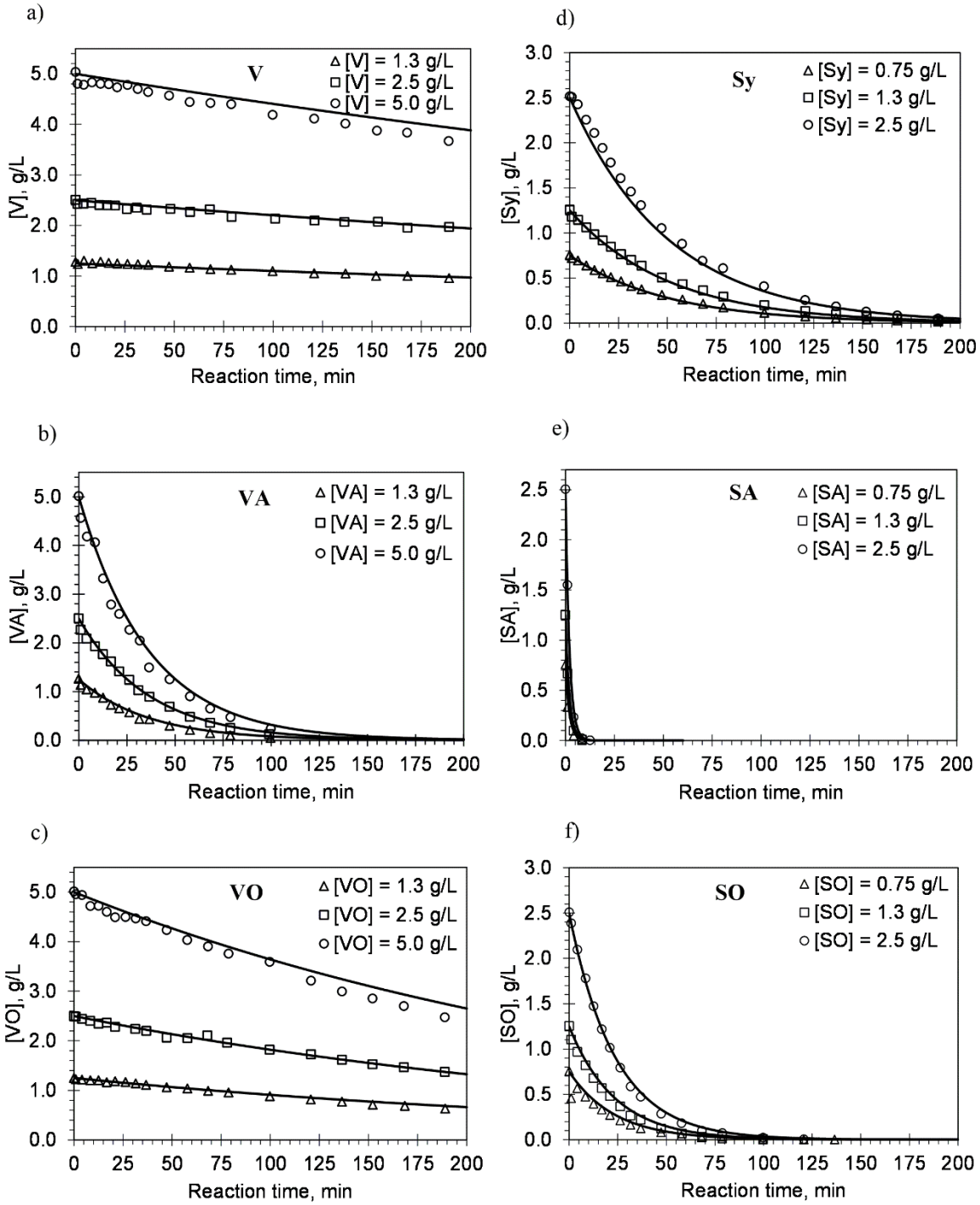

Figure 4.2 - Effect of initial concentration on degradation along oxidation reaction time: (a) V, (b) VA, (c) VO, (d) Sy, (e) SA, (f) SO and the line represents the fitted kinetic model (—). Initial reaction conditions: [NaOH] = 80 g/L; pH≈14; Ti=393 K; pO_2=3 bar; P_T=9.8 bar.

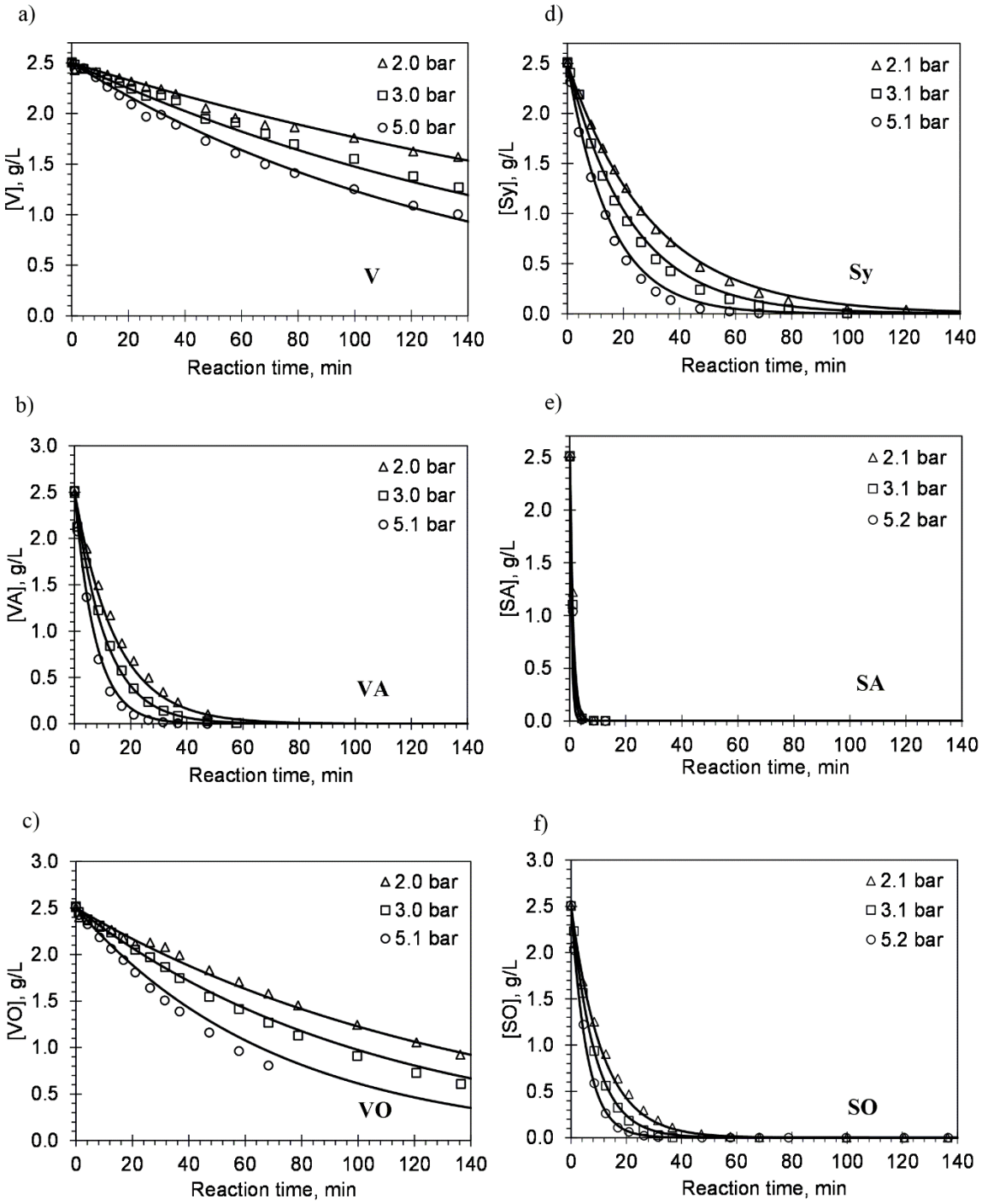

Figure 4.3 - Effect of oxygen partial pressure on degradation as a function of reaction time: (a) V, (b) VA, (c) VO, (d) Sy, (e) SA, (f) SO and the line represents the fitted kinetic model (—). Initial reaction conditions: [NaOH] = 80 g/L; pH ≈ 14; initial concentration of compounds 2.5 g/L; T_i = 413 K; P_T = 9.8 bar.

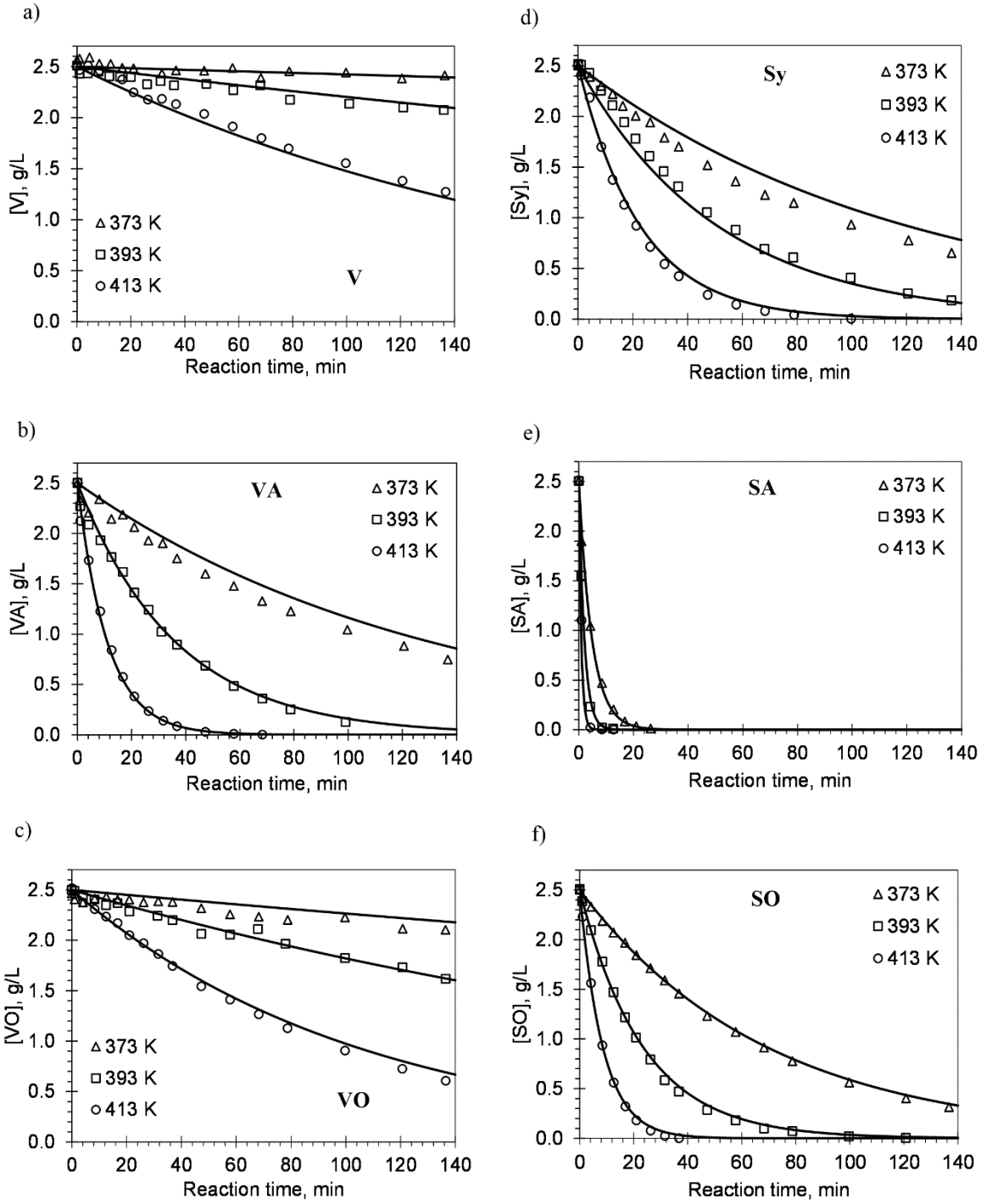

Figure 4.4 - Effect of temperature on degradation as a function of oxidation reaction time: (a) V, (b) VA, (c) VO, (d) Sy, (e) SA, (f) SO and the line represents the fitted kinetic model (—). Initial reaction conditions: [NaOH] = 80 g/L; pH ≈ 14; initial concentration of compound 2.5 g/L; pO_2 = 3.0 bar; P_{total} = 9.8 bar.

4.3.5 Kinetic Parameters

The kinetic parameters used to develop the model that fit the experimental data were described in detail in section 5.3.1. The reaction orders, *n*, and *m*, from equation (4.1), were determined from de slope of the logarithmic representation of *r0* (initial reaction rate for different T) as a function of the logarithmic phenolic initial concentration and logarithmic $[O_2^{liq}]$, respectively. The results showed that, for all the studied phenolics, V, VA, VO, Sy, SA and SO, the reaction order with respect to the phenolic initial concentration, was 1. The first order dependence was also obtained for $[O_2^{liq}]$. Fargues and co-workers have also found a reaction order of 1 with respect to V concentration and to $[O_2^{liq}]$, whereas Alunga and co-workers reported that the kinetic reaction for VO degradation was also of first order (Fargues *et al.*, 1996 (b), Alunga *et al.*, 2015).

The equation describing the reaction kinetics for any of the compound *A* studied, V, VA, VO, Sy, SA and SO, is given by:

$$r_A = k[A]^1[O_2^{liq}]^1 \text{ in g/L·min}^{-1} \quad (4.4)$$

As stated before, temperature has a significant impact on phenolic compounds degradation and its dependence can be explained by the Arrhenius equation (4.5), which was applied for the determination of kinetic parameters.

$$k = k_0\, e^{-\frac{Ea}{RT}} \quad (4.5)$$

where *T* is the absolute temperature (in kelvins); k_0 is the pre-exponential factor; E_a is the activation energy for the reaction (in J·mol^{-1}); and *R* is the universal gas constant. Equation (4.5) can be linearized as:

$$\ln(k) = \ln(k_0) - \frac{Ea}{R}\frac{1}{T} \quad (4.6)$$

The Arrhenius plot, ln (k) *versus* 1/T, for V, VA, VO and Sy, SA, SO degradation kinetics is presented in Figure 4.5. The slope from the graphic representation of the logarithm of k (T) as a function of 1/T allows determine E_a for each phenolic compound.

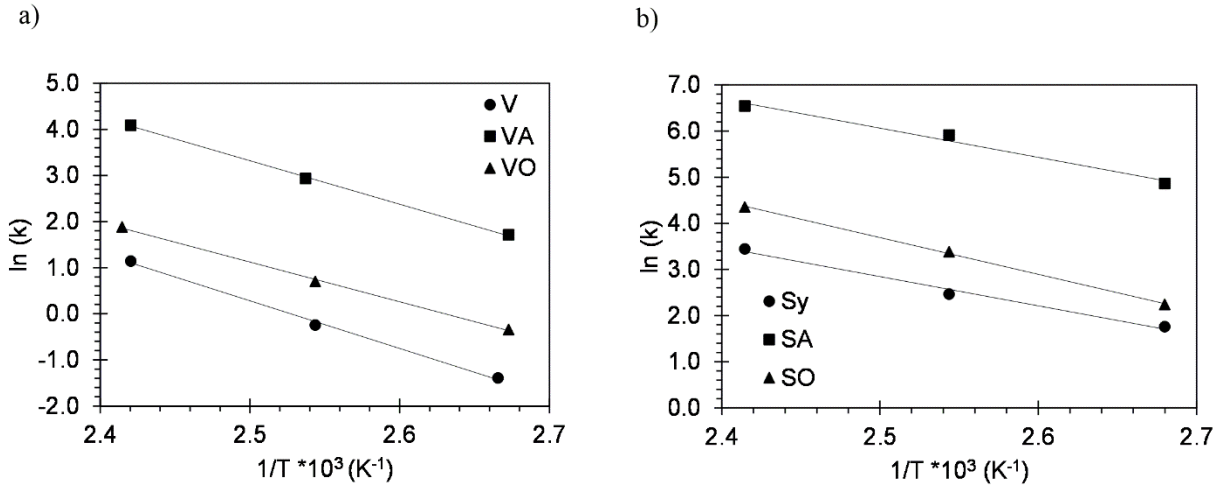

Figure 4.5 - Arrhenius plot, logarithm of k versus 1/T, for the calculation of the activation energy of (a) V, VA, VO and (b) Sy, SA, SO oxidation.

Table 4.1 summarizes the obtained activation parameters for V, VA, VO, Sy, SA and SO oxidation in alkaline medium with oxygen. The calculated E_a values for V (86.0 kJ/mol) is similar to the one determined by Fargues and co-workers or Wallick and Sarkanen (Wallick and Sarkanen, 1983, Fargues *et al.*, 1996 (b)). Also, Alunga and co-workers reported, in a study about VO degradation with heterogeneous catalyst, a value of E_a for VO, 85.3 kJ/mol, similar to that obtained in this work (Alunga *et al.*, 2015). Kalyani and Jamunarani investigated Sy oxidation with hexacyanoferrate (III) in alkaline medium and reported a E_a of 48.40 kJ/mol (Kalyani and Jamunarani, 2015).

Table 4.1 – Summary of activation parameters for V, VA, VO, Sy, SA and SO oxidation in alkaline medium.

	V	**VA**	**VO**	**Sy**	**SA**	**SO**
E_a, **kJ mol^{-1}**	86.0±1	78.4±1	71.6±1	52.7±1	52.7±1	66.2±1
$-E_a/R$	-10348	-9427	-8610	-6336	-6335	-7956
k_0	2.27E+11	4.75E+11	6.84E+09	1.30E+08	3.25E+09	1.74E+10

Concerning the reaction rates, in a general way, the results shown that the increasing in the initial concentration, pO_2 or T enhanced the initial reaction rate for all the studied phenolic compounds. The reaction rate range varies between 9.39E-03 $g/L \cdot min^{-1}$ and 1.34E+00 $g/L \cdot min^{-1}$. The phenolic presenting the highest degradation reaction rate was SA, whereas the one with the lower reaction rate was V.

4.4 CONCLUSIONS

The study of the degradation of valuable phenolic compounds obtained from lignin oxidation in alkaline medium with O_2 was the main objective of this work. The performed kinetic study allowed evaluating the reaction orders with respect to V, VA, VO, Sy, SA, and SO initial concentration, and oxygen concentration, as well as the effect of temperature on the kinetic rate constants. The results showed that the initial concentration of phenolic compounds as well as the oxygen concentration, had no effect on the degradation reaction rate, since a first order dependence for both oxidation parameters was obtained for all the studied compounds. The developed pseudo-first-order model fits well with the experimental data, considering the oxidative degradation of all phenolic compounds studied. The activation parameters were calculated, achieving an activation energy in the range of 53 - 86 kJ/mol was found for V, VA, VO, Sy, SA and SO. Comparing all the tested phenolic, it was possible to conclude that Sy, SA, and SO have higher degradation rate, in comparison with V, VA, and VO. This is an expected behavior since derivatives from S units are more reactive than the G ones due to the presence of two methoxyl groups in the aromatic ring in the later compounds.

4.5 REFERENCES

Alunga, K. R., Y.-Y. Ye, S.-R. Li, D. Wang and Y.-Q. Liu (2015). Catalytic oxidation of lignin-acetoderivatives: a potential new recovery route for value-added aromatic aldehydes from acetoderivatives. *Catalysis Science & Technology* 5(7): 3746-3753.

Ansaloni, S., N. Russo and R. Pirone (2016). Wet Air Oxidation of Acetovanillone over LaFeO3 as Catalyst: A Model Reaction for Lignin Valorization.

Araújo, J. D. P. (2008). Production of vanillin from lignin present in the kraft black liquor of the pulp and paper industry. Ph.D. Dissertation, *Faculty of Engineering University of Porto*.

Benitez, F. J., J. Beltran-Heredia and J. L. Acero (1996). Oxidation of Vanillic acid as a model of polyphenolic compounds in olive oil wastewaters. III. Combined UV radiation-hydrogen peroxide oxidation. *Toxicological & Environmental Chemistry* 56(1-4): 199-210.

Benitez, F. J., F. J. Real, J. L. Acero, A. I. Leal and S. Cotilla (2005). Oxidation of Acetovanillone by Photochemical Processes and Hydroxyl Radicals. *Journal of Environmental Science and Health, Part A* 40(12): 2153-2169.

Fargues, C., Á. Mathias and A. Rodrigues (1996 (a)). Kinetics of vanillin production from kraft lignin oxidation. *Industrial & Engineering Chemistry Research* 35(1): 28-36.

Fargues, C., A. Mathias, J. Silva and A. Rodrigues (1996 (b)). Kinetics of vanillin oxidation. *Chem. Eng. Technol.* 19: 127- 136.

Fawzy, A., I. A. Zaafarany, I. Althagafi, J. Alfahemi and M. Morad (2016). Kinetics and Mechanism of Oxidation of Vanillin by Permanganate in Neutral Medium and the Effect of Different Transition Metal Ion Catalysts.

Fung, B. S. K. and B. F. Hrutfiord, (1987), Oxidation of acetovantillone to vanillin.

Jose, T. P., S. T. Nandibewoor and S. M. Tuwar (2006). Kinetics and Mechanism of the Oxidation of Vanillin by Hexacyanoferrate(III) in Aqueous Alkaline Medium. *Journal of Solution Chemistry* 35(1): 51-62.

Kalyani, A. G. and R. Jamunarani (2015). Oxidation of Syringaldehyde by Alkaline Hexacyanoferrate (III)–A Kinetic and Mechanistic Study.

Liu, C. and C. Zeng (2018). Heterogeneous kinetics of methoxyphenols in the OH-initiated reactions under different experimental conditions. *Chemosphere* 209: 560-567.

Ma, R., M. Guo and X. Zhang (2018). Recent advances in oxidative valorization of lignin. *Catalysis Today* 302: 50-60.

Mathias, A. L. (1993). Produção de Vanilina a partir da Lenhina: Estudo Cinético e do Processo. Ph.D. Thesis, *Faculdade de Engenharia da Universidade do Porto*.

Mathias, A. L., M. I. Lopretti and A. E. Rodrigues (1995). Chemical and biological oxidation of Pinus pinaster lignin of the production of vanillin. *Journal of Chemical Technology & Biotechnology* 64(3): 225-234.

Munavalli, D. S., S. A. Chimatadar and S. T. Nandibewoor (2007). Oxidation of vanillin by a new oxidant diperiodatoargentate(III) in aqueous alkaline medium. *Industrial & Engineering Chemistry Research* 46(5): 1459-1464.

Pandey, M. P. and C. S. Kim (2011). Lignin Depolymerization and Conversion: A Review of Thermochemical Methods. *Chemical Engineering & Technology* 34(1): 29-41.

Pinto, P. C. R., C. E. Costa and A. E. Rodrigues (2013). Oxidation of lignin from *eucalyptus globulus* pulping liquors to produce syringaldehyde and vanillin. *Industrial & Engineering Chemistry Research* 52(12): 4421-4428.

Pinto, P. C. R., E. A. B. Silva and A. E. Rodrigues (2012). Lignin as source of fine chemicals: vanillin and syringaldehyde. Biomass Conversion: The Interface of Biotechnology, Chemistry and Materials Science. *C. Baskar, S. Baskar and S. R. Dhillon*. Berlin, Heidelberg, Springer Berlin Heidelberg**:** 381-420.

Pinto, P. C. R., E. A. B. d. Silva and A. E. Rodrigues (2011). Insights into oxidative conversion of lignin to high-added-value phenolic aldehydes. *Industrial & Engineering Chemistry Research* 50(2): 741-748.

Sales, F. G., L. C. A. Maranhão, N. M. Lima Filho and C. A. M. Abreu (2006). Kinetic Evaluation and Modeling of Lignin Catalytic Wet Oxidation to Selective Production of Aromatic Aldehydes. *Industrial & Engineering Chemistry Research* 45(20): 6627-6631.

Singh, K. and A. Kumar (2018). Kinetics of complex formation of Fe(III) with syringic acid: Experimental and theoretical study. *Food Chemistry* 265: 96-100.

Wallick, S. A. and K. V. Sarkanen (1983). Effect of pH on the autoxidation kinetics of vanillin. *Wood Science and Technology* 17(2): 107-116.

5 Recovery of Vanillin from an Oxidized Mixture of Softwood Lignin from a Pulp Mill Sulfite Liquor

In this chapter, an oxidation mixture of a lignin from a pulp mill softwood sulfite liquor was submitted to a sequential process of filtration and adsorption/desorption experiments aiming the recovery of vanillin. A two-step filtration using ultra and nanomembranes with a molecular weight cut-off of 2 kDa and 800-600 Da, respectively, was used to concentrate the low molecular phenolic compounds of interest, namely the vanillin. The permeate from nanofiltration proceeds to fractionation by adsorption/desorption experiments using a non-polar resin (SP700) to obtain an enriched fraction in vanillin. This fraction will be purified by crystallization, the topic will be discussed in a next chapter.

5.1 INTRODUCTION

As already stated, lignin can be used as a viable source for highly functionalized chemicals however, the recovery of phenolic compounds from lignin oxidation mixtures remains a challenge. Depending on the lignin source, the main products from lignin oxidation in an alkaline medium with oxygen are vanillin (V) and syringaldehyde (Sy). However, vanillic acid (VA), syringic acid (SA), acetovanillone (VO), and acetosyringone (SO), among others, are also products from lignin oxidation but in minor quantities. The similar structure and acid dissociation constant of these compounds make it difficult to separate them from the lignin-rich oxidation medium (Mota *et al.* 2016). The challenging separation of the obtained phenolic compounds in a single separation process implies the need of a sequence of processes for its efficient recovery (Mota *et al.* 2016).

In the perspective of lignin valorization, ultrafiltration or nanofiltration are promising separation technologies to recover the low molecular weight phenolic compounds of interest from the reaction medium of depolymerized lignin (Žabková *et al.* 2007b, Mota *et al.* 2018). Membrane separation can be easily integrated after the oxidation process and constitutes a good alternative over other methods (evaporation, distillation) since it is an environmentally friendly technology with lower energy requirements, good physical and chemical stability, reproducible performance and selectivity (Mota *et al.* 2018).

Zabkova and co-workers have investigated the recovery of vanillin from lignin oxidation medium by ultrafiltration. In this work, the influence of lignin and vanillin concentration, and the pH of the mixture on the ultrafiltration process has been studied (Žabková *et al.* 2007b). The authors found that when a membrane with a low cut-off is used V in permeate shows high purity moreover, also a higher lignin rejection is observed. The fractionation of an oxidized industrial kraft liquor by 3 stages of ultrafiltration was investigated by Mota and co-workers (Mota *et al.* 2018) using a tubular ceramic membrane with molecular weight cut-off of 50, 5, and 1 kDa. It was reported by the authors that the content of total solids in the permeate stream gradually decreases along the sequence, and an enrichment in total phenolics is observed: from 2.8 % (feed) to 3.7 % (permeate from 1 kDa membrane), in terms of composition (%w/$w_{\text{Total solids}}$) (Mota *et al.* 2018).

Adsorption experiments represent an interesting approach for the separation of the phenolic compounds of interest from dilute solutions and it can be integrated with the membrane separation process. This technology can be accessible to design and scale up, and combined with an adsorbent with high capacity and easy to regenerate becomes an

economically viable process (Mota *et al.* 2020). The application of nonpolar macroporous polymeric resins presents a series of advantages, including the wide range of structures and properties available, high adsorption capacity and selectivity, good performance to the recovery of the adsorbed molecules, chemical stability, relatively low cost, and easy regeneration (Soto *et al.* 2012, Mota *et al.* 2016). Many works in literature dealt with recovery of phenolic compounds from standard solutions using polymeric resins, but few of those studies deal with real depolymerized lignin mixtures. Our team in LSRE-LCM studied the separation of phenolic monomers using resins, including a work about the fractionation of acids, ketones and aldehydes from alkaline lignin oxidation solution with a non-polar resin (SP700) (Gomes *et al.* 2018). The author studied the influence of pH of the feed mixture on the separation of phenolic monomers, ranging from 9 to 12, and was found that a pH 12 is better to concentrate aldehydes and ketones (Gomes *et al.* 2018).

In this chapter a lignin solution from an industrial pulp mill softwood sulfite liquor (LSSL), which was previously oxidized in alkaline medium with oxygen, was submitted to a two-step filtration with ultra and nanofiltration membranes, (2 kDa and 600-800 Da). At this stage the low molecular phenolic compounds of interest were concentrated in the permeate from nanofiltration. The mixture was then fractionated by an adsorption/desorption process with a non-polar resin SP700, to obtain an enriched fraction in the target phenolic compound, namely V.

5.2 EXPERIMENTAL SECTION: MATERIALS AND METHODS

5.2.1 Lignin Oxidative Depolymerization

Lignin was obtained from a softwood sulphite liquor (11.3 % w/w_{liquor} total solids), supplied by a pulp mill of Company A, from a mixture of 90 % of spruce and 10 % of beech. The liquor was submitted to ultrafiltration, using a membrane of 5 kDa, and the resulting retentate was freeze-dried to obtain the lignin used in this work. Lignin from softwood sulfite liquor (LSSL) was submitted to oxidative depolymerization in alkaline medium (NaOH 2 M) with oxygen (pO_2 = 3 bar and P_{total} = 9.8 bar) in a batch reactor at 120 ºC. Detailed information about the experimental set-up and the operation conditions were described in the section 3.2.6.

5.2.2 Ultra and Nanofiltration of LSSL Oxidized Stream

The ultra and nanofiltration experiments were performed using a laboratory crossflow module, Figure 5.1, supplied by GE Osmonics, model SEPA CF II. The system comprises a filtration cell connected to a variable speed Hydracell pump (M-3/G-13 model, from Wanner Engineering, Inc.) fitted with a flow meter. Transmembrane pressure (TMP) was controlled by a needle valve located after the membrane module in the retentate side, and the operating pressure used during the ultra and nanofiltration experiments was 18 and 30 bar, respectively. All experiments were carried out in full recycling mode.

Figure 5.1 – Experimental set-up used in ultra and nanofiltrations.

The resulting mixture from LSSL oxidation was treated by a flat sheet membrane system using a two-step sequence of ultra and nanofiltration membranes, with molecular weight cut-off (MWCO) of 2 kDa and 600-800 Da, respectively. Both membranes are made from a thin film composite of polyamide with an effective membrane surface area of 0.014 m^2. The main characteristics of the membranes used are detailed in Table 5.1.

Before filtration of the oxidized mixture, water permeability tests were performed at several pressures, in the range of the operating pressure of each membrane. For each pressure tested, three measurements of volume permeated were made. Membranes were first flushed with deionized water at 25 ºC and a TMP of 18 for GH 2 kDa membrane and 30 bar for NFG 600-800 Da membrane, for 30 minutes. Then, the water flux was measured in the range of operation pressure: 4 - 18 bar for the ultrafiltration membrane and 15 - 30 bar for the nanofiltration membrane.

Total dissolved solids (TDS) were determined for the LSSL oxidized mixture, the permeates, and the retentates resulting from ultra and nanofiltration. For TDS determination,

20.0 mL of each solution was added to prior dried crucibles containing calcined and sieved sand. The crucibles with the solutions were dried at 105 °C until reached constant weight.

Table 5.1 – Characteristics of ultra (GH) and nano (NFG) filtration membranes.

Membrane	**GH**	**NFG**
Manufacturer	GE Power & Water	Synder
Membrane MWCO, Da	2000	600-800
Composition	Polyamide TFC	Polyamide TFC
Max. temperature, ºC	70	50
Max. pressure, bar	27	40
pH range	1-11 (25 ºC)	4-10 (25 ºC)
Typical operating flux, LMH	34.0	93.5 - 102

5.2.3 Fixed Bed Adsorption/Desorption Experiments

The experiments were performed in a chromatographic installation (Figure 5.2) composed by a jacketed glass column (Merck–Darmstadt, diameter of 2.6 cm and length 13.0 cm) connected to a preparative chromatography pump with maximum volumetric flowrate of 50 mL/min (KNAUER, model Smartline P1000).

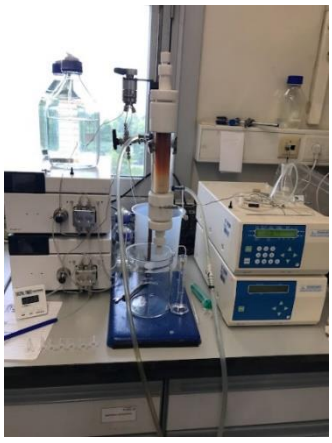

Figure 5.2 - Chromatographic installation used in the adsorption/desorption experiments.

Two more chromatographic pumps (KNAUER, model PUMP 40P) were also coupled to pump the eluents in the desorption phase, each one with maximum flowrate of 50 mL/min. The column was packed with nonpolar SP700 resin previously activated as described in the

next section. The jacketed column was kept at 25 °C by a thermostatic bath (LAUDA, model RE 104). Tracer experiments were performed using blue dextran at 5 mL/min thus allowing the determination of bed porosity of 0.4, and a mean liquid residence time of 372 s.

5.2.3.1 Resin activation

SP700 resin (properties detailed in Table 5.2) was activated following the procedure described by Mota and co-workers (Mota *et al.* 2016). The resin was placed in a flask with excess water, and the floating dry resin was removed. After that, the resin was filtered with vacuum and placed in a flask with excess water and was left in the orbital shaker at 170 rpm for at least 30 minutes. This step was repeated once more and afterwards the resin was rinsed with methanol, filtered, and placed in a flask with methanol acidified with 0.1% (v/v) of formic acid and left in the orbital shaker for another 30 minutes. Then, the resin was filtered out, rinsed with water acidified with 0.1% (v/v) of formic acid, and shaken for 30 minutes with excess acidified water. Finally, the resin was rinsed several times with deionized water and used to pack the column.

Table 5.2 – Physical and chemical properties of SP700 resin.

Property	Value/designation
Resin denomination	SP700
Manufacturer	Mitsubishi Chemical Corp.
Matrix	Poly divinylbenzene-ethylvinylbenzene
Water Content, %	60-70
Particle density, g/ml	1.02
Specific surface area, m^2/g	1100
Particle size, mm	0.25
Pore volume, mL/g	2.2
Pore radius, Å	90

5.2.3.2 Breakthrough experiment

During the breakthrough experiment, the column was fed for 8 h with a multi-component model solution, MMS, composed of VA, V, Sy, and VO. The MMS was prepared in NaOH (2 M) to maintain the pH of the real solution. The phenolic monomers concentration in MMS was prepared based on the respective values in the permeate from

nanofiltration of the oxidized LSSL mixture. Initial concentrations of the phenolic compounds in the MMS are detailed in the Table 5.3. The breakthrough experiment was carried out at a volumetric flow rate of 5 mL/min and the temperature of the jacketed column was kept at 25 ℃. The samples were collected at preset times: two in two minutes until the first 10 minutes, and then five in five minutes until 480 minutes. The concentration of VA, V, Sy, and VO in the samples collected at the outlet of the chromatographic column was determined by HPLC, as described in section 3.2.3.

Table 5.3 – Feed concentrations of the phenolic monomers in MMS used for breakthrough experiment.

	VA	**V**	**Sy**	**VO**
Feed stream, g/L	0.71	2.38	0.06	0.24

5.2.3.3 Adsorption/desorption cycles

The MMS prepared to perform the adsorption/desorption cycles was similar, concerning the pH and the concentrations of the phenolic compounds, to the MMS used for the breakthrough experiment (Table 5.3). The adsorption/desorption cycles were performed by feeding MMS for 90 minutes. Then desorption step was performed using two eluents, first water deionized, for 45 minutes, and then ethanol (99 % v/v) for more 45 minutes, both at a volumetric flowrate of 5 mL/min. Four cycles of adsorption/desorption were performed using MMS and 8 cycles were performed with the permeate from nanofiltration of the LSSL mixture.

5.3 RESULTS AND DISCUSSION

5.3.1 Ultra and Nanofiltration of LSSL Oxidized Stream

5.3.1.1 Water membrane permeability

Water permeability of each membrane was evaluated by measuring deionized water permeate flowrate at different values of TMP, in recirculation mode. The permeate flux was measured over time after the stabilization of the feed flow rate at 156 $L.h^{-1}$, at ambient

temperature. For ultrafiltration membrane (GH 2 kDa) the applied TMP were in the range 4–18 bar and for nanofiltration membrane (NFG 600-800 Da) the range was 15–30 bar.

Water permeate flux (J_w) was determined for each membrane (GH 2 kDa and NFG 600-800 Da) allowing obtaining the membrane hydraulic resistance coefficient (R_m, m^{-1}) by applying the Darcy´s law:

$$J_w = \frac{TMP}{\mu_0 R_m} \quad (5.1)$$

where μ_0 (Pa.s) is the viscosity of water at 25 ºC. The water permeate flux, calculated from equation (5.1), for each TMP is represented in Figure 5.3 for ultra and nanofiltration membranes.

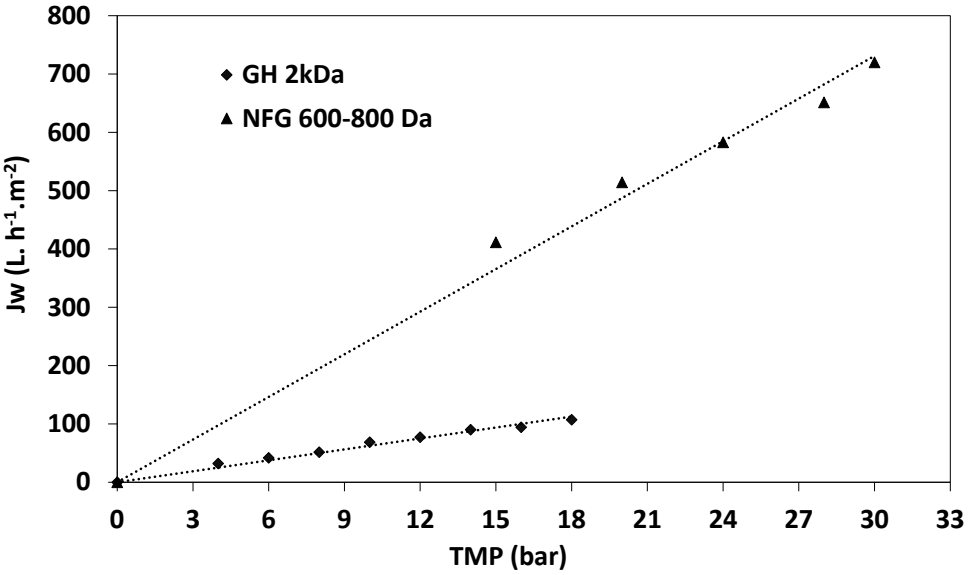

Figure 5.3 - Water permeate fluxes through the membranes of 2 k and 600-800 Da for different TMP at 25 ºC, a feed flowrate set to 156 $L.h^{-1}$ and a membrane surface area of 0.014 m^2.

The water permeate flux increased with the increase of TMP for both membranes. The NFG membrane showed a water permeability of 24.4 L m^{-2} h^{-1} bar^{-1} and GH membrane of 6.2 L m^{-2} h^{-1} bar^{-1}. Moreover, it would be expected that the membrane with higher cut-off show higher value of permeability instead, in the Figure 5.3 it is possible to observe that the water permeate flux is higher for NFG membrane (600-800 Da). This behavior can be explained based on the typical operating flux of this membrane: besides its lower molecular weight cut-off, the NFG membrane (600-800 Da) has a typical operating flux three times higher than the GH 2 kDa membrane (Table 5.1).

5.3.1.2 Filtration of LSSL oxidized mixture

The mixture resulting from the oxidation with O_2 in alkaline medium of LSSL lignin was submitted to ultra and nanofiltration using a GH membrane with a molecular weight cutoff of 2 kDa and a NFG membrane of 600-800 Da, respectively. The experiment was carried out with a total recirculation of the feed solution. Before ultrafiltration, the oxidation mixture was filtered without any neutralization. The sequence of ultra and nanofiltration process applied to oxidized LSSL mixture is represented in Figure 5.4, and the operating conditions of experiments were shown in Table 3.1.

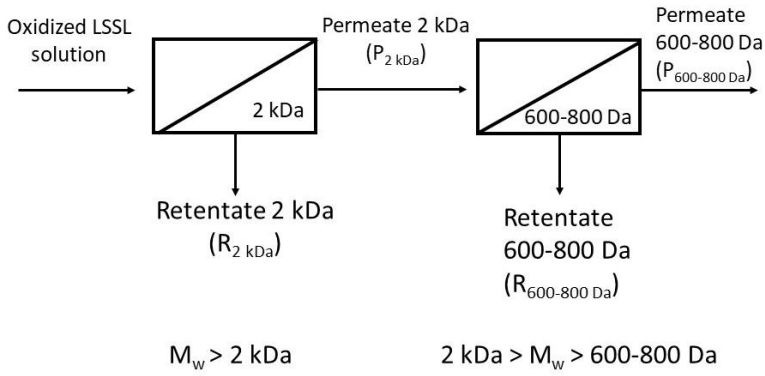

Figure 5.4 - Schematic representation of the ultra and nanofiltration process applied to the oxidized LSSL mixture performed with 2 k and 800-600 Da membranes.

A starting volume of about 6.5 L of oxidized LSSL mixture was processed. In the first step of ultrafiltration, the oxidized mixture was treated with the highest membrane cut-off, 2 kDa, which resulted in a volume reduction (VR, permeate volume divided by initial feed volume) of 0.81. This value means that the initial volume of the mixture from oxidation of LSSL lignin was reduced so that about 19% remained as retentate. Moreover, a volume concentration factor (VCF) of 5.2 (initial feed volume divided by the retentate volume) was reached. In the nanofiltration, the resulting permeate stream from the first step (P_{2kDa}) was further processed using the NFG 800-600 Da cut-off membrane, which resulted in a VR of 0.86 corresponding to a VCF of 7.0. The permeate flux behavior with time observed during the ultra and nanofiltration sequence was graphically represented in Figure 5.5. Permeate flux, J_p ($m^3.s^{-1}.m^{-2}$), was calculated as following:

$$J_p = \frac{Q_p}{A_m} \qquad (5.2)$$

where Qp ($m^3.s^{-1}$) is the permeate flowrate measured for a certain TMP and A_m is the effective membrane surface area (0.014 m^2). The permeate flux, calculated from equation (5.2), in the beginning and at the end of the processing with each membrane is presented in Table 5.4.

Table 5.4 – Ultra and nanofiltration operating conditions.

	Oxidized LSSL mixture	**P_{2kDa}**
Membrane MWCO, Da	2000	600 - 800
Solution pH (25 ºC)	13.2	13.2
Pressure, bar	22	21
Initial volume, mL	6500	5200
Permeate volume, mL	5200	4460
Volume concentration factor (VCF)	5.2	7.0
Initial flux, $L.m^{-2}.h^{-1}$	16.3	69.5
Final flux, $L.m^{-2}.h^{-1}$	10.4	154.1

During ultrafiltration with GH 2 kDa membrane the flux decreased with the processing time (Figure 5.5). The observed decrease of the initial permeate flux could be related with the high molecular weight fractions of oxidized lignin and the high content of solids presents in the oxidation mixture that form a cake layer at the membrane surface, causing a flux reduction. In contrast, the nanofiltration with NFG 600-800 Da membrane showed an increase in their flux during the processing (Figure 5.5). This behavior could be a consequence of the temperature variation of the feed solution (P_{2kDa}), which in the beginning of the processing was lower than 18 ºC and after 2 hours reach 28 ºC. It is well known that when the filtration proceed at high temperatures lower retention is observed since it leads to a better diffusion of the feed solution through the membrane and consequently higher fluxes (Silva 2018). Moreover, the higher initial flux obtained when processing with the 600-800 Da membrane (69.5 $L.m^{-2}.h^{-1}$) could also be related to the fact that fractions with higher molecular weight had already been removed from the feed solution by the ultrafiltration with GH 2 kDa membrane, showing the importance of a membrane sequence in the process productivity.

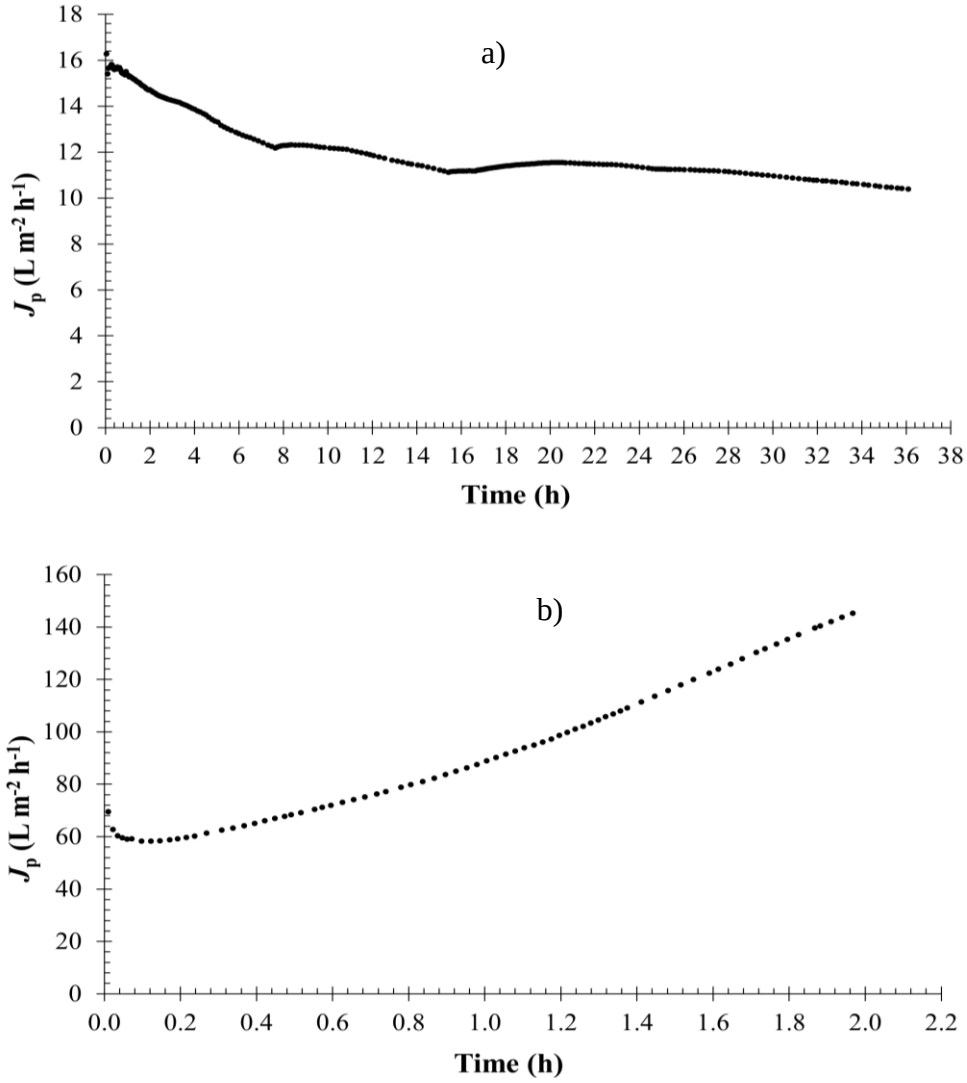

Figure 5.5 – Permeate flux behavior with operating time obtained for the processing with a) ultrafiltration membrane GH 2 kDa, and b) nanofiltration membrane NFG 800-600 Da.

The LSSL mixture, permeate, and retentate resulting from ultra and nanofiltration were analyzed for TDS (Figure 5.6**)**. The most significant difference was observed between the percentage of TDS of the oxidized mixture and the permeate obtained with the GH 2 kDa membrane. The P_{2kDa} presented the lowest value of TDS content, being similar to the content obtained in $P_{800\text{-}600Da}$. What concerns the TDS percentage in the retentates it is possible to observe an increase in R_{2kDa}, confirming the concentration of this constituent in this fraction, which is coherent with the decrease observed in the corresponding permeate.

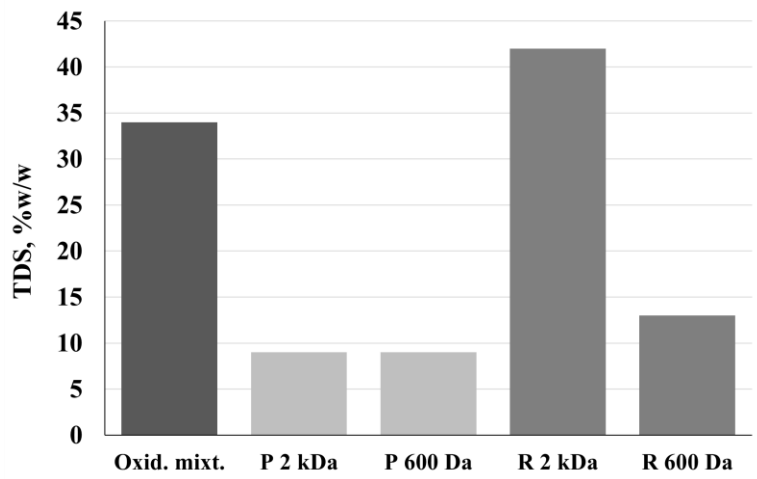

Figure 5.6 – Total dissolved solids of LSSL lignin oxidized mixture, permeates and retentates resulting from ultra and nanofiltration with 2 kDa and 600-800 Da membranes.

5.3.2 Fixed Bed Adsorption/Desorption Experiments

The following fixed bed adsorption/desorption experiments were performed to fractionate the most representative compounds present in the complex mixture obtained from the oxidation of LSSL lignin. To understand the interaction of the main phenolic compounds, present in the permeate from nanofiltration of LSSL mixture, with SP700 resin, a breakthrough curve was performed with an MMS. As mentioned before, concentrations of the phenolic monomers V, VA, VO, and Sy in the MMS were prepared based on the concentrations in the permeate obtained from the nanofiltration of the oxidized LSSL mixture (Table 5.3). In the following sections, the outcomes from breakthrough experiment and adsorption/desorption cycles are presented.

5.3.2.1 Breakthrough experiment

The breakthrough allows the study of the interaction of the phenolic compounds present in the mixture (Table 5.3), VA, V, Sy and VO, with the SP700 resin. The profile of the phenolic monomers studied during the breakthrough experiment with MMS is presented in the Figure 5.7, and the normalized concentration histories of the phenolic monomers are shown in the Figure 5.8.

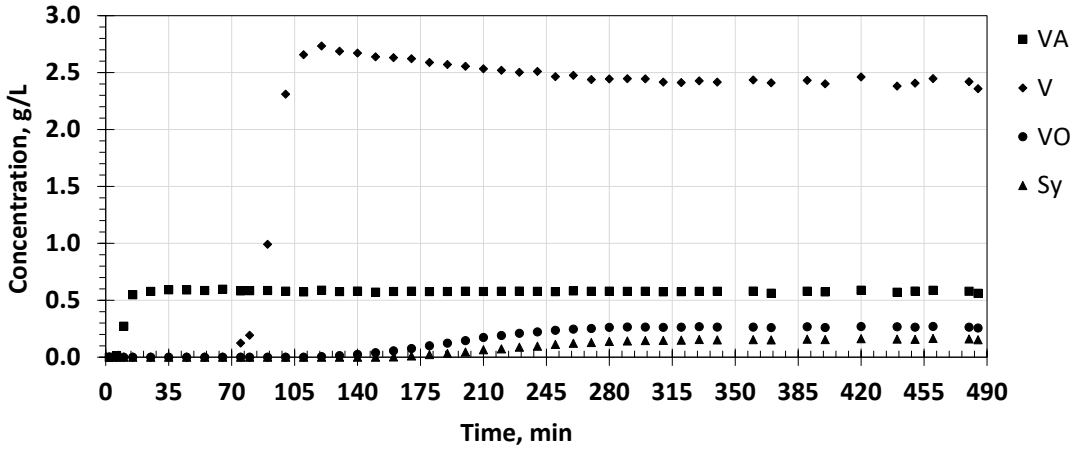

Figure 5.7 - Concentration history of the phenolic monomers in the breakthrough experiment using the MMS. Feed pH: 13.5; *T*=25°C, volumetric flow rate = 5 *ml/min*. Feed of monomers concentration are given in Table 5.3.

The first monomer eluting was VA, six minutes after starting the feed, and the outlet reached a concentration similar to the feed after 25 min. Then, V started to elute after 75 minutes, and reached the feed concentration about 100 min after. VO eluted in 120 min and took over 2.5 h to reach the feed concentration. The last monomer to elute was Sy, which starts to elute after160 minutes and reached the feed concentration after 5.5 hours. It was noticed that when VO started to elute a slight roll-up phenomenon in the V profile was observed, suggesting that V was displaced by VO due to the competitive adsorption. This phenomenon was commonly observed in competitive multicomponent adsorption (Kapoor and Yang 1987, Gu 1995).

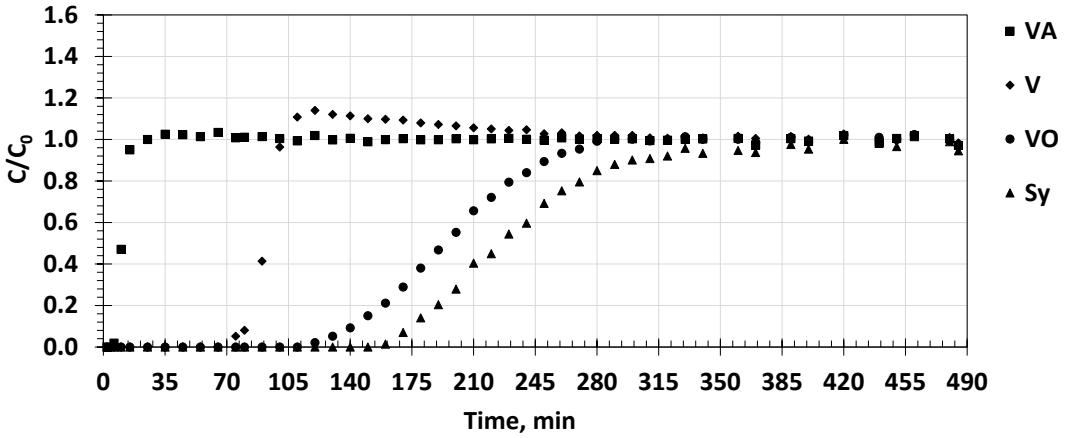

Figure 5.8 - Normalized concentration histories of the phenolic monomers in the breakthrough experiment using the MMS. Feed pH: 13.5; *T*=25°C, volumetric flow rate = 5 *ml/min*. Feed monomers concentration is given in Table 5.3**.**

Phenolic compounds adsorption onto nonpolar resins is commonly explained by the occurrence of weak physical interactions mainly of the van der Waals forces type (e.g. permanent dipole-induced dipole or induced dipole-induced dipole) (Pan *et al.* 2003, Suresh *et al.* 2012). Since the phenolic compounds have hydrogen donors, some authors have studied the effect of functional groups (e.g. phenolic hydroxyl or carbonyl, acetyl, amine or methoxy groups) in polymeric resins as promoters of hydrogen bonding to improve the adsorption capacity for these compounds (Li *et al.* 2002, Jiang *et al.* 2007).

Gomes and co-workers reported that the fact of guaiacyl derived compounds (VA, V and VO) elute early than syringil derived compound (Sy) are related to the different affinities of the compounds with the active sites of the SP700 resin (Gomes *et al.* 2018). This difference can be explained by the fact of syringil units have two methoxyl groups and guaiacyl units have only one methoxyl group (Payne *et al.* 1989, Wang *et al.* 2004, Mota *et al.* 2016). Moreover, since the resin is non-polar, it is expected that the phenolic compounds eluting from most to least polar, that is, acids, aldehydes, and ketones.

5.3.2.2 Adsorption/desorption cycles using MMS

The adsorption/desorption cycles were started with the feed step and after that, the recovery of the main phenolic monomers was attained in the desorption phase using two eluents, water, and ethanol. The desorption step with water can recover the aldehydes, V and Sy, with minor amounts of VO, and the desorption step with ethanol is able to recover the ketones with low quantities of aldehydes that might remain in the column after desorption with water. The selected solvent must overcome van der Waals's attractive forces that bind the adsorbate to the resin, and assure enough solubility of the adsorbate after solvent diffusion to and from the adsorptive site (Mota *et al.* 2016). Mota and co-workers stated that using only water as desorption solvent to desorb V and Sy from a column packed with SP700 resin can be a very time-consuming process (Mota *et al.* 2016). Thus, employing two-eluent technique, with water and ethanol, to desorb phenolic monomers from this macroporous resin benefit the desorption step, which was in agreement with the results found in other works (Zhang *et al.* 2008, Mota *et al.* 2016, Mota 2017, Gomes *et al.* 2018, Mota *et al.* 2019, Gomes and Rodrigues 2019b). Furthermore, ethanol was chosen due to its nontoxic and wide acceptance in several industrial applications as perfumes and flavors (Scordino *et al.* 2005, Kammerer *et al.* 2010). To perform these experiments, it was adopted a cyclic mode operation. The set duration of the feed period in the cycles of adsorption/desorption was

selected based on the breakthrough time of V, the target phenolic compound, which was around 70 minutes. To assure that the resin was saturated by V, the time of the column feed was for 90 minutes. Then, desorption step with water was performed for 45 minutes, after that desorption with ethanol was performed for more 45 minutes. During the water phase desorption three different fractions were collected to recover an enriched fraction in V with less quantities of other phenolic compounds as VA, VO and Sy. The same cyclic mode configuration was performed for both solutions, MMS and permeate from nanofiltration of LSSL mixture, and the fractionation scheme is detailed in Table 5.5.

Table 5.5 – Fractionation scheme of cyclic operation mode for MMS and permeate from LSSL mixture nanofiltration.

Cycle number	Feed solution	Duration, min	Eluate solution
Cycle 1 – cycle n	LSSL mixture (permeate from nanofiltration) or MMS	[0-90]	Feed phase
	Water	[90-95]	Water desorption fraction I
		[95-115]	Water desorption fraction II
		[115-135]	Water desorption fraction III
	Ethanol	[135-180]	EtOH fraction

Adsorption/desorption experiments using MMS were performed for 4 cycles. The feed solution has V, VA, Sy and VO in its composition with the concentrations shown in Table 5.3. Concentration profiles of the studied monomers during the cyclic mode operation are shown in Figure 5.9, and the respective representation of the normalized concentration is presented in Figure 5.10.

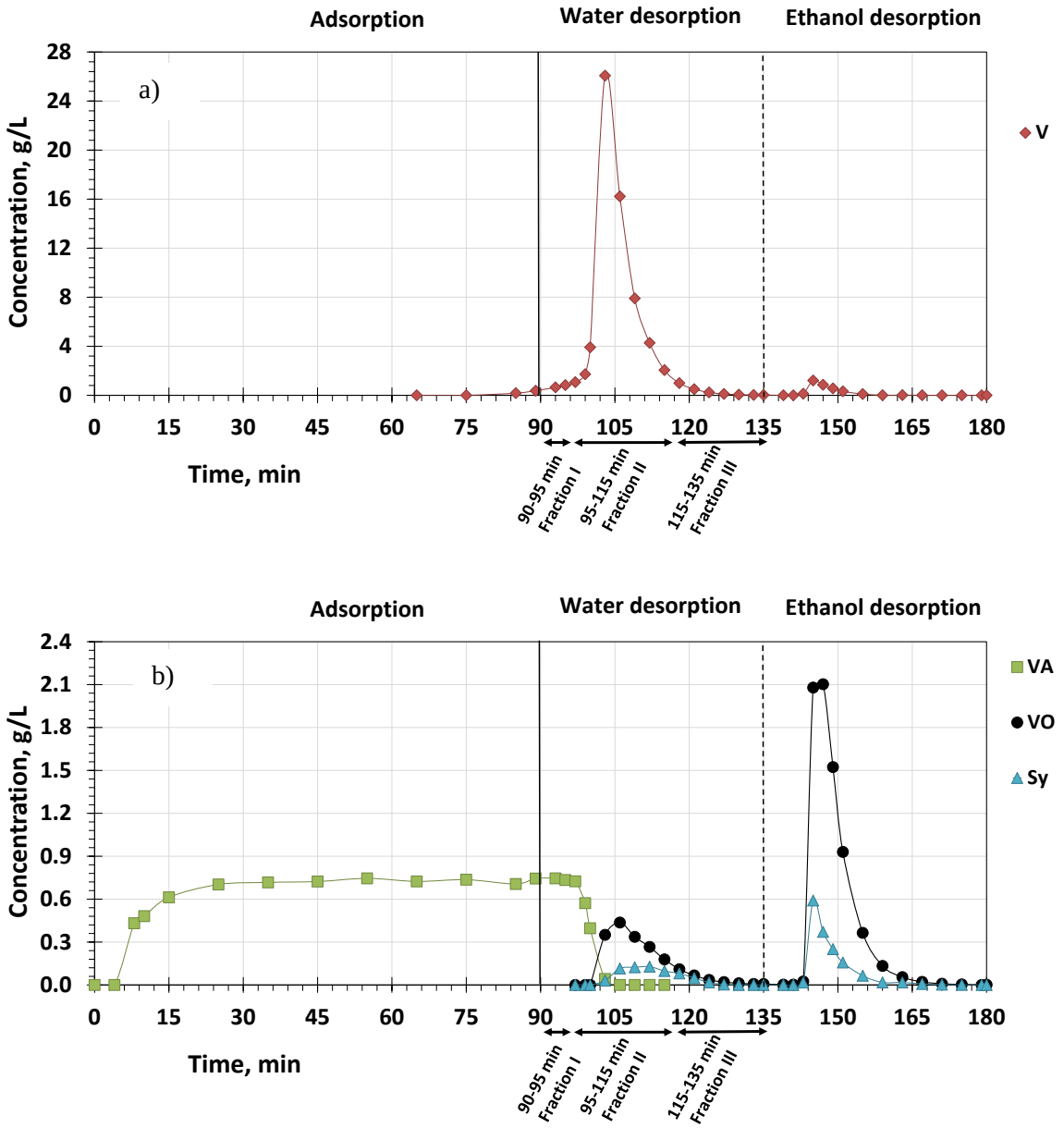

Figure 5.9 - Concentration history of the studied monomers: a) V, and b) VA, VO, and Sy, in the one adsorption/desorption cycle experiment with MMS. The first vertical line represents the beginning of the water desorption phase, and the vertical dotted line represents the beginning of the ethanol desorption phase. Feed pH: 13.5, T = 25 °C, volumetric flow rate = 5 ml/min. Feed monomers concentration is given in Table 5.3.

During the feed phase, VA eluted with the same concentration (0.71 g/L) as the feed mixture after 25 minutes. The pH of the elution solution is constant (around 13.5) during the feed phase. When the water desorption phase began, V started to elute, and it was possible to see the concentration increasing up to almost 11 times the feed concentration in the minute 103. Sy and VO also eluted in this phase, increasing about 2 times its feed concentration. However, it was in the ethanol desorption phase that Sy and VO had preference to desorb,

increasing concentration up to 10 and 9 times of the feed concentration, respectively. In the Table 5.6 it is possible to see the summary of the concentrations obtained for V, VA, Sy and VO in each fraction collected during one adsorption/desorption cycle experiment. During all the cycles performed, no significant differences in the values of concentrations were observed for the monomers studied, and the mass balance can be seen in the Figure 5.11.

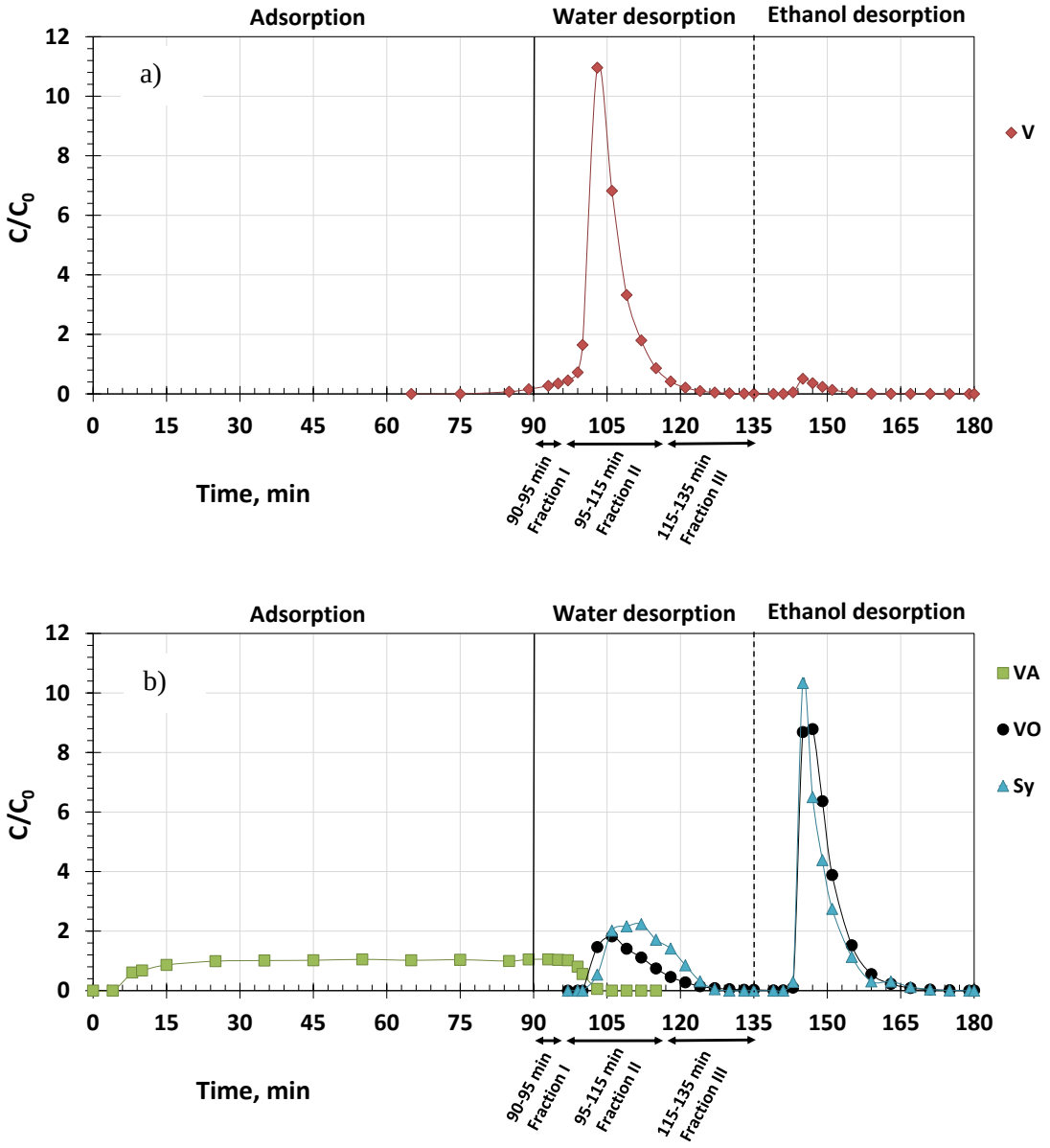

Figure 5.10 - Normalized concentration history of the studied monomers a) V, and b) VA, VO, and Sy in the one adsorption/desorption cycle experiment with MMS. The first vertical line represents the beginning of the water desorption phase, and the vertical dotted line represents the beginning of the ethanol desorption phase. Feed pH: 13, T = 25°C, volumetric flow rate = 5 mL/min. Feed monomers concentration is given in Table 5.3.

Table 5.6 – The concentration of V, VA, Sy, and VO in each fraction collected during one adsorption/desorption cycle experiment using MMS.

Monomers	Concentration, g/L				
	Feed phase	Water desorption phase			Ethanol desorption phase
		Fraction I	Fraction II	Fraction III	
VA	0.71	0.75	0.16	-	-
V	0.001	0.62	10.0	0.47	0.15
Sy	-	-	0.02	0.03	0.07
VO	-	-	0.22	0.06	0.37

Considering V, which was collected mainly in water desorption phase (fraction II), a concentration of 10.0 g/L was obtained in this fraction. Moreover, 94 % of recovery and 96 % of purity were obtained for V.

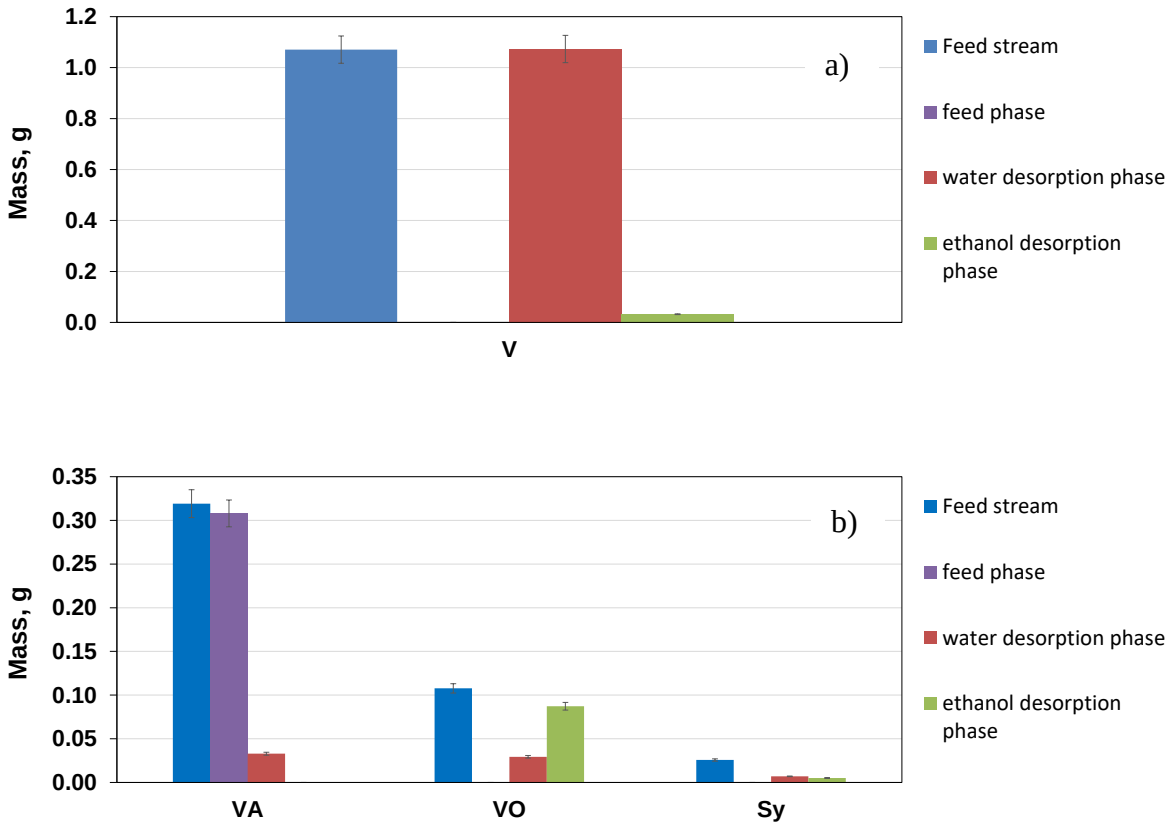

Figure 5.11 - Mass balance to the species fed and recovered at each phase: a) V, b) VA, VO, and Sy with MMS.

Recovery was calculated based on the mass of the compound obtained in the eluate stream of a selected fraction comparatively to the feed stream. Purity was calculated considering the mass of a monomer in a particular fraction of the eluate stream relatively to the total mass of all the monomers identified in the same fraction. The initial VA mass fed to the column, was mainly recovered during the feed phase, and a small amount during the water desorption phase (Fraction I). Moreover, VA was not detected during the desorption phase with ethanol. Concerning Sy and VO, both compounds were collected mainly in the ethanolic fraction, with a recovery of about 59 % and 78 %, respectively. During the water desorption phase about 22 % and 25 % were recovered of Sy and VO, respectively.

5.3.2.3 Adsorption/desorption cycles using the permeate from nanofiltration of LSSL mixture

After the adsorption/desorption cycles with MMS, fixed bed experiments were performed using the permeate from nanofiltration of the oxidized mixture from softwood sulfite liquor. Among the several monomers, VA, V, Sy, and VO were the main phenolic compounds identified in the mixture. The mixture was fed to the column without pH adjustment, and the concentration of the phenolic monomers studied are detailed in Table 5.7. Eight adsorption/desorption cycles were performed according to the fractionation scheme previously mentioned (Table 5.5). In the cycles 1 and 8 samples were collected at preset times. In the adsorption phase, samples were collected every 2 minutes until 10 minutes of adsorption and then every 5 minutes until 90 minutes. During the first 10 minutes of the water desorption phase samples were collected every minute and after that and during ethanol phase samples were collected every 2 minutes. The quantification of the phenolic compounds was performed by HPLC. For all the cycles, the concentration profiles of monomers were similar, and no significant differences were observed. Figure 5.12 and Figure 5.13 shows the concentration profiles of the studied monomers and the normalized concentration profiles in one cycle, respectively.

Table 5.7 – Concentration of the feed stream of the permeate from LSSL mixture nanofiltration in the adsorption/desorption cycle's experiments.

	VA	**V**	**Sy**	**VO**
Feed stream, g/L	0.35	1.31	0.02	0.17

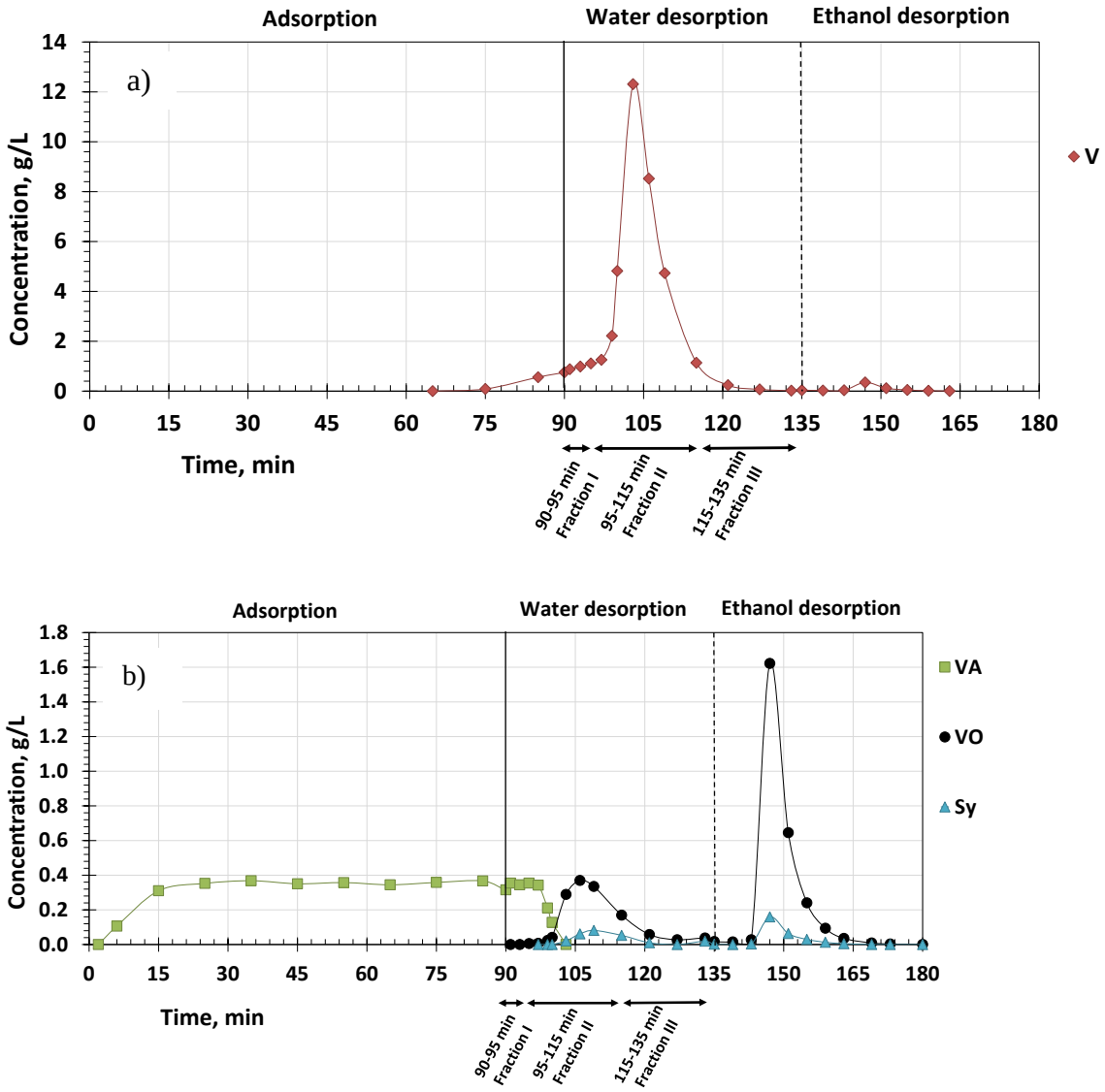

Figure 5.12 - Representation of concentration history of the monomers studied, a) V and b) VA, VO and Sy, in one adsorption/desorption cycle using the permeate from nanofiltration of LSSL mixture. The first vertical line represents the beginning of the water desorption phase, and the vertical dotted line represents the beginning of the ethanol desorption phase. Feed pH: 13.5; T=25°C, volumetric flow rate = 5 ml/min. Feed monomer concentrations is given in Table 5.7.

Regarding the concentration history of all the compounds, it was possible to see that VA desorb just after 15 minutes after the start of the feed phase, confirming the low adsorption of the phenolic acids into the SP700 resin. Then, V started to elute after 75 minutes of feed reaching a maximum of 12.31 g/L after about 100 minutes of the experiment (water desorption phase), a concentration value that corresponds to 9 times the feed concentration. Sy, started to elute at minute 100 and increase the concentration by 2 times of feed concentration after that time. Although VO and Sy started to elute during the water

desorption phase, it was in the ethanolic desorption phase that both compounds have a higher intensity peak, increasing feed concentration by 8 and 5 times, respectively. Concerning all the eight cycles performed using the permeate from LSSL mixture nanofiltration, no significant differences were found between the concentrations of the monomers, or the recoveries achieved for each monomer. Table 5.8 summarizes the concentration of the monomers, VA, V, Sy, and VO attained during one adsorption/desorption cycle experiment. The mass balance for the recovery of V, VA, VO, and Sy is presented in the Figure 5.14.

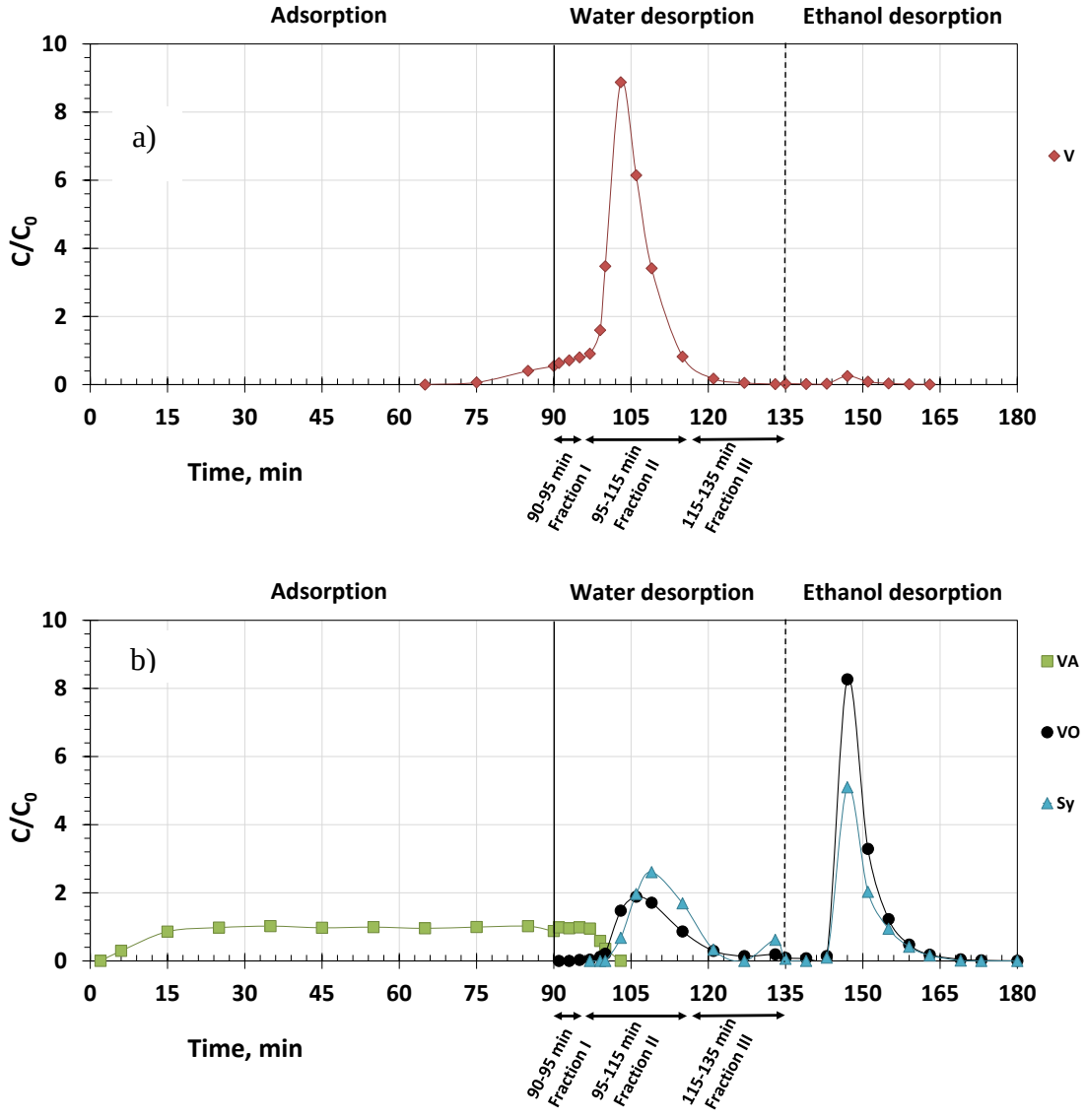

Figure 5.13 - Representation normalized concentration history of the monomers studied, a) V and b) VA, VO and Sy, in one adsorption/desorption cycle using the permeate from nanofiltration of LSSL mixture. The first vertical line represents the beginning of the water desorption phase, and the vertical dotted line represents the beginning of the ethanol desorption phase. Feed pH: 13.5; T=25°C, volumetric flow rate = 5 ml/min. Feed monomer concentrations is given in Table 5.7**.**

Table 5.8 – Concentration of VA, V, Sy and VO in each fraction collected during an adsorption/desorption cycle experiment with the permeate from nanofiltration of LSSL mixture.

Monomers	Concentration, g/L				
	Feed phase	Water desorption phase			Ethanol desorption phase
		Fraction I	Fraction II	Fraction III	
VA	0.32	0.35	0.08	-	-
V	0.04	1.01	5.44	0.21	0.02
Sy	-	-	0.03	0.006	0.01
VO	-	-	0.20	0.05	0.25

Regarding V, it is well known that the higher recovery of this phenolic compound is obtained during the water desorption phase (fraction II), reaching 92 % of recovery. VA, VO, and Sy were present in minor quantities, being recovered in the water desorption phase with percentages of 11, 33, and 64 %, respectively. Moreover, 40 % and 73 % of the total amount desorbed of Sy and VO, respectively, were recovered in the ethanolic desorption phase. V was also detected in the ethanolic phase but in tracer amounts, corresponding less than 1 % of the total amount desorbed.

Comparing the phenolic profiles in the adsorption/desorption cycles using MMS and using the permeate from the nanofiltration of the LSSL solution, it is possible to observe some differences. Between minute 75 and 90 of the adsorption step it was verified the existence of a tail in the profile of V when the permeate from nanofiltration of LSSL mixture is used. This could be related to the different feed concentration of this aldehyde in both mixtures. Another reason could be the non-identification of all the compounds present in the permeate from nanofiltration of LSSL mixture since it is a real mixture, and it is difficult to identify all the compounds present on it. Moreover, during the desorption phase with water the maximum peak obtained for V, in terms of C/C0, was slightly lower when using the permeate from the nanofiltration of the LSSL mixture. The same behavior was verified for Sy in the ethanol desorption phase, where C/C0 at the maximum peak in the permeate from the nanofiltration of the LSSL solution was half of the value obtained with the MMS.

Concerning VA and VO, the differences found for adsorption/desorption profiles of both solutions were not significant. Besides the differences found in the experiments performed with the two mixtures, it is important to carry out the adsorption/desorption cycles

with the model solution, since it allows predict the concentration profiles of the studied phenolic compounds during the adsorption/desorption experiments using the permeate from the nanofiltration of the LSSL solution.

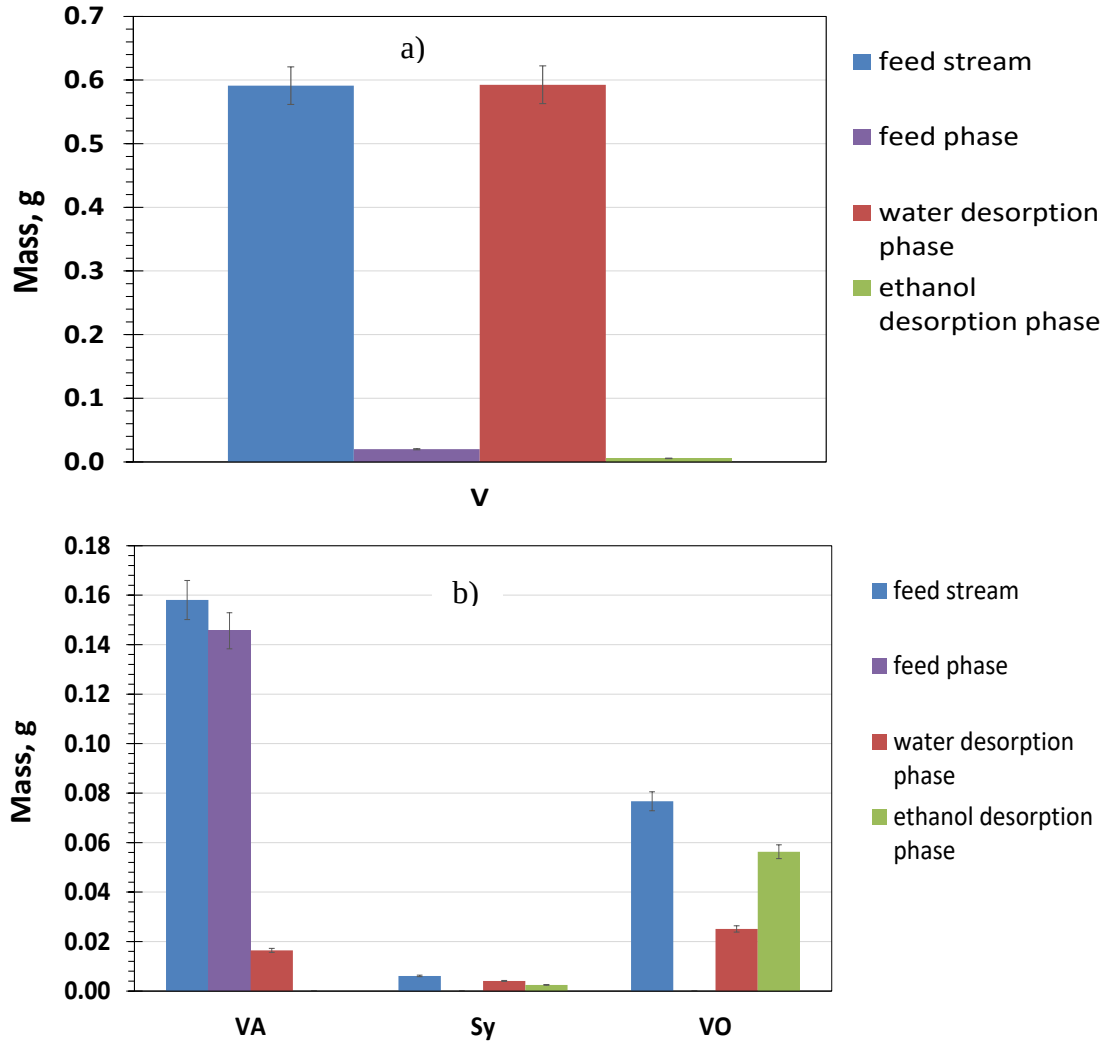

Figure 5.14 - Mass balance to the species fed and recovered at each phase: a) V, b) VA, VO and Sy with permeate from nanofiltration of LSSL mixture.

5.4 CONCLUSIONS

The permeate obtained from the fractionation process of oxidized LSSL stream was submitted to adsorption/desorption studies employing a polymeric resin SP700 without any pH adjustment. Before the chromatographic step, the oxidized LSSL mixture was submitted to a two-step membrane filtration that reduces the TDS from the initial 34 % w/w_{lignin} to 9 % w/ w/w_{lignin} before being fed to the chromatographic column.

A complete breakthrough curve with a model solution was performed for 8 hours, pH of 13.5, and a volumetric flow rate of 5 mL/min. The breakthrough curve enabled to understand the adsorption of the phenolic compounds into the resin and determining the times at which cycles of adsorption/desorption would be performed. Four cycles were performed for the model solution and 8 cycles in the case of permeate from oxidized LSSL mixture nanofiltration.

The resulting fractions from adsorption/desorption cycles differ considerably from the feed mixture and the monomers are successful fractionated through their functional groups: phenolic acids, phenolic aldehydes, and phenolic ketones. The fraction collected during the feed phase has mostly VA. Phenolic aldehydes were mainly collected in the water desorption phase. In order to get a higher purity of V, three fractions were collected in the water desorption phase: fraction I, where the residual VA is collected, fraction II, where V is collected with a recovery of 92 % although with small amounts of Sy and VO, and fraction III, where small concentrations of Sy and VO were collected. In the ethanol desorption phase, VO and Sy were collected with a recovery of 40% and 73 %, respectively.

5.5 REFERENCES

Gomes, E. D., M. I. Mota and A. E. Rodrigues (2018). Fractionation of acids, ketones and aldehydes from alkaline lignin oxidation solution with SP700 resin. *Separation and Purification Technology* 194: 256-264.

Gomes, E. D. and A. E. Rodrigues (2019b). Lignin biorefinery: Separation of vanillin, vanillic acid and acetovanillone by adsorption. *Separation and Purification Technology* 216: 92-101.

Gu, T. (1995). Mathematical Modeling and Scale-up of Liquid Chromatography, Springer Berlin, Heidelberg.

Jiang, Z.-m., A.-m. Li, J.-g. Cai, C. Wang and Q.-x. Zhang (2007). Adsorption of phenolic compounds from aqueous solutions by aminated hypercrosslinked polymers. *Journal of Environmental Sciences* 19(2): 135-140.

Kammerer, D. R., R. Carle, R. A. Stanley and Z. S. Saleh (2010). Pilot-Scale Resin Adsorption as a Means To Recover and Fractionate Apple Polyphenols. *Journal of Agricultural and Food Chemistry* 58(11): 6787-6796.

Kapoor, A. and R. T. Yang (1987). Roll-up in fixed-bed, multicomponent adsorption under pore-diffusion limitation. *AIChE Journal* 33(7): 1215-1217.

Li, A., C. Long, Y. Sun, Q. Zhang, F. Liu and J. Chen (2002). A new phenolic hydroxyl modified polystyrene adsorbent for the removal of phenolic compounds from their aqueous solutions. *Separation Science and Technology* 37(14): 3211-3226.

Mota, I. F., P. R. Pinto, J. M. Loureiro and A. E. Rodrigues (2020). Purification of syringaldehyde and vanillin from an oxidized industrial kraft liquor by chromatographic processes. *Separation and Purification Technology* 234: 116083.

Mota, I. F., P. R. Pinto, A. M. Ribeiro, J. M. Loureiro and A. E. Rodrigues (2018). Downstream processing of an oxidized industrial kraft liquor by membrane fractionation for vanillin and syringaldehyde recovery. *Separation and Purification Technology* 197: 360-371.

Mota, M. I. F., S. Barbosa, P. C. R. Pinto, A. M. Ribeiro, A. Ferreira, J. M. Loureiro and A. E. Rodrigues (2019). Adsorption of vanillic and syringic acids onto a macroporous polymeric resin and recovery with ethanol:water (90:10 %V/V) solution. *Separation and Purification Technology* 217: 108-117.

Mota, M. I. F., P. C. R. Pinto, J. M. Loureiro and A. E. Rodrigues (2016). Adsorption of vanillin and syringaldehyde onto a macroporous polymeric resin. *Chemical Engineering Journal* 288: 869-879.

Mota, M. I. F., P. C. R. Pinto, J. M. Loureiro and A. E. Rodrigues (2016). Successful recovery and concentration of vanillin and syringaldehyde onto a polymeric adsorbent with ethanol/water solution. *Chemical Engineering Journal* 294: 73-82.

Mota, M. I. F., P. C. Rodrigues Pinto, J. M. Loureiro and A. E. Rodrigues (2016). Recovery of Vanillin and Syringaldehyde from Lignin Oxidation: A Review of Separation and Purification Processes. *Separation & Purification Reviews* 45(3): 227-259.

Mota, M. I. F. d. (2017). Fractionation and purification of syringaldehyde and vanillin from oxidation of lignin. PhD *Faculty of Engineering, University of Porto*.

Pan, B. C., Y. Xiong, Q. Su, A. M. Li, J. L. Chen and Q. X. Zhang (2003). Role of amination of a polymeric adsorbent on phenol adsorption from aqueous solution. *Chemosphere* 51(9): 953-962.

Payne, G. F., N. N. Payne, Y. Ninomiya and M. L. Shuler (1989). Adsorption of Nonpolar Solutes onto Neutral Polymeric Sorbents. *Separation Science and Technology* 24(5-6): 457-465.

Scordino, M., A. Di Mauro, A. Passerini and E. Maccarone (2005). Selective Recovery of Anthocyanins and Hydroxycinnamates from a Byproduct of Citrus Processing. *Journal of Agricultural and Food Chemistry* 53(3): 651-658.

Silva, F. C. (2018). Nanofiltration. Rijeka, IntechOpen.

Soto, M. L., E. Conde, N. González-López, M. J. Conde, A. Moure, J. Sineiro, E. Falqué, H. Domínguez, M. J. Núñez and J. C. Parajó (2012). Recovery and concentration of antioxidants from winery wastes. *Molecules* 17(3): 3008-3024.

Suresh, S., V. C. Srivastava and I. M. Mishra (2012). Adsorption of catechol, resorcinol, hydroquinone, and their derivatives: a review. *International Journal of Energy and Environmental Engineering* 3(1): 32.

Wang, X. J., J. F. Zhao, S. Q. Xia, A. M. Li and L. Chen (2004). Adsorption mechanism of phenolic compounds from aqueous solution on hypercrosslinked polymeric adsorbent. *J Environ Sci (China)* 16(6): 919-924.

Žabková, M., E. A. B. da Silva and A. E. Rodrigues (2007b). Recovery of vanillin from lignin/vanillin mixture by using tubular ceramic ultrafiltration membranes. *Journal of Membrane Science* 301(1): 221-237.

Zhang, Q.-F., Z.-T. Jiang, H.-J. Gao and R. Li (2008). Recovery of vanillin from aqueous solutions using macroporous adsorption resins. *European Food Research and Technology* 226(3): 377-383.

6 Recovery of Phenolic Aldehydes from an Oxidation Mixture of a Hardwood Lignin Isolated from a Pulp Mill Sulfite Liquor

In this chapter, an oxidized mixture of a lignin isolated from a pulp mill hardwood sulfite liquor, rich in phenolic products, was dealt with a sequential process to obtain the phenolic aldehydes of interest, namely vanillin and syringaldehyde. The first stage was a three-step filtration of the oxidized mixture using ultra and nanofiltration membranes with molecular weight cut-off of 5 kDa, 2 kDa and 600-800 Da. After that, the permeate from nanofiltration was treated by an adsorption/desorption process in a chromatographic column packed with non-polar resin SP700. To desorb the compounds, two eluents were applied, water and ethanol (99% v/v). In the water desorption phase, an enriched fraction in the target phenolic monomers, syringaldehyde and vanillin, was obtained, with minor amounts of phenolic acids (vanillic acid and syringic acid), and phenolic ketones (acetovanillone and acetosyringone). Ethanolic desorption phase desorbed phenolic ketones with higher recoveries than in water desorption phase.

6.1 INTRODUCTION

As stated previously in this thesis, lignin is composed of three main moieties: *p*-hydroxyphenyl (H), guaiacyl (G), and syringil (S) units. These units have a similar chemical structure however, its main difference depends on the degree of substitution of methoxy functional groups in the aromatic ring. Based on the S:G:H ratio lignin can be classified into softwood, with a high preponderance of G units, hardwood, with a shared composition of G and S units, and a very small proportion of H units (Sethupathy *et al.* 2022).

Lignin can potentially be converted into valuable phenolic compounds through depolymerization reactions in an alkaline environment at high temperatures and under high pressure (Fache *et al.* 2016, Rodrigues *et al.* 2018). The oxidative depolymerization of a hardwood lignin in an alkaline medium using O_2 as oxidant generates a complex mixture of lignin fragments and low molecular weight compounds. The resulting oxidation mixture should be submitted to a sequence of separation and purification processes concerning lignin valorization through the recovery of the added-value phenolic monomers produced. However, due to the structural similarities of the phenolic compounds of interest, V and Sy, its effective separation remains a huge challenge.

The complex mixture from oxidation stream of a hardwood lignosulfonate can be fractionated and concentrated, through ultra and nanofiltration, into different streams: partially depolymerized lignin, intermediate molecular weight oligomers, and phenolate monomers. The ultra and nanofiltration process concentrates the low molecular weight phenolic compounds taking advantage of their solubility in an alkaline medium, producing a stream containing phenolate monomers to proceed for the separation step. The efficiency of the recovery of phenolic monomers, like V and Sy, from model solutions andoxidized kraft lignin mixtures by ultra and nanofiltration was demonstrated in previous works of our research team (Žabková *et al.* 2007b, Gomes *et al.* 2018, Mota *et al.* 2018, Gomes and Rodrigues 2019b).

In this chapter, a lignin from a pulp mill hardwood sulfite liquor (LHSL) was oxidized in an alkaline medium with oxygen, and then submitted to a three-step filtration with ultra and nanofiltration membranes of 5 kDa, 2 kDa, and 600-800 Da, to concentrate the low molecular phenolic compounds of interest in the permeate from nanofiltration.

The permeate obtained in the last membrane (nanofiltration) was then fractionated by an adsorption/desorption process in a chromatographic column packed with a non-polar resin SP700. This is an important step to the efficient purification of the phenolic aldehydes of

interest. The aqueous fraction with the rich in vanillin and syringaldehyde will proceed to liquid-liquid extraction and crystallization (processes discussed in the next chapter). Adsorption/desorption studies with the SP700 resin have already been reported using softwood lignin as raw material (Gomes *et al.* 2018, Gomes and Rodrigues 2019b, Gomes and Rodrigues 2020a). From the author's knowledge, in this work it is reported for the first-time adsorption/desorption studies with SP700 resin using hardwood lignin from a pulp mill sulfite liquor as a raw material.

6.2 EXPERIMENTAL SECTION: MATERIALS AND METHODS

6.2.1 Oxidized LHSL Solution

Lignin isolated from hardwood (*Eucalyptus globulus*) sulfite liquor (LHSL), gently provided by Caima (Constância, Portugal), was submitted to oxidative depolymerization in an alkaline medium (NaOH 2M) with oxygen (pO_2 of 3 bar and P_T of 9.8 bar) in a batch reactor at an initial temperature of 120 ℃. Information about lignin source and its structural characterization is detailed in section 3.2.1 and 3.3, respectively. Experimental setup and the operating conditions used in the oxidative depolymerization were described in section 3.2.6.

The oxidized LHSL solution proceeded to concentration and separation processes: ultra and nanofiltration and adsorption/desorption experiments.

6.2.2 Ultra and Nanofiltration

The ultra and nanofiltration experiments were performed using a laboratory crossflow module as described in section 5.2.2. As already stated, the transmembrane pressure (TMP) was controlled by a needle valve located after the membrane module in the retentate side (Figure 5.1). All experiments were carried out in full recycling mode. A three-step membrane filtration was performed, using flat sheet membranes with a molecular weight cut-off (MWCO) of 5 kDa, 2 kDa, and 600-800 Da. The operating pressure used during the ultra and nanofiltration experiments were 10, 18, and 30 bar for 5 kDa, 2 kDa, and 600-800 Da membrane, respectively. All the membranes have an effective membrane surface area of 0.014 m^2. The main characteristics of the ultra and nanofiltration membranes were detailed in Table 6.1.

Table 6.1 – Characteristics of ultra (MT and GH) and nano (NFG) filtration membranes**.**

Membrane	MT	GH	NFG
Manufacturer	Synder	GE Power & Water	Synder
Membrane MWCO, Da	5000	2000	600-800
Composition	PES	Polyamide TFC	Polyamide TFC
Max. temperature, ºC	55	70	50
Max. pressure, bar	12	27	40
Operating TMP (used in the experiments), bar	4-10	4-18	15-30
pH range (25 ºC)	1-11	1-11	4-10
Typical operating flux, LMH	226-348	34.0	93-102

Water permeability tests were performed in the range of the operating TMP of each membrane, in recirculation mode. For MT (5 kDa) membrane the applied TMP were in the range 4-10 bar, for GH membrane (2 kDa) the applied TMP were in the range 4–18 bar and for NF membrane (NFG 600-800 Da) the range was 15–30 bar. For each pressure tested, the permeate flux was measured three times, after the stabilization of the feed flow rate at 168 $L.h^{-1}$, at ambient temperature. Prior to water permeability tests, membranes were flushed with deionized water at 25 ºC for 30 minutes. Total dissolved solids (TDS) were determined for the LHSL oxidized mixture, the permeates, and the retentates from ultra and nanofiltration, as already described in section 5.2.2.

6.2.3 Adsorption and Desorption Experiments

6.2.3.1 Batch adsorption experiments

To evaluate the adsorption isotherms of the phenolic aldehydes onto the surface of the adsorbent, resin SP700, batch adsorption experiments were performed. Different amounts of SP700 resin, ranging from 0.1 to 0.5 g of dry weight, were added to 0.04 L of a NaOH 2M aqueous solution with about 4.0 g/L of V and 1.0 g/L of Sy. The resin was activated according to the description given in section 5.2.4.1. Three different pH values were used in the batch adsorption experiments: 6.5, 10, and 13 (Figure 6.1), all of them at 25 ºC. The initial NaOH solution with V and Sy has a pH value near to 13 and the acidification was performed using an aqueous solution of sulfuric acid (1:1 v/v). Batch samples were placed

in an orbital shaker for a total of 72 h and 160 rpm to ensure that the equilibrium was achieved. The samples were collected every 24 h and analyzed by HPLC (as described in section 3.2.3) as well as the initial feed concentration of each pH value.

Figure 6.1 - Multicomponent model solution with different pH values, 6.5, 10, and 13.

6.2.3.2 Breakthrough curves and cycles of adsorption/desorption

Breakthrough experiments were carried out by feeding the column during 8 h with a model solution, composed of VA, V, SA, Sy, VO and SO, at a volumetric flowrate of 5 mL/min. The model solution was prepared considering the phenolic monomers and respective concentrations present in the permeate from the nanofiltration (600-800 Da membrane) of the oxidized LHSL solution, Table 5.3. The jacketed column was kept at 25 ºC using a thermostatic bath, and the samples were collected at preset times: every 2 minutes until 10 minutes of the experiment, and then every 5 minutes until 480 minutes. The phenolic compounds present in the samples collected at the outlet of the chromatographic column were quantified by HPLC analysis, as described in section 3.2.3.

The adsorption/desorption cycles were performed based on the information from the breakthrough curve. For both model solution and permeate from the nanofiltration of the LHSL solution, the feeding phase was performed for 260 minutes, initial concentrations of phenolic compounds are presented in Table 6.2 for the model solution and for the permeate from nanofiltration of LHSL oxidation mixture.

The desorption phase was performed using two eluents, first with water for 50 minutes and then ethanol (99 % v/v) for more 50 minutes, both at a volumetric flowrate of 5 mL/min. Samples were collected every five minutes during adsorption. During the water desorption phase samples were collected every 2 minutes until 35 minutes of desorption, and every 3 minutes between 35 and 50 minutes. During the ethanol desorption phase samples were collected every 3 minutes until the end of the experiment. In total, eight cycles of

adsorption/desorption were performed using the model solution and 2 cycles were performed using the permeate from nanofiltration of LHSL solution. In the chromatographic experiments, the phenolic compounds were quantified by HPLC analysis, as described in section 3.2.3.

Table 6.2 – Feed stream concentrations of the phenolic monomers in the solutions used in the experiments of breakthrough and adsorption/desorption cycles.

	Model solution, g/L	**Permeate from nanofiltration of LHSL oxidation mixture, g/L**
VA	0.14	0.11
V	0.35	0.35
SA	0.15	0.12
Sy	0.89	0.73
VO	0.05	0.05
SO	0.13	0.18

6.3 RESULTS AND DISCUSSION

6.3.1 Ultra and Nanofiltration of LHSL Oxidation Stream

6.3.1.1 Water membrane permeability

The water permeability of each membrane was evaluated by measuring deionized water permeate flowrate at different values of TMP. Water permeates flux (J_w), determined, using the equation (5.1), presented in the section 5.3.1.1, is represented in the Figure 6.2 for MT, GH and NFG membranes. From the figure, it is possible to observe that water permeate flux increase with the increase of TMP for all the membranes. The NFG membrane has a permeability to the water of 24.4 L m^{-2} h^{-1} bar^{-1}, GH membrane a permeability of 7.4 L m^{-2} h^{-1} bar^{-1}, and MT membrane a permeability of 48.7 L m^{-2} h^{-1} bar^{-1}.The lowest value of water permeability was observed for the membrane of GH (2 kDa) when compared to MT (5 kDa) or NFG (800-600 Da) membranes. Moreover, the membrane with higher cut-off (MT, 5 kDa) show the higher value of permeability (Figure 6.2). Considering GH and NFG membranes, it would be expected that the membrane with higher cut-off show higher value of permeability however, this is not observed. This behavior can be explained based on the

typical operating flux of each membrane: besides its lower molecular weight cut-off, the NFG membrane (600-800 Da) has a typical operating flux three times higher than the 2 kDa membrane (Table 6.1). In the previous chapter similar results were obtained for NFG membrane comparatively to GH membrane.

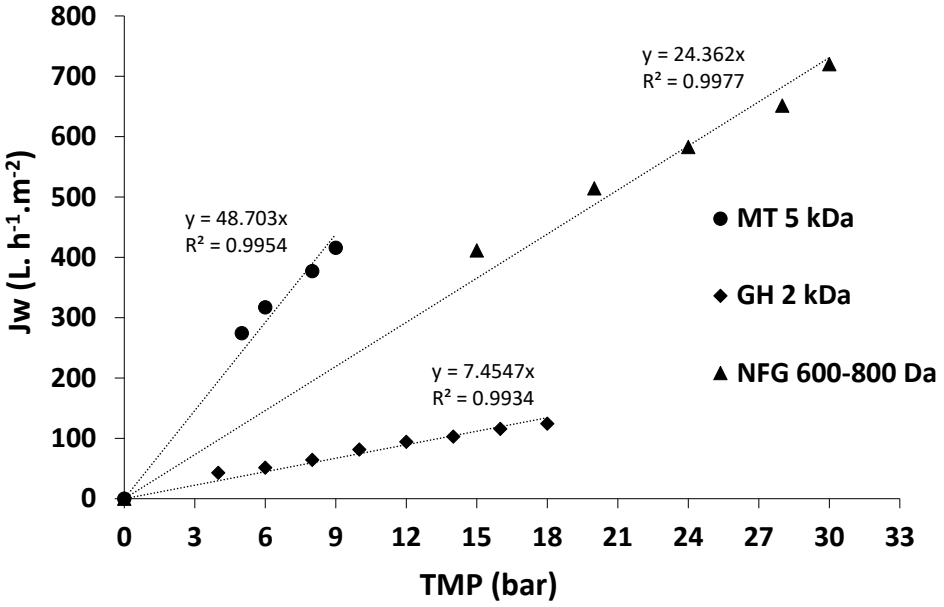

Figure 6.2 - Water permeate fluxes through the membranes of 5 k, 2 k, and 600-800 Da at different TMP, constant temperature of 25 ºC, and feed flowrate set to 168 $L.h^{-1}$.

6.3.1.2 Ultra and nanofiltration of oxidized LHSL solution

As already stated, during alkaline oxidative depolymerization, lignin can be broken into low molecular weight phenolic compounds but also can give origin oligomeric lignin structures. These lignin structures have molecular weights between the starting lignin and the molecular weight of aromatic monomers, typically around 150 g/mol. The content of oligomeric structures presents in the solution resulting from the oxidative depolymerization of LHSL lignin with O_2 in an alkaline medium could be minimized through the filtration process.

The experiment was carried out with a total recirculation of the feed solution, without any pH adjustment. A sequence of three membranes, with a molecular weight cut-off of 5k Da, 2k Da, and 600-800 Da, was employed to reduce the amount of lignin oligomeric products in the solution. The scheme of ultra and nanofiltration process applied to the oxidized LHSL solution is represented in Figure 6.3. A summary of the conditions of each step is presented in Table 6.3.

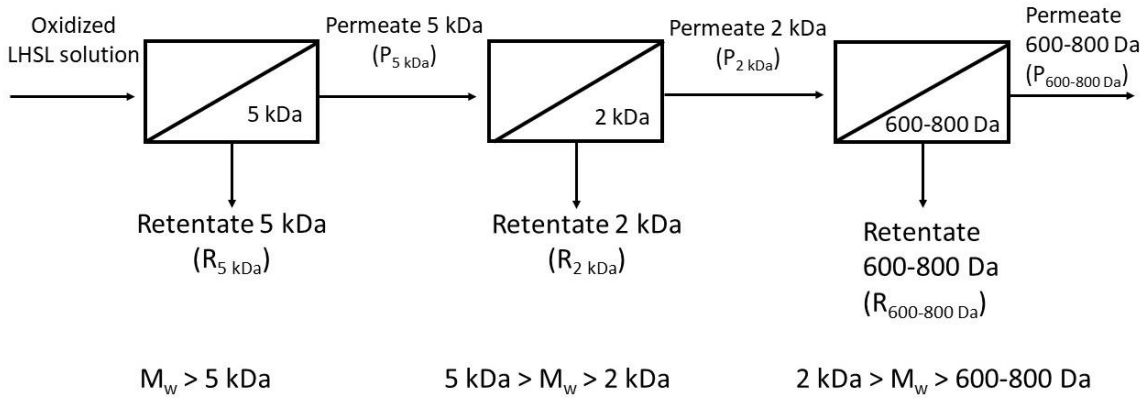

Figure 6.3 - Schematic representation of the ultra and nanofiltration process applied to the mixture from oxidation of LHSL lignin performed with 5 k, 2 k and 600-800 Da membranes.

Table 6.3 – Ultra and nanofiltration operating conditions.

	Feed Solution		
Parameter	**Oxidized LHSL solution**	**$P_{5\ kDa}$**	**$P_{2\ kDa}$**
Membrane MWCO, Da	5,000	2,000	600 - 800
Solution pH (25 ºC)	13.2	13.2	13.2
Pressure, bar	10	22	30
Initial volume, L	5.8	4.7	4.2
Permeate volume, L	4.7	4.2	3.7
Volume concentration factor (VCF)	5.3	9.4	8.4
Initial flux, $L.m^{-2}.h^{-1}$	65.9	38.4	57.1
Final flux, $L.m^{-2}.h^{-1}$	4.7	26.4	129.8

The total volume of oxidized LHSL solution was about 5.8 L. In the first stage of ultrafiltration, the oxidized LHSL solution was processed with the highest membrane cut-off, 5 kDa, which resulted in a volume reduction (VR, permeate volume divided by initial feed volume) of 0.81, in which the initial volume of the oxidized LHSL solution was reduced so that about 19% remained as retentate. Moreover, a VCF of 5.3 (initial feed volume divided by the retentate volume) was reached. Then, the permeate from the first stage, $P_{5\ kDa}$ membrane (4.7 L), was processed with a GH membrane with a molecular weight cut-off of

2 kDa. In this second stage, a VR of 0.89 was obtained which means that the volume was reduced in 89 %. Additionally, a value of 9.4 of VCF was achieved.

In the nanofiltration, the resulting permeate stream from the second stage (P_{2kDa}) was further processed using the 600-800 Da cut-off membrane, which resulted in a VR of 0.88 corresponding to a VCF of 8.4. Temperature was monitored during all the filtration experiments. Assays were performed with a feed flowrate of 198 $L.h^{-1}$.

During the ultra and nanofiltration stages, the variation of the permeate flux with time was calculated according to the equation (5.2), presented in the section 5.3.1.2, and it is graphically represented in the Figure 6.4 for each membrane.

Regarding the ultrafiltration with MT 5 kDa membrane, the permeate flux profile decreases around 74 % in 30 minutes of ultrafiltration, after that the flux decreases slowly. The initial decline in permeate flux can be explained by the increase of osmotic pressure of the solution moreover, the decline may be considered as a combined effect of the deposited layer on the membrane surface and the accumulation of solute particles in the membrane pores (Satyanarayana *et al.* 2000). During ultrafiltration with 2 kDa membrane the permeate flux also decreases with time but not as shortly as the 5 kDa membrane permeate flux (Figure 6.4). On the other hand, the nanofiltration with 600-800 Da membrane showed an increase in their permeate flux during the processing (Figure 6.4)(c). This behavior could be a consequence of the temperature variation of the feed solution (P_{2kDa}), which in the beginning of the processing was lower than 18 º C and after 45 minutes reach 29 ºC. In the previous chapter the same behavior was observed for the NFG membrane, in which permeate flux increase with time processing. Moreover, the higher initial flux obtained using the 600-800 Da membrane (57.1 $L.m^{-2}.h^{-1}$) could also be related to the fact that fractions with higher molecular weight had already been removed from the feed solution by the ultrafiltration with 5 and 2 kDa membranes, showing the importance of a membrane sequence in the process productivity. Gomes and co-workers confirm the importance of membrane sequence in order to reduce the amount of oligomeric products of lignin in solution (Gomes and Rodrigues 2019b).

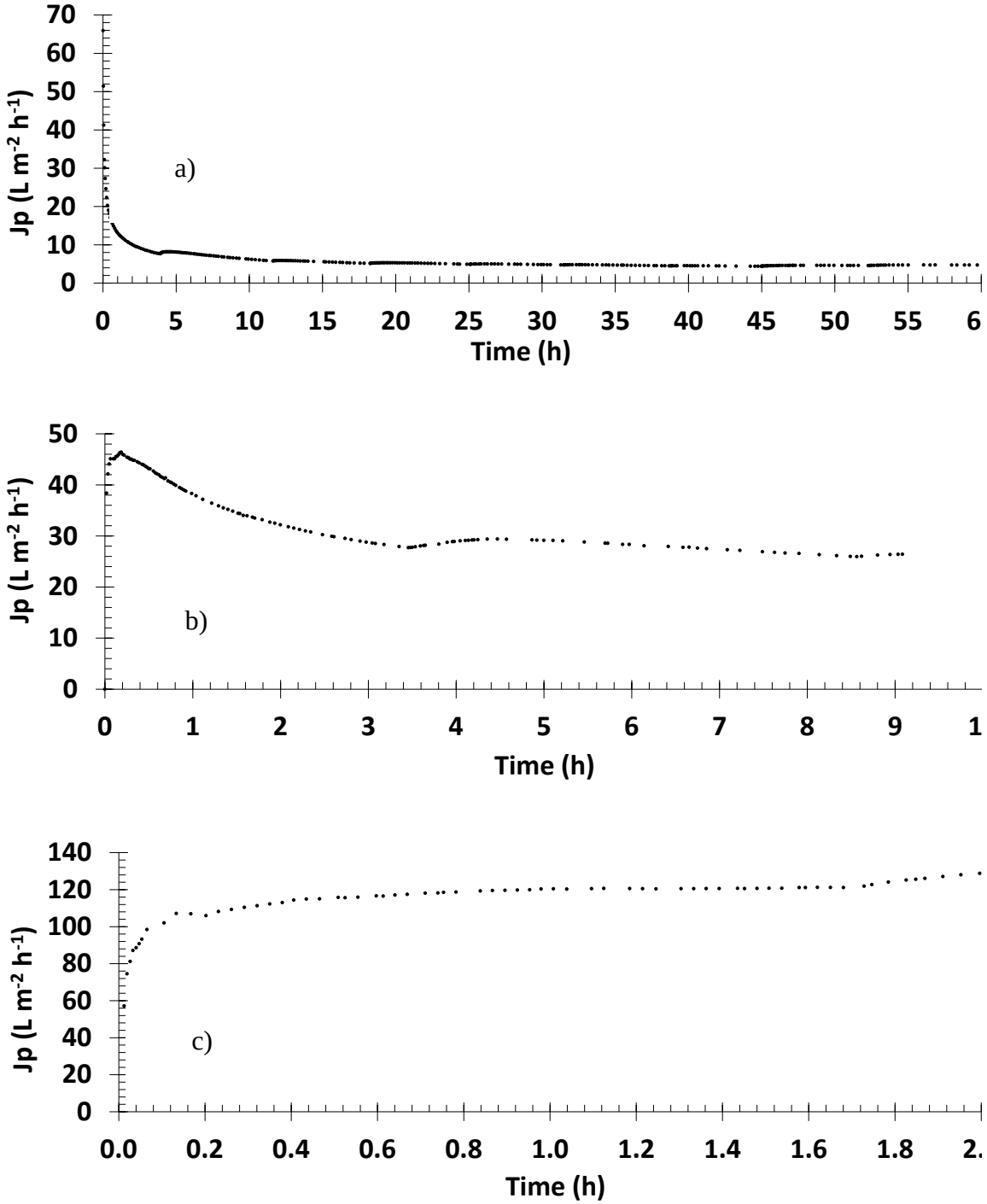

Figure 6.4 – Permeate flux behaviour with operating time obtained for the processing with: a) ultrafiltration membrane MT (5 kDa), b) ultrafiltration membrane GH (2 kDa), and c) nanofiltration membrane NFG (600-800 Da).

Total dissolved solids (TDS) were analyzed for the oxidized LHSL solution, permeates, and retentates resulting from ultra and nanofiltration. The results can be seen in Figure 6.5. The lowest value of TDS content was obtained for $P_{600\text{-}800Da}$, being similar to the content obtained in P_{2kDa}. Concerning the TDS percentage in the retentates it is possible to

observe a decrease in R_{5kDa} compared to the oxidized LHSL solution, but an increase in the R_{2kDa}. This could be explained by the presence of oligomeric structures of lignin, as well as the TDS was being retained with a higher percentage in this fraction between 5 kDa and 2 kDa

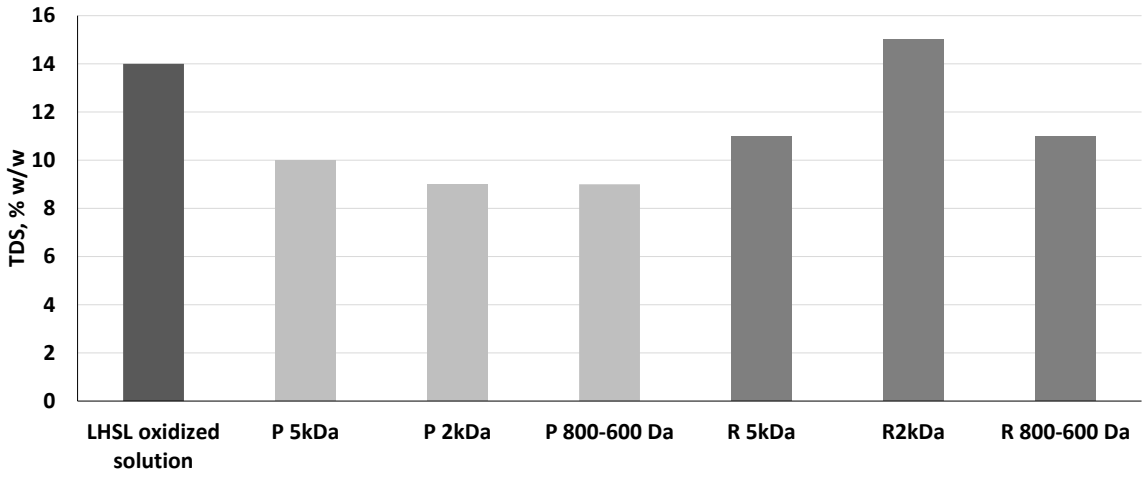

Figure 6.5 – Total dissolved solids of LHSL lignin oxidized mixture, permeates and retentates resulting from ultra and nanofiltration with 5 kDa, 2 kDa and 800-600 Da membranes.

6.3.2 Adsorption and Desorption Experiments

Preparative liquid chromatography was used to fractionate the mixture obtained from the oxidation of hardwood lignin isolated from the sulfite liquor (LHSL) after nanofiltration, into its monomer phenolic compounds by adsorption process.

The equilibrium adsorption in batch mode allows evaluating the adsorbent performance before application in larger scale as fixed bed column. The adsorption capacity of the SP700 resin with phenolic aldehydes, V and Sy, was evaluated using three different pH values, 6.5, 10, and 13. Mota and co-workers studied the adsorption capacity with aqueous solutions of V, Sy, VA and SA onto SP700 resin (Mota *et al.* 2016). In their study the pH used in the solutions was 4.5-4.9 for V, 5.7-6.2 for Sy, 3.3-3.5 for VA, and 3.5-3.6 for SA, in all cases the pH was below of pka of the studied phenolic compounds. In the present work, the pH used in the binary mixtures was selected based on acid dissociation constants of V and Sy, also considering that V and Sy are in phenolate form above 7.4 and 7.3 for V and Sy, respectively (Ragnar *et al.* 2000).

The study of the interaction of the main phenolic compounds contained in the permeate from nanofiltration of LHSL solution with SP700 resin was evaluated by performing a breakthrough curve, which also serves for the assessment of the duration of the feeding phase during the adsorption/desorption cycles. The breakthrough curve as well as adsorption/desorption cycles for the standard solution and permeate of nanofiltration are presented in the following sections.

6.3.2.1 Batch adsorption experiments

Batch adsorption experiments were conducted to study equilibrium isotherms for V and Sy from aqueous solutions onto SP700 resin. The effect of pH was evaluated, and three different values were selected: 6.5, 10, and 13. All the experiments were performed at a constant temperature of 25 ℃. The main experimental conditions and results obtained from batch experiments are presented in Table 6.4, for V and Sy.

The adsorption capacity of an adsorbent for a specific solute corresponds to the adsorbed amount reached in a saturated solution. In the case of the batch experiments performed for V and Sy, the equilibrium was reached after 48 hours. In batch adsorption experiments, the amount of solute that disappears from the solution is adsorbed onto the adsorbent. The adsorption capacity can be calculated from a mass balance between the adsorbent and liquid phases:

$$q_e = \frac{(C_{feed} - C_e) \cdot V}{W}; \quad (6.1)$$

where q_e (g/g$_{\text{dry resin}}$) is the adsorption capacity at equilibrium, C_{feed} (g/L) is the initial concentration of solute in the solution, C_e (g/L) is the equilibrium concentration of solute in the solution, V (L) is the initial volume solution and W (g) is the weight of dry resin.

The adsorption capacity of V and Sy as a function of liquid phase concentration at equilibrium (48 h) for the different pH values can be seen in the Figure 6.6. The adsorption capacity for the three different pH values studied were similar for V and Sy, both phenolics were most adsorbed at pH 6.5 and least at pH 13.

Table 6.4 - Conditions and results of batch experiments of V and Sy at constant temperature of 25 °C: $C_{i,feed}$ - initial feed concentration, $W_{dry\ resin}$ - weight of the dry SP700 resin, pH of C_i - pH of initial concentration, C - concentration at equilibrium, q_{ads} - adsorption capacity.

$C_{i,feed}$ (g/L)	$W_{dry\ resin}$ (g)	T (K)	pH of C_i	C (g/L)	q_{ads} ($g/g_{dry\ resin}$)
VANILLIN					
3.660	0.1	298	6.5	2.764	0.359
	0.2			2.046	0.323
	0.3			1.451	0.295
	0.4			1.104	0.256
	0.5			0.941	0.218
3.781	0.1		10	3.279	0.201
	0.2			2.969	0.162
	0.3			2.779	0.134
	0.4			2.625	0.116
	0.5			2.465	0.105
4.067	0.1		13	3.644	0.169
	0.2			3.358	0.142
	0.3			3.199	0.116
	0.4			3.066	0.100
	0.5			2.909	0.093
SYRINGALDEHYDE					
0.826	0.1	298	6.5	0.509	0.127
	0.2			0.313	0.103
	0.3			0.185	0.085
	0.4			0.117	0.071
	0.5			0.087	0.059
0.809	0.1		10	0.570	0.096
	0.2			0.487	0.064
	0.3			0.423	0.052
	0.4			0.389	0.042
	0.5			0.350	0.037
0.887	0.1		13	0.654	0.093
	0.2			0.571	0.063
	0.3			0.501	0.051
	0.4			0.454	0.043
	0.5			0.403	0.039

In literature it is reported that the amount of V adsorbed decreased as pH increased (Zabkova *et al.* 2006, Mota *et al.* 2016). This is related with the charge/structure of V and Sy that changes at different pH values of the solution due to of the hydroxyl groups (Zhang *et al.* 2008). V and Sy have a pKa of 7.4 and 7.2, respectively, when the pH of the solution is 6.5 both compounds are in the protonated form. On the other hand, when the pH of the starting solution is 10, V and Sy are deprotonated to become negatively charged. In the Figure 6.6 it is possible to observe that the adsorption capacity was higher for V than Sy. This is expected since Sy is less soluble in water than V and due to this limitation, the maximum adsorption capacity of Sy (0.13 $g/g_{dry\ resin}$) is smaller than the value found for V (0.36 $g/g_{dry\ resin}$). Mota and co-workers reported higher values for the adsorptive capacity of V and Sy onto SP700 resin. This may be due to the competitive adsorption between these phenolic compounds, since in this work, the experiments were performed with V and Sy in the same solution (Mota *et al.* 2016).

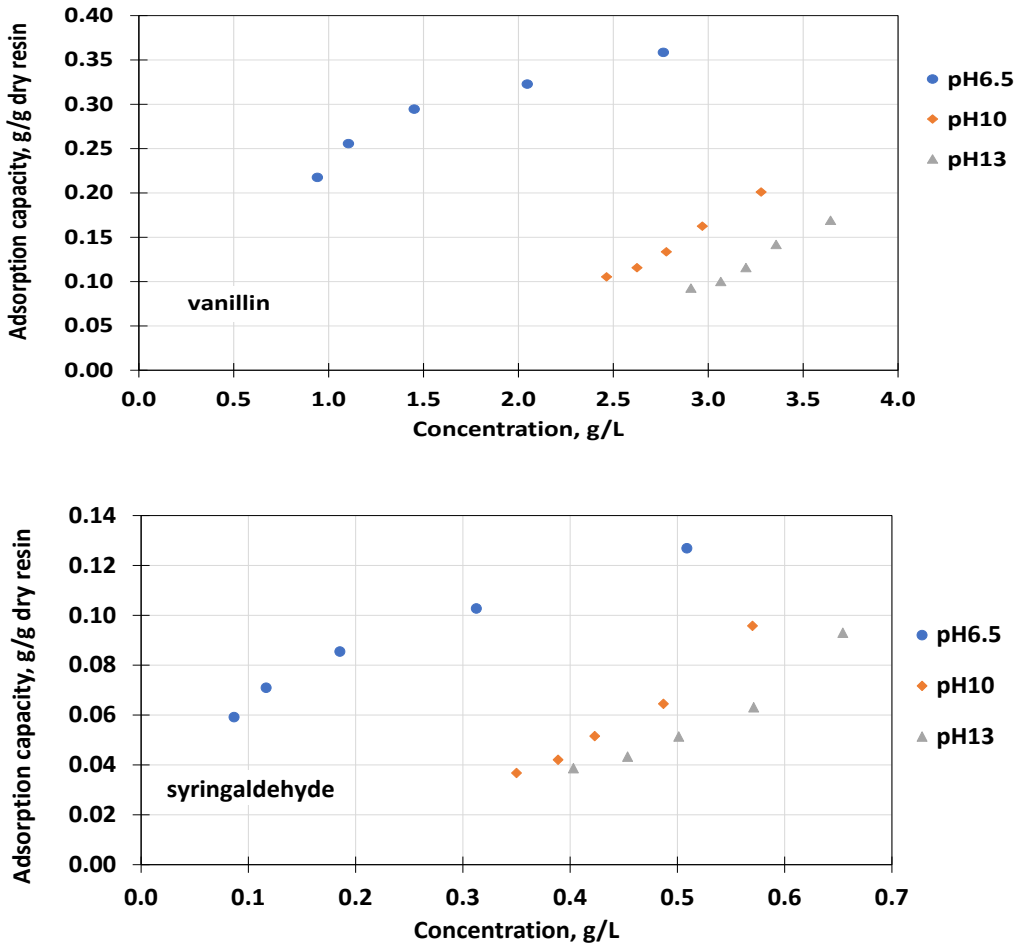

Figure 6.6 – The equilibrium adsorption isotherms of V and Sy onto the adsorbent SP700 resin at different pH values, at 25 °C.

The lowest adsorption capacity observed for V corresponds to 10.4 % of the initial concentration and this was observed for pH 13 and 0.1 g of dry resin and the highest one (72.3%) was obtained for pH 6.5 and 0.5 of dry resin. Regarding Sy, it was observed the same behavior, the lowest percentage corresponds to 26.2 % of the initial concentration and the highest corresponds to 90.5 %.

6.3.2.2 Breakthrough experiments

The breakthrough experiment allows to study the interaction of the main phenolic compounds present in the studied mixture, VA, V, SA, Sy, VO and SO, with the SP700 resin until equilibrium is reached. The equilibrium is achieved when the outlet and feed concentrations are similar. The breakthrough was performed using a model solution at a feed volumetric flow rate of 5 mL/min and a constant temperature (25 ℃). Feed concentrations are detailed in Table 6.2.

Concentration and normalized concentration history of the phenolic monomers studied are shown in Figure 6.7 and Figure 6.8, respectively.

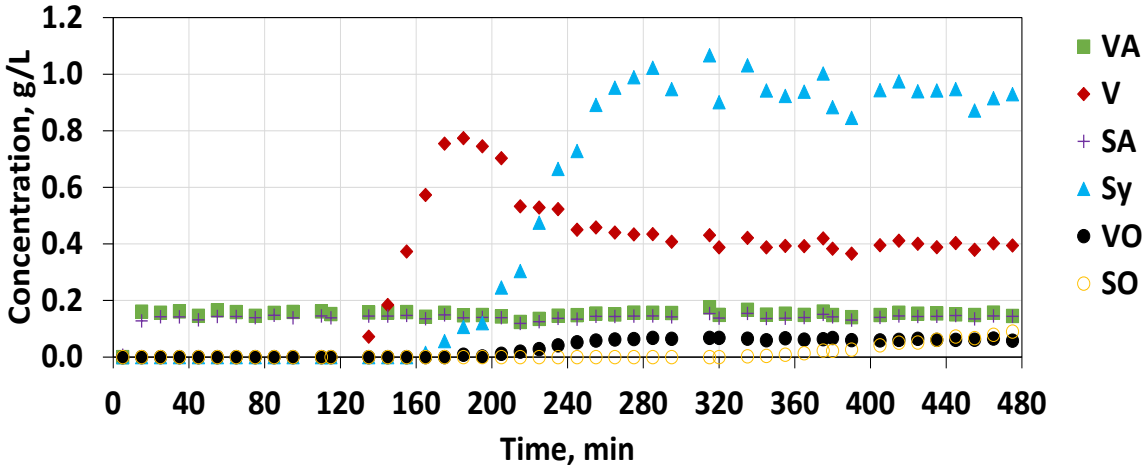

Figure 6.7 - Concentration history of the phenolic monomers during the breakthrough experiment. Feed pH: 13.2; *T*=25°C, volumetric flow rate = 5 *ml/min*. Feed monomer concentrations are given in Table 5.3.

The breakthrough experiment was performed for 8 hours. The phenolic acids, VA and SA reaches the feed concentration 15 minutes after the beginning of the experiment. Then, V starts to elute after 135 minutes and takes over 4 hours to reach the equilibrium. Between 160 min and 240 min, it is observed a roll-up effect for V, which coincides with the beginning of Sy elution. This phenomenon confirms that there is competitive adsorption between these two aldehydes. Sy starts to elute after 175 minutes and reach the equilibrium

after 280 min (4.7 h). VO elute in 200 min and takes over 4.3 h to reach the feed concentration. The last monomer to elute is SO, which elute after 345 minutes and reaches the feed concentration after 8 hours.

The elution order observed in the breakthrough experiment, acids, aldehydes and ketones, was also be confirmed in the work of Gomes and Rodrigues (Gomes and Rodrigues 2019b). The authors reported that the elution order could be explained based on acid dissociation constants (pKa) of each phenolic monomer, which means that compounds with lower pKa elute first such as the phenolic acids (pKa of 4.3 and 4.4 for VA and SA, respectively). While aldehydes and ketones have a pKa in the range of 7.2 - 8.0 ending up eluting later. The authors also reported that higher pH values, as in the present work (pH of 13.2) are associated with lower adsorption capacities of the ionizable phenolic compounds due to the formation of more hydrogen bonds between adsorbate and water leading to higher hydrophilicity and hindering the full extent of adsorption (Lin and Juang 2009, Jin *et al.* 2015, Gomes and Rodrigues 2019b). Suggesting that with higher pH values of the solution, the time of the breakthrough curve can be higher than expected.

Gomes and co-workers reported a breakthrough curve using an annual plant as a raw material, which implies a different S:G:H ratio (Gomes *et al.* 2018). While the hardwood lignin (present work) has an S:G:H ratio of 64:30:6, the lignin from an annual plant has more H units with a ratio of 38:48:18. Thus it is expected that the referred work, reported by Gomes and co-workers, it is observed a notorious competitive adsorption since it has more phenolic aldehydes (same family) competing with the SP700 resin. The breakthrough performed in this work has different behavior on the phenolic monomer profile when compared with the results obtained by Gomes and co-workers (Gomes *et al.* 2018). Phenolic acids VA and SA had the same profile in both works, but when phenolic aldehydes or phenolic ketones are compared it was possible to see that Gomes and co-workers achieved higher ratios for C/C0 during the breakthrough curve.

Comparing the breakthrough curve with 6 compounds (LHSL lignin), and the breakthrough obtained with 4 compounds (LSSL lignin) it is possible to observe some differences between them. Regarding V, when the solution has more competing compounds (LHSL lignin) for the adsorption sites, it takes double of time to start eluting. Also depending on the functional group of the compound, phenolic acids have low affinity with the SP700 resin eluting in the first minutes of feeding, on contrary, the aldehydes and ketones have more impact due to the similarity of functional groups, and consequently have more affinity

with the SP700 resin. Other variable is the phenolic concentration, where phenolic compounds with higher concentrations takes longer time to elute.

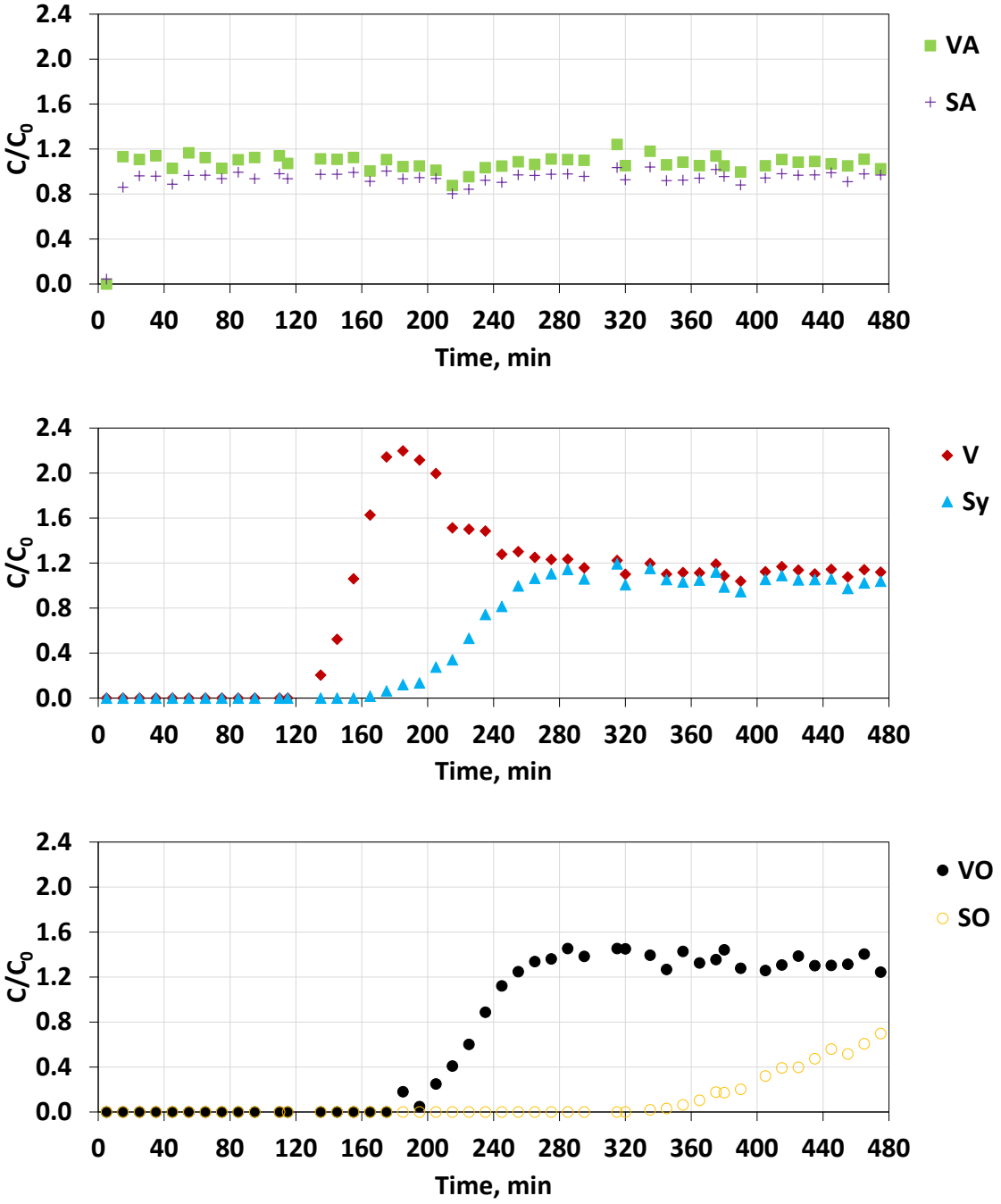

Figure 6.8 - Normalized concentration histories of the phenolic monomers from a multicomponent model solution in the breakthrough experiment: a) acids, VA and SA; b) aldehydes, V and Sy; and c) ketones, VO and SO. Feed pH: 13.2; *T*=25°C, volumetric flow rate = 5 *ml/min*. Feed monomer concentrations are given in Table 5.3**.**

Considering the elution order and time of the phenolic compounds studied in the breakthrough, the selected time 260 min was the reference for the feed phase duration in the adsorption/desorption cycles that are presented in the next sections. This time was selected with the aim of obtaining a fraction rich in our compounds of interest. At 260 min Sy almost achieve the equilibrium, and the column is almost saturated with Sy, this is the time that the feeding phase was stopped. Regarding vanillin, it is possible to obtain a maximum ratio of 1.2 (C/C0) during the breakthrough curve with 4 compounds at 110 minutes, while in the breakthrough with six compounds a ratio of 2.2 (C/C0) was obtained at 175 minutes. Despite being the same compound, V, and the resin-composite interaction are also the same, the feed concentration of V is higher in the breakthrough curve with 4 compounds than in the breakthrough curve with 6 compounds. Concluding that the concentration has a significant influence on the elution time and therefore on the maximum C/C0 ratio obtained for the phenolic compounds studied.

To proceed to the cycles of adsorption and desorption experiments was performed a test to choose the best time feeding with the objective to get higher concentration in phenolic aldehydes. The feeding time was selected based on the two preliminary tests performed. According to the breakthrough curve performed and presented in the previous section it was chosen 175 (Test 1) and 260 (Test 2) minutes of feeding, Table 6.5.

Table 6.5 – Main results obtained in the preliminary tests performed to select feeding time. Test 1 with feeding time of 175 min and Test 2 with feeding time of 260 min.

		Phenolic compounds	
		V	**Sy**
Test 1 – 175 min.	**Feed stream, g/L**	0.36	0.84
	Fraction II – water desorption phase, g/L	2.3	5.8
	Fraction II recovery, %	72	79
Test 2 – 260 min.	**Feed stream, g/L**	0.29	0.67
	Fraction II – water desorption phase, g/L	1.41	7.5
	Fraction II recovery, %	38	85

The concentration and recovery obtained during the water desorption phase for the target phenolic compound, Sy, were the main parameters evaluated to select the feeding

time. Higher recovery and higher concentration of Sy were obtained when 260 min of feed was used. The concentration of Sy obtained during fraction II of the water desorption phase was an important parameter since this fraction will be used to further the purification process.

The adsorption/desorption experiments were accomplished in a cyclic mode operation without regeneration of SP700 resin. The column was fed for 260 minutes, to ensure that phenolic aldehydes, V and Sy, saturate the resin. The main phenolic monomers present in the solution were desorbed with water and ethanol (99 % v/v). The desorption step with water was performed for 50 minutes, after that desorption with ethanol was performed for more 50 minutes. During the water phase desorption three different fractions were collected at preset times to recover Sy in high concentration with lower quantities of other phenolic compounds present in the mixture. Fractionation scheme of cyclic mode operation applied to the model solution and to the permeate from nanofiltration of LHSL solution is detailed in Figure 6.9. In both solutions the same cyclic configuration was adopted, the results are presented in the following sections.

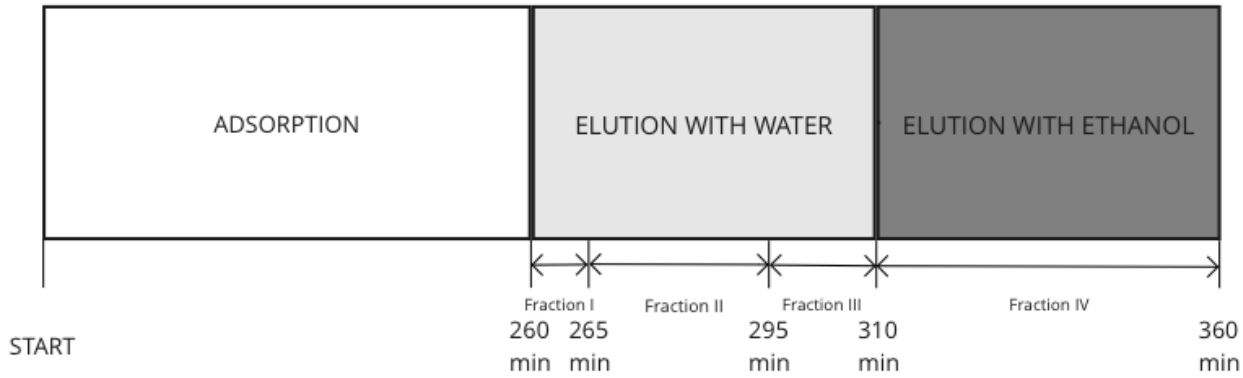

Figure 6.9 - Sequence of steps of the cycles of adsorption/desorption experiments**.**

6.3.2.3 Adsorption/desorption cycles using model solution

In order to study the capacity of the resin to operate in a continuous cyclic mode, eight cycles of adsorption/desorption were performed using a model solution. The feed solution for all the cycles was composed by VA, V, SA, Sy, VO and SO, with the concentrations shown in Table 5.3. The mixture was fed at a volumetric flow rate of 5 mL/min and the column was kept at 25 ℃. The concentration history and the representation of the normalized concentration of the studied monomers can be shown in Figure 6.10 and Figure 6.11, respectively.

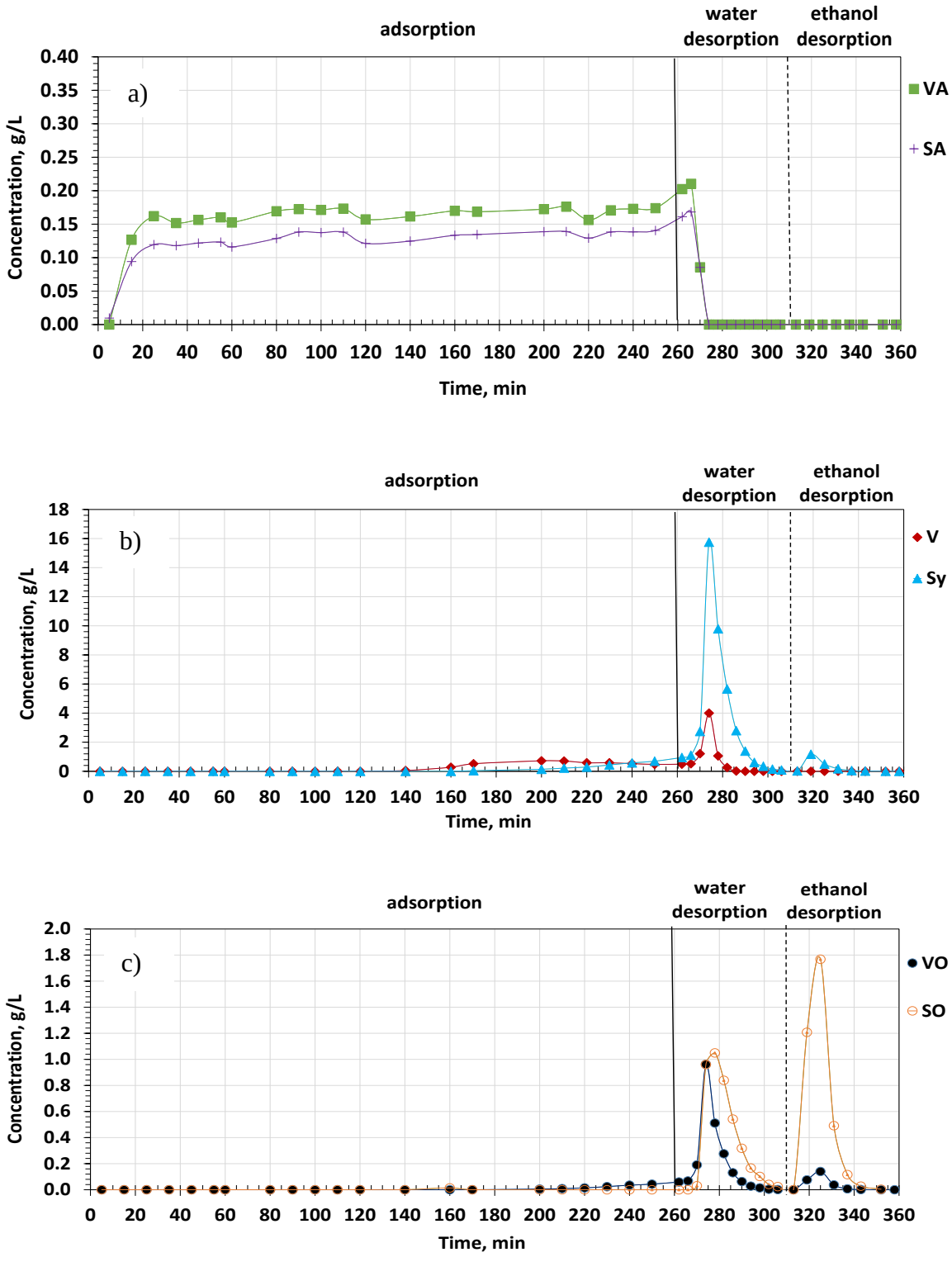

Figure 6.10 – Concentration history of the monomers in the cycle experiment with model solution by families: a) phenolic acids b) phenolic aldehydes, and c) phenolic ketones. The first vertical line represents the beginning of the water desorption phase, and the vertical dotted line represents the beginning of the ethanol desorption phase. Feed pH: 13.2, T=25 °C, volumetric flow rate = 5 mL/min. Feed monomer concentration is given in Table 6.2.

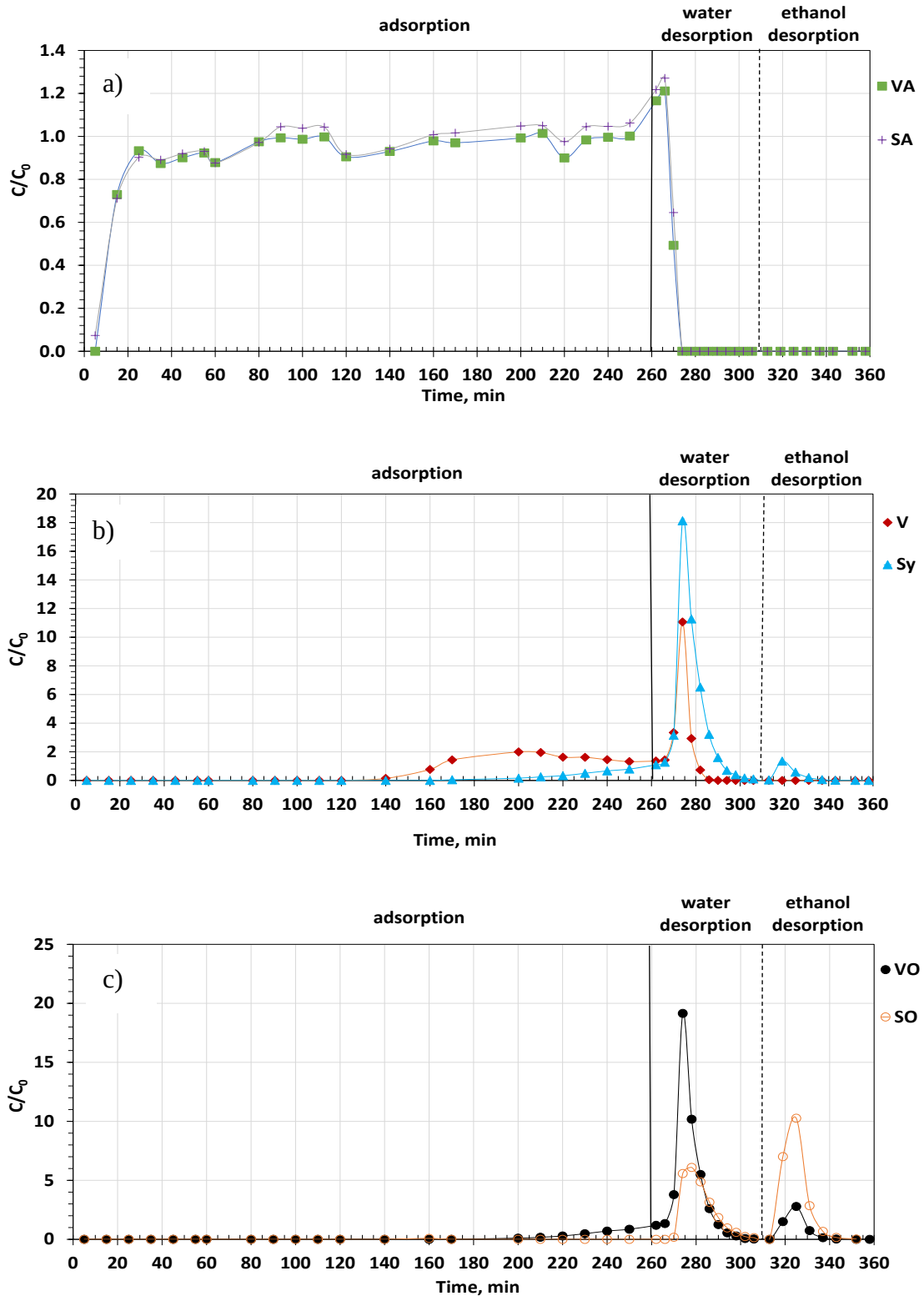

Figure 6.11 – Normalized concentration history of the monomers in the cycle experiment with model solution by families: a) phenolic acids b) phenolic aldehydes, and c) phenolic ketones. The first vertical line represents the beginning of the water desorption phase, and the vertical dotted line represents the beginning of the ethanol desorption phase. Feed pH**:** 13.2, T=25 ℃, volumetric flow rate = 5 mL/min. Feed monomer concentration is given in Table 6.2.

During the feed phase, VA and SA eluted with a similar concentration (0.16 g/L and 0.12 g/L, respectively) as the feed mixture after 15 minutes. The pH of the feed solution was measured during the elution and a constant value, around 13.2, was found. The aldehyde V started to elute after 140 minutes of adsorption and reached twice the feed concentration in the minute 200. VO also started to elute during the feed phase at time around 230 minutes, while the ketone SO is not detected during the feed phase. When the water desorption phase began, V and Sy started to elute, and it was possible to see that its concentration increases up to almost 11 and 18 times of the feed concentration, respectively, in the minute 274 (14 minutes of water desorption phase). Moreover, VO and SO also elute in the water desorption phase reaching 19 and 6 times of the feed concentration (minute 274), respectively. Additionally, in the ethanol desorption phase a small amount of Sy eluted in the minute 325 (15 minutes after the beginning of ethanol phase desorption). Moreover, in this phase elute mainly SO, it is possible to see in Figure 6.11 that this ketone elutes after minute 325, reaching 10 times the feed concentration. VO also elutes at the same time but reaching only almost 3 times of the feed concentration.

The concentrations obtained for the studied compounds in each fraction collected in one of the adsorption/desorption cycle's experiments are shown in the Table 6.6. It is important to note that the concentration values obtained in the different fractions were similar for all the cycles performed.

Table 6.6 – Concentration of VA, V, SA, Sy, VO and SO in each fraction collected and feed stream during adsorption/desorption cycle experiment with model solution**.**

		Concentration, g/L			
Monomers	**Feed stream**	**Water desorption phase**			**Ethanol desorption phase**
		Fraction I	**Fraction II**	**Fraction III**	
VA	0.17	0.16	0.02	--	--
V	0.35	0.40	1.14	--	--
SA	0.13	0.13	0.04	--	--
Sy	0.85	0.85	6.5	0.17	0.13
VO	0.05	0.05	0.36	--	0.03
SO	0.17	--	0.63	0.06	0.46

The mass balance, in grams, of each phenolic compound fed to the column and recovered during the feed phase and during both desorption phases was presented in Figure 6.12.

Sy, which was our main target monomer considering the hardwood lignin, was collected mainly in fraction II of the water desorption phase, with a concentration of 6.5 g/L. Therefore, 87 % of recovery and 75 % of purity were obtained for Sy in this fraction. Considering V, it was possible to see that 40 % of the recovery was achieved in the water desorption phase. However, the compounds that elute during the feed phase can be recovered by passing the solution through the column again. Since our main objective was to have a fraction enriched in Sy, that is, with a high concentration of Sy, some of the mass of V was lost. It would be expected that in the ethanol desorption phase, VO and SO elute with high recovery. But in the case of VO, was in the water desorption phase that this compound had a higher recovery reaching 88 %. In contrast, the recovery of SO is divided by the water desorption phase and ethanol desorption phase reaching a recovery of about 45 and 50 %, respectively.

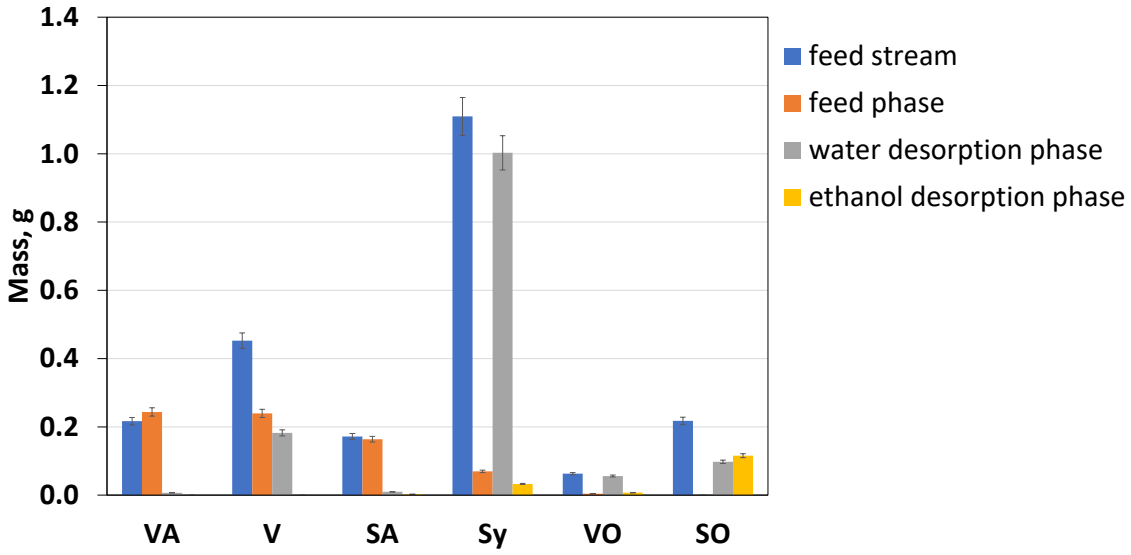

Figure 6.12 – Mass balance related to the monomers studied in the different collected phases with model solution.

Comparing the cycles performed in this chapter and the cycles performed in the previous chapter both with model solutions, it can be observed that the concentration history of the phenolic compounds had some differences. Looking at phenolic acids, the normalized

concentration history (C/C_0) of both model solutions (Figure 5.10 and Figure 6.11) do not show significant differences, due to the weak interaction between phenolic acids and the adsorbent, SP700 resin. Concerning the phenolic aldehyde, V, the C/C_0 achieved in the water desorption phase presented in the previous chapter and the present work was 11 times the feed concentration although, the model solution in the present work had a lower concentration than the model solution presented in the previous chapter. The same does not happen with Sy or the phenolic ketones VO and SO. For these compounds, it was observed that higher concentrations of the phenolic compounds, increase the ratio C/C_0 observed. This suggests that these compounds have more interaction with the SP700 resin, and higher competitive adsorption between them.

6.3.2.4 Fixed bed experiments: cycles of adsorption/desorption using the permeate from nanofiltration of LHSL solution

The mixture obtained from the oxidation of lignin from hardwood sulfite liquor in an alkaline medium with oxygen was submitted to a three-step membrane filtration (ultra and nanofiltration). The permeate obtained in the nanofiltration, $P_{600\text{-}800\ Da}$, was used in the chromatographic experiments. The main phenolic compounds present in the mixture are VA, V, SA, Sy, VO and SO. The mixture was fed to the column with volumetric flow rate of 5 mL/min, without pH adjustment, and the temperature of the jacketed column was kept at 25 ºC. Initial concentrations of monomers are detailed in Table 6.2. According to the fractionation scheme previously mentioned (Figure 6.9) 2 cycles of adsorption/desorption were performed. During adsorption/desorption experiments in cycle 1, samples were collected, and then concentration of the studied monomers were analyzed by HPLC and represented in the Figure 6.13. The normalized concentration histories of the studied monomers are shown in the Figure 6.14.

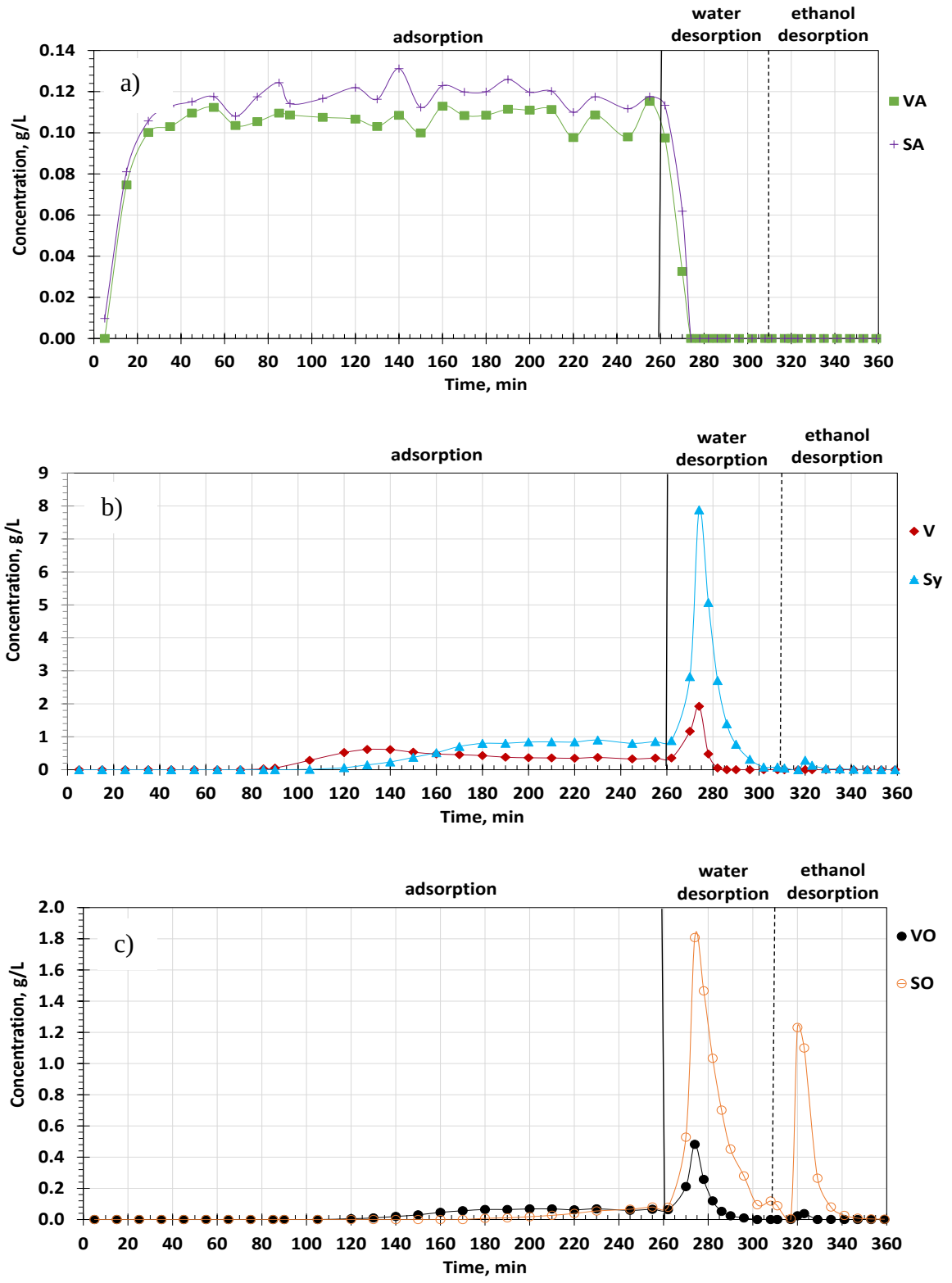

Figure 6.13 – Representation of concentration history of the monomers in the adsorption/desorption experiment, with permeate from nanofiltration of LHSL solution by families: a) phenolic acids, b) phenolic aldehydes, c) phenolic ketones. The first vertical line represents the beginning of the water desorption phase, and the vertical dotted line represents the beginning of the ethanol desorption phase. Feed pH:13.2, T=25 ºC, volumetric flow rate of 5 mL/min. Feed monomer concentrations is given in Table 6.2.

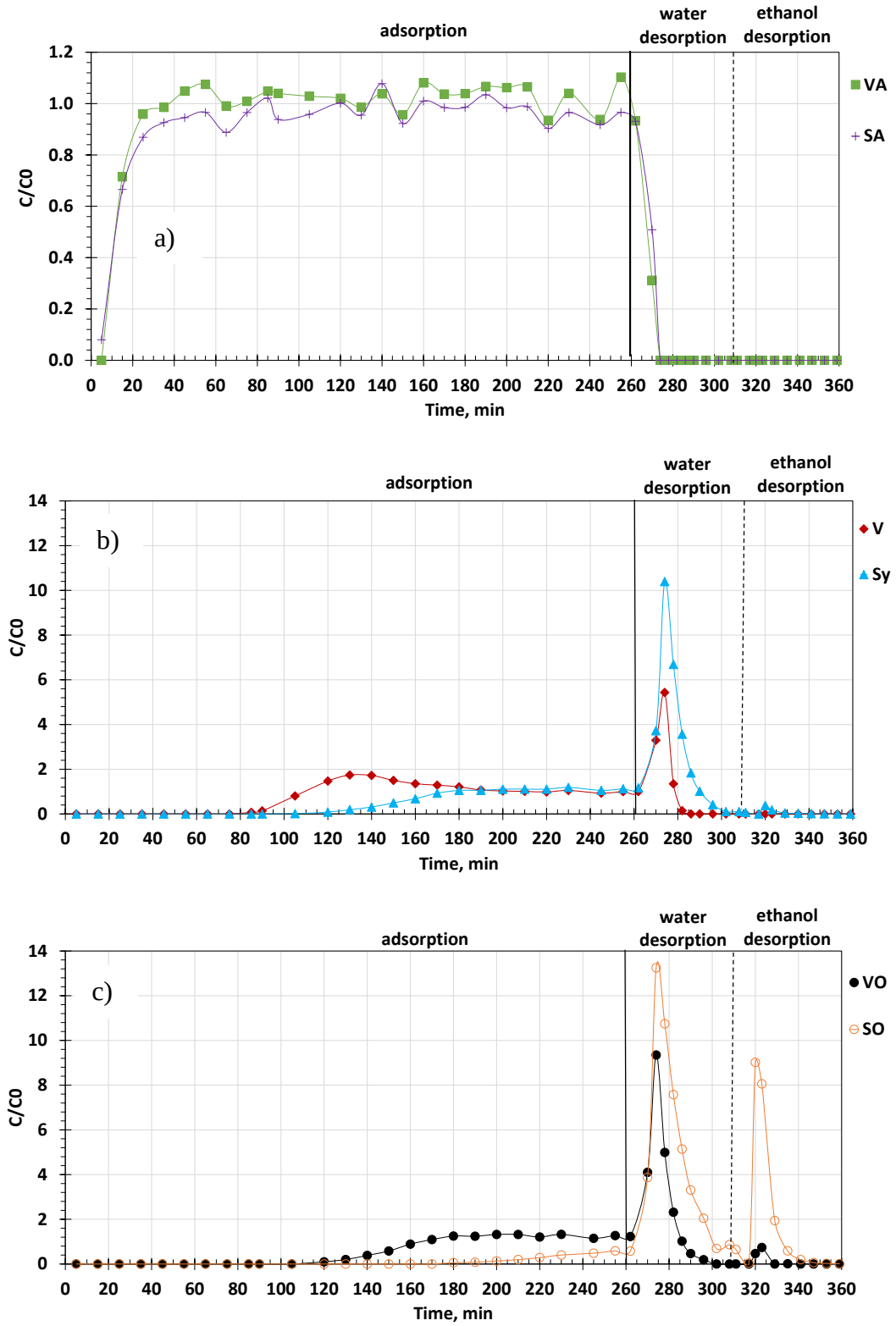

Figure 6.14 - Representation of normalized concentration history of the monomers in the adsorption/desorption experiment, with permeate from nanofiltration of LHSL solution by families: a) phenolic acids, b) phenolic aldehydes, c) phenolic ketones. The first vertical line represents the beginning of the water desorption phase, and the vertical dotted line represents the beginning of the ethanol desorption phase. Feed pH:13.2, T=25 ºC, volumetric flow rate of 5 mL/min. Feed monomer concentrations is given in Table 6.2.

Regarding the concentration history for all the compounds, it is possible to see that the acids VA and SA desorb after 15 minutes of the feed phase, which means that acids are not adsorbed. The aldehydes, V and Sy, start to elute around 90 and 120 minutes of feed, respectively. In minute 180 both compounds reach the saturation point. In the experiment using standard solution, the saturation point is observed after 260 minutes of feed, which is quite later when compared to the permeate from LHSL solution nanofiltration. This behavior could be explained by the presence of other compounds that are not identified and could compete with V and Sy for the active sites of the adsorbent. During the desorption with water the aldehydes, V and Sy, have a higher peak in the minute 274 reaching a concentration of 6 and 10 times of feed concentration with 1.9 and 7.8 g/L, respectively.

Concerning the ketones, during the feed phase in the minute, 120 and 200 of feed VO and SO elutes, respectively. During the water desorption phase, VO and SO reach 9 and 13 times of feed concentration, with a concentration of 0.5 and 1.8 g/L, respectively. Although the ketone SO also elute during the water desorption phase, during the ethanol desorption phase elute reaching a concentration of 1.2 g/L in the minute 320 which is 9 times of feed concentration. Table 6.7 summarizes the concentrations of the monomers, VA, V, SA, Sy, VO and SO, attained during the cycle's experiment with the permeate from nanofiltration of oxidized LHSL solution.

Table 6.7 – Concentration of VA, V, SA, Sy, VO and SO in each fraction collected during adsorption/desorption cycle experiment with permeate from nanofiltration of LHSL solution.

Monomers	**Concentration, g/L**				
	Feed phase	**Water desorption phase**			**Ethanol desorption phase**
		Fraction I	**Fraction II**	**Fraction III**	
VA	0.11	0.11	--	--	--
V	0.27	0.37	0.54	--	--
SA	0.11	0.11	--	--	--
Sy	0.30	0.86	2.9	0.18	0.05
VO	0.02	0.07	0.17	0.006	0.004
SO	--	0.12	0.92	0.21	0.22

No significant differences were observed for the 2 performed cycles. The mass recovered of phenolic compounds in water and ethanol desorption phases is presented in

Figure 6.15. From the initial mass of VA (0.14 g) fed to the column, 0.13 g was recovered during the feed phase. No VA was detected during the desorption phase with ethanol. From the initial mass of SA (0.16 g) fed to the column, 0.14 g was recovered during the feed phase. No SA was detected during the desorption phase with ethanol. From the mass of V (0.45 g) fed initially to the column, 0.35 g was recovered during the feed phase, and during desorption phase with water 0.1 g of V were recovered. No V was detected during the desorption phase with ethanol. From the mass of Sy (0.95 g) fed initially to the column, 0.39 g was recovered during the feed phase, and during desorption phase with water 0.47 g of Sy were recovered. In the ethanol desorption phase traces of Sy were detected. From the mass of VO (0.06 g) fed initially to the column, 0.03 g was recovered during the feed phase, and during desorption phase with water 0.02 g of VO were recovered, and traces of VO were detected in the ethanol desorption phase. From the mass of SO (0.23 g) fed initially to the column, during desorption phase with water 0.15 g of SO were recovered, and 0.10 g of SO in the ethanol desorption phase.

Overall, most of the mass of the phenolic acids VA and SA were recovered during the feed phase with minimal mass being lost to the water desorption phase. The aldehydes Sy and V the recovery is divided in the feed phase and in the water desorption phase along with a small contamination from the phenolic ketones SO and VO. In the ethanol desorption phase, SO is the major phenolic compound, with a small quantity of Sy. From the total mass of each compound fed to the column, it was possible to recover 19 % of V, 50 % of the Sy, 67 % of the SO, and 42 % of VO during the water desorption phase. The recoveries during the ethanol desorption phase were lower comparing to the water desorption phase, having only 24 % of SO mass recovered, 2 % of VO, and 1 % of Sy.

Making a comparative approach of the adsorption/desorption studies with the two real solutions (hardwood and softwood lignin coming from the pulp mill sulfite liquor) it was possible to observe that the hardwood solution has an S:G:H ratio of 64:30:6 while the softwood solution has mainly G units with an S:G:H ratio of 18:75:7 (Chapter 3). Consequently, the LHSL solution shows a higher competitive adsorption between the phenolic monomers than the LSSL solution, due to the presence of more phenolic monomers which was verified by the obtained results in Chapter 5 (Figure 5.14) and the results obtained in the present chapter (Figure 6.15). Other difference was the feed concentrations, where in the LHSL solution the highest monomer concentration belongs to Sy and in the LSSL solution the highest monomer concentration belongs to V.

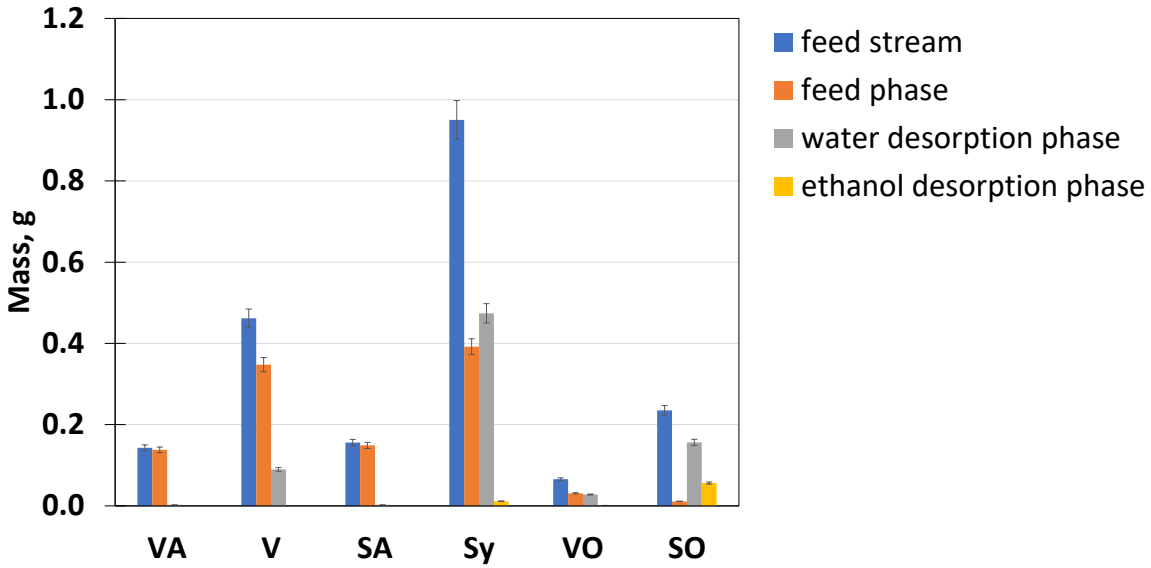

Figure 6.15 - Mass balance to the species fed and recovered at each phase for LHSL mixture.

6.4 CONCLUSIONS

In this work, the most abundant low molecular weight phenolic compounds, Sy, V, VA, SA, VO and SO, obtained in the alkaline oxidation of LHSL were fractionated in a chromatographic step that employs water and ethanol as eluents and the polymeric resin SP700. Prior to the chromatographic step, the feed mixture was submitted to a three-step membrane filtration, 5 k, 2 k and 600-800 Da, where the organic solids content was reduced in 5% before being fed to the chromatographic column.

A complete breakthrough with a standard solution was performed for 8 hours, with a pH of 13.2, and a volumetric flow rate of 5 mL/min. The breakthrough curve allows determining the time at which cycle of adsorption/desorption would be performed. Eight cycles were performed in the case of standard solution and two cycles in the case of permeate from oxidized LHSL solution nanofiltration. All the cycles performed, with the model solution or with the oxidation mixture, had very similar behaviors.

The resulting fractions from chromatographic phase were fractionated by dominant functional groups: phenolic acids, phenolic aldehydes, and phenolic ketones.

Regarding the cycles performed with the model solution, it was possible to obtain recoveries of about 88 % for Sy, 40 % for V, 81% for VO, and 45 % for SO during the water desorption phase. In the ethanol desorption phase phenolic ketones, VO and SO, had

recoveries of about 20% and 80 %, respectively. Considering the permeate from oxidized LHSL solution nanofiltration different recoveries were obtained. From the total mass of each compound fed to the column, it was possible to recover 19 % of V, 50 % of the Sy, 67 % of the SO, and 42 % of VO during the water desorption phase. The recoveries during the ethanol desorption phase were lower comparing to the water desorption phase, having only 24 % of SO mass recovered, 2 % of VO, and 1 % of Sy.

6.5 REFERENCES

Fache, M., B. Boutevin and S. Caillol (2016). Vanillin Production from Lignin and Its Use as a Renewable Chemical. *ACS Sustainable Chemistry & Engineering* 4(1): 35-46.

Gomes, E. D., M. I. Mota and A. E. Rodrigues (2018). Fractionation of acids, ketones and aldehydes from alkaline lignin oxidation solution with SP700 resin. *Separation and Purification Technology* 194: 256-264.

Gomes, E. D. and A. E. Rodrigues (2019b). Lignin biorefinery: Separation of vanillin, vanillic acid and acetovanillone by adsorption. *Separation and Purification Technology* 216: 92-101.

Gomes, E. D. and A. E. Rodrigues (2020a). Recovery of vanillin from kraft lignin depolymerization with water as desorption eluent. *Separation and Purification Technology* 239: 116551.

Jin, Z., X. Wang, Y. Sun, Y. Ai and X. Wang (2015). Adsorption of 4-n-Nonylphenol and Bisphenol-A on Magnetic Reduced Graphene Oxides: A Combined Experimental and Theoretical Studies. *Environmental Science & Technology* 49(15): 9168-9175.

Lin, S.-H. and R.-S. Juang (2009). Adsorption of phenol and its derivatives from water using synthetic resins and low-cost natural adsorbents: A review. *Journal of Environmental Management* 90(3): 1336-1349.

Mota, I. F., P. R. Pinto, A. M. Ribeiro, J. M. Loureiro and A. E. Rodrigues (2018). Downstream processing of an oxidized industrial kraft liquor by membrane fractionation for vanillin and syringaldehyde recovery. *Separation and Purification Technology* 197: 360-371.

Mota, M. I. F., P. C. R. Pinto, J. M. Loureiro and A. E. Rodrigues (2016). Adsorption of vanillin and syringaldehyde onto a macroporous polymeric resin. *Chemical Engineering Journal* 288: 869-879.

Ragnar, M., C. T. Lindgren and N.-O. Nilvebrant (2000). pKa-Values of Guaiacyl and Syringyl Phenols Related to Lignin. *Journal of Wood Chemistry and Technology* 20(3): 277-305.

Rodrigues, A., P. Pinto, F. Barreiro;, C. A. E. Costa, M. I. F. Mota and I. Fernandes (2018). An Integrated Approach for Added-Value Products from Lignocellulosic Biorefineries. Springer Nature Switzerland AG, Springer International Publishing.

Satyanarayana, S. V., P. K. Bhattacharya and S. De (2000). Flux decline during ultrafiltration of kraft black liquor using different flow modules: a comparative study. *Separation and Purification Technology* 20(2): 155-167.

Sethupathy, S., G. Murillo Morales, L. Gao, H. Wang, B. Yang, J. Jiang, J. Sun and D. Zhu (2022). Lignin valorization: Status, challenges and opportunities. *Bioresource Technology* 347: 126696.

Žabková, M., E. A. B. da Silva and A. E. Rodrigues (2007b). Recovery of vanillin from lignin/vanillin mixture by using tubular ceramic ultrafiltration membranes. *Journal of Membrane Science* 301(1): 221-237.

Zabkova, M., M. Otero, M. Minceva, M. Zabka and A. E. Rodrigues (2006). Separation of synthetic vanillin at different pH onto polymeric adsorbent sephabeads SP206. *Chemical Engineering and Processing: Process Intensification* 45(7): 598-607.

Zhang, Q.-F., Z.-T. Jiang, H.-J. Gao and R. Li (2008). Recovery of vanillin from aqueous solutions using macroporous adsorption resins. *European Food Research and Technology* 226(3): 377-383.

7 From Sulfite Liquors to Phenolic Aldehydes: Vanillin and Syringaldehyde

This chapter contemplates, V and Sy crystallization using aqueous solutions with low concentrations of these potential food and pharmaceutical phenolic compounds. The crystallization processes were performed using the aqueous solutions enriched with V and Sy obtained from the steps of filtration and preparative chromatography, described in the previous chapters.

In the case of V, different approaches of cooling and evaporative crystallization were attempted using the aqueous solution from LSSL. The processes yield, and purity of the V crystals were determined, and the thermal stability of the two resulted polymorphic forms were analysed by DSC.

For Sy, using the aqueous solution from LHSL, crystallization was performed based on the solubility of the compounds present in the solution and taking advantage of the lower solubility of this phenolic compound in water.

7.1 INTRODUCTION

V (4-hydroxy-3-methoxy-benzaldehyde, Figure 7.1) is a phenolic aldehyde and a moderate hydrogen bond acceptor with reactive methoxyl, hydroxyl, and aldehyde sites (Zhang *et al.* 2015). It has a strong aroma and is one of the most demanded ingredients in flavour industry. In the global market, about 60 % of industrial V is used as a food additive, while the remaining 40 % is used as cosmetic ingredients (approximately 33 %) and pharmaceuticals (roughly 7 %) (Bajpai 2018). Due to its valuable antimicrobial, antioxidant, anticarcinogenic, and antislicking properties, V shows great potential as a chemical intermediate to produce pharmaceuticals such as papaverine, levodopa, ethamivan, and cyclovalone, and fine chemicals such as veratraldehyde, protocatechualdehyde (Wong *et al.* 2020, Zhou *et al.* 2022). The rising demand for V for end-use industries is expected to substantially influence market growth in the next years. In 2016, the global demand for V was about 18 600 tons and will grow by 6.2 % by 2025 (Martău *et al.* 2021).

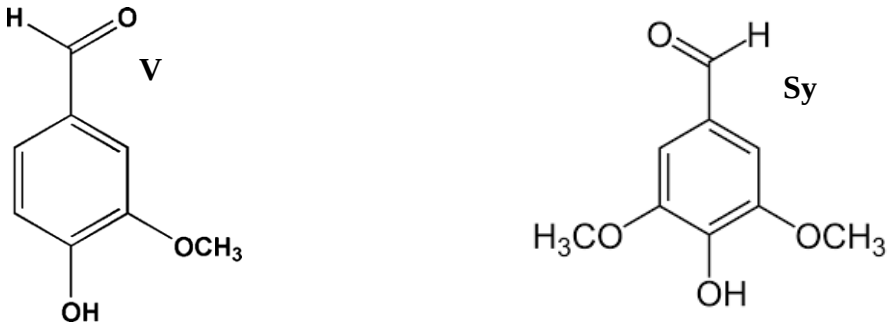

Figure 7.1 – Structure of V (4-hydroxy-3-methoxy-benzaldehyde) and Sy (4-Hydroxy-3,5-dimethoxy-benzaldhyde).

Sy (4-Hydroxy-3,5-dimethoxy-benzaldhyde, Figure 7.1) is very similar in structure to V, and it has similar applications. Although it is not as well-commercialized as V, Sy has been gaining prominence, especially after the discovery of its role as an essential intermediate of the antibacterial drugs Trimethoprim, Bactrim, and Biseptol (Manchand, 1978). Sy is a naturally occurring unique compound with assorted bioactive characteristics that belongs to the phenolic aldehyde family. This phenolic is important in pharmaceutical applications due to their antioxidant, anti-inflammatory, antimicrobial and antifungal properties (Yancheva *et al.*, 2016). Sy can be synthesized from gallic acid, pyrogallol,

vanillin, or *p*-cresol and its market value is about 22 USD per kilogram (Osorio-González *et al.*, 2019). An excellent natural source of Sy lies within the cell walls of plants.

Recently, the demand for chemicals from renewable sources has brought new life on the lignin route to produce V. Furthermore, there is an increasing interest also for homologous compounds such as Sy, for direct applications, or as precursors of fine chemicals and drugs (Erofeev *et al.* 1990, Lee *et al.* 2009, Ibrahim *et al.* 2012), and it is expected that the market of Sy will grow significantly in the period from 2021 to 2028.

Considering the environmental sustainability and economic relevance, lignin, the second most available renewable raw material with around 50 million tons per year produced, is identified as a promising source of V and Sy production (Rodrigues *et al.* 2018). Currently, the production of V from wood accounts for about 15 % of the total V production and Borregaard is the world's largest producer of bio-based V, which produces V from lignin via sulphite pulping method. Lignin derived V, which is marketed as a premium product, is priced at $100-200 per kilogram (Martău *et al.* 2021) .

Crystallization is widely used as a method to isolate and purify products with specific physicochemical properties in pharmaceutical, food, fine chemicals, and bulk chemical industries. Depending on the final product obtained, and the efficiency of the process, the process can be classified into crystallization, where crystals of specific shape and size are produced or precipitation, where amorphous solids are obtained (Haan 2015). Crystallization usually is a very time-consuming process compared to precipitation. Precipitation can be carried out in one step to remove a large number of compounds in a single precipitate. This is the most effortless application and is the most common. However, fractional precipitation can also be applied as a series of steps, with each step optimized to precipitate one desired component.

Cooling of a compound from a supersaturated solution by decreasing the temperature, has been the most common method of crystallization for the past 50 years, although antisolvent, reactive, and evaporative methods are also commonly employed (Mullin 2001, Zhao *et al.* 2012). Crystallization is a complex and challenging process, where the purity, crystal size, and polymorphic forms obtained need to be controlled and understood. Polymorphism is the ability of a chemical entity to crystallize into different structures where the atoms, ions or molecules are packed differently within the crystal lattice (Kavuru *et al.* 2016). Moreover, for each polymorph the physicochemical properties, such as melting point, solubility, density, and stability, are influenced by the differences in crystal packing and/or structural conformation. The control of polymorphism is an important factor in maintaining

high product quality and reproducibility in the food and pharmaceutical industry and it is a key issue in several scientific, technological, and industrial fields (Kavuru *et al.* 2016, Sundareswaran and Karuppannan 2021). In 1950, W. C. McCrone has reported that vanillin crystallization could occur in four different polymorphic forms: (i) Form I, the stable crystalline form; (ii) Form II, the metastable form; (iii) Form III, and (iv) Form IV (Kavuru *et al.* 2016). Most of the literature reports disclose only the crystallization of stable polymorph of vanillin - Form I, which can be easily crystallized at normal growth conditions and has many industrial applications (Kavuru *et al.* 2016, Parimaladevi *et al.* 2018). On the other hand, very few reports exist on the crystallization of metastable polymorph of vanillin - Form II, whose nucleation occurs only in specific conditions. Form III and Form IV are highly unstable, and their crystallization process is not completely understood.

In this work, crystallization and/or precipitation attempts were studied to obtain V and Sy. The starting solutions were obtained from the fixed bed adsorption/desorption experiments already discussed in the previous chapters, in Chapter 5 in the case of LSSL aqueous solution, which is enriched in V, and in Chapter 6 for the case of LHSL aqueous solution, enriched in Sy.

Different approaches of cooling and evaporative crystallization of V were attempted. In the case of Sy, the purification was made based on the solubility of the compounds present in the mixture. To the best of the author's knowledge, it is the first time that the recovery and purification of Sy were made from pulp mill hardwood sulfite liquor.

7.2 EXPERIMENTAL SECTION: MATERIAL AND METHODS

7.2.1 Vanillin Crystallization

In the process of V purification, crystallization is considered the key step that strongly influences the type and purity of the final product. In this work, the aqueous solutions that proceed for crystallization have low concentrations of V, in contrast to most of the studies in literature about V crystallization, which work with saturated and supersaturated solutions. V is sparsely water soluble, 10 g/1000 mL water at 25 °C, and its partial water solubility arises from formation of hydrogen bonds between the surrounding water molecules and polar groups in the V molecule (Havkin-Frenkel 2018).

7.2.1.1 LSSL aqueous solution

The aqueous solution used, rich in V, was obtained from the fixed bed adsorption/desorption process (Chapter 5) applied to the permeated from nanofiltration of the LSSL oxidation mixture. Detailed information about LSSL oxidative depolymerization in alkaline medium with O_2 is presented in Chapter 3. Table 7.1 summarize the concentrations of the main phenolic compounds present in the LSSL aqueous solution.

Table 7.1 – Concentration of phenolic monomers in the LSSL aqueous solution from fixed bed adsorption/desorption experiment.

	Concentration, g/L					
	VA	**V**	**SA**	**Sy**	**VO**	**SO**
LSSL mixture	0.08	5.20	ND	0.05	0.23	ND

ND – not detected

7.2.1.2 Liquid-liquid extraction (LLE)

The aqueous fraction rich in V, obtained from the adsorption/desorption experiments, was subjected to an LLE step before crystallization. The LLE was performed at a controlled pH to allow the separation of phenolic ketones, acids and aldehydes based in their acid dissociation constants (pKa). The pKa of the main low molecular weight phenolic compounds present in solution is between 4.3 and 8.3. Thus, it is expected that these compounds have negative charge in strong alkaline solutions, as the water fraction from desorption, which has a pH around 13. Moreover, it is expected that at the end of the LLE the organic solvent, ethyl acetate, extracts all the phenolate species.

Two different LLE approaches were performed, the first with two sequential extractions and another one with only one extraction step. The first LLE approach (Figure 7.2) started with the aqueous solution rich in V (100 mL) acidified, with an aqueous solution of H_2SO_4 (1:1 v/v), until pH around 8.0. The extraction was made with 100 mL of ethyl acetate. Then, the resulting aqueous phase from the first extraction was acidified until pH 6.0 and used for a second LLE. The second extraction was made with the same organic solvent.

The second approach was performed with only one step of LLE, with ethyl acetate, and the aqueous solution rich in V (100 mL) acidified until a pH near 6.0, also with an

aqueous solution of H_2SO_4 (1:1 v/v). After the LLE, for both approaches, the organic phase obtained was evaporated in a rotavapor, and the evaporated material was dissolved in 50 mL of water. The aqueous and organic phases and the solution resulting after evaporation and dissolution with water of the organic phase were analysed by HPLC for the quantification of all the main phenolic compounds, already described in the section 3.2.3.

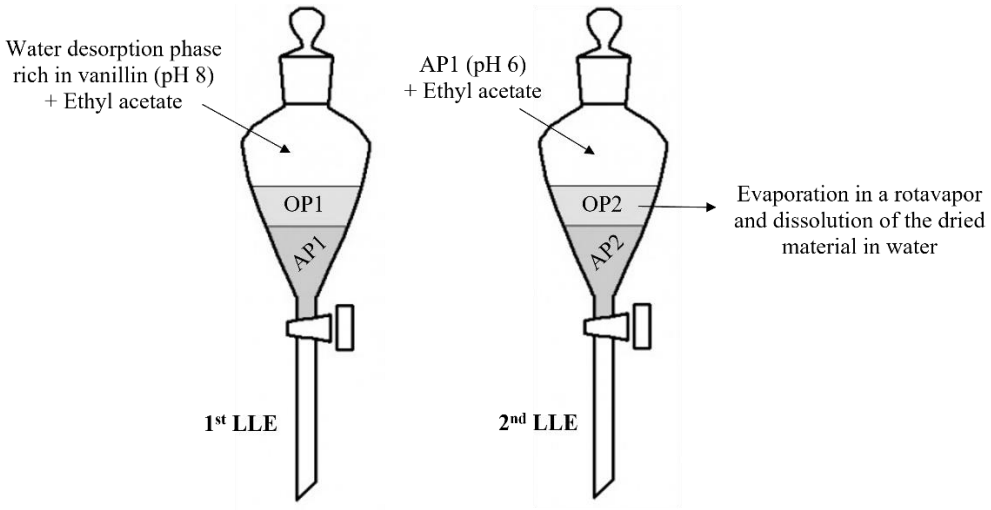

Figure 7.2 – Scheme of the two-step LLE (OP1 and OP2 - organic phase from the first and second LLE, respectively; AP1 and AP2 - aqueous phase from the first and second LLE, respectively).

7.2.1.3 Cooling crystallization

For the cooling crystallization, 50 mL of the aqueous solution from one-step LLE, after evaporation and dissolution of the evaporated material in water, was filled out into a 500 mL double-walled glass bottle, stirred at 250 rpm, and kept at 40 ºC for a few minutes. This slight heating guarantees the total dissolution of the phenolic compounds in the solution since the solubility of V in all solvents increases with an increase in temperature (Zhao *et al.* 2012). After that, the temperature was ramped down from 40 ºC to 5.0 ºC at 0.1 ºC/min. The temperature inside of the double-walled bottle was controlled using a thermostatic circulating water bath (VWR model AP07R-40-V12V) and the agitation maintained at 250 rpm using a magnetic stirrer impeller type. After several hours at 5.0 ºC, without the formation of V crystals, the solution was left in a glass crystallizer at room temperature (~25 °C) during about 48 hours until the complete crystallization of the final product.

The temperature for the cooling crystallization process (5 ºC) was selected based on the solubility of V in water (Svärd *et al.* 2007). In literature it is stated that the solubility

curve of this compound, in the range of 4 to 80 ºC, follows the polynomial equation $c = 0.0066T^2 + 0.1392T + 2.6530$, where '$c$' is the concentration of V in g/L and 'T' is the saturation temperature in °C (Gomes and Rodrigues 2020b). Therefore, at 5 ºC the saturation is reached with a concentration of 3.5 g/L, a lower value than V concentration in the solution that proceed for crystallization.

7.2.1.4 Swift cooling crystallization

The aqueous solution from one-step LLE was heated at 40 ºC at a stirring speed of 250 rpm for a few minutes. Then, was swiftly transferred to a double-walled glass bottle of 500 mL that was kept cooled to 5.0 ºC and stirred at 250 rpm using a magnetic stirrer impeller type, to originate V saturation in the aqueous solution. After 4 hours at 5.0 ºC and without V crystallization, the solution was transferred to a 600 mL glass crystallizer and left to evaporate slowly at room temperature (25 ºC) for about 48 hours.

7.2.1.5 Slow evaporative crystallization

Evaporative crystallization was carried out using the material obtained from the evaporation of the organic phase after one-step LLE. Before crystallization, the aqueous solution (50 mL) was kept at 40 °C for a few minutes. Then, the heated solution was left to evaporate slowly in a glass crystallizer at room temperature (~25 °C). The resulting crystals were collected after the evaporation of the solvent, which took around 48 hours.

7.2.1.6 Evaporative crystallization with heat

The aqueous solution from one-step LLE was transferred into a glass crystallizer and heated with constant agitation at 250 rpm. The set temperature of the heating plate was 80 ºC. After the evaporation started, and when only about 10 mL of the solution remain, some drops of oily phase started to form. The heat was stopped, and 10 mL of water was added to the evaporated solution, to revert the oily phase. The resulting solution, about 20 mL, was left to evaporate at room temperature until complete evaporation of the solvent and crystallization of the final product.

7.2.1.7 Yield and purity of vanillin crystals

About 3.0 mg of the final dry product, obtained from each crystallization process, was dissolved in 5 mL of methanol until complete dissolution. The solution was analysed by gas chromatography - mass spectrometry (GC-MS) and HPLC for identification of contaminants, such as VO or Sy, and quantification of V purity. GC-MS analyses were assessed using a SHIMADZU GC-MS (model TQ8040) equipped with an automatic split/splitless injector. The column used is a RESTEK Rxi-5Sil MS (30 m x 0.25 mm x 0.25 μm film thickness). The GC oven temperature was programmed from 100°C (2 min) to 180°C at 3°C/min, then to 200°C (5 min) at 3°C/min and then to 250°C (3 min) at 15°C/min. The temperatures of injector and detector were 250˚C and 280˚C, respectively. The carrier gas was helium (Air Liquide) at a column volumetric flow of 1.32 mL/min.

7.2.1.8 Identification of vanillin polymorphs

The morphology of the different forms of V crystals obtained from the different crystallization processes was observed using an Axiotech 100 HD optical microscope coupled to a high-resolution digital camera AxioCam 105 color. Images were processed using Zen software.

7.2.1.9 Polymorphs characterization by differential scanning calorimetry (DSC)

To study the thermal stability and possible polymorphic phase transformation of the grown polymorphic forms of V, the DSC thermogram was recorded. About 10 mg of each polymorphic sample was analyzed under nitrogen atmosphere at a heating rate of 10 °C/min from 40 to 200 °C, using a STA 490 PC/4/H Luxx 134 Netzsch thermal analyser.

7.2.2 Syringaldehyde Crystallization

Concerning the path for Sy purification, the solubility of the phenolic compounds in water could be the key to obtain the final product (Tarabanko *et al.* 2013). Since Sy has a low solubility compared to the other compounds present in the mixture, we can take advantage of this property and separate Sy from the remaining compounds, V, VO, and SO.

The aqueous solution used for Sy crystallization was obtained from the fixed bed adsorption / desorption process applied to the permeated from nanofiltration of the LHSL

oxidation mixture. Detailed information about LHSL depolymerization in alkaline medium with O_2 is presented in Chapter 3. The concentrations of the main phenolic compounds present in the LHSL aqueous solution is summarized in the Table 7.2.

Table 7.2 – Concentration of phenolic monomers in the LHSL aqueous solution from fixed bed adsorption/desorption experiment.

	Concentration, g/L					
	VA	**V**	**SA**	**Sy**	**VO**	**SO**
LHSL mixture	ND	0.52	0.03	2.9	0.17	0.92

ND – not detected

With LHSL aqueous solution one-step LLE was performed. The LHSL aqueous solution (150 mL) was acidified until pH 6, with an aqueous solution of H_2SO_4 (1:1 v/v) and extracted with the same amount of ethyl acetate.

After LLE, the ethyl acetate was evaporated from the organic phase, and the precipitate formed was washed with 50 mL of water and then filtered (Figure 7.3). The quantification of all the main phenolic compounds present in the samples from the different steps of the process was made by HPLC, using the same equipment and conditions as described in section 3.2.3.

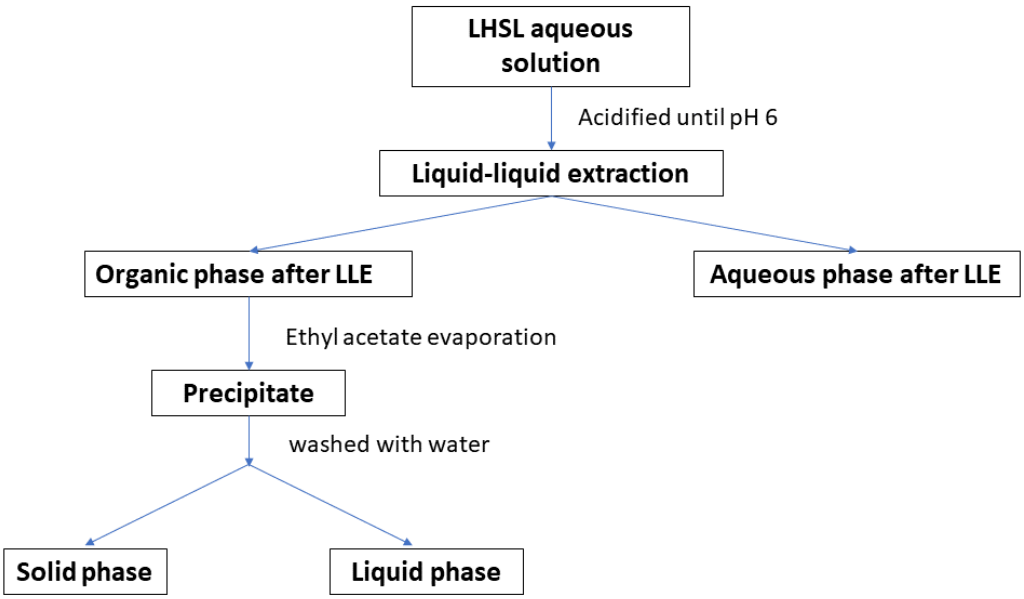

Figure 7.3 – Procedure to obtain the purified Sy from the aqueous solution obtained in the adsorption/desorption experiments.

7.3 RESULTS AND DISCUSSION

7.3.1 From LSSL Mixture to Vanillin

7.3.1.1 Liquid-liquid extraction (LLE)

As already described in the experimental section, two different LLE approaches, both using ethyl acetate, were performed. The first with two consecutive extractions (Figure 7.2), starting with the acidification of the aqueous solution rich in V until pH around 8.0. Then the resulting aqueous phase was used for another LLE at a pH around 6.0. The second LLE approach had only one extraction step with the aqueous solution rich in V acidified until a pH around 6.0. The objective of the two LLE approaches was to study the effect of consequent extractions on the recovery of phenolic compounds, mainly V. As already stated, in the aqueous fraction rich in V from adsorption/desorption experiments, with a pH value around 13, all the phenolic compounds are in the phenolate form. However, the studied phenolic compounds present in alkaline media (VA, V, Sy, and VO) have different pKa, between 4.3 and 8.3, and therefore the separation among aldehydes, acids, and ketones can be somewhat tuned by the pH of the aqueous solution due to differences in acid dissociation constants. When the pH of the solution decrease until a value near to 8.0, VO, with pKa around 8.3, leaves the phenolate form and is extracted by the organic solvent. The acids and aldehydes, with pKa values lower than 8, remains in the phenolate form and it was expected that they continue in the aqueous phase that will proceeds for the second step of LLE. However, in Figure 7.4 it can be observed that around 30 % and 40 % of the total mass of V and Sy, respectively, were extracted, as about 55 % of VO, by the organic solvent (ethyl acetate). Only VA, which has the lower pKa value, remains, in the totality, in the aqueous phase from the first step of LLE.

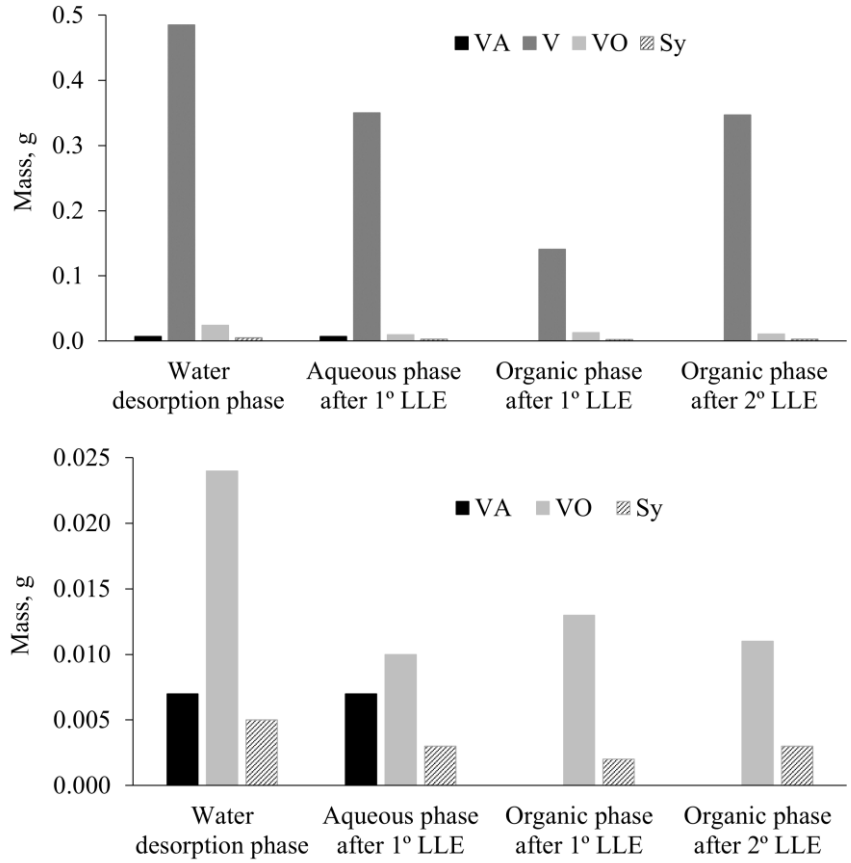

Figure 7.4 – V, VA, VO and Sy in water desorption fraction and aqueous and organic phases obtained from two-step LLE.

In conclusion, only 70 % of V, 55 % of VO, and 60 % of Sy remain in the aqueous phase that proceeds for the second extraction. The two-step approach is not advantageous since a significant amount of V is lost for the aqueous phase from the first step extraction and higher quantities of solvents are consumed.

In the procedure with only one extraction step (Figure 7.5), the initial fraction rich in V was acidified until pH 6.0, to guarantee that all the phenolic aldehydes and ketones (V, VO, and Sy) were extracted by ethyl acetate to the organic phase which will proceed to crystallization, after evaporation and dissolution of the evaporated material with water. VA is the only compound with a pKa lower than the pH of the solution, and consequently is the only compound that keeps in the phenolate form remaining in the aqueous phase. With this LLE approach, an extraction yield of 96 %, 91 %, and 99 % was observed for V, Sy and VO, respectively.

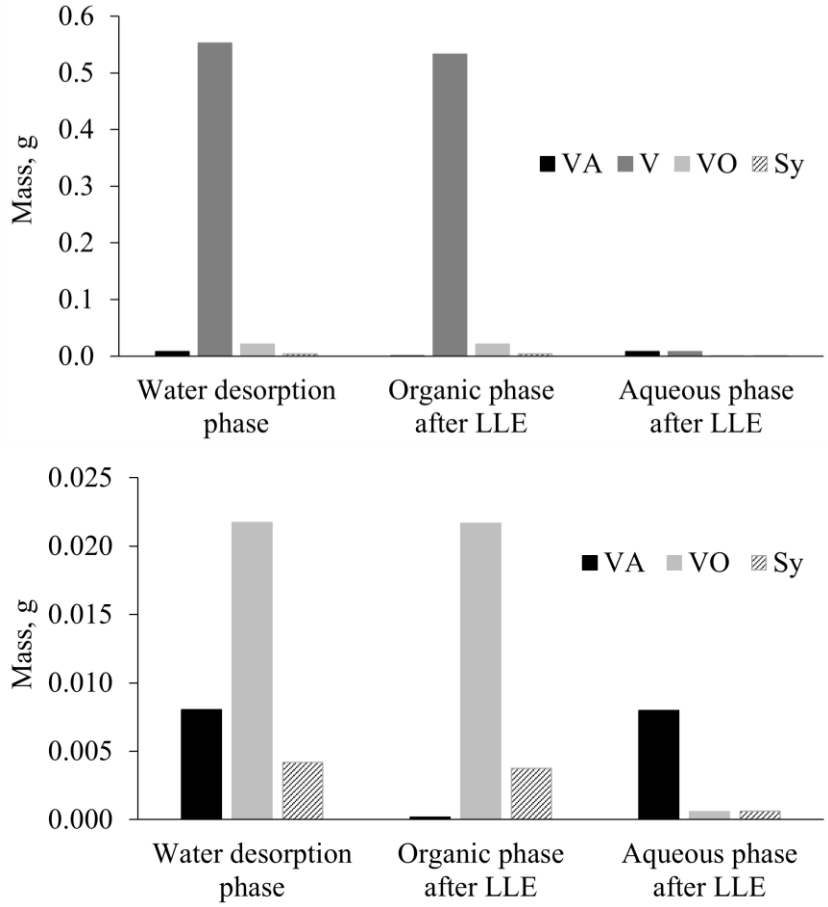

Figure 7.5 – V, VA, VO and Sy in water desorption fraction and aqueous and organic phases obtained from one-step LLE.

Considering the results coming from the two LLE approaches, it was established to proceed with only one-step of LLE, since the integrated process to obtain V from lignin will benefit from a smaller number of extraction steps and a lower consumption of organic reagents. Consequently, the organic phase from the one-step LLE, after evaporation and dissolution of the evaporated material with water, will proceed for crystallization as already described in section 7.2.1.

7.3.1.2 Yield and purity of vanillin crystals

A crystallization process could be optimized depending on its main objectives, such as crystallized mass, yield, crystal size distribution, crystal polymorphic form, and process time. In Table 7.3, the form and colour of the crystals, purity, and yield obtained from the evaporative and cooling crystallization processes are detailed.

Table 7.3 – Structural characteristics, purity, and yield of the V polymorphic forms obtained from the different crystallization processes**.**

Crystallization process	Form	Colour	Yield, %*	Purity, %
Slow evaporation	Form I	Yellow	80	95
Cooling	Form I	Yellow	75	99
Swift cooling	Form II	White	52	98
Evaporation with heat	Form II	Yellow	55	95

*Taking as reference the total content of V in the water desorption fraction before LLE.

A significant difference between the crystallization yields of the different processes was observed. From the slow evaporative and cooling process, V crystallizes into stable polymorphic Form I with a yield of 80 and 75 %, respectively. For swift cooling and evaporation with heat, the crystallization process shows a lower yield, between 52 and 55 %, respectively, and gives origin to crystals with metastable Form II. It seems that, besides the influence of the crystallization process, the type of polymorphic form of V formed also influences the process yield. The crystallization processes that give origin to V polymorphs of Form II, the metastable form, have lower yields.

The purity of the crystals that resulted from the evaporative crystallization are slight lower than that from the cooling crystallization processes. From evaporation, V crystals present a purity of about 95 %, while for cooling processes the purity is slightly higher, with values around 99 %. When the aqueous solution rich in V is submitted to low temperatures (5 ºC), apart from the cooling range, the purity of the V crystals is higher. Considering this, in opposition to that observed for yield values, it seems that the results are influenced by the crystallization process instead the resulting polymorphic form of V. Moreover, from GC-MS analyses, it can be stated that the only impurity present in the crystals from evaporative crystallization, with purity of 95 % and without any type of cooling step, is VO, in very low amounts.

7.3.1.3 Polymorphic forms of vanillin

During the different crystallization processes, two distinct polymorphic forms of V were observed: the stable Form I and the metastable Form II (Figure 7.6). In the stable monoclinic Form I the molecules in each of the pairs of its asymmetric unit are linked by the

hydrogen bonds between the aldehyde (C=O) and hydroxyl (O-H) groups of neighbouring molecules (Sundareswaran and Karuppannan 2021). While in the metastable orthorhombic Form II the molecules are linked by the hydrogen bonds between hydroxyl groups of the neighbouring molecules (Sundareswaran and Karuppannan 2021).

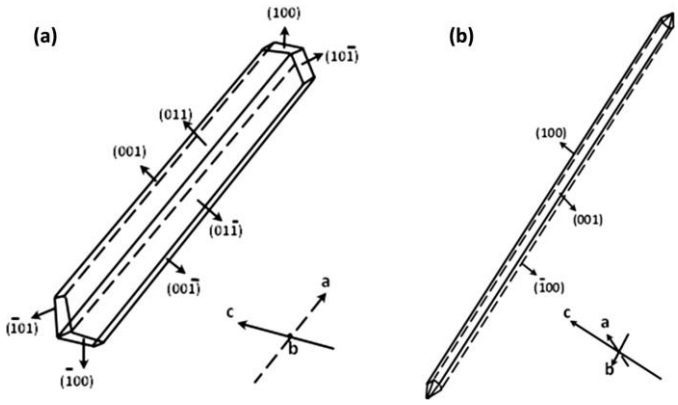

Figure 7.6 - Morphology of V polymorphs from aqueous solution: (a) stable Form I and (b) metastable Form II (Parimaladevi *et al.* 2018).

The occurrence of a metastable crystal form depends on a combination of the saturation and solvent composition of the system (Hussain *et al.* 2001, Ouyang *et al.* 2022). In a study about the nucleation of V polymorphs in different solvents under a series of supersaturation ratios with the presence of different silica templates, the authors found that Form I and Form II could be obtained in water with low supersaturation ratio and high supersaturation ratio, respectively (Sundareswaran and Karuppannan 2022). Moreover, a high content of water in the solvent seems to increase the possibility of the precipitation of a metastable phase (V Form II) in the system. In ethanol, isopropanol and ethyl acetate, only form I was obtained (Ouyang *et al.* 2022).

In this work, all the crystallization processes were performed using aqueous solutions. The cooling crystallization process was carried out at 5.0 ºC with a slow decrease of temperature at a rate of 0.1 ºC/min, while during the slow evaporative crystallization the solution was left at room temperature until crystals were formed. In these crystallization processes there are no sudden temperature changes, and both yielded the nucleation of the stable polymorph Form I of V (Table 7.3). On the other hand, during swift cooling crystallization the temperature is drastically changed from 30 ºC to 5 ºC and in crystallization by evaporation with heat the solution is submitted to a swift increase of temperature. Considering the polymorphic form of V that results from these processes, it

could be concluded that the processes with high and sudden variations of temperature favour the nucleation of thinner and lengthy V crystals with the metastable Form II. From Table 7.3 it could be stated that cooling and slow evaporative crystallization gives origin to V crystals with Form I, which presents a rod-like shape (Figure 7.7 (a)), while during swift cooling crystallization and crystallization by evaporation with heat V crystals with a thin needle-like form were obtained (Form II, Figure 7.7 (b)).

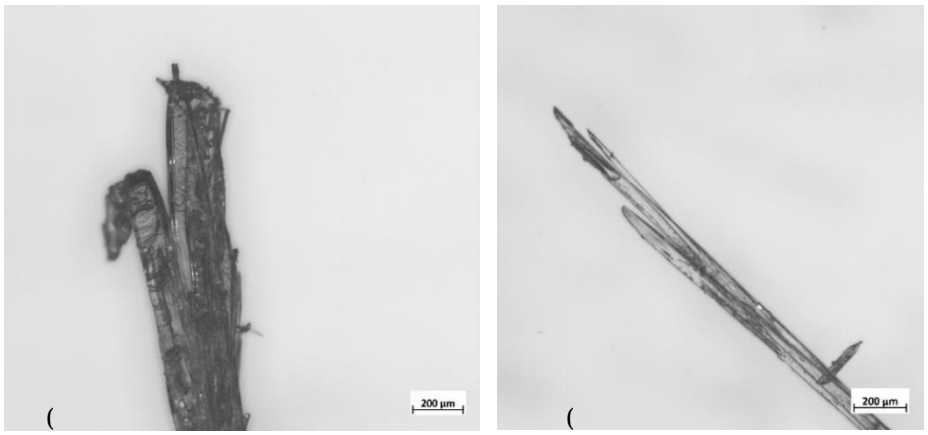

Figure 7.7 - Microscope images of V polymorph Forms I (a) and Form II (b).

It is clear that a temperature variation in the order of minutes (crystallization by evaporation with heat and swift cooling crystallization), instead of hours or days (slow evaporative and cooling crystallization), promotes a sudden saturation of the solution achieving a quasi-steady state distribution of molecular crystals that favours the nucleation of metastable Form II (Kavuru *et al.* 2016, Sundareswaran and Karuppannan 2021). In opposition, the rod-like stable monoclinic Form I crystals grew under lower saturation conditions, promoting a slow growth rate of the crystals. According to Ostwald's rule of stages, during crystallization, the system moves to equilibrium from an initial high energy stage to a lower energy state through minimal changes in free energy (Nývlt 1995). Therefore, at a higher supersaturation level, the metastable polymorph Form II nucleated possesses higher energy and transforms into the stable Form I by attaining the minimum energy (Findlay 1904, Hussain *et al.* 2001). Other authors in literature also noticed the influence of temperature variation on the resulting polymorphic forms of V. All of them reported the effect of the cooling and evaporation rate on the crystallization of V in stable Form I, metastable Form II or a mixture of both (Kavuru *et al.* 2016, Sundareswaran and Karuppannan 2021).

7.3.1.4 Polymorphs characterization by DSC

The thermal stability and melting point of the stable Form I and metastable Form II of V crystals were analyzed through DSC and the recorded thermograms, in the temperature range from 40 to 200 °C with a heating rate of 10 °C/min, are shown in Figure 7.8. Pure V has a melting point between 81 - 83 ºC (Vidal 2006).

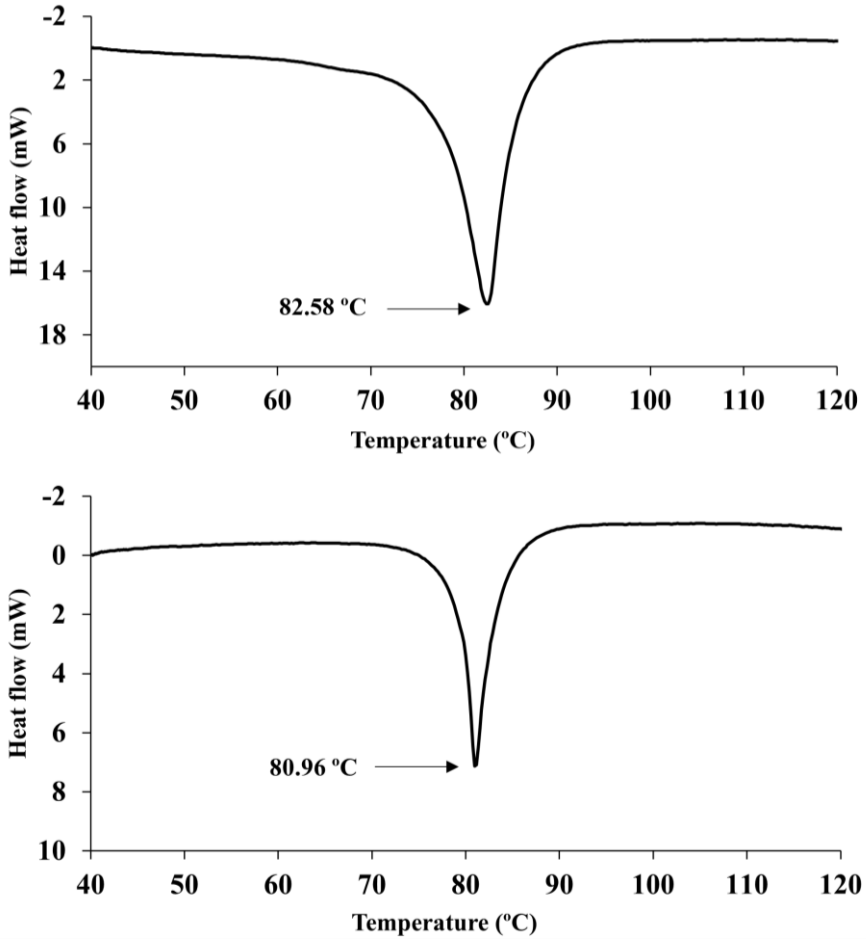

Figure 7.8 - DSC thermograms of the V polymorphs from aqueous solution: a) stable Form I and b) metastable Form II.

The DSC curve obtained for the stable monoclinic Form I of V crystals shows a sharp endothermic peak at 82.6 °C, which corresponds to the melting point. No phase transformation was observed during the heating cycle until the melting point. What concerns the orthorhombic metastable Form II of V crystals the sharp endothermic peak was noticed at 81.0 °C. In this case, it was also no phase transformation observed during the heating cycle. Considering the melting point found for Form I and Form II it is evidenced that Form I is the most thermodynamically stable crystal form. According to the literature, the V

polymorphic stable Form I has valuable non-linear optical properties useful in industry, increasing its relevancy to materials science (Sundareswaran and Karuppannan 2021). On the other hand, the metastable Form II has better second harmonic generation efficiency and may have other applications relevant to the food and pharmaceutical industries (Vidal 2006, Sundareswaran and Karuppannan 2021).

7.3.2 From LHSL Mixture to Syringaldehyde

7.3.2.1 Liquid-liquid extraction (LLE)

As already stated, in the aqueous fraction rich in Sy from adsorption/desorption experiments, with a pH value of around 13, all the phenolic compounds (VA, V, SA, Sy, VO and SO) are in the phenolate form. Moreover, the studied phenolic compounds have different pKa, between 4.3 and 7.9 therefore, the separation among aldehydes, acids, and ketones can be performed based on this chemical property. Some physico-chemical properties of the phenolic monomers present in the LHSL mixture are summarized in Table 7.4.

Table 7.4 – Physico-chemical properties of the main phenolic monomers present in the LHSL mixture.

Phenolic monomer	pKa	Solubility in water, g/L	Mw, g/mol	Boiling Point, °C	Melting Point, °C
VA	4.42	1.5	168.14	353	211
V	7.40	10	152.15	285	81-83
SA	4.34	5.8	198.17	379	208
Sy	7.34	Insoluble	182.17	193	113
VO	7.81	3.0	166.17	297	115
SO	7.88	4.0	196.2	293	126

In LLE, the aqueous solution rich in Sy, was acidified until a pH around 6.0, to guarantee that all the phenolic aldehydes and ketones (V, Sy, VO and SO) were extracted by ethyl acetate to the organic phase. VA and SA have a lower pKa than the pH of the solution and consequently, both compounds keep in the phenolate form remaining in the aqueous phase. At this stage, an extraction yield of 98 %, 95 %, 96 %, and 91 % was observed for V, Sy, VO and SO, respectively (Figure 7.9). The organic phase from the LLE, after evaporation will proceed for a crystallization step as already described in section 7.2.2.3.

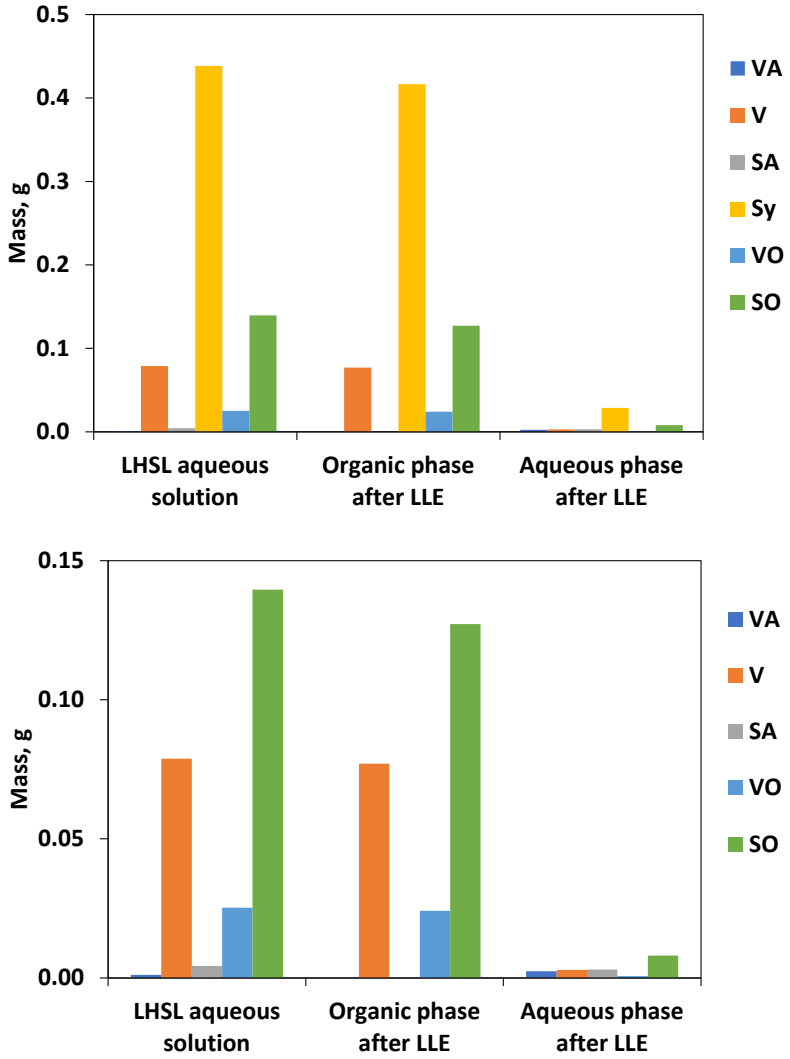

Figure 7.9 - VA, V, SA, Sy, VO and SO in LHSL aqueous solution, and aqueous and organic phases obtained from LLE.

7.3.2.2 Crystallization of Sy: yield and purity

In literature, it was reported that Sy is insoluble or has very low solubility in water, while the remaining phenolic compounds have a solubility in water in the range of 1.5 – 10 g/L (Tarabanko *et al.* 2013).

Once the crystallization of V was successfully achieved, it was decided to carry out a preliminary test with the organic phase coming from the LLE applied to the LHSL aqueous solution. The organic phase from the one-step LLE was evaporated. At this point, it was observed the formation of a precipitate (Figure 7.10). After that, the precipitate was placed

in a desiccator overnight (Figure 7.10 B). HPLC analysis showed that the precipitate was composed of 16 %, 55 %, 5 %, and 25 % of V, Sy, VO, and SO, respectively.

The precipitate was washed with 50 mL of water (Figure 7.10 C) and filtered, obtaining two phases, the solid (Figure 7.10 D) and the liquid one.

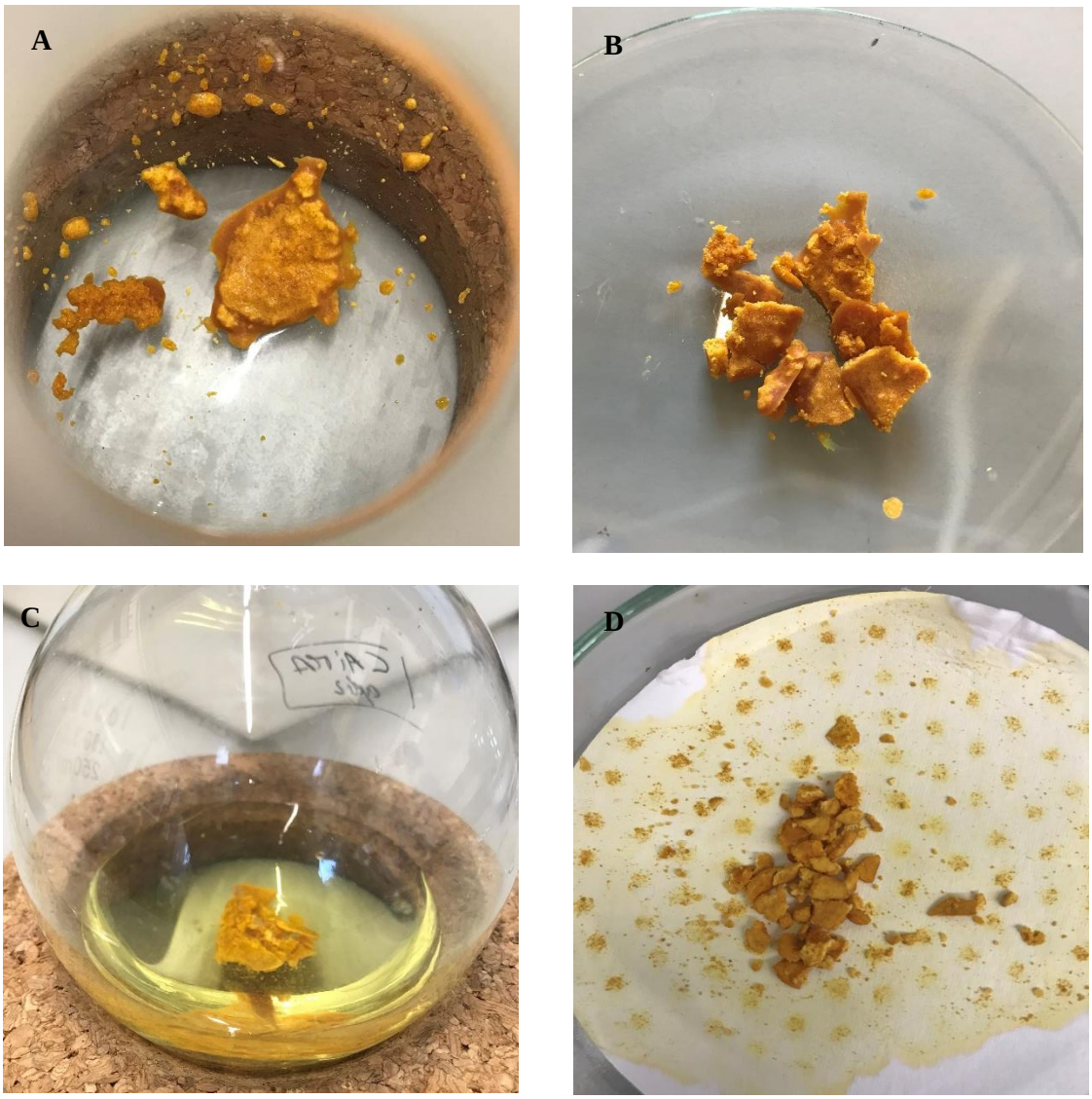

Figure 7.10 – Precipitate: A) after evaporation, B) after overnight in the desiccator, C) washed with water and D) after filtration.

The solid phase was dissolved in 1.5 mL of eluent B, which is methanol:water solution (95:5 % v/v), acidified with formic acid (0.1 % v/v), and analyzed by HPLC, and it was observed that besides Sy it contains 3 % of V and 5 % of SO. Concerning the target phenolic compound, Sy, it was possible to obtain a process yield of around 70 %, relative to the initial mass of Sy present in the initial aqueous solution, with a purity of 92%.

7.4 CONCLUSIONS

The influence of the crystallization process on the yield, purity, and polymorphic forms of V crystals was achieved. The polymorphic form of V was found to be dependent on the crystallization method as well as the temperature variation during the process. The slow evaporation method and cooling crystallization give origin to the stable polymorph Form I, with a yield of 80 and 75 %, respectively, while swift cooling and evaporative process with heat favour the nucleation of V polymorphic Form II, with a yield of 52 and 55 %, respectively. Moreover, from evaporative processes, the V crystals present a purity of about 95 %, while for cooling processes the purity is slightly higher, with values around 99 %. The melting points, observed in the DSC thermograms, of the stable Form I and metastable Form II of V were found to be 82.6 ºC and 81.0 ºC, respectively. Since the metastable Form II is less stable and highly energetic, the melting point of V Form II is lower than that of the stable Form I. Moreover, there was no polymorphic phase transformation obtained for both polymorphic forms of V during heating until melting point. The evaporative and cooling crystallization processes studied in this work proved to be consistent and valuable considering the attaining of V crystals. Moreover, each of the polymorphic forms of V may have different industrial applications due to their different physicochemical properties.

In the case of Sy, the final product obtained, presents a purity of 92 % with a process yield of 70 %, considering the mass of Sy present in the aqueous solution obtained from the adsorption/desorption experiments.

7.5 REFERENCES

Bajpai, P. (2018). Value-Added Products from Lignin. Biotechnology for Pulp and Paper Processing. *P. Bajpai*. Singapore, Springer Singapore**:** 561-571.

Erofeev, Y. V., V. L. Afanas'eva and R. G. Glushkov (1990). Synthetic routes to 3,4,5-trimethoxybenzaldehyde (review). *Pharmaceutical Chemistry Journal* 24(7): 501-510.

Findlay, A. (1904). The phase rule and its applications, Longmans, Green.

Gomes, E. D. and A. E. Rodrigues (2020b). Crystallization of vanillin from kraft lignin oxidation. *Separation and Purification Technology* 247: 116977.

Haan, A. B. d. (2015). 13. Crystallization and precipitation. Process Technology. Berlin, München, Boston, De Gruyter**:** 273-296.

Havkin-Frenkel, D. (2018). Vanillin. Kirk-Othmer Encyclopedia of Chemical Technology**:** 1-12.

Hussain, K., G. Thorsen and D. Malthe-Sørenssen (2001). Nucleation and metastability in crystallization of vanillin and ethyl vanillin. *Chemical Engineering Science* 56(7): 2295-2304.

Ibrahim, M., R. B. Sriprasanthi, S. Shamsudeen, F. Adam and S. Bhawani (2012). A concise review of the natural existence, synthesis, properties, and applications of syringaldehyde.

Kavuru, P., S. J. Grebinoski, M. A. Patel, L. Wojtas and K. Chadwick (2016). Polymorphism of vanillin revisited: the discovery and selective crystallization of a rare crystal structure. *CrystEngComm* 18(7): 1118-1122.

Lee, C. Y., A. Sharma, J. E. Cheong and J. L. Nelson (2009). Synthesis and antioxidant properties of dendritic polyphenols. *Bioorganic & Medicinal Chemistry Letters* 19(22): 6326-6330.

Martău, G. A., L. F. Călinoiu and D. C. Vodnar (2021). Bio-vanillin: Towards a sustainable industrial production. *Trends in Food Science & Technology* 109: 579-592.

Mullin, J. W. (2001). Crystallization, Elsevier Science.

Nývlt, J. (1995). The Ostwald rule of stages. *Crystal Research and Technology* 30(4): 443-449.

Ouyang, J., X. Xing, J. Chen, L. Zhou, Z. Liu and J. Y. Y. Heng (2022). Effects of solvent, supersaturation ratio and silica template on morphology and polymorph evolution of vanillin during swift cooling crystallization. *Particuology* 65: 93-104.

Parimaladevi, P., S. Supriya and K. Srinivasan (2018). The role of ultrasound in controlling the liquid-liquid phase separation and nucleation of vanillin polymorphs I and II. *Journal of Crystal Growth* 484: 21-30.

Rodrigues, A. E., P. C. d. O. R. Pinto, M. F. Barreiro, C. A. Esteves da Costa, M. I. Ferreira da Mota and I. Fernandes (2018). An integrated approach for added-value products from lignocellulosic biorefineries: Vanillin, syringaldehyde, polyphenols and polyurethane, Springer International Publishing.

Sundareswaran, S. and S. Karuppannan (2021). Nucleation control and separation of vanillin polymorphs I and II through the swift cooling crystallization process. *CrystEngComm* 23(7): 1634-1642.

Sundareswaran, S. and S. Karuppannan (2022). Isolation and stabilization of the metastable Form-II polymorph of vanillin. *Chemical Engineering & Technology* 45(4): 687-693.

Svärd, M., S. Gracin and Å. C. Rasmuson (2007). Oiling out or molten hydrate-liquid-liquid phase separation in the system vanillin-water. *Journal of Pharmaceutical Sciences* 96(9): 2390-2398.

Tarabanko, V. E., Y. V. Chelbina, A. V. Kudryashev and N. V. Tarabanko (2013). Separation of Vanillin and Syringaldehyde Produced from Lignins. *Separation Science and Technology* 48(1): 127-132.

Vidal, J. P. (2006). Vanillin. Kirk-Othmer Encyclopedia of Chemical Technology**:** 1-14.

Wong, S. S., R. Shu, J. Zhang, H. Liu and N. Yan (2020). Downstream processing of lignin derived feedstock into end products. *Chemical Society Reviews* 49(15): 5510-5560.

Zhang, C., S. A. Madbouly and M. R. Kessler (2015). Renewable polymers prepared from vanillin and its derivatives. *Macromolecular Chemistry and Physics* 216(17): 1816-1822.

Zhao, H., C. Xie, Z. Xu, Y. Wang, L. Bian, Z. Chen and H. Hao (2012). Solution crystallization of vanillin in the presence of a liquid–liquid phase separation. *Industrial & Engineering Chemistry Research* 51(45): 14646-14652.

Zhou, N., W. P. D. W. Thilakarathna, Q. S. He and H. P. V. Rupasinghe (2022). A Review: Depolymerization of Lignin to Generate High-Value Bio-Products: Opportunities, Challenges, and Prospects. *Frontiers in Energy Research* 9.

8 Final Conclusions and Suggestions for Future Work

8.1 GENERAL CONCLUSIONS

This work addresses the valorization of sulfite liquor streams from pulp and paper mills for the sustainable production of value-added compounds by an integrated process. The sequential process contemplates membrane and chromatographic procedures to be combined with the depolymerization of lignin into V and Sy in an alkaline medium with oxygen, and a final purification step including LLE followed by crystallization. The scheme of the integrated process from oxidation until crystallization is presented in Figure 8.1. In this thesis, two real oxidized lignin solutions, from hardwood and softwood sulfite liquors, were studied. The most relevant conclusions obtained will be made in the following paragraphs.

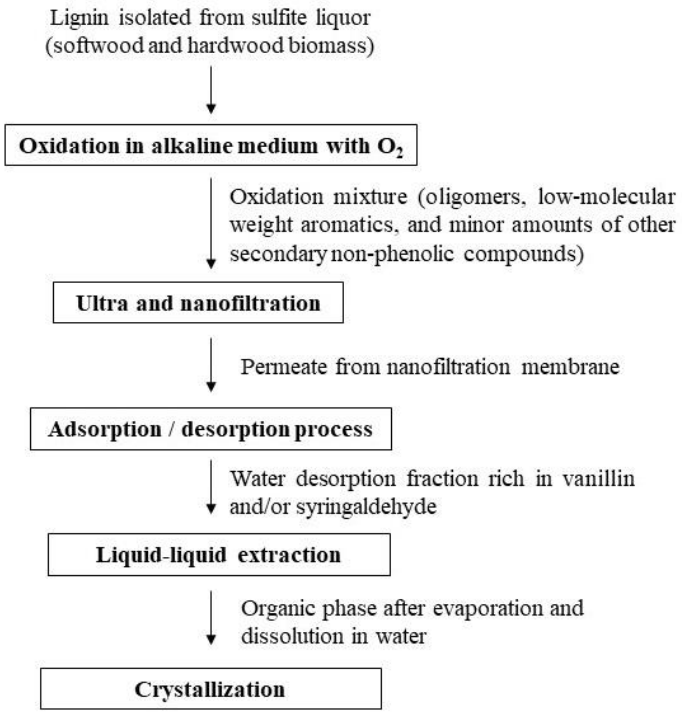

Figure 8.1 – Scheme of the sequential process since the oxidation of lignin from sulfite liquor until crystallization.

The lignins from hardwood and softwood pulp mill sulfite liquors were comprehensively analyzed by selected characterization techniques and methods, evaluating the most important features of their structure. The LHSL, lignin from hardwood biomass, presents the lowest value of DC and the highest number of β-*O*-4 structures, consequently this lignin give origin to higher yields of phenolic monomers through depolymerization by nitrobenzene oxidation. Concerning the LSSL, lignin from softwood biomass, the GPC

analysis confirmed its highest value of molecular weight, which is coherent with the presence of more condensed moieties in its structure, related with the higher availability of G units in this lignin. Both lignins were subjected to alkaline oxidation with O_2 and the yield of aromatic monomers and the selectivity of the target products were evaluated. With the experimental conditions optimized, LSSL produced a maximum of 2.7 $g.L^{-1}$ of V in the final oxidation mixture achieving a yield of 5 % w/w_{lignin}, while LHSL produced a maximum of 1.5 $g.L^{-1}$ of Sy in the final oxidation mixture with a yield of 2.6 % w/w_{lignin}.

The degradation of valuable phenolic compounds obtained from lignin oxidation in alkaline medium with O_2 was studied. An evaluation of the reaction orders with respect to V, VA, VO, Sy, SA, and SO initial concentration, and oxygen concentration was performed, as well as the effect of temperature on the kinetic rate constants. The results showed that the initial concentration of phenolic compounds as well as the oxygen concentration, had no effect on the degradation reaction rate, since a first order dependence for both oxidation parameters was obtained for all the studied compounds. Comparing all the tested phenolic compounds, it was possible to conclude that Sy, SA, and SO have higher degradation rate, in comparison with V, VA, and VO. This is an expected behavior since derivatives from S units are more reactive than the G ones due to the presence of two methoxyl groups in their aromatic rings.

The oxidized LSSL stream was submitted to a two-step membrane filtration, ultra and nanofiltration, that reduces the TDS from the initial 34 % w/w_{lignin} to 9 % w/ w/w_{lignin} before fixed bed experiments.

The breakthrough curve performed with a model solution, composed by VA, V, VO and Sy, enabled the selection of the times at which cycles of adsorption/desorption would be made. Four cycles were performed using the model solution and 8 cycles in the case of permeate from nanofiltration of oxidized LSSL solution.

The resulting fractions from adsorption/desorption cycles differ considerably from the feed mixture since the monomers are successful fractionated through their functional groups: phenolic acids, phenolic aldehydes, and phenolic ketones. Three fractions were collected in the water desorption phase using the permeate from nanofiltration of LSSL oxidized mixture: the fraction I, where the residual VA is collected, fraction II, where V is collected with a recovery of 92 % with small amounts of Sy and VO, and fraction III, where small

concentrations of Sy and VO were collected. In the ethanol desorption phase, VO and Sy were collected with a recovery of 40% and 73 %, respectively.

Considering LHSL oxidized stream, it was fractionated in a chromatographic step that employs the same eluents and resin used with LSSL mixture. Prior to the fixed bed experiments, the feed mixture was submitted to a three-step membrane filtration, 5 kDa, 2 kDa and 600-800 Da, where the organic solids content was reduced in 5% comparing the oxidation mixture and the solution fed to the chromatographic column. A complete breakthrough with a standard solution, composed by VA, V, SA, Sy, VO, and SO, was performed, and allows determining the time at which cycle of adsorption/desorption would be performed. Eight cycles were performed in the case of the standard solution and two cycles using the permeate from oxidized LHSL solution submits to nanofiltration. Considering the cycles performed with the model solution, it was possible to obtain recoveries of about 88 % for Sy, 40 % for V, 81% for VO, and 45 % for SO during the water desorption phase. In the ethanol desorption phase phenolic ketones, VO and SO, had recoveries of about 20% and 80 %, respectively. Considering the permeate from nanofiltration of oxidized LHSL solution different recoveries were obtained. Considering the total mass of each compound fed to the column, it was possible to recover 19 % of V, 50 % of the Sy, 67 % of the SO, and 42 % of VO during the water desorption phase. The recoveries during the ethanol desorption phase were lower comparing to the water desorption phase, only 24 % of SO mass recovered, 2 % of VO, and 1 % of Sy.

Furthermore, the aqueous solutions obtained from the water desorption phase were submitted to an LLE followed by crystallization processes. Several approaches were performed regarding LSSL aqueous solution. The influence of the crystallization process on the yield, purity, and polymorphic forms of V crystals was evaluated. The slow evaporation method and cooling crystallization give origin to the stable polymorph Form I, with a yield of 80 and 75 %, respectively, while swift cooling and evaporative process with heat favour the nucleation of V polymorphic Form II, with a yield of 52 and 55 %, respectively. Moreover, from evaporative processes, the V crystals present a purity of about 95 %, while for cooling processes the purity is slightly higher, with values around 99 %. The evaporative and cooling crystallization processes studied with LSSL aqueous solution proved to be consistent and valuable considering the attaining of V crystals. An attempt of evaporative crystallization was made with LHSL aqueous solution, and a final product with a purity of

92 % and a yield of 70 %, considering the initial mass of Sy present in the aqueous solution obtained from the adsorption/desorption process.

At the end of this work, it can be seen as a proof of concept that oxidation, membrane separation, adsorption/desorption, and crystallization processes can be integrated to process a pulp mill sulfite liquor, valorizing these streams as source of value-added phenolic compounds.

8.2 SUGGESTIONS FOR FUTURE WORK

The results attained in this thesis, using two lignins isolated from pulp mill sulfite liquors to produce valuable compounds, namely vanillin and syringaldehyde, reveal that some topics contemplated in this work should be more explored. Thus, some suggestions for future work are proposed:

A future research line that can be considered is the application of the integrated process to lignins from different processes and biomass sources, as kraft lignins.

The separation of vanillin and syringaldehyde by fixed bed adsorption/desorption experiments was evaluated in this thesis however, several improvements could be attained in the separation of these two similar phenolic aldehydes. A continuous Simulated Moving Bed (SMB) based process for the fractionation of oxidized lignin mixture should be applied to study the separation of the main families of phenolic products obtained: acids, aldehydes, and ketones. SMB is commonly used to separate chemically similar compounds in petroleum (Broughton 1984), sugar (Beste *et al.* 2000), and pharmaceutical industry (Negawa and Shoji 1992, Pais *et al.* 1997, Pais *et al.* 1998).

8.3 REFERENCES

Beste, Y. A., M. Lisso, G. Wozny and W. Arlt (2000). Optimization of simulated moving bed plants with low efficient stationary phases: separation of fructose and glucose. *Journal of Chromatography A* 868(2): 169-188.

Broughton, D. B. (1984). Production-Scale Adsorptive Separations of Liquid Mixtures by Simulated Moving-Bed Technology. *Separation Science and Technology* 19(11-12): 723-736.

Negawa, M. and F. Shoji (1992). Optical resolution by simulated moving-bed adsorption technology. *Journal of Chromatography A* 590(1): 113-117.

Pais, L. S., J. M. Loureiro and A. E. Rodrigues (1998). Modeling strategies for enantiomers separation by SMB chromatography. *AIChE Journal* 44(3): 561-569.

Pais, L. s. S., J. M. Loureiro and A. r. E. Rodrigues (1997). Modeling, simulation and operation of a simulated moving bed for continuous chromatographic separation of 1,1′-bi-2-naphthol enantiomers. *Journal of Chromatography A* 769(1): 25-35.